Institut für Chemie und Dynamik der Geosphäre 3:
Atmosphärische Chemie

Measurements of Atmospheric Trace Gas Concentrations during the Field Campaign in Jülich 1988

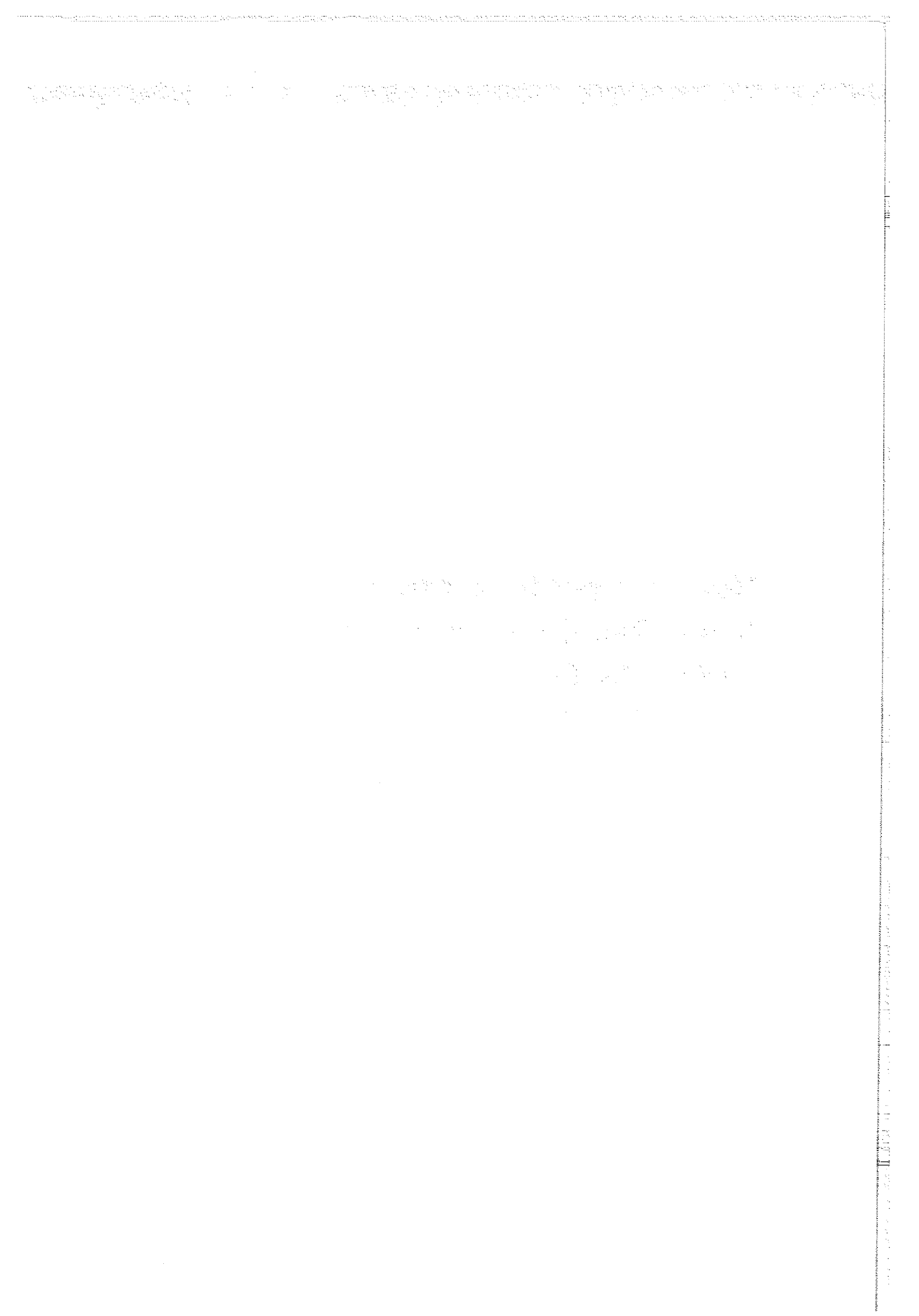

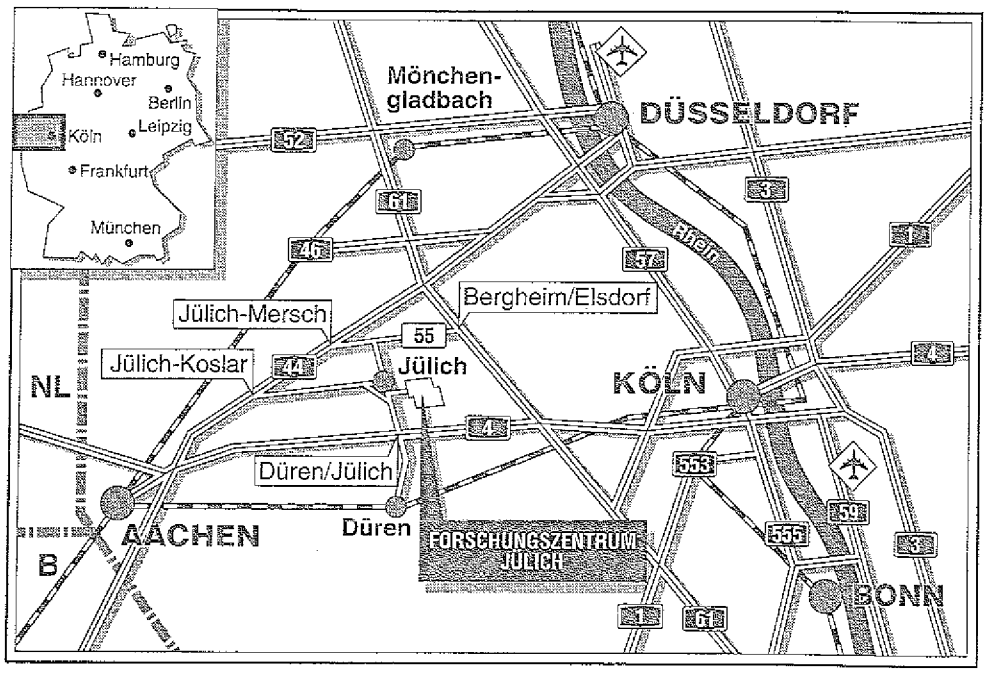

Berichte des Forschungszentrums Jülich ; 2731
ISSN 0366-0885
Institut für Chemie und Dynamik der Geosphäre 3:
Atmosphärische Chemie Jül-2731

Zu beziehen durch: Forschungszentrum Jülich GmbH · Zentralbibliothek
Postfach 1913 · D-5170 Jülich · Bundesrepublik Deutschland
Telefon: 02461/61-6102 · Telefax: 02461/61-6103 · Telex: 833556-70 kfa d

Measurements of Atmospheric Trace Gas Concentrations during the Field Campaign in Jülich 1988

D. Poppe R. Bauer T. Brauers D. Brüning J. Callies
H.-P. Dorn A. Hofzumahaus F.-J. Johnen A. Khedim
R. Koppmann H. London K.-P. Müller R. Neuroth
Ch. Plaß-Dülmer U. Platt F. Rohrer J. Rudolph
U. Schmidt M. Wallasch D.H. Ehhalt

Abstract

Our current understanding of the gas phase chemistry of the lower troposphere is based on measurements of trace gas concentrations in the atmosphere, laboratory studies of gas phase reactions and model calculations of the relevant chemical processes. The ultimate validation of a reaction scheme can only be derived from a comparison of model results with experimental data from measurements in the atmosphere. In order to establish an extended and reliable experimental data set on which such a comparison could be based the Institut für Atmosphärische Chemie of the Forschungszentrum Jülich (KFA) has been conducting field campaigns for a number of years. One such campaign took place in Jülich from May 9 - June 10 in 1988. Many of the relevant trace species were measured on a continuous basis together with photolysis frequencies and meteorological parameters. All measurements were ground based and included OH, O_3, NO, and NO_2, NO_y, HCHO, SO_2, CH_4, CO, non methane hydrocarbons up to C_5, peroxyacetylnitrate, and aldehydes. The photolysis frequencies of O_3 and NO_2 were also monitored, as were atmospheric temperature, relative humidity, wind speed, and wind direction.

All quantities were measured in-situ except OH and SO_2, which were exclusively measured by a long path differential optical absorption technique. HCHO, NO_2, and O_3 were determined by in-situ and also by long-path-absorption methods for intercomparison.

Jülich (lat.: 50.9°N, long.: 6.3°E, alt.: 100 m) is a moderately polluted area about 5 km from motorways with heavy traffic and about 20 to 40 km away from industrialized zones in the Rhine valley.

The NO_x mixing ratio showed large variability with a mean value of 9 ppb and 16- and 84-percentiles of 4 ppb and 22 ppb, respectively. The ozone concentration reached mean values of 24 ppb with peak values up to 84 ppb. The SO_2 burden was usually below 7.5 ppb with a mean concentration of 1.2 ppb. CO ranges from 200 ppb to 374 ppb (16- and 84-percentile) with an average concentration of 267 ppb and peak values up to 881 ppb. The measured average non methane hydrocarbon concentration was 29 ppbC. All trace gases except CH_4 showed significant diurnal variations. The trace gas scenario is typical for large parts of Germany (Umweltbundesamt, 1989).

The paper describes the purpose and design of the campaign and presents diurnal profiles of all measured species in a first evaluation of the experimental material. A brief description of the experimental setup and an analysis of the experimental uncertainties are also given. The access to the data in computerized form for further interpretation and processing is indicated.

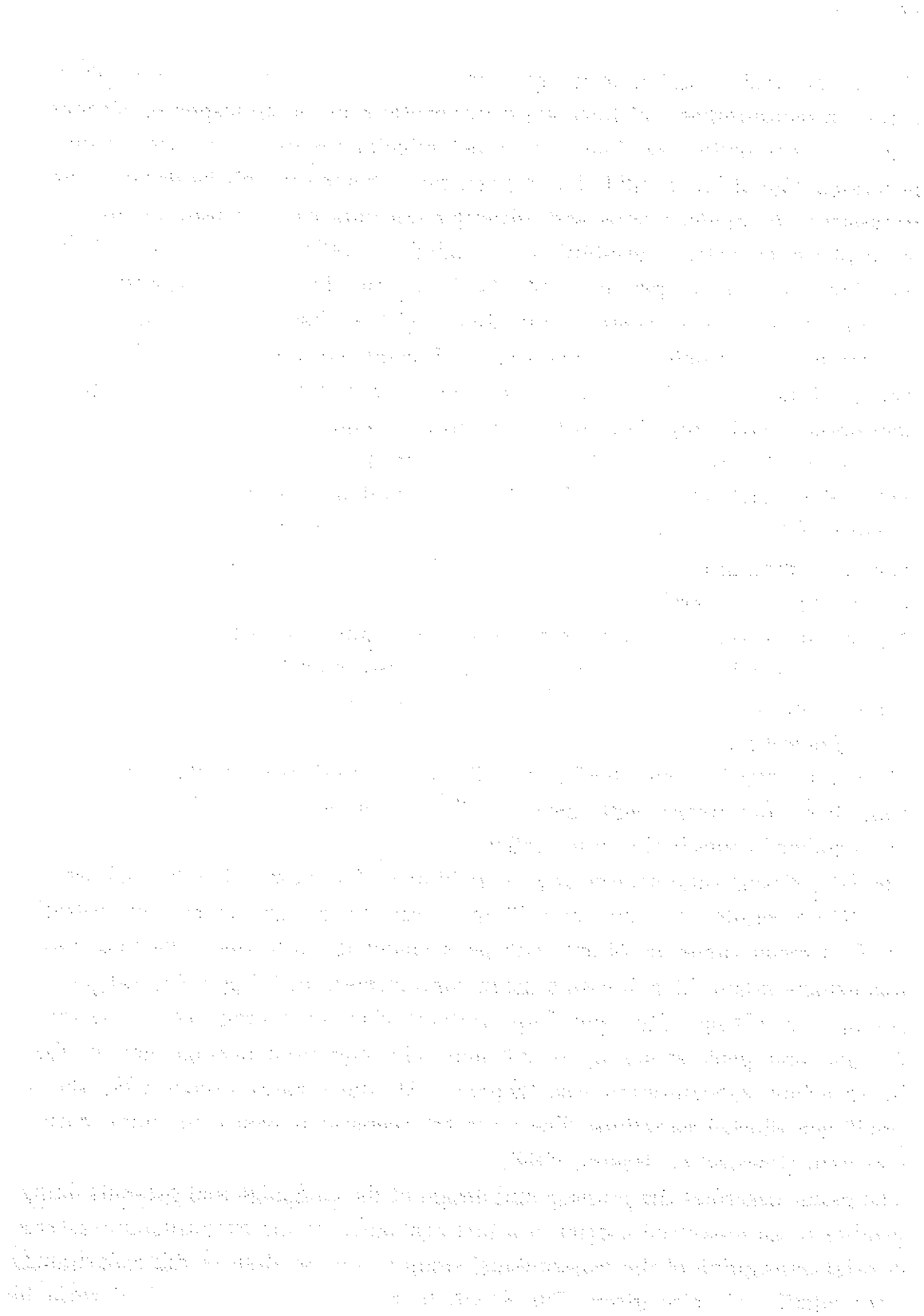

Contents

1. Introduction 1

2. Design of the Campaign 3

3. Measurement Sites 6

4. Experimental Techniques 7

4.1 Trace Gas Concentrations 9
4.1.1 Measurement of NO, NO_2, NO_y, and O_3 9
4.1.2 Measurement of OH by Long Path Absorption 11
4.1.3 O_3, NO_2, HCHO, and SO_2 Measurements by Long Path Differential Absorption Spectroscopy 14
4.1.4 Measurement of Nonmethane Hydrocarbons 17
4.1.5 Measurement of Carbon Monoxide 18
4.1.6 Measurement of Peroxyacetylnitrate 19

4.2 Photolysis Frequencies of Ozone and Nitrogen Dioxide 20

4.3 Meteorological Parameters 21

5. Results 22

6. Access to the Data 25

Literature 27

Appendix A Diurnal Cycles of all Measured Quantities ..... A

NO (chemiluminescence) A-1

NO_2 (chemiluminescence) A-4

NO_y (chemiluminescence) A-7

O_3 (DASIBI) A-10

O_3 (DOAS) A-13

NO_2 (DOAS, 450 nm) A-15

NO_2 (DOAS, 333 nm) A-17

SO_2 (DOAS) A-19

HCHO (DOAS) A-21
Acetaldehyde A-22
OH A-24
CO (grab sample) A-25
Methane A-27
PAN A-29
CO (in situ) A-32
Ethane A-35
Propane A-37
i-Butane A-39
n-Butane A-41
i-Pentane A-43
n-Pentane A-45
Ethene A-47
Propene A-49
1-Butene A-51
Acetylene A-53
Benzene A-55
Toluene A-57
o-Xylene A-59
p+m-Xylene A-61
Radon Activity A-63
$j(O_3)$ A-66
$j(NO_2)$ A-69
Relative Humidity A-72
Temperature (10 m) A-75

Temperature (2 m) A-78

Stability class A-81

Wind Speed A-84

Wind direction A-87

Total Radiation A-90

Scattering Coefficient A-93

Appendix B Weather Maps ..... B

1. Introduction

One way of investigating the completeness of a chemical reaction scheme and its applicability to environmental problems is to compare the model results with data from smog chamber experiments which are designed to simulate atmospheric processes. Often, however, the experimental setup enforces conditions which are not fulfilled in the atmosphere. For example the smog chamber can only be run with concentrations of the reactants that are larger than the atmospheric abundance by orders of magnitude. Moreover, reactions on the wall of the chamber can play a dominant role and change the apparent chemical behavior completely. Also there may exist processes in the natural atmosphere, for example reactions of trace gases on aerosol surfaces or uptake by vegetation that are not covered by the model. Therefore the ultimate validation needs experimental data from atmospheric field studies in comparison with corresponding model calculations. Such a data set should cover different meteorological situations and pollution scenarios to explore the chemistry over a wide range of trace gas concentrations and transport conditions.

Naturally such a study cannot deal with all aspects of atmospheric chemistry, here we concentrate on the following topics:

(1) Measurement of OH
It is well known that the OH radical plays a very important role, since it is the dominant oxidizing agent in the troposphere. It is produced everywhere in the sunlit atmosphere and reaches concentrations of the order of some 10^6 OH molecules cm^{-3}. It is produced solely by gas phase chemical reactions and has no external sources. Its impact on the chemical transformation of biogenically and anthropogenically emitted pollutants can hardly be overestimated. It initiates reaction chains for almost all oxidizable species leading to their final removal from the atmosphere. Thorough knowledge of the parameters controlling the ambient OH concentration are essential for any progress in our understanding of atmospheric chemistry. A benchmark in the validation of the OH chemistry is the comparison of model calculations with experimental data from field studies. The determination of OH concentrations is therefore one of the objectives of this campaign.

(2) Chemical characterisation of air mass
The ambient concentration of the short lived OH is mainly determined by its chemical precursors and chemical sinks. A careful investigation of the air mass containing OH is therefore another purpose of this campaign. Measurements of ozone, nitrogen oxides, water content, and hydrocarbons should accompany the OH field data to establish a as comprehensive as

possible chemical characterization of an air mass. These data provide for example the necessary input for the model calculation of OH. They have also a value in themselves as a measured continuous record of the trace gas scenario in surface near air.

(3) Applicability of model
Finally the campaign addresses problems with respect to the comparison of model data and measurements. Models usually make approximations, for example the assumption of horizontal homogeneity or the neglect of vertical transport that may be justified or not for the situation under consideration. Measurements, on the other hand, take place at not exactly the same place and the same time. For example the OH-measurements are done by long path absorption probing a volume of air of 6 km length, a diameter of about 30 cm, and about 50 m above ground, while the majority of hydrocarbons are probed in-situ about 10 m above the surface. Their comparability is limited by small scale transport processes and the influence of point sources. The analysis of the data could improve the models and the design of the campaign to meet even better the goal of validating certain aspects of atmospheric chemistry.

The Institut für Atmosphärische Chemie of the Forschungszentrum Jülich has performed an intense field experiment in Jülich (lat.: 6.3°, long.: 50.9°, alt.: 100 m) in Germany lasting from May 6 to June 10, 1988 in order to contribute to such a data set. The campaign investigated air masses near the surface during a period of summerly weather with nearly no precipitation. Jülich is a moderately polluted area (see section 3) being typical for large parts of Germany.
The location in Jülich was mainly chosen for logistic reasons. As pointed out in section 2 and 3 the site is not an optimal choice for the desired purpose of comparison with model data.

This report describes the purpose of the campaign and gives a first overview over the experimental results. The discussion of the strategy of the campaign in section 2 is followed by a short description of the measurement site and the topography of the area in section 3. The experimental methods, the uncertainties of the measured quantities, and the performance of the instruments are reported in section 4. First results are presented in section 5. All experimental results are collected in a common (computer adapted) data format for further interpretation. The access is indicated in section 6.

2. Design of the Campaign

The ambient concentrations of trace gases in the atmosphere are determined by three factors, namely strength and distribution of the sources, transport processes, and chemical reactions. For the local concentrations near the ground the relevant phenomena besides chemistry are vertical displacement within the planetary boundary layer (PBL), deposition and emission at the earth's surface, exchange with the free troposphere (above the PBL) and (horizontal) advection. In contrast to the deterministic chemistry the motion of air has an inherently nondeterministic component due to the strong nonlinearity of the equations of motion. It is present on all length and time scales and introduces spatial and temporal fluctuations of all measured quantities. For the design of a field experiment one has to be aware of this source of variability of the trace gas abundances. It is superimposed on other variabilities for example from sources. The relative influence of transport and chemistry depends on the lifetime of the species in the atmosphere. An increasing lifetime also implies in general an increasing influence of atmospheric transport on the temporal variation of the concentration of the compound.

Since the campaign is mainly devoted to an investigation of the chemical processes, it is desirable to measure at least one species whose concentration is dominantly determined by chemistry and only very little affected by transport. It must be one of the short-lived and therefore very reactive substances in the air. This requirement leads again to OH as a key observational parameter. The hydroxyl radical is short-lived with a chemical lifetime of less than 1 sec. Since OH is coupled to the chemistry of the peroxyradicals, which have lifetimes of minutes, the time to reach quasi-steady state concentrations of OH is about 1 minute. Transport processes influence OH only indirectly via the changing abundances of the longer-lived reaction partners. Since the OH measurements were well above the ground (see Figure 3), dry deposition of OH is negligible.

The NO and NO_2 which are also radicals are another short-lived species with a chemical lifetime on the order of minutes. It is, however, emitted by numerous surface sources. It's local concentration is, therefore, inevitably disturbed by transport processes and the temporal variability and spatial distribution of its sources.

The chemical lifetime of the short-lived substances like OH, NO_2, and NO introduces a natural time scale which carries over into the strategy of the campaign. Species with a larger atmospheric lifetime are dominantly influenced by local transport. They provide the chemical environment in which the short-lived compounds approach quasistationary concentrations within their chemical lifetimes. Measurements of both types of species are necessary to achieve a

comprehensive chemical characterization of the air masses passing the experimental site.

The set of the measured species is the largest one ever taken during a field experiment of the institute. It includes 8 inorganic species, 18 organic compounds, meteorological parameters and photolysis rates (see section 4). The quantities to be measured were chosen to meet the following requirements:

(1) The short-lived radicals OH, NO, and NO_2 were measured. In the first step a comparison with models is intended only for OH, since NO_2 and NO are also influenced by transport from local sources. The nitrogen oxides are important parameters controlling the OH concentration: The reaction with NO_2 is the dominant loss of OH under polluted conditions while the reaction of NO with HO_2 influences OH via the cycling of radicals between OH and HO_2. The nitrogen oxides determine the branching between the two NO_x radical destruction paths via reaction of OH with NO_2 and the recombination reaction of peroxyradicals to longlived peroxides. Both compounds are further important for an estimate of the chemical ozone production.

(2) The dominant driving force of the daytime chemistry is the flux of solar UV photons which enters through the photolysis of several species. The photolytic dissociation of O_3 and NO_2 are the most important ones and their photolysis rates were continuously monitored. The major source of OH radicals is the photolysis of O_3 followed by the reaction of O^1D-atoms with H_2O molecules.
The distribution of nitrogen oxides between the two components NO and NO_2 is largely determined by the photolysis rate of NO_2 and the ambient ozone concentration.

(3) The trace gases CO, O_3, and H_2O are known to have an important impact on the OH chemistry. Ozone and H_2O largely control the OH radical production, while the dominant OH degradation is the reaction with CO. They should be supplemented by measurements of several primary and secondary trace gases for resolving the details of the chemical composition of the air.
Primary trace gases are those emitted from various sources. Their concentrations depend mainly on transport processes and the source strengths. Through their chemical degradation they influence the chemistry according to their chemical reactivity. Therefore the measurement program of the campaign included the longer-lived alkanes like methane, ethane, and propane. Also measured were the light alkenes and some aromatics; both groups have a substantially higher reactivity than the alkanes (see Table 1).

Even more important are the secondary trace gases which are to a large extent produced in atmospheric chemical reactions. The aldehydes, peroxides, organic and inorganic acids, and the peroxy radicals are of this kind. With decreasing lifetime their abundances are more and more controlled by chemistry and transport becomes less effective. Since they are not directly affected by sources they are also possible candidates for a comparison with model calculations. The measurement program included HCHO, CH_3CHO, peroxyacetylnitrate PAN, and HNO_3.

(4) Wind speed and wind direction, pressure, temperature, and height of the PBL give an indication about the locally effective transport processes. The temperature is also a controlling factor of the reaction rates. With the exception of the height of the PBL all quantities were monitored continuously.

(5) The location of the experimental sites should allow for consistent probing i.e. all apparatus should probe the same air parcel. Because of the concentration fluctuations in space and time this requirement is difficult to fulfill. Only the thorough analysis of the experimental data will reveal to what extent this could be achieved. In this respect simultaneous measurements of the same species at different locations are particularly valuable. Therefore during this campaign some hydrocarbons were measured at the institute and simultaneously in about 3 km distance at the end of the OH absorption light path.

(6) For the evaluation of the data and comparison with models it is desirable to have homogeneous air masses. The short-lived compounds should have reached steady state concentrations within the considered airmass at the experimental site. Then the calculations can be made with a transport independent model. For example assuming a horizontal wind speed of 2 m/sec and a time scale of 1 min one requires horizontal uniformity over a length of at least 120 m. Obviously, this is only approximately true for some wind directions in the vicinity of the institute building where nearly all measurements were done (see section 3).

(7) The sampling strategy should provide a representative picture of the chemical composition of air. It is desirable to make the measurements of the various parameters simultaneously, with compatible temporal integration intervals and regular repetition rates, to exclude the disturbing effects from different time averages and from transport induced fluctuations. Only in cases where the temporal and spatial variance of a compound is known to be

small this influence is negligible. For technical reasons, however, it was not always possible to fulfil these requirements.

3. Measurement Sites

Hydrocarbons, CO, O_3, NO, NO_2, aldehydes, PAN were measured in-situ. The majority of these measurements were done in the vicinity of the building of the institute (see Figure 1). It is part of the Forschungszentrum Jülich and located in a park with a deciduous forest. A small car park is close to the south side of the building. Gas inlets were installed several meters height to be well above the surface near layer where strong vertical gradients are to be expected. The photolysis rates were measured on the roof of the building (Figure 1).

Gas samples for analysis of hydrocarbon abundances were also taken on the Sophienhöhe. It is an artificial hill with a height of 220 m in approximately 3 km distance and covers an area of 3 km by 4 km. A browncoal strip mining site of 12 km^2 size and a depth of roughly 200 m is located south east of the hill. It is known that the topography gives rise to local perturbations of the windfield near the surface. The area is embedded into a rather flat landscape which extends over 10 km into all directions. The mean height above sea level is about 100 m.

OH, O_3, NO_2, HCHO, and SO_2 were studied by a long path optical absorption technique. The light path run from the roof of the building to a plane mirror placed on the Sophienhöhe and back to the detection apparatus (see Figure 2). The mean height of the beam above ground was 50 m.

The main sources of pollutants are to some extent the immediate surroundings of the institute, the town of Jülich and several power plants within distances between 15 km and 35 km burning brown coal. The site is surrounded by three motor ways with heavy traffic. The distance to the motorways is between 10 km and 20 km.

Local meteorological data were obtained from sensors at the institute and from the meteorological tower of the KFA (see section 4.3). The horizontal distance to the institute is roughly 200 m. The height of the PBL, was provided by the data of the Deutscher Wetterdienst Station in Essen.

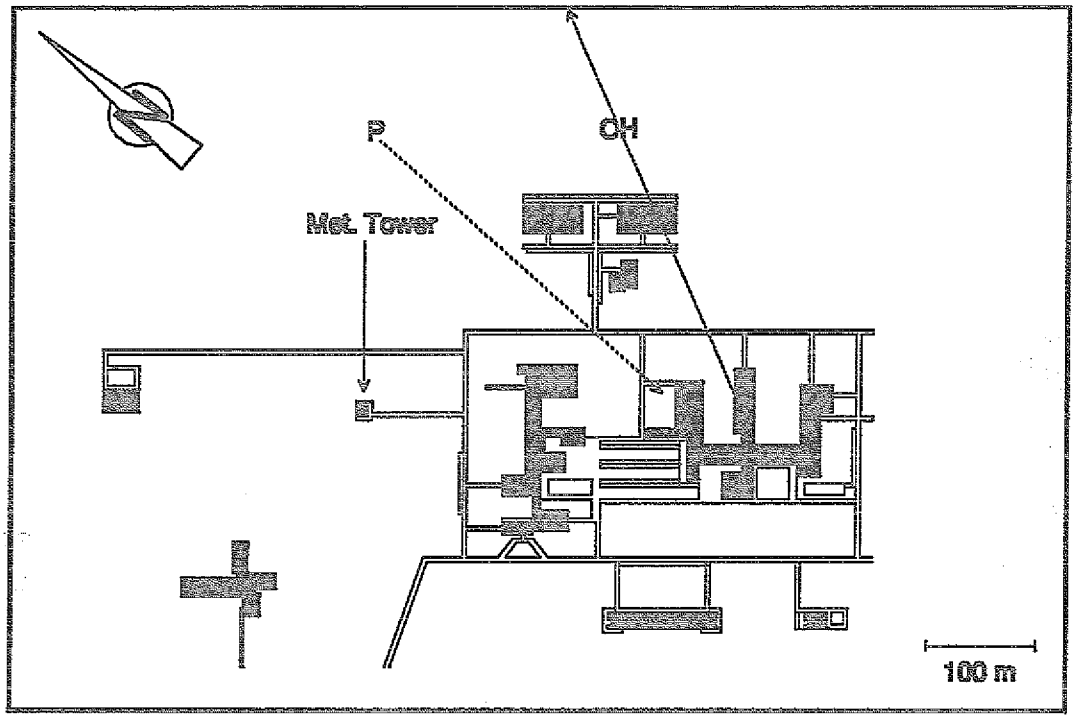

Figure 1: Measurement site. The location of the gas inlets (P) and the OH apparatus (OH) as well as the light path are indicated.

4. Experimental Techniques

This section presents a brief description of the experimental techniques and an uncertainty analysis of the data. It also discusses the program of the measurements, and the performance of the instruments.

An overview over the experimental material is given in Table 1. Frequency and integration time of the measurements and the total number of data obtained are entered for each species.

quantity	section[a)]	total number of measurements	time between subsequent measurements	time of integration
NO	4.1.1	3989	10 min	10 min
NO2	4.1.1	4576	10 min	10 min
NOy	4.1.1	4709	10 min	10 min
Ozone	4.1.1	4950	10 min	10 min
OH	4.1.2	36	-	3-42 min
Ozone	4.1.3	111	-	2-24 min
NO2 (450 nm)	4.1.3	149	-	2-24 min
NO2 (333 nm)	4.1.3	108	-	2-24 min
SO2	4.1.3	331	-	2-24 min
Formaldehyde	4.1.3	48	-	2-24 min
PAN	4.1.6	2169	15 min	1 min
CO (automated samples)	4.1.5	3203	15 min	1 min
CO (flask samples)	4.1.4	79	3 h	1 min
methane (")		79	3 h	1 min
acetaldehyde	4.1.4	141	3 h	1 h
ethane	4.1.4	141	3 h	1 h
propane	4.1.4	141	3 h	1 h
i-butane	4.1.4	141	3 h	1 h
n-butane	4.1.4	141	3 h	1 h
i-pentane	4.1.4	141	3 h	1 h
n-pentane	4.1.4	141	3 h	1 h
ethene	4.1.4	141	3 h	1 h
propene	4.1.4	141	3 h	1 h
1-butene	4.1.4	141	3 h	1 h
acetylene	4.1.4	141	3 h	1 h
benzene	4.1.4	141	3 h	1 h
toluene	4.1.4	141	3 h	1 h
o-xylene	4.1.4	141	3 h	1 h
p+m-xylene	4.1.4	141	3 h	1 h
radon activity		1543	30 min	30 min
relative humidity	4.3.1	4568	10 min	10 min
temperature	4.3.1	4404	10 min	10 min
stability class	4.3.1	760	1 h	1 h
windspeed		4422	10 min	10 min
winddirection		4422	10 min	10 min
air pressure		1468	30 min	30 min
scattering coefficient		4685	10 min	10 min
total radiation		4444	10 min	10 min
J(O3)	4.2	4656	10 min	10 min
J(NO2)	4.2	4564	10 min	10 min

Table 1: Overview of the measured quantities during the campaign in Jülich 1988.

NO_y : $NO + NO_2 + NO_3 + 2\,N_2O_5 + HNO_2 + HNO_3 + HNO_4$ + PAN + nitrate aerosol

PAN : Peroxyacetylnitrate

$J(O_3)$: photolysis frequency $O_3 \rightarrow O(^1D) + O_2$

$J(NO_2)$: photolysis frequency $NO_2 \rightarrow NO + O(^3P)$

a) The experimental method is discussed here.

4.1 Trace Gas Concentrations

4.1.1 Measurement of NO, NO_2, NO_y, and O_3

NO, NO_2 and NO_y were measured by the chemiluminescence technique described by Drummond et al. (1985). Two detectors were used, one for NO and NO_2 (after conversion to NO) and the second detector for all reactive nitrogen compounds, NO_y (after conversion to NO). The data were measured with a time resolution of 30 s and then averaged over time intervalls of 10 minutes. The inlet point was located 12 m west of the institute building, 10 m above ground. Ambient air was pumped at a flow rate of 15 l/min through the 17 m Teflon inlet line (inner diameter 4 mm). NO and NO_2 were corrected for the reaction with ozone during the residence time of 0.9 s inside the inlet line.
The detectors were calibrated once a day using a mixture of synthetic air and NO-calibration gas (2 ppm NO/N2, SPECTRASEAL). The calibration factors showed day to day fluctuations of not more than 3%. Two different NO-calibration gases were used giving calibration factors that differ by less than 1%. The accuracy of the calibration mixtures is specified with 2% by the manufacturer. The calibration mixtures were not checked against an absolute calibration method in our own laboratory. The systematic error of NO and NO_2 due to calibration uncertainties is estimated to be less than 10%. For the data analysis, the calibration factors were linearly interpolated between calibration times.

NO was measured by the NO/NO_2-detector with the light source for photodissociation of NO_2 blocked. The measured NO-mixing ratios were corrected for the reaction of NO with ozone in the converter volume taking a residence time of 15 s. The possible error arising from this correction is estimated to be 5% at 50 ppb ozone and 10% at 100 ppb ozone. The noise of the NO-signal was 3 ppt at zero level, 10 ppt at 5 ppb NO. Combining the systematic error of 10% and the random errors of 3% (fluctuations of the calibration factors) and 5%-10% (correction for the reaction with ozone), the accuracy of the given NO-mixing ratios is estimated to be 3 ppt plus 16% of the NO-signal at 50 ppb ozone and 20% at 100 ppb ozone.

NO_2 was measured by the same detector using the light of a 300 W Xe-lamp for photodissociation (Rohrer and Brüning, 1992). The conversion efficiency was determined each day using a NO_2-calibration mixture in synthetic air by measuring the ratio of the NO_2-detector signal and the NO_y-detector signal . The efficiency was typically 0.5 and showed day to day fluctuations of 5%. A possible error arises here from the NO_y-converter. Its efficiency was not measured separately. Earlier experience showed here a maximum error of 10% for the conversion efficiency of NO_2 by the NO_y-converter. The efficiency for photodissociation of NO_2, which was

determined at calibration time, was corrected for the reaction of NO with ozone in ambient air inside the photolytic converter. A simple chemical reaction scheme including the reactions of NO, NO_2, and O_3 was solved numerically. The calculations were tested experimentally for ozone concentrations up to 600 ppb. The comparison between measured and calculated efficiency was better than 5%. The noise of the NO_2-detector was around 15 ppt NO_2 at zero level and 50 ppt at 5 ppb NO_2. The overall accuracy of the given NO_2-mixing ratios is estimated to be 15 ppt plus 22% of the NO_2-signal, calculated from the systematic error of 10% and the random errors of 3% (fluctuations of the calibration factors), 5% (fluctuation of the NO_2-conversion efficiency), 10% (efficiency of the NO_y-converter), and 5% (correction for the reaction with ozone) . Because some of the possible error sources affect both NO and NO_2 by the same amount, the accuracy of the NO/NO_2-ratio depends mainly on the day to day fluctuations of the calibration factors and the efficiency of the NO_y-converter. It is estimated to be 11% for NO- and NO_2-signals higher than 100 ppt.

NO_y was measured by NO chemiluminescence after conversion of NO_y to NO (Fahey et al., 1985). Since HNO_3 is absorbed at the surface of the long inlet line, the detector did not measure any contribution from HNO_3. Potentially this is a source for large errors of the NO_y measurement, possibly up to a factor of two. Using synthetic air the detector showed a signal corresponding to 500 - 1000 ppt NO_y. This background signal was determined at calibration time and used for correction of the ambient air data. The day to day fluctuations of this background signal were less than 200 ppt NO_y. The conversion efficiency of the NO_y-converter was not tested experimentally. Other experiments showed here a maximum error of 10% for the conversion efficiency of NO_2. The noise of the NO_y-detector was around 5 ppt NO_y at zero level and 15 ppt at 5 ppb NO_y. For the NO_y-signal arising from NO, NO_2 and PAN, the accuracy of the given NO_y-mixing ratios is estimated to be 200 ppt plus 20% of the NO_y-signal, calculated from the systematic error of 10% and the random errors of 3% (fluctuations of the calibration factors) and 10% (efficiency of the NO_y-converter) .

Ozone was measured by a UV-photometer (DASIBI type 1003 AH). It shared the inlet line with the NO-detectors. The accuracy and precision of the instrument stated by the manufacturer is 3% and 1 ppb ozone. For a comparison with a reference instrument (DASIBI type 1008 PC), the actual precision of the instrument is estimated to be 2 ppb.

4.1.2 Measurement of OH by Long Path Absorption

The concentration of tropospheric hydroxyl radicals, OH, was measured by differential optical absorption spectroscopy (DOAS). This technique needs no external calibration. Its accuracy only depends on the error of the OH absorption coefficient. As shown in Figure 1 the absorption path extended from the roof of the institute building to the top of the Sophienhöhe where a plane mirror was mounted (Fig. 2). The total light path length was 5.8 km. The distance to the ground is indicated in Figure 3. Because the instrumental setup is already described in the literature (Perner et al. 1987, Callies 1988, Callies et al. 1988, Dorn et al. 1988, Platt et al. 1988) only a short description will be given here. The instrument consists of four main parts: light source, absorption path, spectrometer, and spectral detector.

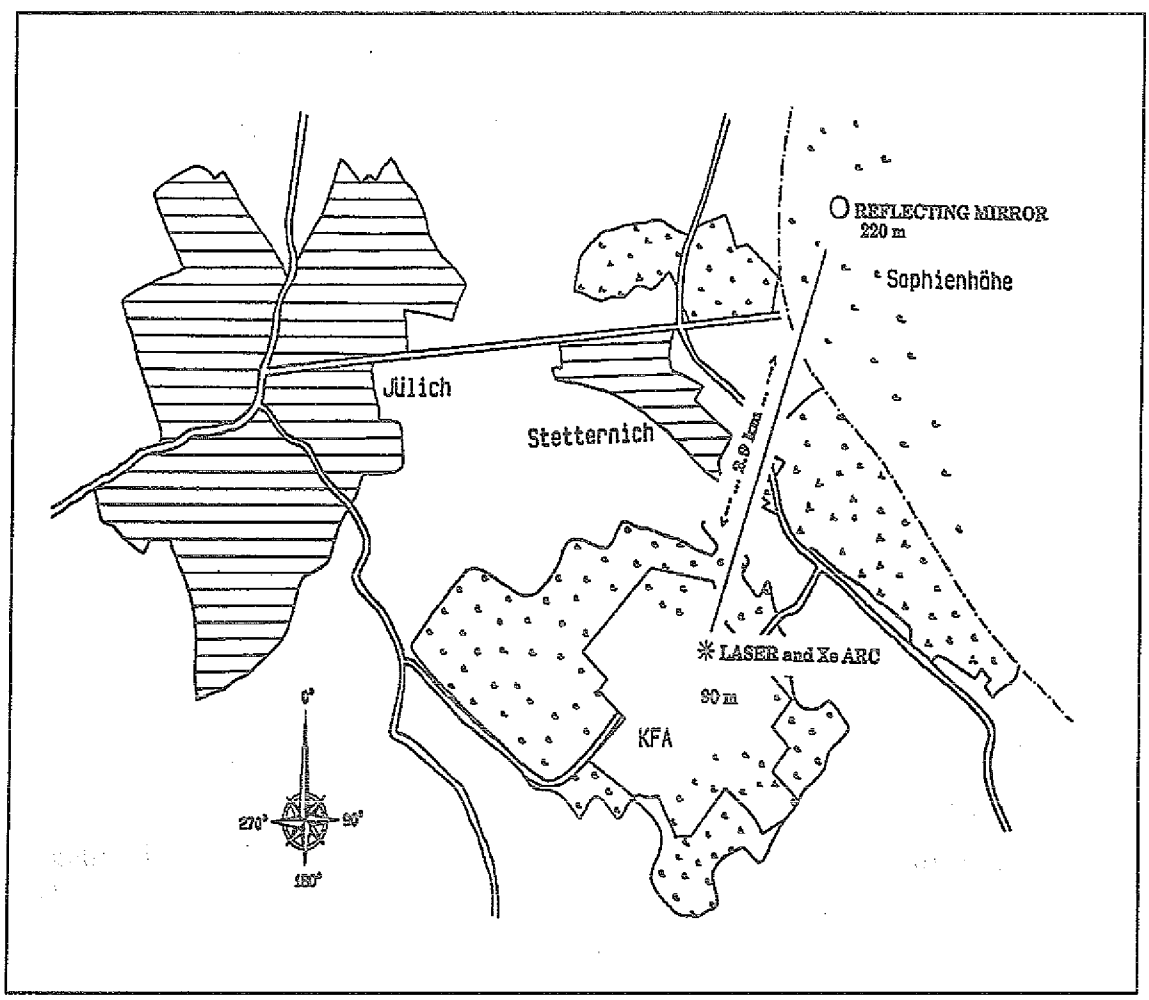

Figure 2: Location of the light path for the OH- and the DOAS-experiment (section 4.1.3). The light sources and the spectrometers were located on the roof of the building of the Institute of Atmospheric Chemistry (altitude 100 m). The reflector was mounted near the top of the Sophienhöhe (altitude 220 m). The total lengths of the light path was 5.8 km.

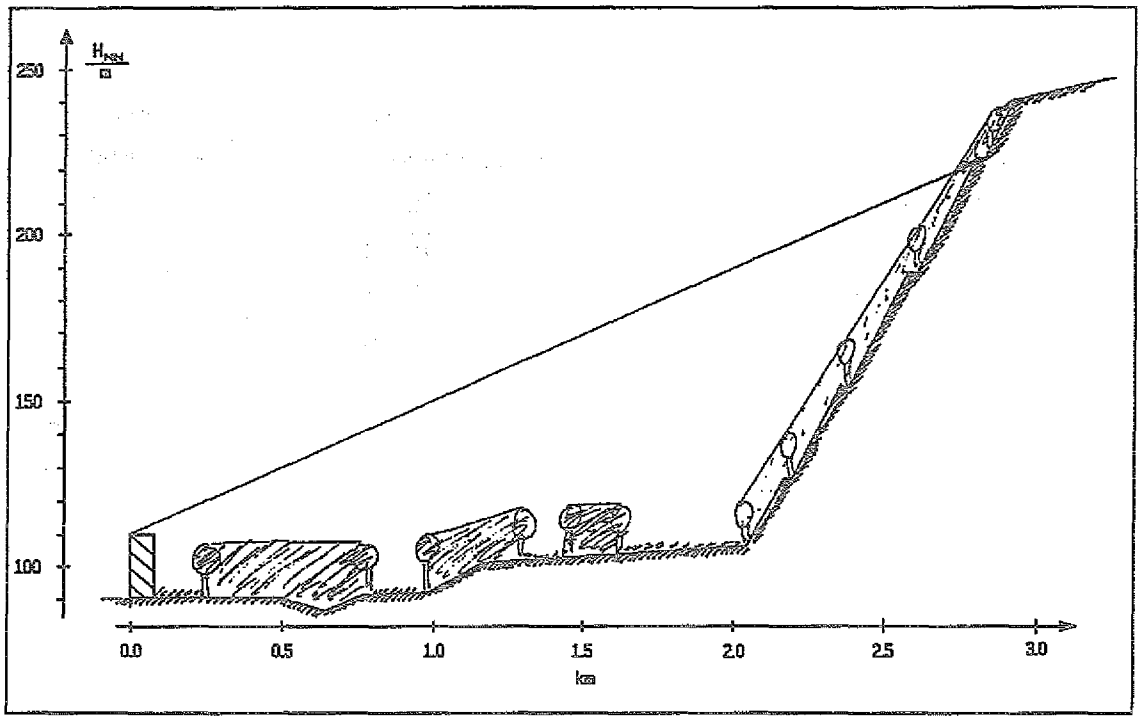

Figure 3: Height profile of the OH- and DOAS-absorption path.

Light source

Because the rotational lines of OH have a very narrow bandwidth (2.3 pm under atmospheric conditions) the high spectral irradiance essential for absorption spectroscopy can only be provided by a UV laser. The system used in our measurements was a frequency doubled picosecond dye laser which was synchronously pumped by a mode-locked argon ion laser. The dye laser generates nearly transform limited picosecond pulses with a spectrum of large bandwidth (about 0.15 nm after frequency doubling to 308 nm) and very little spectral substructures. Both features are of decisive importance for tropospheric trace species measurements especially under polluted conditions. Typical UV output power was 15 mW.

Absorption path

Before entering the free troposphere, the laser beam was expanded by about a factor of 50 using a Cassegrain telescope in order to reduce the beam divergence and the level of self generated OH radicals by laser induced photolysis of ambient ozone and subsequent formation of OH.

Spectrometer

After passing the absorption path light was collected by a Newton telescope (f = 2400 mm, d = 300 mm) and was focused onto the entrance slit of a high resolution double grating spectrometer ($\lambda/\Delta\lambda$ = 171000).

Detection system

Spectra were recorded using a linear photodiode array as a multichannel spectrometric detector.
The spectrum was imaged from the exit plane of the spectrograph onto the diode array using a 3 element UV achromat with a magnification factor of about 11. This resulted in oversampling since the smallest resolvable spectral element was covered by 5-6 diodes of the array.

Measurement procedure

In order to use diode array spectrometers for very sensitive absorption measurements two properties of those detectors must be taken into account. The first is the nonuniform response of the individual light sensitive elements which varies between one and two percent between the diodes. The second is the temperature dependent dark current and its associated dark current noise which can be the limiting factor at long integration times. The latter can be suppressed by cooling the detector to sufficiently low temperatures (210 K). The influence of the former must be eliminated by dividing the recorded air spectrum that carries the absorption structures by a reference spectrum i.e. the laser spectrum without absorption features (for more details, see Dorn et al. 1988). In order to improve the signal to noise ratio, usually between 100 and 1000 scans were averaged. Thus one measurement point resembles the mean OH value over integration times between about 5 and 60 minutes. (For a more complete discussion of S/N problems see Dorn et al., 1988).

Sources of error

Because of the relatively high level of air pollution found during the campaign, low OH concentrations, in many cases below the detection limit of the instrument, are to be expected. The detection limit ranged between $1.5\text{-}2.5 \cdot 10^6$ OH radicals/cm^3 and was limited by the baseline noise due to several factors:

- Error in determination of the absorption pathlength: less than 1%.
- Presence of absorption features of unidentified species.
- Residuals of known overlapping absorptions by other molecules (like SO_2 and HCHO (see Callies, 1988, Dorn et al. 1988, and Callies et al. 1989, Neuroth, 1992)) that remain after subtraction of their spectra.

- Periodic baseline modulations due to beam interferences at plane parallel surfaces (etalon effects). These were minimized using wedged and high quality anti-reflection coated surfaces.

- Artificial structures generated by the detector. These seem to originate from variations of the illumination direction of gratings and detector during the recording of measurement- and reference-spectra due to atmospheric turbulences ('illumination noise'). These are sometimes hard to control and can limit the detection sensitivity. The effect is still subject of intensive studies.

- Electronic sources of noise, which are presently negligible, because they vanish when large number of spectra are averaged.

Although the total integrated line absorption cross-section of OH is known within 3% the effective cross-section at the line center (which is used for data evaluation) is more uncertain due to the following reasons:

- Because the instrumental spectral resolution is not sufficient to fully resolve the absorption lines the effective cross-section depends on the instrumental response function which can be measured within 10-15 percent precision.

- Literature data of the pressure broadening of OH in air differ within 50%. We have used the data by Leonard (1990) which lead to an overall accuracy of the effective cross section of 12%.

- The precision of OH absorption measurement is determined by the ratio of the OH absorption strength to the strength of residual structures in the spectra. Observed values attained 85%.

4.1.3 O_3, NO_2, HCHO, and SO_2 Measurements by Long Path Differential Absorption Spectroscopy

Long Path Differential Optical Absorption Spectroscopy (DOAS) was used for the simultaneous measurements of ozone (O_3), nitrogen dioxide (NO_2), formaldehyde (CH_2O), and sulfur dioxide (SO_2) using nearly the same light path as the OH measurements. The following will briefly describe the experimental technique and the evaluation of the data.

Experimental

DOAS with low spectral resolution (0.3 nm) uses the characteristic vibrational structure of electronic transitions in the visible and ultraviolet spectral region for the detection of trace gases. The method has been previously described in detail by Platt et al. (1979), Platt and Perner (1984).

The collimated beam of a 500 W high pressure Xe arc lamp on the roof of KFA building (see Figure 2) was directed to a remote controlled flat mirror (30 cm diameter) on the top of the Sophienhöhe. This mirror was also used by the OH long path absorption experiment (see section 4.1.2). The reflected light was collected by a Newton type telescope (f = 1.8 m, 30 cm diameter) and focused into a spectrometer (SPEX 1870, f = 0.5 m, 600 l/mm) both located on the same roof. The total absorption path length was 5.8 km. A 30 nm spectral range was repetitively scanned (100 Hz) by a rotating slotted disk mounted in the focal plane of the spectrometer. The light passing the slit was detected using a photomultiplier tube (EMI 9659QB, 2" diameter) and its output signal was digitized with a 12-Bit-ADC at a sampling frequency of 40 kHz. 50000-100000 scans were added and after offset correction this averaged signal was stored on a LSI11 computer as one spectrum.

Data evaluation, calibration, and errors

The concentrations c of the trace gases were determined from the spectra by applying Lambert-Beer's-law

$$c = \frac{\ln (I'_0 / I)}{\ell \cdot \sigma'}$$

where I'_0 and I are the light intensity beside and in the center of a selected absorption band, respectively, while ℓ denotes the optical path length and σ' the differential absorption cross section of the species being measured. The differential absorption cross sections were taken from the literature and are listed in Table 2.

The optical density ($\ln(I'_0/I)$) was calculated by fitting reference spectra of the respective trace gases to the air spectra. This could easily be done in the case of the spectra recorded in the blue spectral region (420 nm - 455 nm), where NO_2 absorption dominates the spectrum. Similar considerations apply for SO_2 in the UV range (290 nm - 310 nm). The evaluation of O_3 and CH_2O (320 - 340 nm) required a more sophisticated procedure: first the superimposed NO_2 and O_3 spectra are fitted simultaneously. The respective fit coefficients yield concentrations for these species. Then the air spectrum was divided by the above

fitted reference spectra, to remove the NO_2 and O_3 absorption features. A reference spectrum for CH_2O was fitted to the residual spectrum in the spectral band listed in Table 2. Since O_3 and NO_2 absorption signals dominate the air spectrum in many cases, often only an upper limit of CH_2O concentrations could be obtained.

The errors of the optical densities were calculated from the least square fit using an algorithm given by Bevington (1969). The 1-σ estimated error of the fitting procedure represents the precision of the measurement and these errors are entered in the data files. The values depend on the noise in the spectra as they change with the intensity. The systematic errors caused by the uncertainties of the absorption cross section and the light path are not included. While the error of the lightpath length is less than 1% the contribution of the absorption cross section to the accuracy of the measurements depends on the species as can be seen from Table 2.

Measurements

We recorded about 350 air spectra during the campaign: one third in each of the 3 wavelength intervals (Table 2). Since the spectra were normally accumulated for a period of 20 min, the turn-over rate was about 1 h for each species with the exception of NO_2 which was detected at two wavelength.

The spectra were recorded mainly during periods, when the long-path-absorption OH experiment was operated (May 14 - 18, May 20 - 21, May 24 - 26, May 30 - 31, June 2, June 4 - 7). Moreover the data are restricted to daytime hours (8:00 - 21:00).

Species	Wavel. λ nm	σ' cm^{-2}	wave length (nm) region used for fit	reference
NO_2	450	$2.7 \cdot 10^{-19}$ ± 5%	445-455	Schneider et al. 1987
NO_2	333	$4.86 \cdot 10^{-20}$ ± 5%	320-335	Schneider et al. 1987
O_3	322	$6.5 \cdot 10^{-21}$ ± 5%	320-335	Molina and Molina 1986
CH_2O	326	$7.8 \cdot 10^{-20}$ ±20%	323-333	Platt et al. 1979
SO_2	300	$5.7 \cdot 10^{-19}$ ±10%	290-310	Platt et al. 1979

Table 2: Absorption Bands and differential cross sections (σ') used for the evaluation of the DOAS spectra.

4.1.4 Measurement of Nonmethane Hydrocarbons

Most of the nonmethane hydrocarbon (NMHC) measurements were made by in-situ gas chromatography. The instrument was located in a container near the institute building. The air intake was located on top of a 10 m mast 5 m from the container. The distance to the nearest building was 12 m. The experimental technique is described in detail by Rudolph et al. (1986).

The time required for one measurement including preconcentration from about 1 dm^3 of air was 3 h. The instrument was operated for 24 h a day from May 5, 1988, 9:00 UT until June 10, 1988, 0:00 UT. Between May 12, 1988, 18:00 UT and May 13, 1988, 12:00 UT no measurements were made due to an instrument failure. The samples were analyzed for the C_2 - C_5-alkanes, C_2- and C_3-alkenes, acetylene, acetaldehyde, benzene, toluene and the xylenes.

The atmospheric mixing ratios were calculated by comparing the sample with a reference air of known composition. The mixing ratio of the different hydrocarbons in the reference air were in the range of a fraction of a ppb to a few ppt, comparable with the levels in ambient air. Reproducibility and calibration errors are given in Table 3. The raw data were acquired with a personal computer using a commercial chromatography software and stored on tape. During the campaign 141 air samples were measured.

	error of calibration [%]	reproducibility [%]
alkanes		
ethane	10	5
propane	10	10
i-butane	30	9
n-butane	30	7
i-pentane	25	<10
n-pentane	25	<10
alkenes		
ethene	10	6
propene	25	19
1-butene	30	19
acetylene	10	13
aromates		
benzine	20	<20
toluene	30	<20

Table 3: Calibration error and reproducibility for the measurements of non-methane hydrocarbons.

In addition, 102 whole air grab samples were collected in 2 dm^3 stainless steel containers (see also section 4.1.5). These samples were analyzed for CO and CH_4 later on in the laboratory. Only the 20 samples collected at the Sophienhöhe were analyzed for NMHC. These measurements were made with a similar gas chromatographic system as mentioned above.

The measurement and calibration of CO is described in chapter 4.1.5. CH_4 was measured with the same gas chromatograph and the same calibration technique as CO. The reproducibility of the methane measurements was 0.5%, the total error of the measurement 1%.

4.1.5 Measurement of Carbon Monoxide

Two different methods were used to measure the CO mixing ratio. First, 102 whole air grab samples were collected in 2 l stainless steel containers. 82 of these samples were collected above a lawn near to the institute (on the average 8 samples per day), 20 samples on top of the Sophienhöhe. The samples were analyzed for CO using a gas chromatograph (Packard) with a molecular sieve column (5 Å). For the detection with a flame ionization detector CO is reduced catalytically into CH_4. The quantization is done by comparing the sample with reference air with a CO mixing ratio representative for the remote troposphere. The reproducibility of the CO measurements is 1.5%, the total error of the measurement 2%.

Second, a Reduction Gas Analyzer (RGA 3, Trace Analytical Inc., USA) was operated in an automatic mode throughout the full campaign period. The instrument employes the mercury oxide technique developed by Seiler and Junge (1970), which is based on the reaction of CO with mercury oxide (HgO) at elevated temperatures (about 100°C),

$$HgO + CO \longrightarrow CO_2 + Hg$$

The mercury vapor released through this reaction is monitored in an optical cell by atomic absorption at 253 nm. Because atmospheric hydrogen also reacts with HgO (Schmidt and Seiler, 1970), both trace gases are separated on a short chromatographic column (molecular sieve, 5 Å) before the sample volume passes through the reaction cell. An automated sampling system was used to inject alternatively ambient air or a calibration standard. One measurement was made every 14 minutes. The analytical precision as derived from the series of standard analyses was better than 1%.

The sensitivity of the chemical detector of the RGA 3 changes if contaminants such as hydrocarbons or water vapor enter the reaction cell. Therefore, the sampled air was dried and purified prior to injection. During this campaign the sampled air was taken from a bulk air flow supplied to the GC-laboratory from the same air intake line as used for the measurements of nonmethane hydrocarbons (cf. section 4.1.4). It was purified by means of a calcium chloride packed absorber and a molecular sieve trap (10 Å).

For reasons that have not been identified yet the sensitivity of the instrument increased on 29 May by about a factor of two. On the next day the sensitivity dropped again, however after stabilization of the chemical detector, it was still larger than before. The data set obtained with the RGA 3 detector during the campaign was therefore split into two sets: (1) from 9 May (day no 130) until 29 May (day no 150); (2) from 30 May (day no 151) until 10 June (day no 162). For absolute calibration the CO mixing ratio derived from the RGA 3 analyses during both periods was adjusted to the analyses of the two series of flask samples. The original RGA 3 data were corrected on the basis of the following empirical functions that were derived from the correlation of the RGA3 data against the flask sample data.

Period (1): $CO_{(RGA3,\ corr)} = 0.49 \times CO_{(RGA3,\ orig)} + 47\ ppb$

Period (2): $CO_{(RGA3,\ corr)} = 0.63 \times CO_{(RGA3,\ orig)} + 63\ ppb$

The CO mixing ratio is given in ppb.

4.1.6 Measurement of Peroxyacetylnitrate

The peroxyacetylnitrate (PAN) measurements were made by in situ gaschromatography. The instrument was situated inside the laboratory. The air intake was located on top of a 10 m mast at a distance of 12 m from the institute's building. The PTFE inlet line had a total length of 25 m. It was continuously flushed by a pump and the resulting delay time was about 0.8 seconds. The experimental technique is described in general by B. Vierkorn-Rudolph et al. (1985). The system used during the 1988-campaign was modified as described by K. P. Müller et al. (1989).

The instrument was operated for 24 h a day from May 9, 1988, 11:00 UT until June 10, 1988, 15:00 UT. The time between measurements varied between 10 min and half an hour. The shorter times were used during intensive measuring periods. Between May 18, 13:45 UT and May 20. 12:30 UT the instrument was calibrated.

Therefore no measurements of PAN concentrations were made. Due to an instrument failure on June 3 between 9:30 and 15:00 UT also no samples were taken. During the campaign 2170 air samples could be analyzed.

The atmospheric mixing ratios of PAN were calculated by comparing the air sample with a reference of a known PAN concentration. This reference gas was generated in a dynamic calibration source. After discontinuous hydrolysis it was quantified as nitrite ion by a colorimetric method. Reproducibility, calibration error and detection limits of the instrument were given by Müller et al. (1989). The raw data were acquired with a personal computer using a commercial chromatography software and stored on tape.

4.2 Photolysis Frequencies of Ozone and Nitrogen Dioxide

In this section the experimental technique for the determination of the photolysis frequencies $J(O_3)$ of ozone for

$$O_3 + h\nu \rightarrow O(^1D) + O_2$$

and $J(NO_2)$ of nitrogen dioxide for

$$NO_2 + h\nu \rightarrow NO + O(^3P)$$

is described.

Both photolysis frequencies were continuously measured using two calibrated filter radiometers which were sensitive to the actinic solar flux at 290 - 320 nm and 290 - 380 nm, respectively. The detectors were designed and built in our laboratory. Only a brief technical description follows because details were reported previously (Junkermann et al. 1989).

The detectors were equipped with an optical input system gathering light from 2π sr solid angle. The deviation from uniform sensitivity over the hemisphere was ±5%. The overall spectral sensitivity of the detectors was chosen to match closely to the spectral shape of the photodissociation spectra of O_3 and NO_2, respectively. This was achieved by the appropriate combination of optical filters and photoelectric sensors (for details see Junkermann et al. 1989). Therefore the detector's signals were proportional to the photolysis frequencies. The calibration factor for the $J(O_3)$ detector was determined by comparison with a chemical actinometer in 1989 (Junkermann et al. 1989, Hofzumahaus et al. 1992). The accuracy of the conversion factor was calculated to be ±26% (1σ) (Hofzumahaus et

al. 1992). In addition a dimensionless function F was applied correcting systematic deviations from the linear relationship between detector signal and $J(O_3)$. The deviations are caused by imperfect spectral match between the detector sensitivity and $J(O_3)$ and vary with overhead ozone column and solar zenith angle. Moreover the correction function F includes the temperature dependence of the ozone photodissociation spectrum. For the present work ozone column densities measured with a Dobson photometer at Hohenpeissenberg (Deutscher Wetterdienst, 1989) have been used for the calculation of F. It ranges between 0.9 to 1.5 for zenith angles of up to 70°.

The calibration constant of the $J(NO_2)$-photolysis detector was determined indirectly using the empirical correlation of $J(NO_2)$ and global broadband radiation (0.3 - 3 μm) reported by Bahe et al. (1980). We used long-term simultaneous runs of the $J(NO_2)$ detector and a calibrated pyranometer (CM6) in Jülich during 1987 and 1990. Several sources of error contribute to the total uncertainty of about ±10% (Brauers and Hofzumahaus 1992).

The reliability of the $J(O_3)$ and $J(NO_2)$ detectors used for this work could be demonstrated by analyzing the data that were collected a few month later during a ship cruise from Europe to South America in September/October 1988. A comparison with the literature yielded reasonable agreement within the error limits quoted above (Brauers and Hofzumahaus 1992, Hofzumahaus et al. 1992).

The detectors were mounted on the roof of the institute's building at an altitude of 25 m above ground. Due to height neither direct nor indirect light from the upper hemisphere was significantly obstructed. The time constant of the detectors is about 2 s. The output voltage was digitized using a 12 bit ADC at a sampling frequency of 1 Hz. The data were accumulated and stored as 10 min-averages with standard deviations.

4.3 Meteorological Parameters

Meteorological measurements are continuously carried out by the " Abteilung Sicherheit und Strahlenschutz der KFA Jülich" (Polster et al., 1986 and 1989). The following time series were kindly provided for the duration of the campaign:

- 10 min -averages of relative humidity at 2 m elevation above ground at the KFA meteorological tower.
- 10 min -averages of the temperature at 2 m elevation above ground at the KFA meteorological tower.

- 10 min -averages of the temperature at 10 m elevation above ground at the KFA meteorological tower.
- 1 h -data of the Pasquill-Gifford stability class (Pasquill, 1974).

The reported errors (G. Polster, personal communication) are:

temperature:	± 0.1 K
relative humidity:	± 5% r.h.

For further details concerning the methods and location of the measurements, the cited literature should be referenced.

5. Results

The diurnal cycles of all experimental data are shown in Appendix A. They give a continuous record of the chemical state of the air masses investigated during May 9 - June 10 in Jülich, and exhibit the usual diurnal pattern.

1) The diurnal cycle of ozone reflects the photochemical activity during daytime giving rise to the usual maximum ozone concentration in the early afternoon. Interestingly the daily profiles of the other secondary pollutants HCHO and also PAN vary parallel to ozone.

2) The diurnal cycles of NO_x reflect the local traffic pattern. There are high concentrations during the early morning and late evening hours of heavy automobile traffic caused by employees.

3) The diurnal cycles of NO_x and the anthrogenic non-methane hydrocarbon are correlated.

The weather varied considerably during the campaign. See for example the weather maps in Appendix B kindly provided by the Deutscher Wetterdienst. Cloudy skies were encountered at several days causing low photolytic activity as is shown in the diurnal cycles of $J(NO_2)$ and $J(O_3)$. Wind came from all directions during the campaign with rather low mean velocities of 2 m/sec and always lower than 6 m/sec. The global radiation and the temperature leads to a natural division of the campaign into three periods (see Figure 4). A period of high global radiation and also photolytic activity during daytime started at May 10 and lasted til May 19. During this period the average ozone concentrations were also high. After the change in weather the second period of high daily means of temperature, global radiation, and ozone began May 20 and ended at May 28. After May 29 there were considerable variations of the global radiation and ozone from day to

day with values less than during the previous periods indicating mixed meteorological conditions.

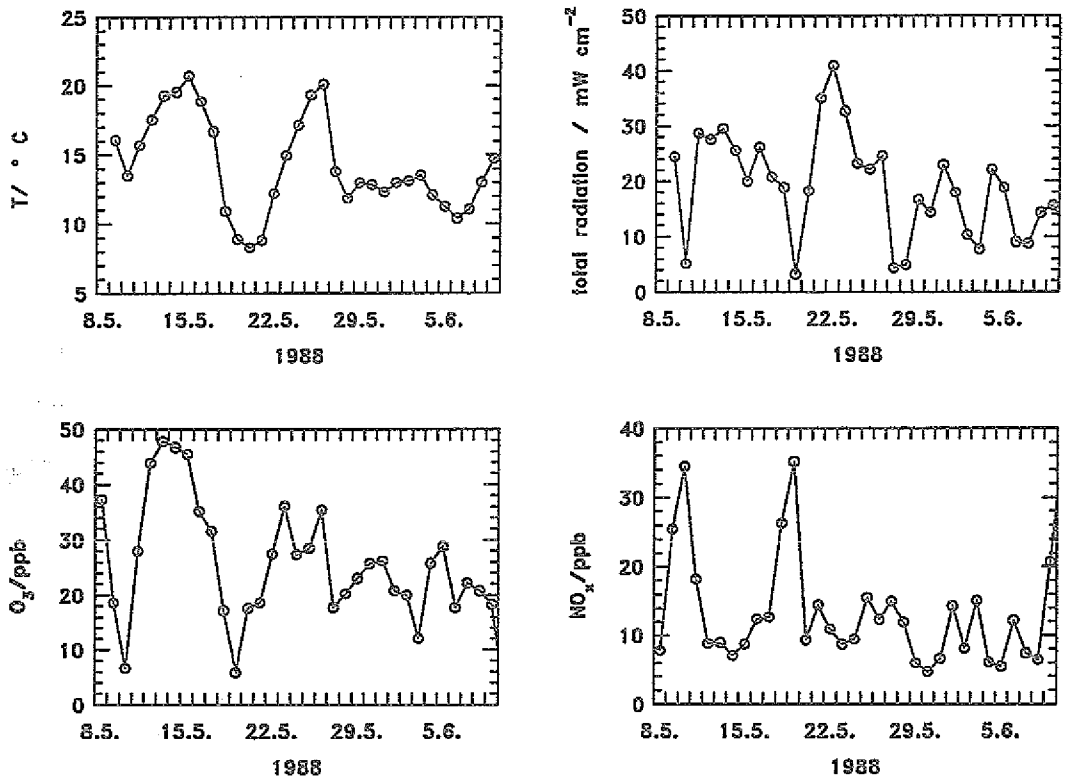

Figure 4: Daily means of global radiation, temperature, NO_x and ozone during the campaign.

To access more quantitatively the variability of all quantities minimum and maximum values, median, as well as the 16- and 84-percentiles for the time of the campaign are entered into Table 4.

Quantity/Unit (Comments)		MI	Q16	MD	Q84	MA	ME	SD
NO/ppb	(CL)	0.00	0.03	0.67	4.03	54.82	3.03	6.92
NO_2/ppb	(CL)	0.83	3.75	8.70	18.05	54.05	10.62	7.46
NO_y/ppb	(CL)	2.77	8.56	14.77	27.55	103.4	18.90	14.22
Ozone/ppb	(Dasibi)	0.00	9.5	24.	40.	81.	25.	16.
Ozone	(DA)	0.02	5.29	9.49	15.2	18.1	9.72	4.29
NO_2 (333 nm)	(DA)	0.22	0.80	2.10	5.09	9.56	2.83	2.17
NO_2 (450 nm)	(DA)	0.06	0.94	2.68	5.25	17.0	3.33	2.67
SO_2	(DA)	0.14	0.42	1.17	2.81	7.59	1.63	1.44
HCHO	(DA)	0.19	0.33	0.49	0.71	0.93	0.50	0.18
$OH/10^6 cm^3$	(DA)			0.87	2.5	5.2	0.9	1.9
CO/ppb	(GS)	144.	213.	292.	411.	655.	313.	104.
Methane/ppm	(GS)	1.81	1.84	1.91	2.13	2.67	1.99	0.20
PAN/ppb	(GC)	0.01	0.25	0.57	1.49	2.66	0.78	0.56
CO/ppb	(GC)	134.	201.	267.	374.	881.	297.	110.
CH_3CHO/ppb	(GC)	0.01	0.07	0.17	0.30	1.05	0.19	0.13
Ethane/ppb	(GC)	0.18	1.75	2.49	3.74	9.92	2.77	1.40
Propane/ppb	(GC)	0.41	0.66	1.22	2.29	12.81	1.63	1.43
i-Butane/ppb	(GC)	0.11	0.23	0.40	0.93	4.51	0.65	0.69
n-Butane/ppb	(GC)	0.12	0.33	0.62	1.32	5.42	0.89	0.88
i-Pentane/ppb	(GC)	0.12	0.36	0.73	1.51	5.60	1.01	0.87
n-Pentane/ppb	(GC)	0.09	0.29	0.63	1.27	3.39	0.80	0.61
Ethene/ppb	(GC)	0.20	0.53	1.22	3.03	15.31	1.89	2.04
Propene/ppb	(GC)	0.06	0.13	0.27	0.79	22.5	0.81	2.30
1-Butene/ppb	(GC)	0.00	0.03	0.05	0.20	1.00	0.11	0.17
Acetylene/ppb	(GC)	0.25	0.62	1.12	2.33	6.74	1.43	1.05
Benzene/ppb	(GC)	0.06	0.21	0.43	0.84	2.93	0.55	0.45
Toluene/ppb	(GC)	0.03	0.11	0.23	0.56	1.63	0.33	0.29
o-Xylene/ppt	(GC)	0.00	0.00	13.0	38.0	317.	24.0	42.0
p+m-Xylene/ppt	(GC)	0.00	6.00	36.0	104.	714.	72.0	106.
Radon activity	(RU)	11	41	90	176	518	109	74
relative humidity / %		23.5	46.2	78.6	96.2	97.7	73.5	22.6
Temperature/ °C		0.4	10.0	14.7	19.0	27.0	14.3	4.6
Windspeed / m s^{-1}		0.0	0.8	2.0	3.1	6.2	2.0	1.1
Air Pressure / hPa		991	996	1000	1005	1018	1001	15.2
Scatt. coeff./10^{-5} m^{-1}		1.7	4.2	8.1	18.7	29.0	10.7	7.7
Tot. Radiation/mW cm^{-2}		0.	0.	7.6	45.2	96.7	18.6	23.7
$j(O_3)$/ 10^{-6} s^{-1}		0.	0.	0.3	7.2	19.0	2.8	4.4
$j(NO_2)$/ 10^{-3} s^{-1}		0.	0.	0.7	4.4	11.1	1.8	2.3

Table 4: Abundances of trace gases and other parameters during the field campaign in Jülich, 1988.

Q16:	*16- Percentile*	*Dasibi:*	*Commercial instrument*
Q84:	*84- Percentile*	*GC:*	*Gas chromatography*
MI:	*Minimum*	*MA:*	*Maximum*
MD:	*Median*	*ME:*	*Mean*
SD:	*Standard Deviation*	*GS:*	*Grab sample*
CL:	*Chemiluminescence*	*RU:*	*Relative unit: counts per 30 min*
DA:	*Differential optical absorption spectroscopy concentrations in units of* $10^{11} cm^{-3}$		

6. Access to the Data

The data are entered into clear-text data files with a common format for further evaluation using a computer. For practical reasons we distinguish between the Institute Data Format (IDF) and another format (ENZ from German EiNZel) (see Table 5). The format specifications are explained in H. London et al. (1992). Files of type IDF contain the experimental data of at least one quantity. These are experimental data sometimes still uncalibrated as they are collected by the experimentalists. The files are also provided with the necessary information on calibration procedures, experimental methods and uncertainties etc. to fully verify the reliability of the entered data. For further processing the data are transferred into files of type ENZ. One ENZ-file is created for every measured quantity. Thereby necessary calibrations and scalings are also performed. The entries in files of both types are self-explanatory to a large extent. The whole data set is stored (and also archived) at the computer center (ZAM) of the KFA. For copies of the data on disc, contact D. Poppe, Institut für Atmosphärische Chemie.

quantity (comments)	ENZ-filename	IDF-filename
NO (Chemilum.) NO_2 (Chemilum.) NO_y (Chemilum.) Ozone (Dasibi)	NO NO2_CHML NOY O3DASIBI	NO_CHEMI NO2PHKNV NOYAUKNV O3DASIBI
Ozone (DOAS) NO_2 (450 nm) (DOAS)*) NO_2 (333 nm) (DOAS) SO_2 (DOAS) HCHO (DOAS)	O3UVF NO2BLAU2 NO2UVF SO2UV HCHOUVF	O3UFDOAS NO2B2DOA NO2UFDOA SO2UDOAS HCHOFDOAS
OH	OH	OH88ALLF
CO (Grab sample) methane	CO_BHLTR CH4	CO_GC_B CH4_GC_B
PAN	PAN	PAN_GCIS
CO (GC) uncorrected corrected	CO_INSI COINSIK	COGCINSI ---
acetaldehyde ethane propane i-butane n-butane i-pentane n-pentane ethene propene 1-butene acetylene benzene toluene o-xylene p+m-xylene	ACETALD ETHAN PROPAN I-BUTAN N-BUTAN I-PENTAN N-PENTAN ETHEN PROPEN 1-BUTEN ACETYLEN BENZOL TOLUOL O-XYLOL PM-XYLOL	KW1_GCIS KW1_GCIS KW1_GCIS KW1_GCIS KW1_GCIS KW1_GCIS KW2_GCIS KW1_GCIS KW1_GCIS KW1_GCIS KW1_GCIS KW2_GCIS KW2_GCIS KW2_GCIS KW2_GCIS
radon activity	RADON	RADON
$j(O_3)$ $j(NO_2)$	JO3CALC JNO2_MET	JO3ADC (JNO2ADCM)
rel. humidity (2 m) temperature (2 m) temperature (10 m) stability class	H2OMT02 TEMPMT02 TEMPMT10 DIFK	H2OPSYCH TEMPMT02 TEMPMTRM DIFFKTG
windspeed winddirection air pressure scatt. coeff. tot. radiation	WINDGSCH WINDRICH LUFTDRCK STREU GSTRHLNG	WINDVMET WINDRMET LUFTDRCK STREUNPH GLOBMET

Table 5: Access to the data of the campaign in Jülich 1988. The names of the files of ENZ- and IDF-format (see section 6) are entered into the table.

*) *For details see section 4.1.3*

Literature:

Bevington, P. R., 1969,
Data reduction and error analysis for the physical sciences, McGraw-Hill Book Company, New York.

Brauers, T., and Hofzumahaus, A., 1992,
Latitudinal variation of measured NO_2 photolysis frequencies over the atlantic ocean between 50°N and 30°S, J. Atmos. Chem. 3/4, 269-282.

Callies, J., 1988,
Absorptionsspektroskopischer Nachweis von Hydroxyl-Radikalen in der Troposphäre, Thesis, University of Cologne.

Callies, J., Dorn, H.-P., Platt, U., and Ehhalt, D. H., 1989,
Tropospheric OH-concentration measurements by laser long-path absorption spectroscopy, in R. D. Bojkov and P. Fabian (eds.), Ozone in the Atmosphere, Proc. of the Quadrennial Ozone Symposium 1988 Deepak Publishing, Hampton/VA, pp. 772-775.

Dorn, H.-P., Callies, J., Platt, U., and Ehhalt, D. H., 1988,
Measurement of tropospheric OH concentrations by laser long-path absorption spectroscopy, Tellus 40 B, 437-445.

Drummond, J. W., Ehhalt, D. H., and Volz, A., 1985,
An optimized chemiluminescence detector for tropospheric NO measurements, J. Atmos. Chem. 2, 287-306.

Engleman, R., 1969,
Collision broadening of transient spectra I. Hydroxyl line width in the (0,0) (A-X) transition at low temperatures, J. Quant. Spectrosc. Radiat. Tansfer, 9, 391-400.

Fahey, D. W., Eubank, C. S., Hübler, G., and Fehsenfeld, F. C., 1985,
Evaluation of a catalytic reduction technique for the measurement of total reactive odd-nitrogen NO_y in the atmosphere, J. Atmos. Chem. 3, 435-468.

Hofzumahaus, A., Brauers, T., Platt, U., and Callies, J., 1992,
Latitudinal variation of measured O_3 photolysis frequencies $J(O^1D)$ and primary OH production rates over the atlantic ocean between 50°N and 30°S, J. Atmos. Chem. 3/4, 283-298.

Junkermann, W., Platt, U., and Volz-Thomas, A., 1989,
A photoelectric detector for the measurement of photolysis frequencies of ozone and other atmospheric molecules, J. Atmos. Chem. 8, 203-227.

Leonard, Ch., 1990,
Entwicklung eines UV-laserspektroskopischen Nachweisverfahrens für OH-Radikale und spektroskopische Untersuchungen an Spurengasen unter troposphärischen Bedingungen, Thesis, University of Hannover.

London, H., Neuwohner, Th., Poppe, D., Wallasch, M., and Johänning, S., 1992
ICG-3 Programme zur Auswertung von Feldkampagnen, Jül-Report no. 2648, Jülich.

Molina, L. T., and Molina, M. J., 1986,
Absolute absorption cross sections of ozone in the 185- to 350-nm wavelength range, J. Geophys. Res. 91, 14, 501-14, 508.

Müller, K. P. and Rudolph, J., 1989,
An automated technique for the measurement of peroxyacetylnitrate in ambient air at ppb and ppt levels, Intern. J. Environm. Anal. Chem. 37, 262.

Neuroth, R., 1992,
Messung troposphärischer Hydroxylradikale mit Laser-Langweg Absorptionsspektroskopie, Thesis, University of Cologne.

Pasquill, F., 1974,
"Atmospheric Diffusion", Wiley, New York.

Perner, D., Platt, U., Trainer, M., Huebler, G., Drummond, J. W.,
Junkermann, W., Rudolph, J., Schubert, B., Volz, A., Ehhalt, D. H.,
Rumpel, K. J., and Helas, G., 1987,
Measurement of Tropospheric OH concentrations: A comparison of field data with model predictions, J. Atmos. Chem. 5, 185-216.

Platt, U., Perner, D., and Paetz, H., 1979,
Simultaneous measurement of atmospheric CH_2O, O_3, and NO_2 by differential optical absorption, J. Geophys. Res. 84, 6329-6335.

Platt, U., and Perner, D., 1984,
Ein Instrument zur spektroskopischen Spurenstoffmessung in der Atmosphäre, Fresenius Z. Anal. Chem. 317, 309-313.

Platt, U., Rateike, M., Junkermann, W., Rudolph, J., and Ehhalt, D. H., 1988,
New tropospheric OH measurements, J. Geophys. Res. 93, 5159-5166.

Polster, G., H. Geiß, and Heinemann, K., 1986,
Der Meteorologische Turm der Kernforschungsanlage Jülich, Jül-Report no. 2035, Jülich.

Polster, G., W. Bergs, and Brunen, E., 1989,
Meteorologische Messungen, in: Arbeitsbericht 1988 der Abteilung Sicherheit und Strahelenschutz, p. 177, ASS-Bericht Nr. 0493, Jülich.

Rohrer, F. and Brüning, D., 1992,
Surface NO- and NO_2-mixing ratios measured between 30°N and 30°S in the atlantic region, J. Atmos. Chem. 15, 253-268.

Rudolph, J., Johnen, F.J., and Khedim, A. 1986,
Problems connected with the analysis of halocarbons and hydrocarbons in the non-urban atmosphere, Intern. J. Environ. Anal. Chem. 27, 97-122.

Schmidt, U. and Seiler, W., 1970,
A new method for recording molecular hydrogen in atmospheric air, J. Geophys. Res. 75, 1713-1716.

Schneider, W., Moortgat, G. K., Tyndall, G. S., and Burrows, J. P., 1987,
Absorption cross-sections of NO_2 in the UV and visible region (200 - 700 nm) at 298 K, J. Photochem. Photobiol. 40, 195-217.

Seiler, W. and Junge, C., 1970,
Carbon monoxide in the atmosphere, J. Geophys. Res. 75, 2217-2226.

Umweltbundesamt (ed.), 1989,
Daten zur Umwelt 1988/89, Berlin.

Vierkorn-Rudolph, B., Rudolph, J., and Diederich, S., 1985,
Determination of peroxyacetylnitrate in unpolluted areas, Intern. J. Environm. Anal. Chem. 20, 131-148.

Deutscher Wetterdienst, 1989,
Sonderbeobachtungen des Meterologischen Observatoriums Hohenpeissenberg, Nr. 59

Appendix A Diurnal Cycles of all Measured Quantities during the Campaign. The time is given in UT.

In this appendix the diurnal cycles of all measured quantities are shown in diagrams for each quantity separately on a daily basis. For easy comparison between different days the same scale was used for all diagramms of a species with a few exceptions where the variability is very large. The time is given in UT and the date is indicated below the corresponding diagram. The quantity and the unit used are given at the bottom together with the name of the file which contains the data.

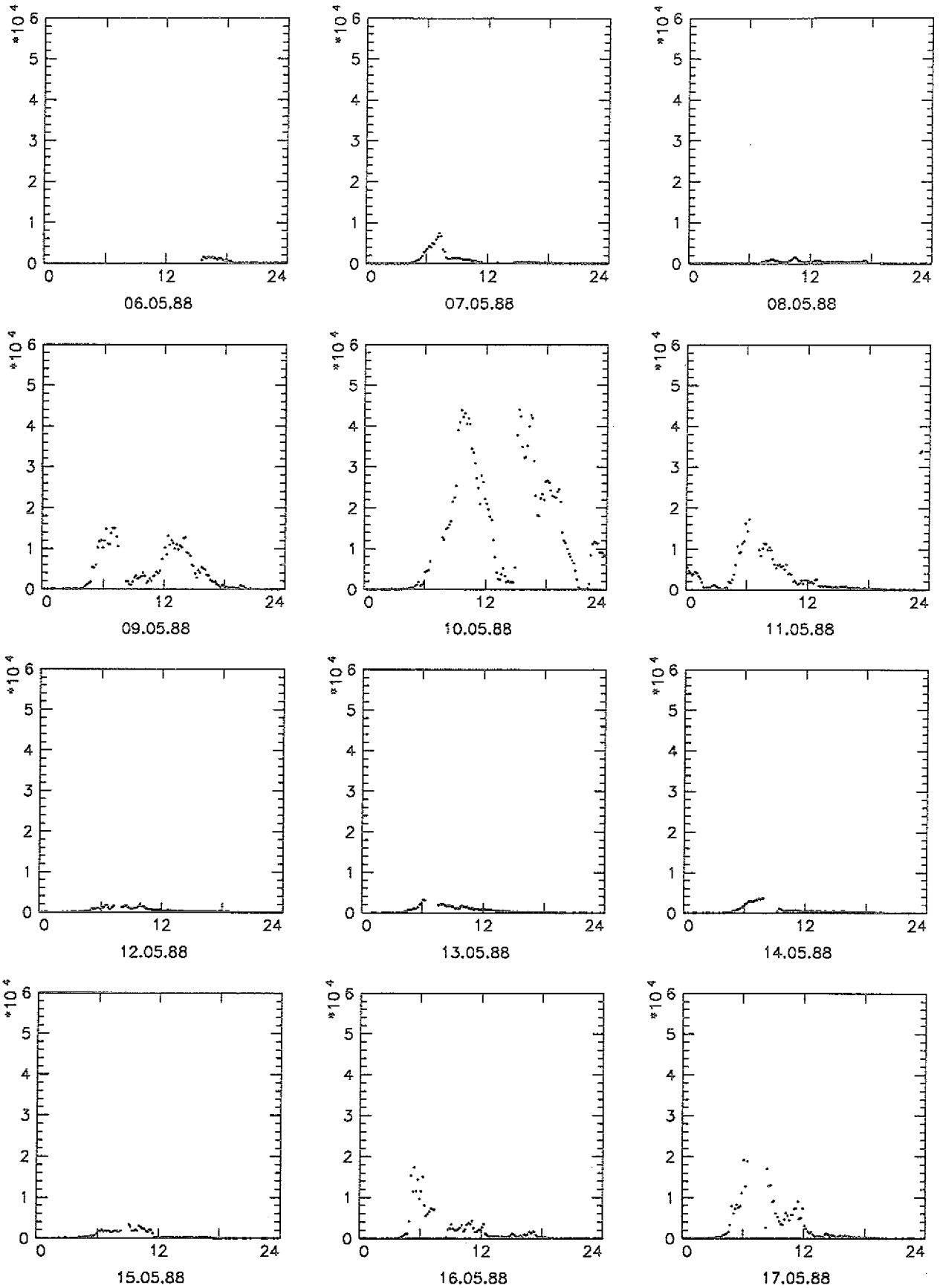

NO (chemilum.) / ppt *File: NO ENZ880HJ*

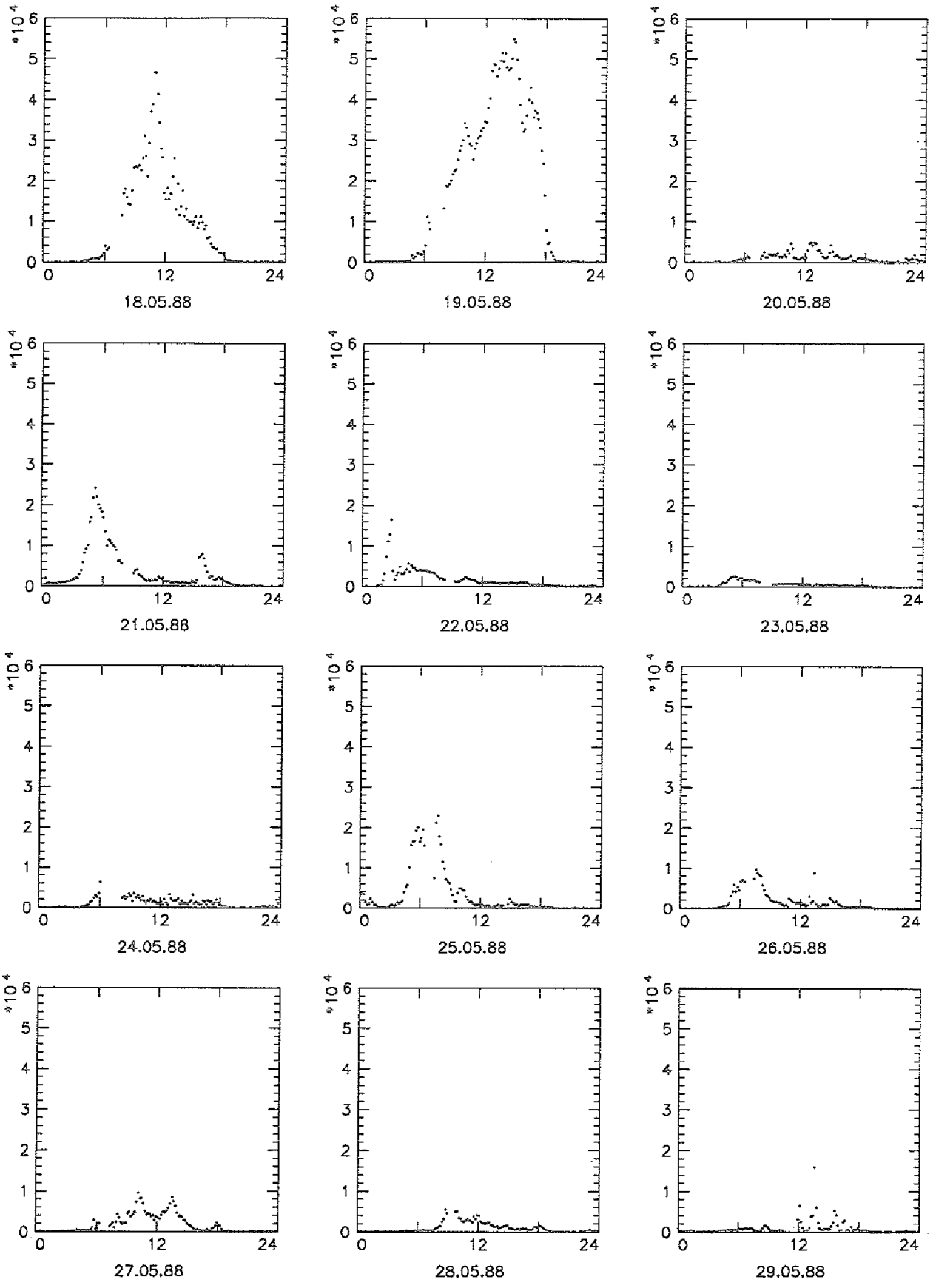

NO (chemilum.) / ppt *File: NO ENZ880HJ*

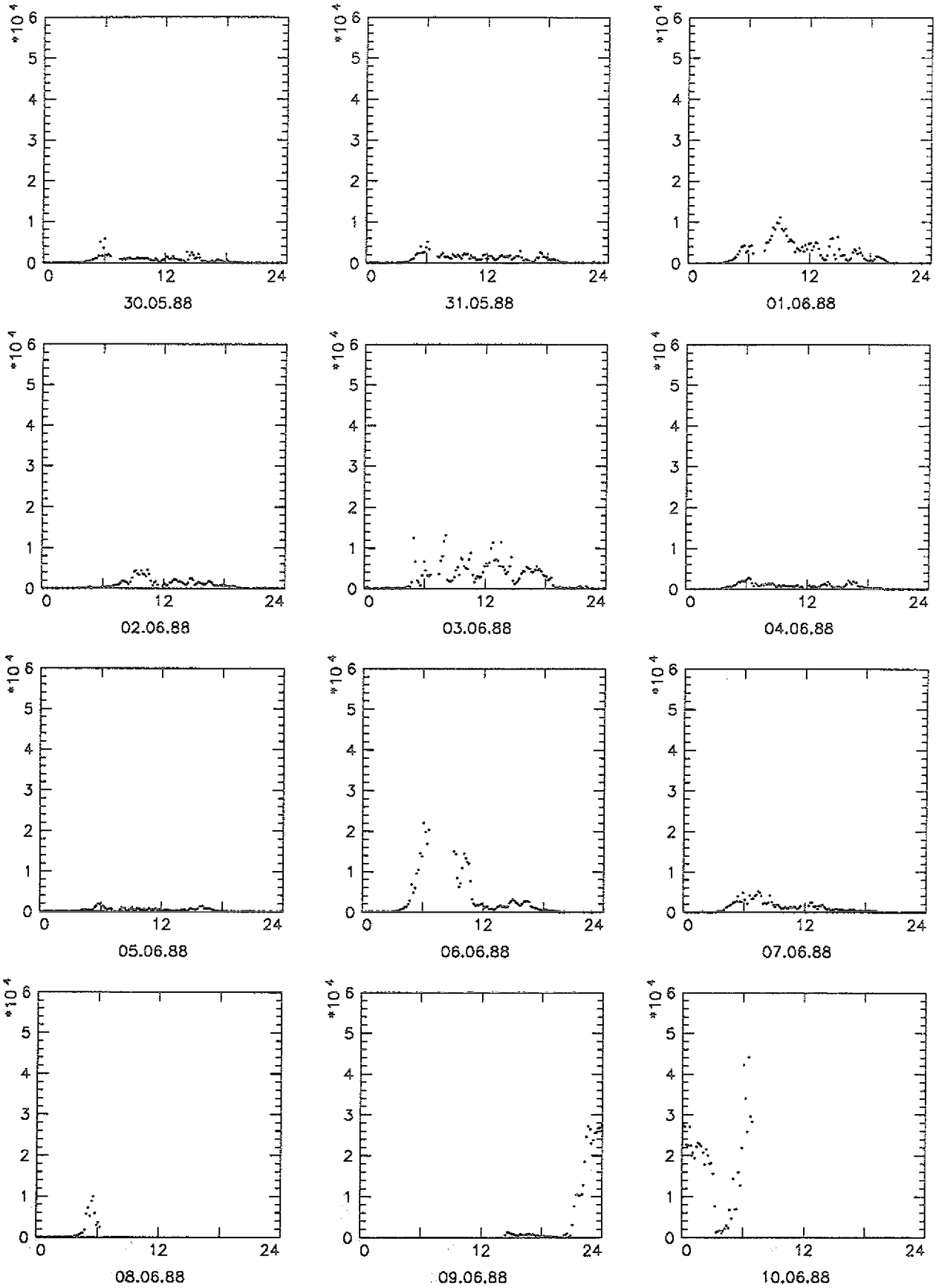

NO (chemilum.) / ppt *File: NO ENZ880HJ*

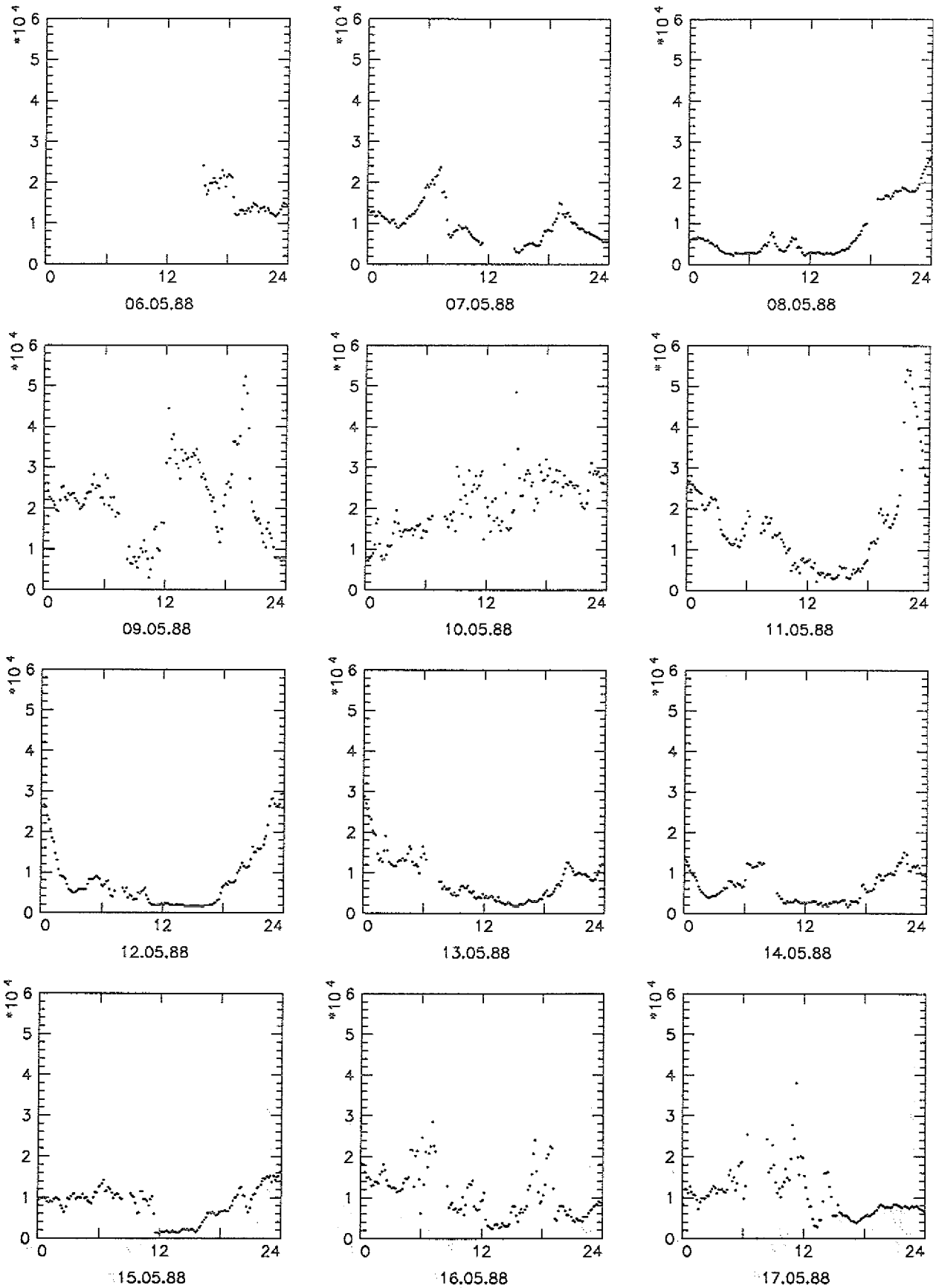

NO_2 (chemilum.) / ppt *File: NO2_CHML ENZ880HJ*

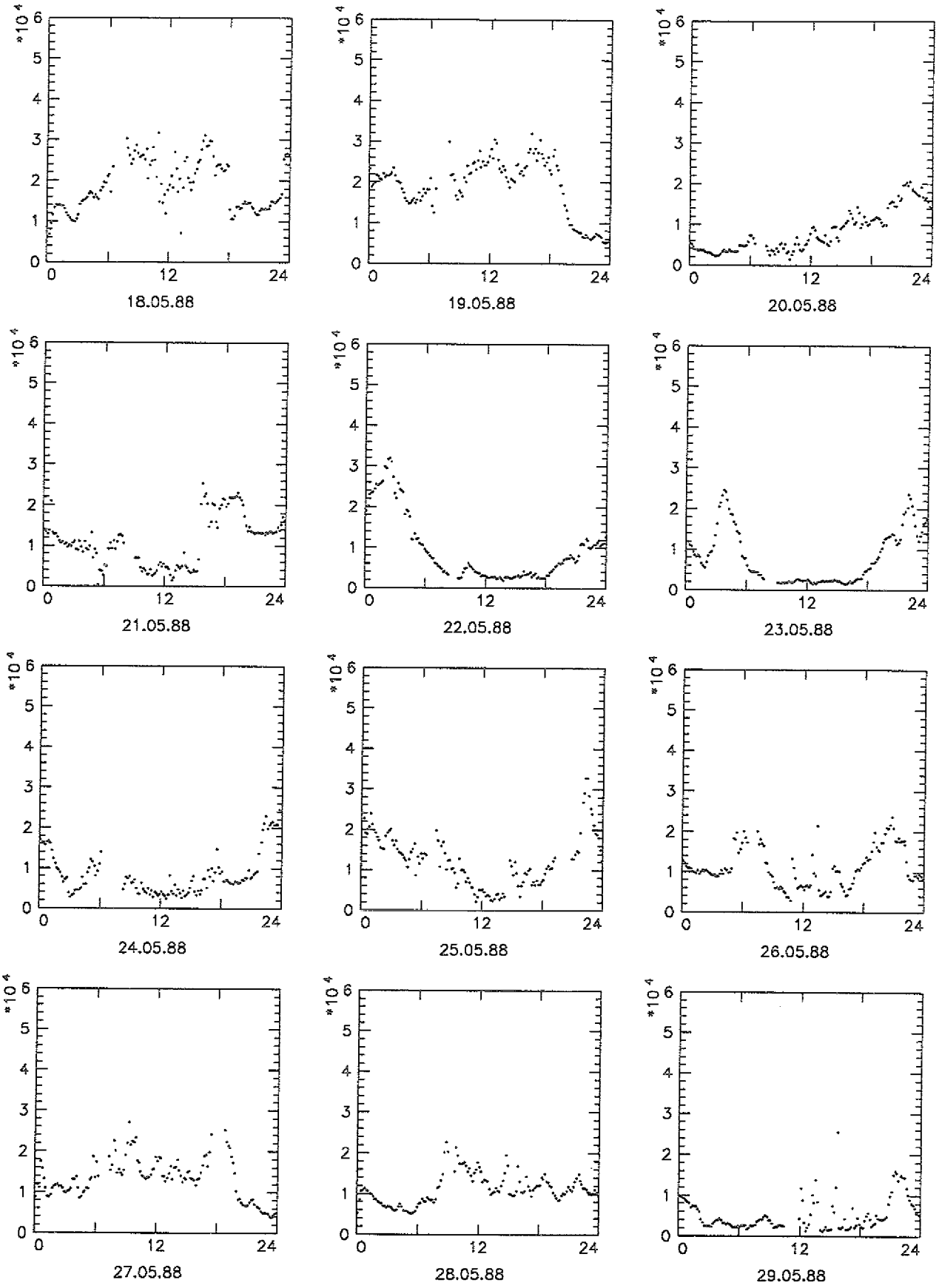

NO_2 (chemilum.) / ppt *File: NO2_CHML ENZ880HJ*

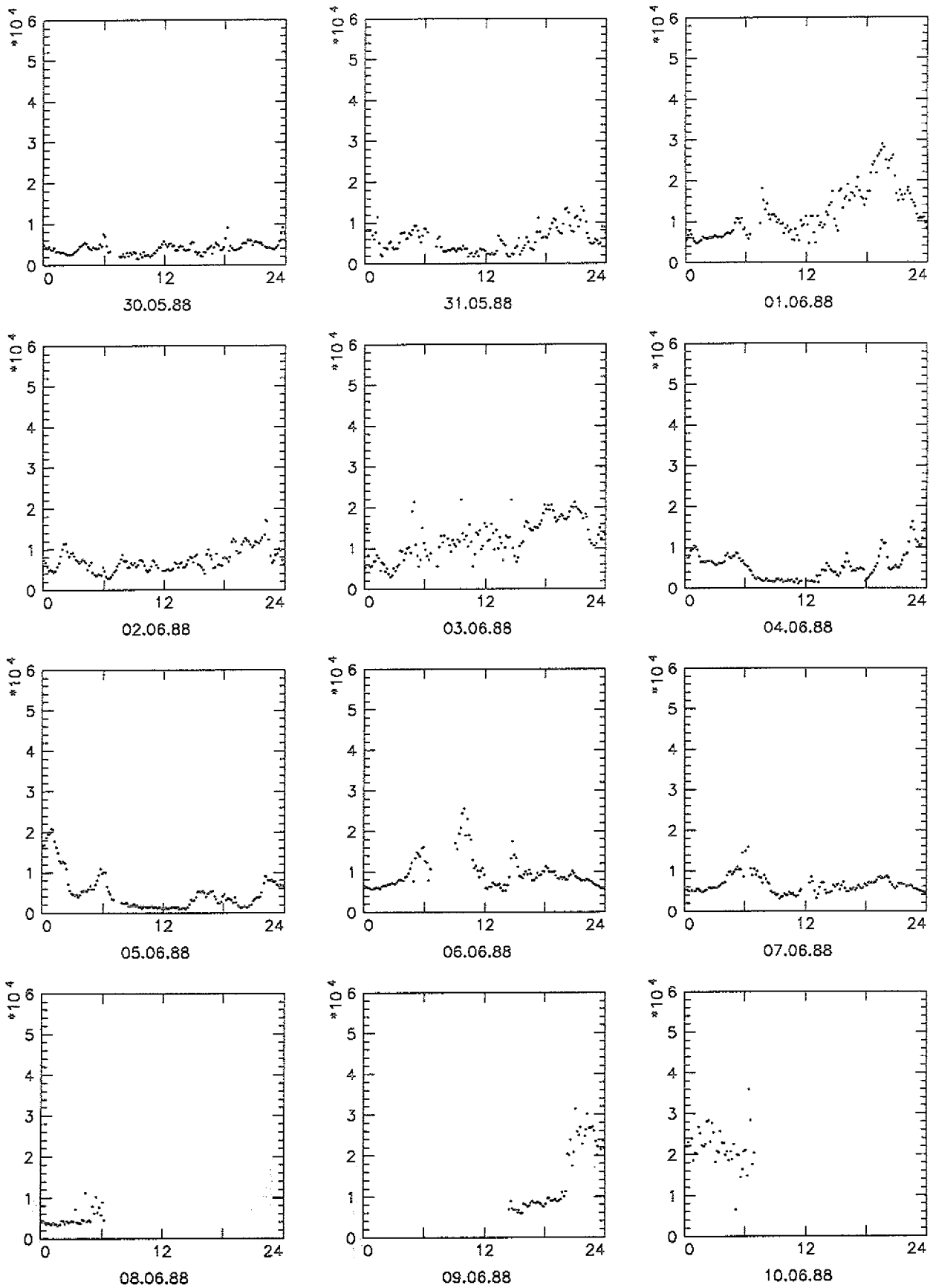

NO_2 *(chemilum.) / ppt* *File: NO2_CHML ENZ880HJ*

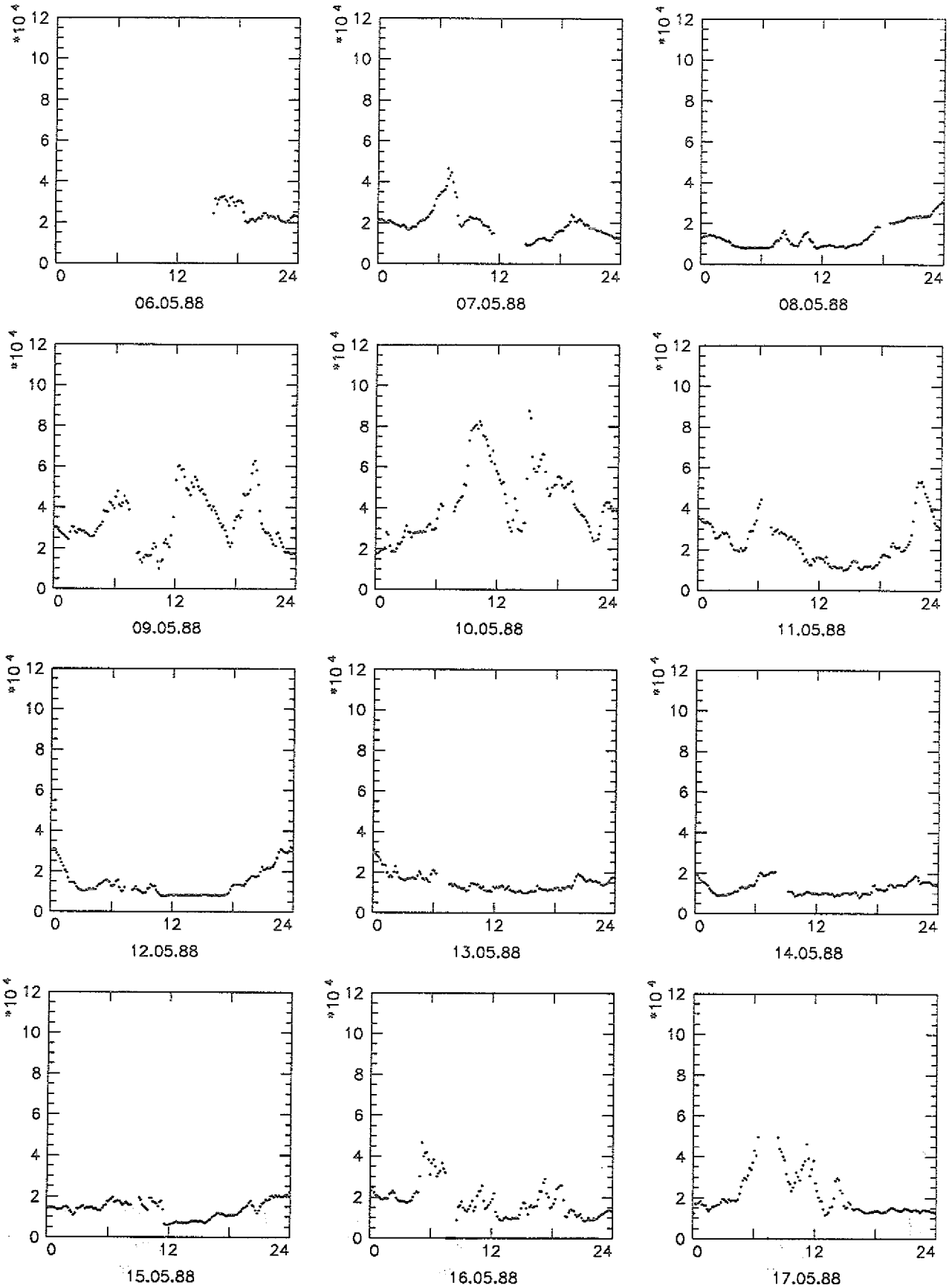

NO_y (chemilum.) / ppt *File: NOY ENZ880HJ*

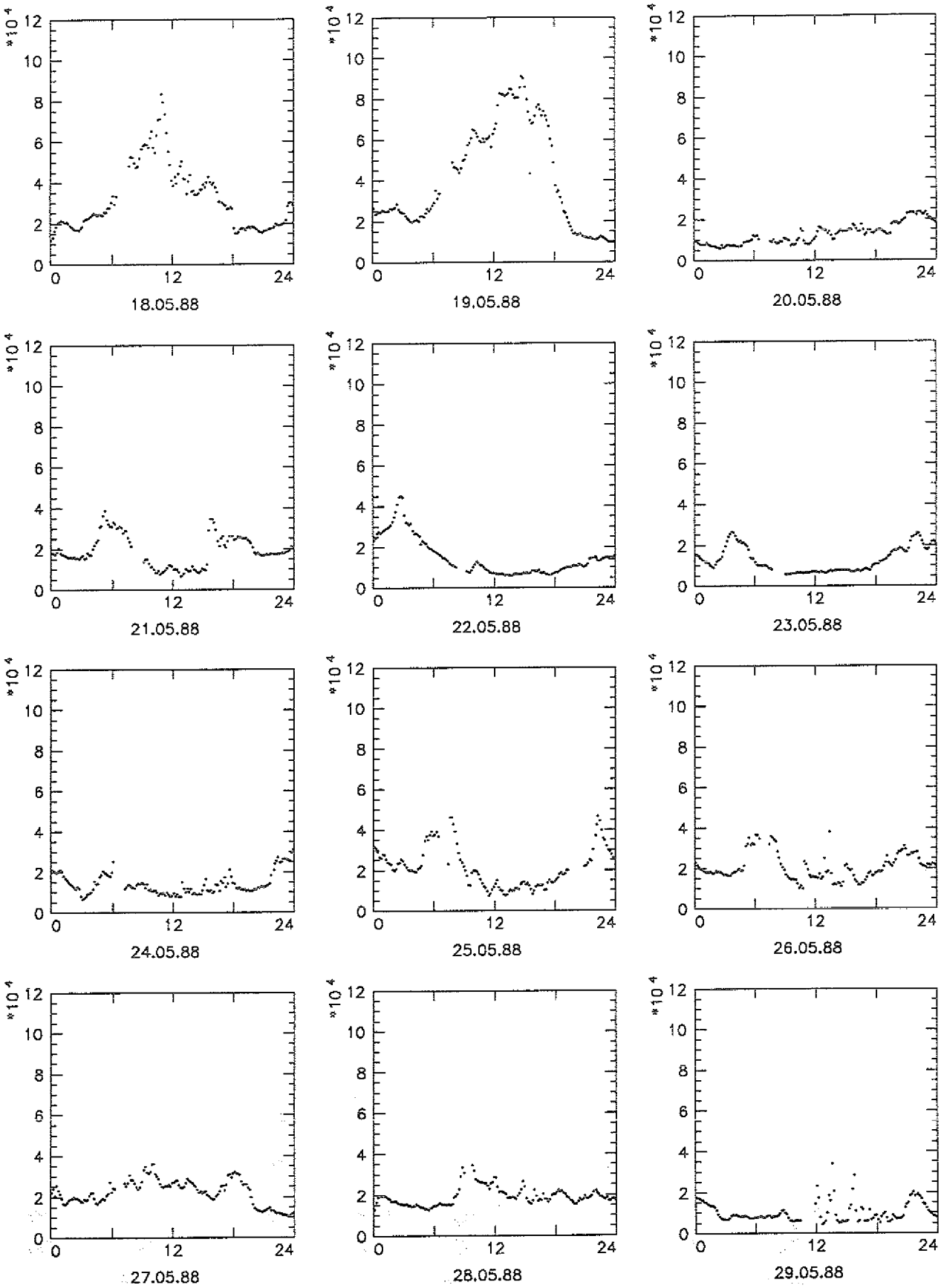

NO_y (chemilum.) / ppt *File: NOY* *ENZ880HJ*

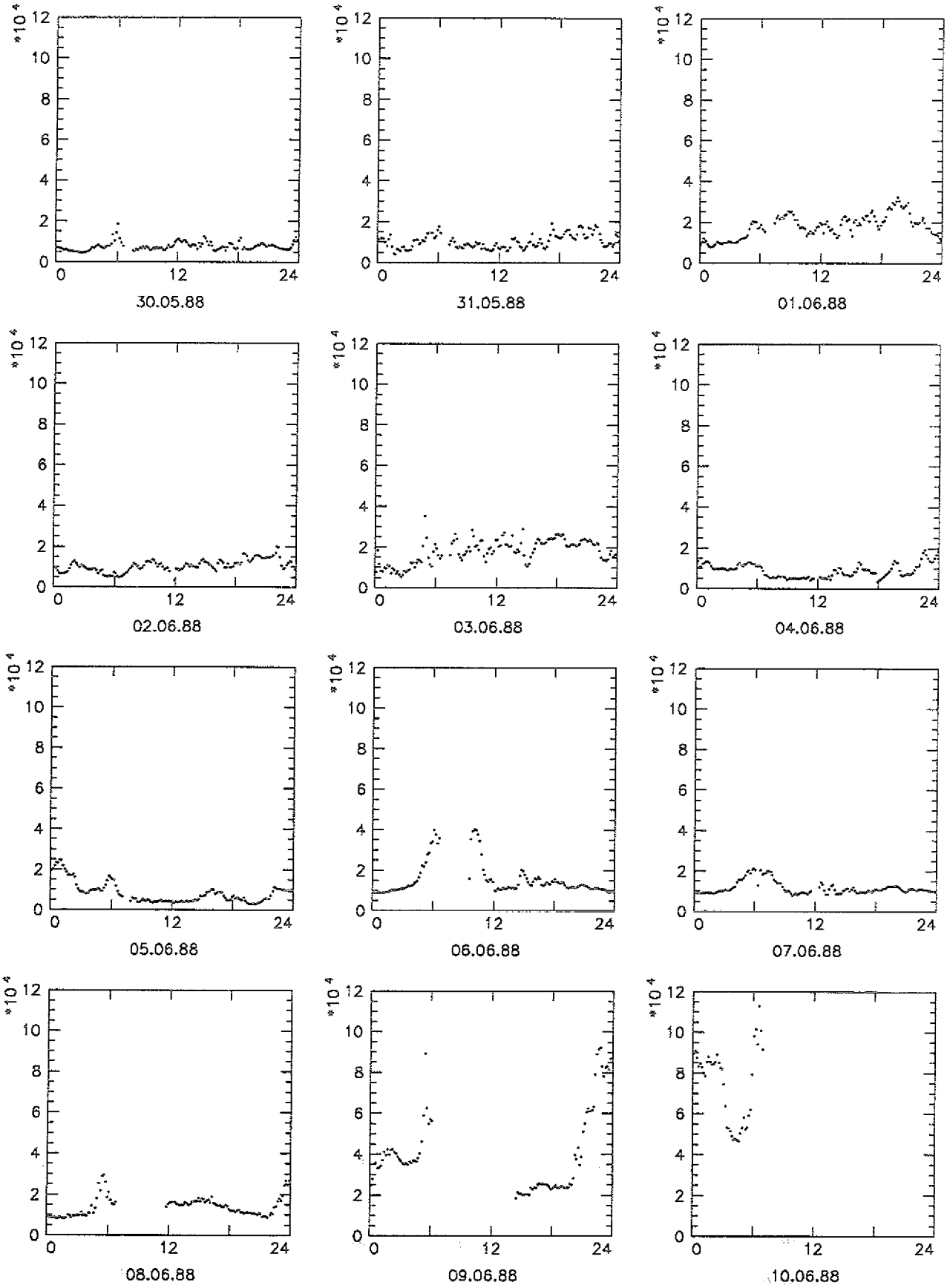

NO_y (chemilum.) / ppt *File: NOY* *ENZ880HJ*

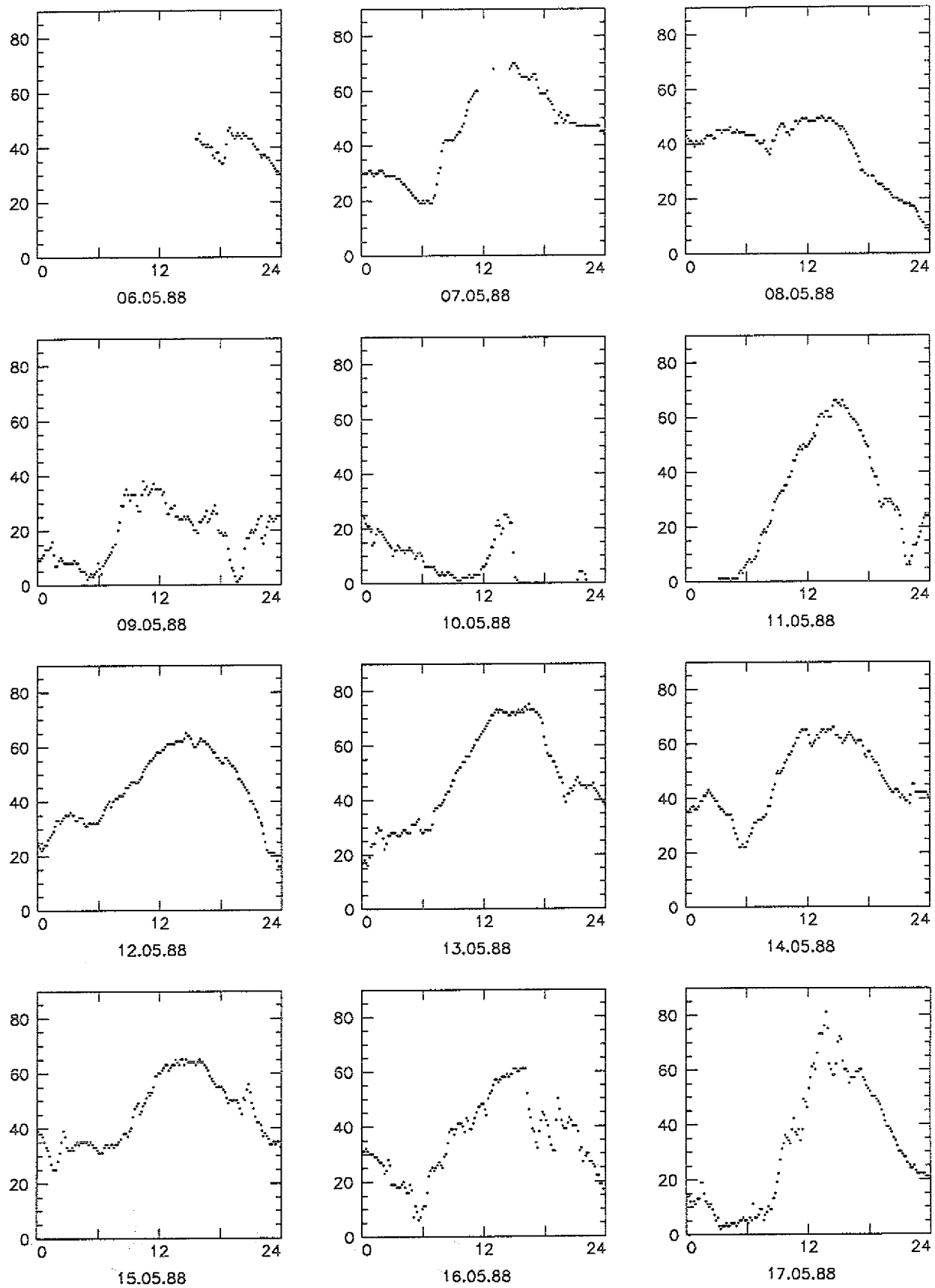

O_3 (DASIBI) / ppb

File: 03DASIBI ENZ880HJ

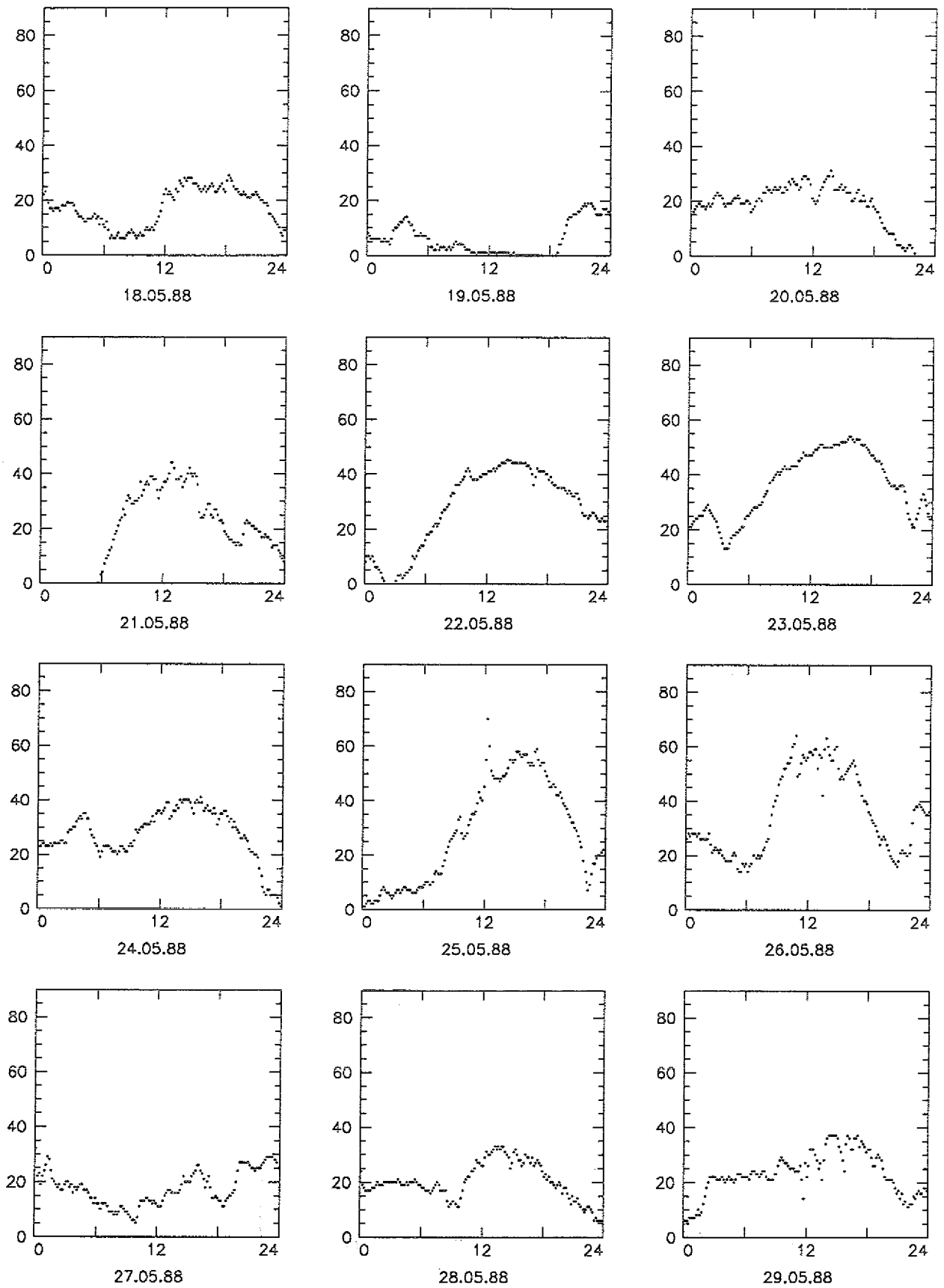

O_3 (DASIBI) / ppb

File: 03DASIBI ENZ880HJ

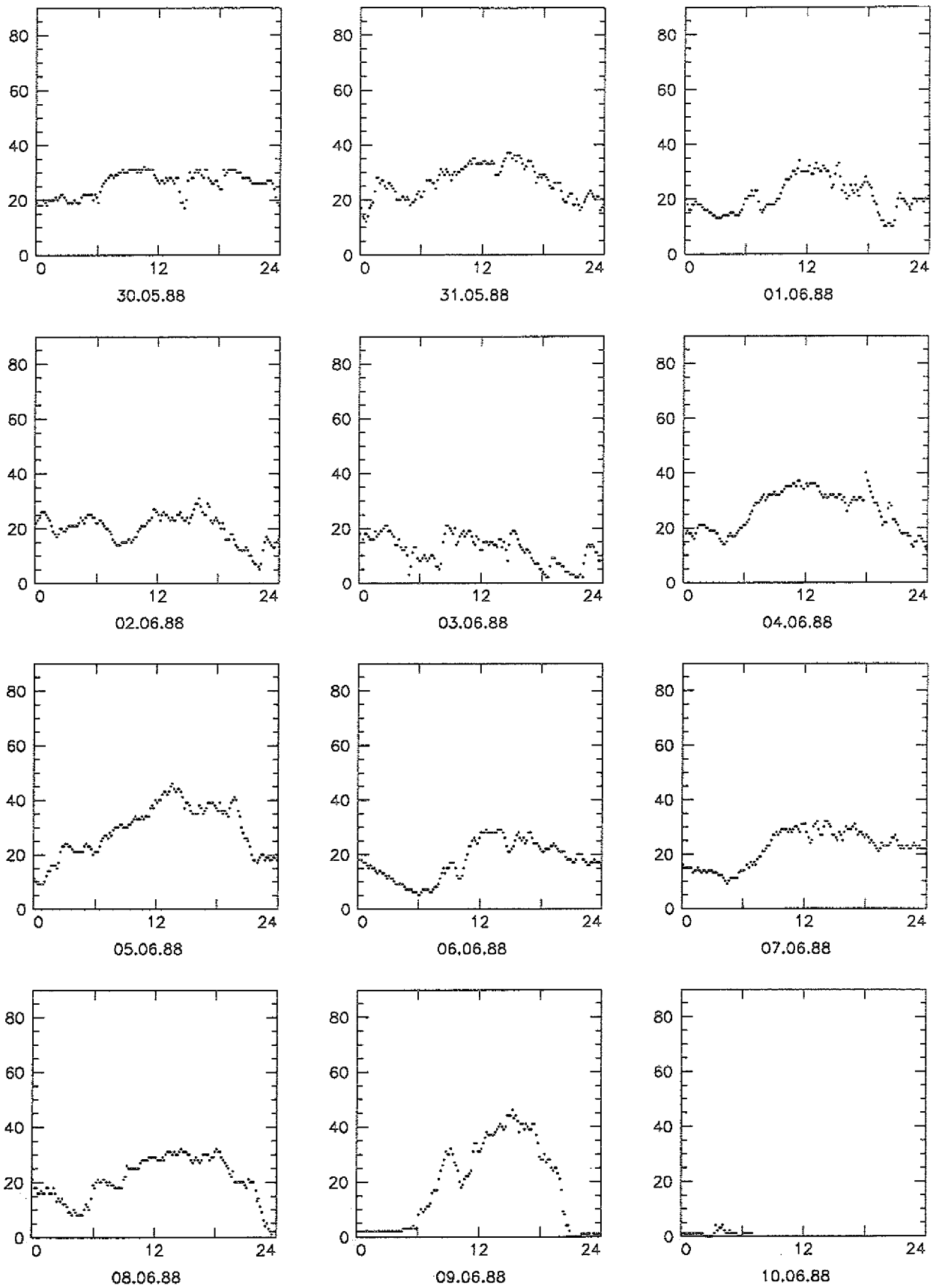

O_3 (DASIBI) / ppb

File: 03DASIBI ENZ880HJ

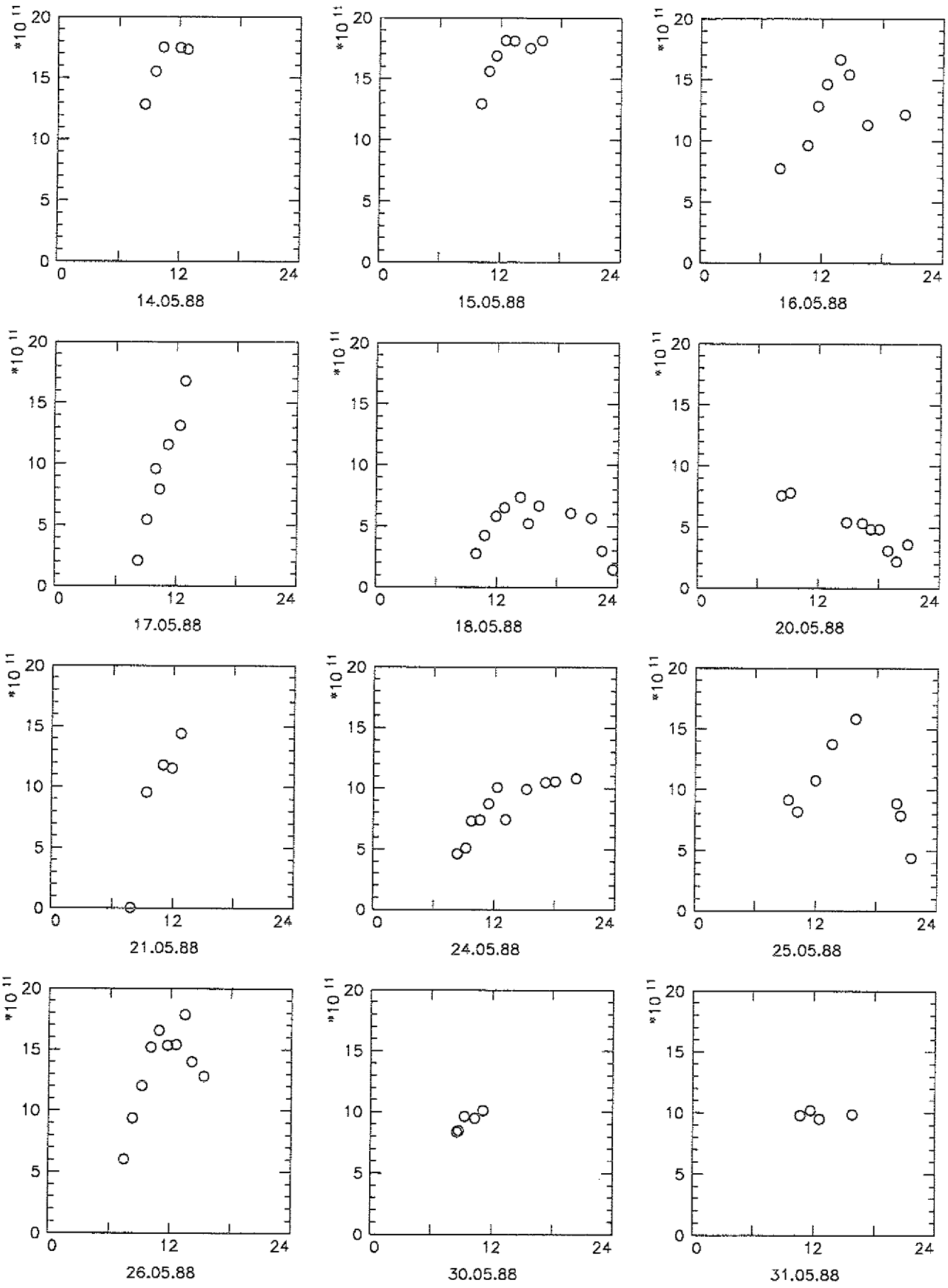

O_3 (DOAS) / cm^{-3}

File: O3UVF ENZ880HJ

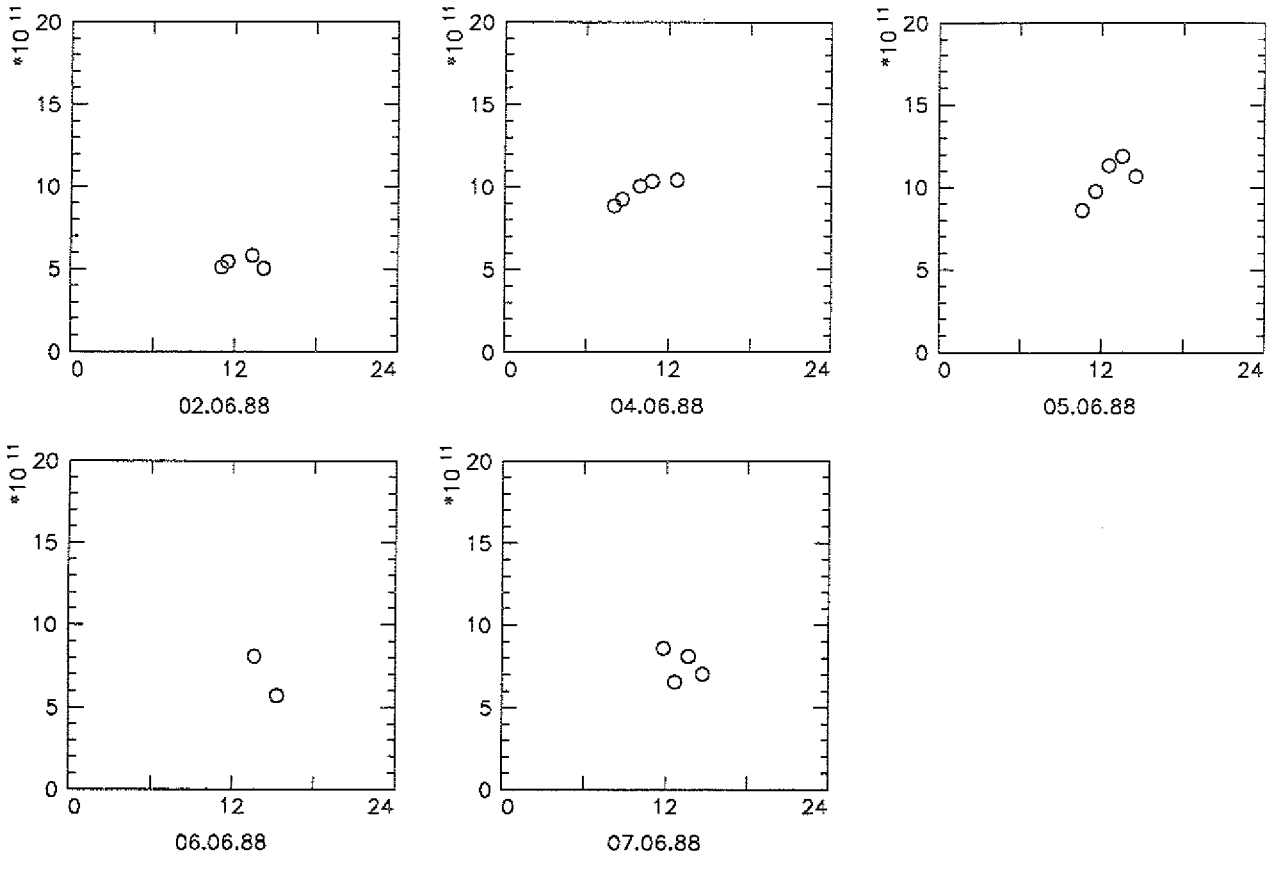

O_3 (DOAS) / cm^{-3} File: O3UVF ENZ880HJ

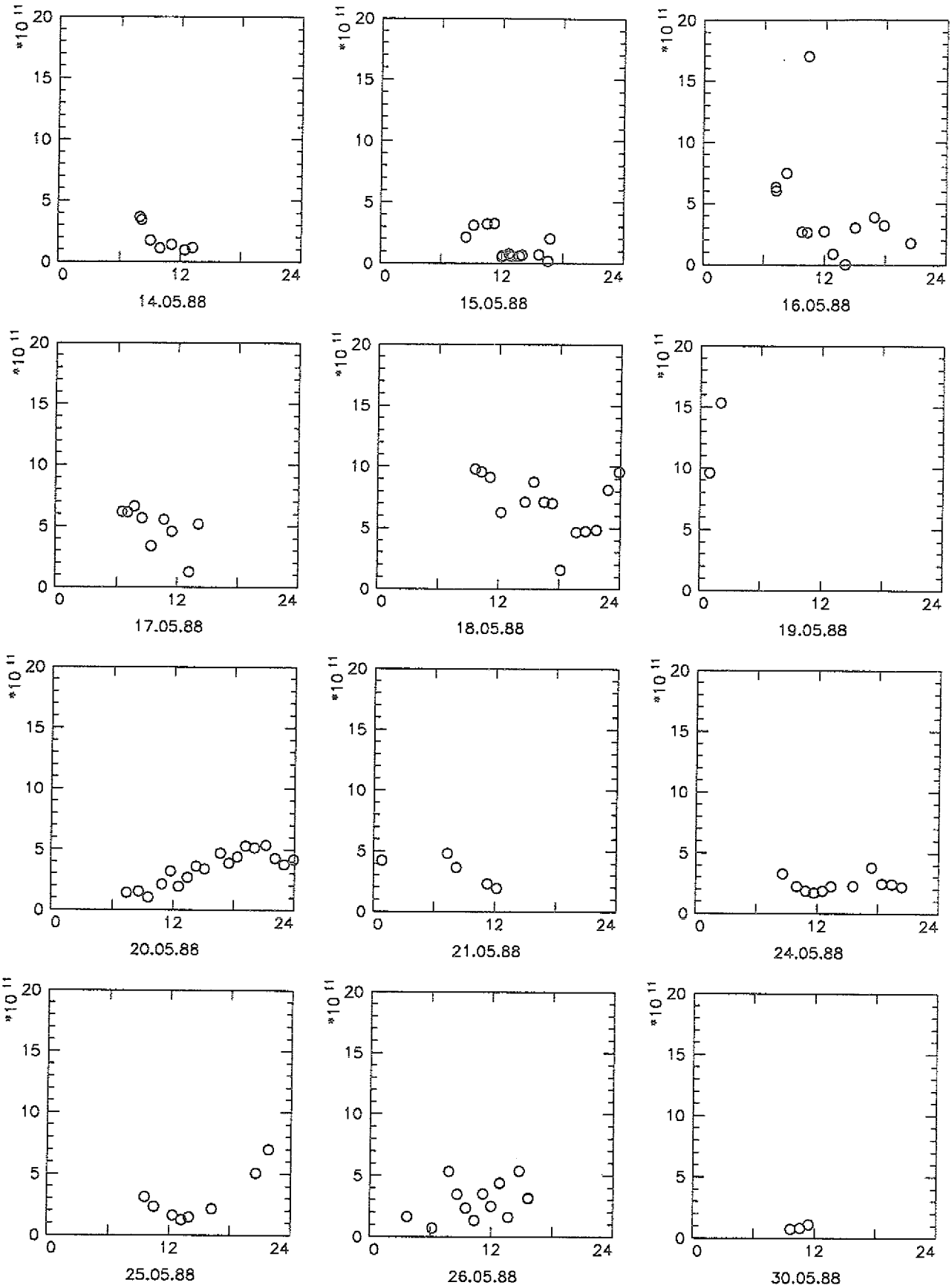

NO_2 (DOAS, 450 nm) / cm^{-3} *File: NO2BLAU2 ENZ880HJ*

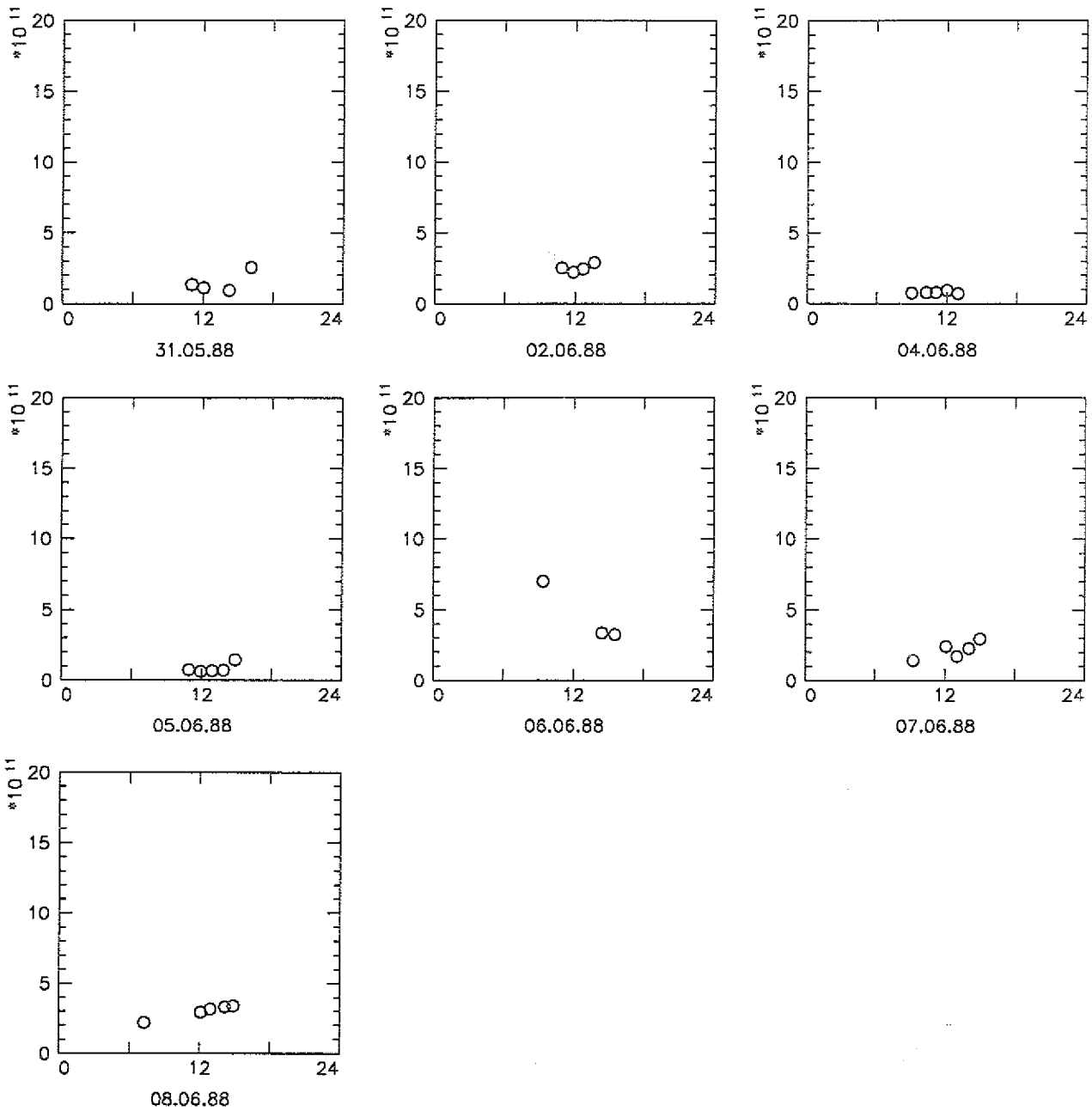

NO_2 (DOAS, 450 nm) / cm^{-3} File: N02BLAU2 ENZ880HJ

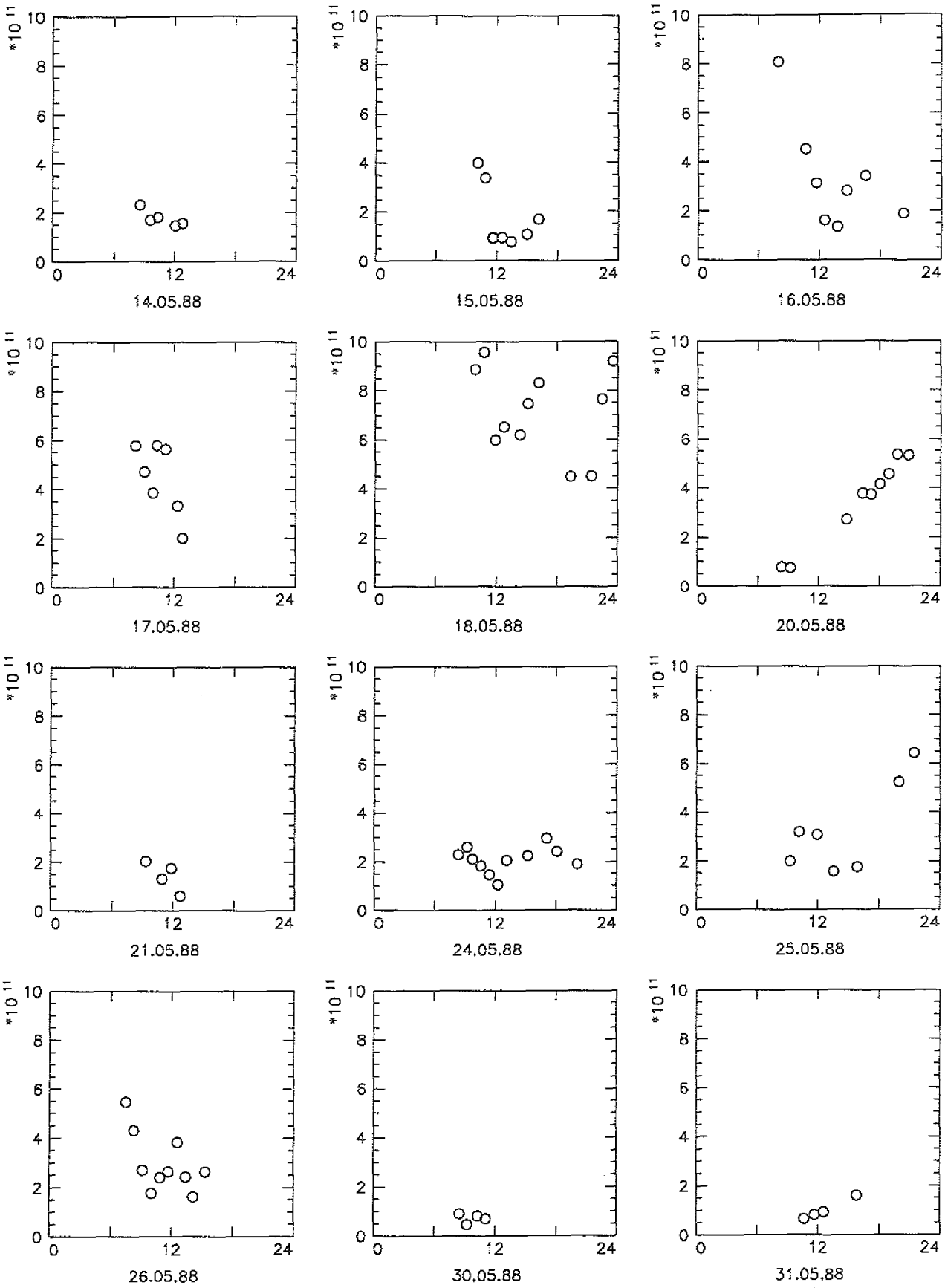

NO_2 (DOAS, 333 nm) / cm^{-3} *File: NO2UVF ENZ880HJ*

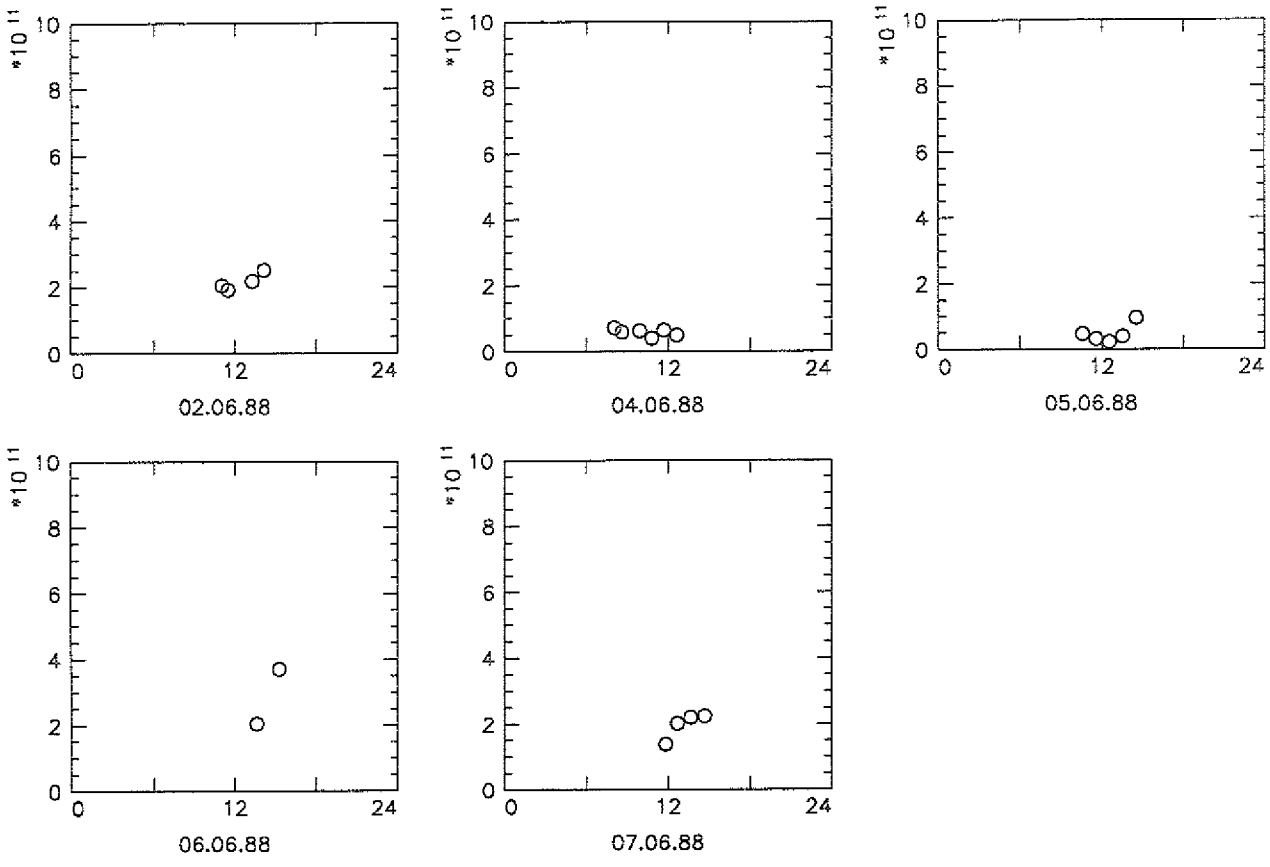

NO_2 (DOAS, 333 nm) / cm^{-3} *File: NO2UVF ENZ880HJ*

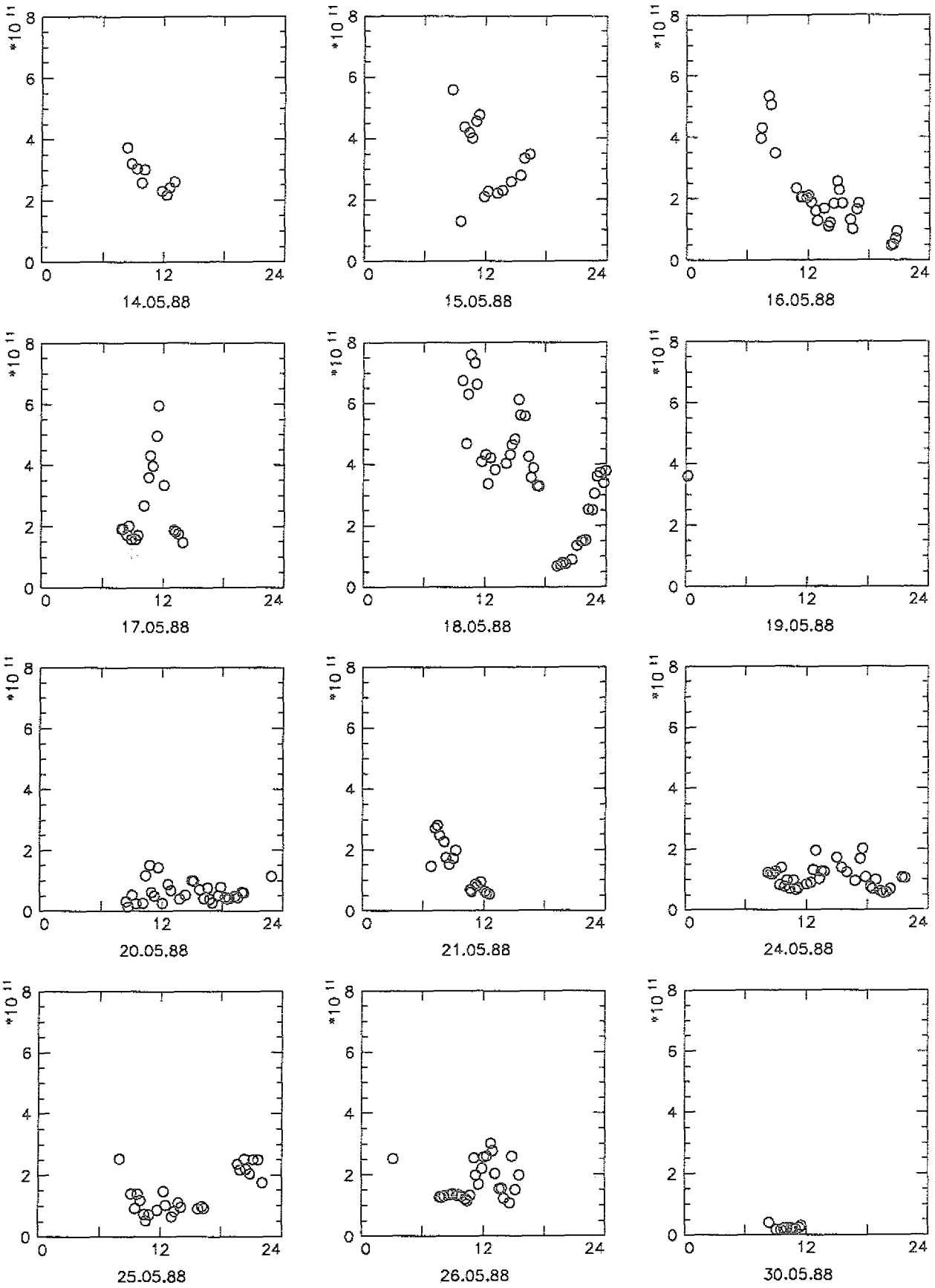

SO_2 (DOAS) / cm^{-3}

File: S02UV ENZ880HJ

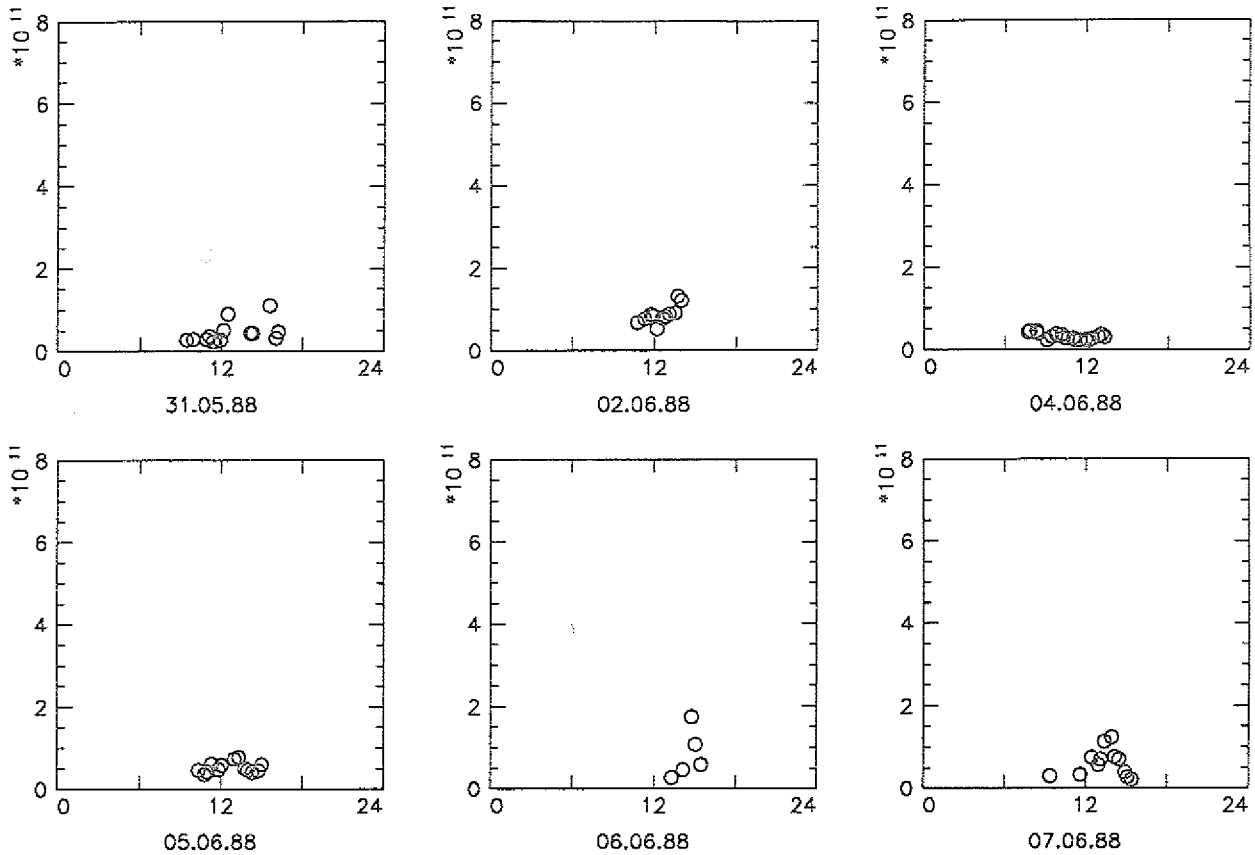

SO_2 (DOAS) / cm^{-3} File: SO2UV ENZ880HJ

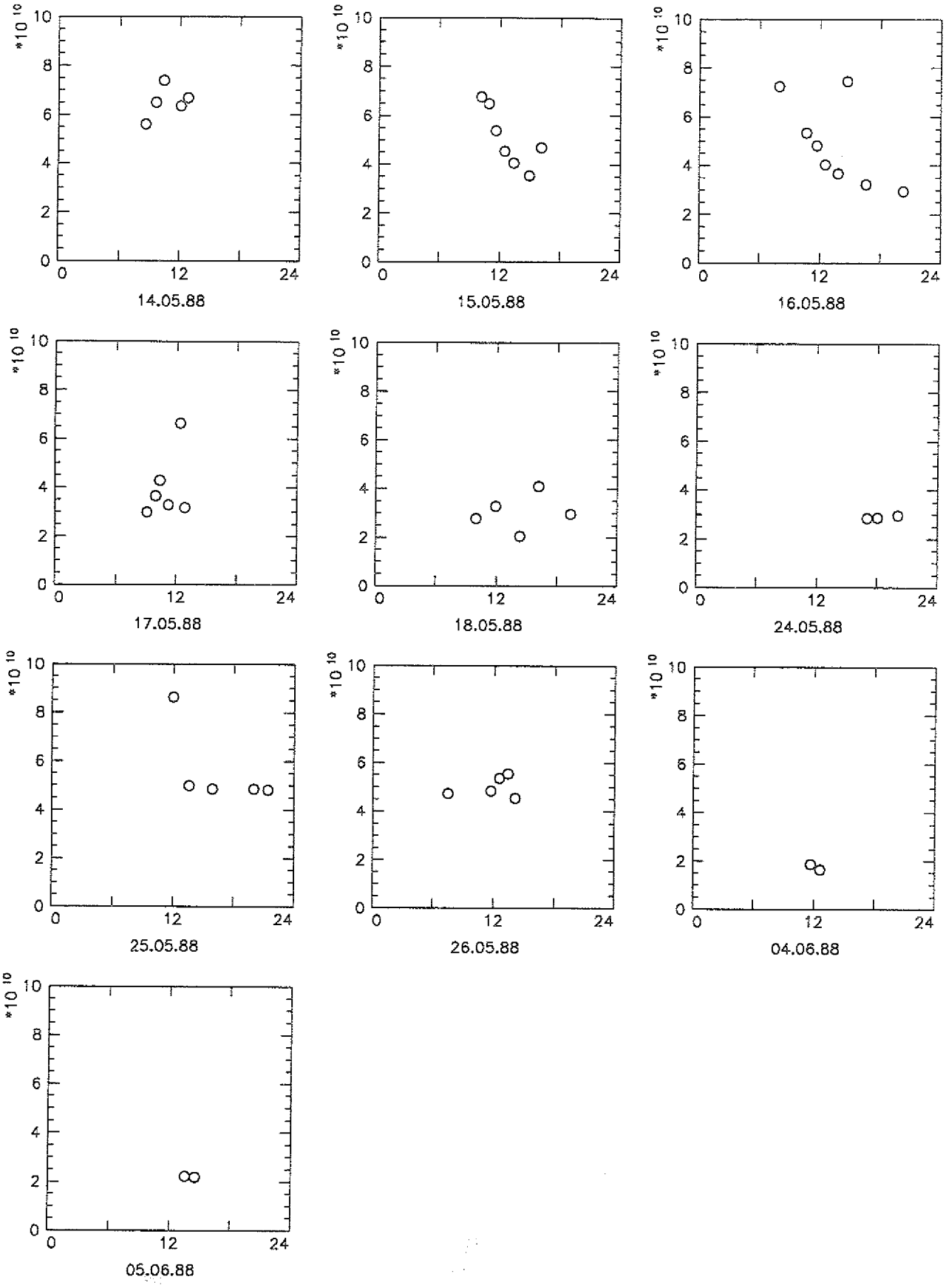

HCHO (DOAS) / cm^{-3}

File: HCHOUVF ENZ880HJ

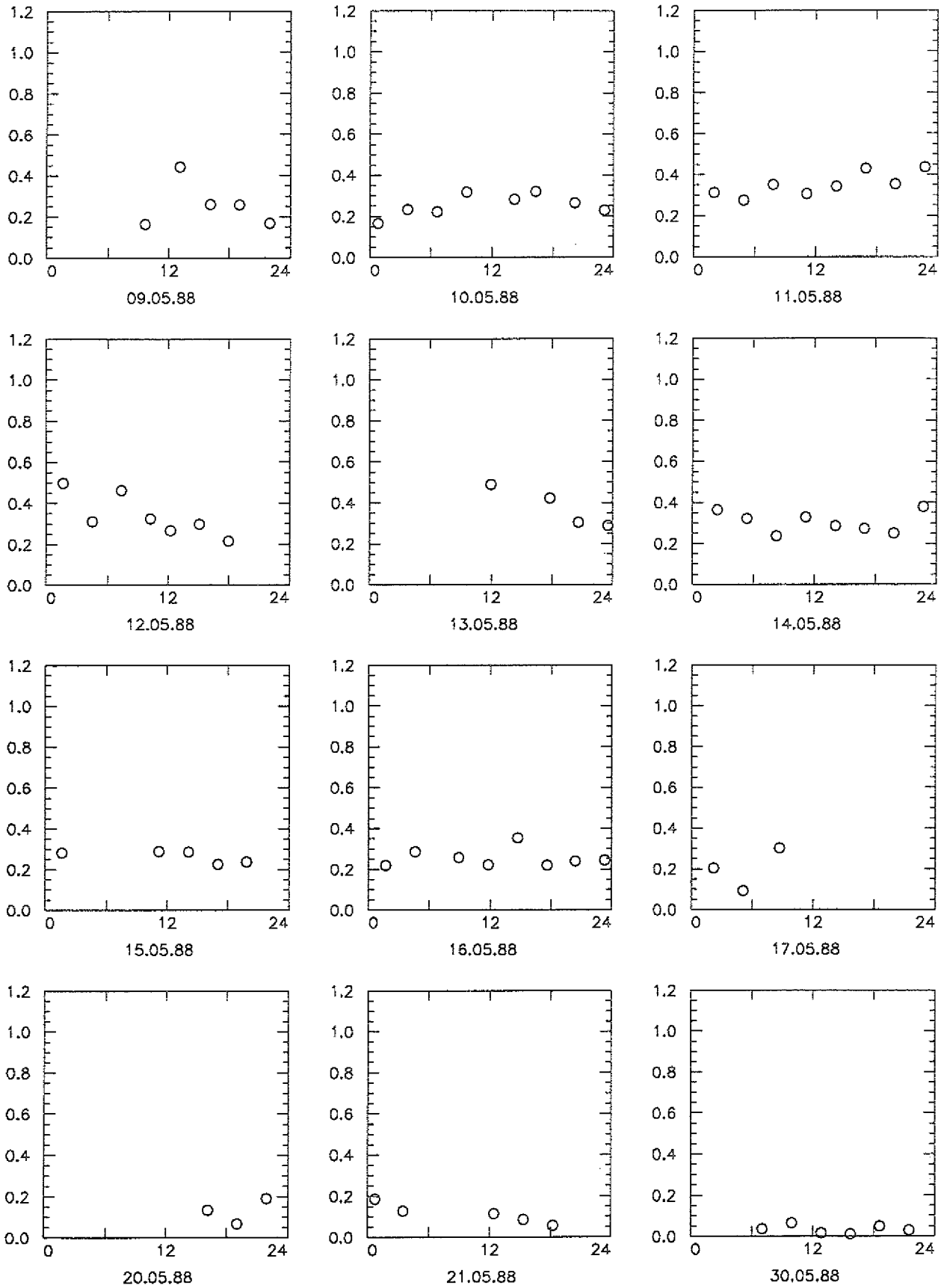

acetaldehyde / ppb

File: ACETALD ENZ880HJ

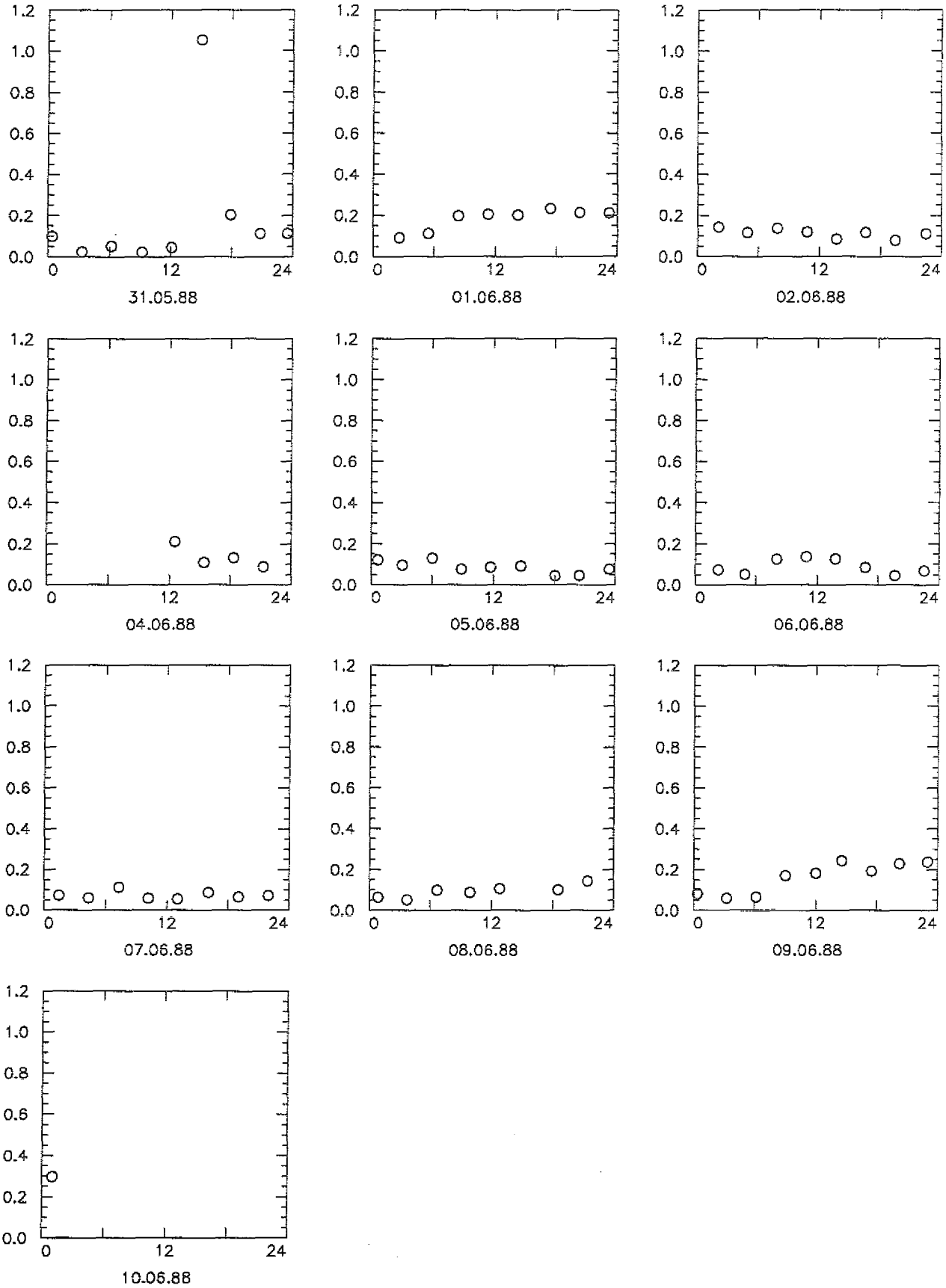

acetaldehyde / ppb

File: ACETALD ENZ880HJ

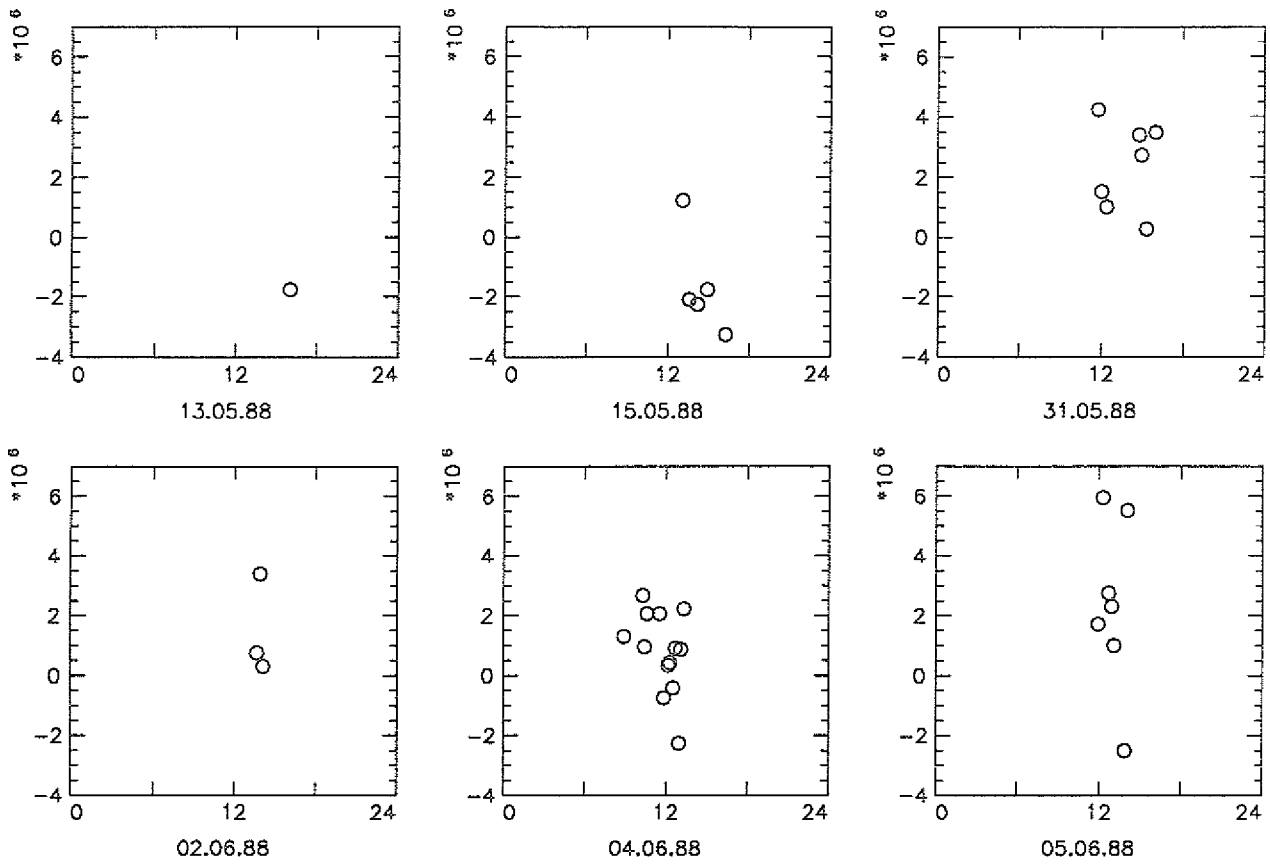

OH / cm^{-3} *File: OH ENZ880HJ*

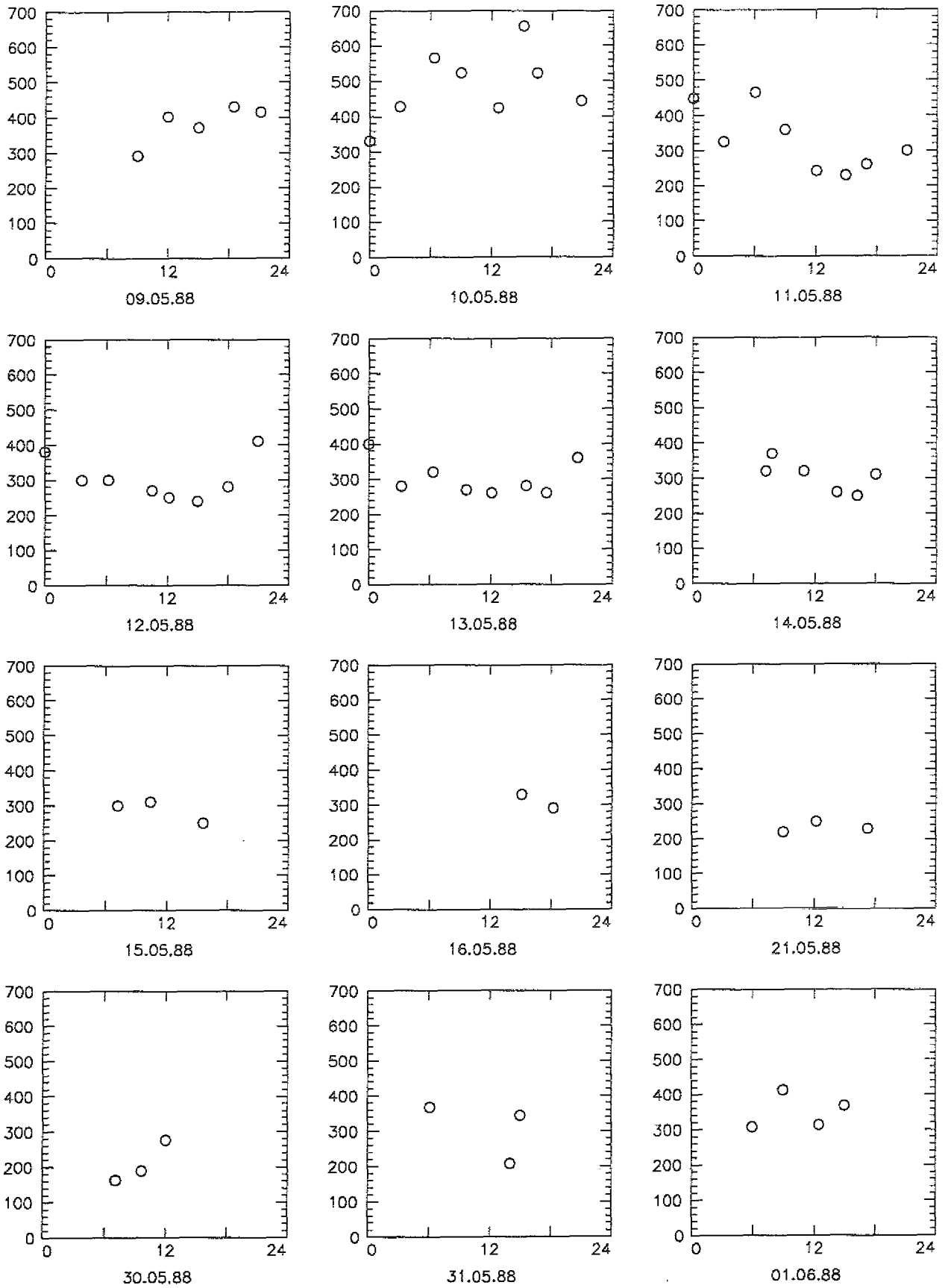

CO (grab sample) / ppb *File: CO_BHLTR ENZ880HJ*

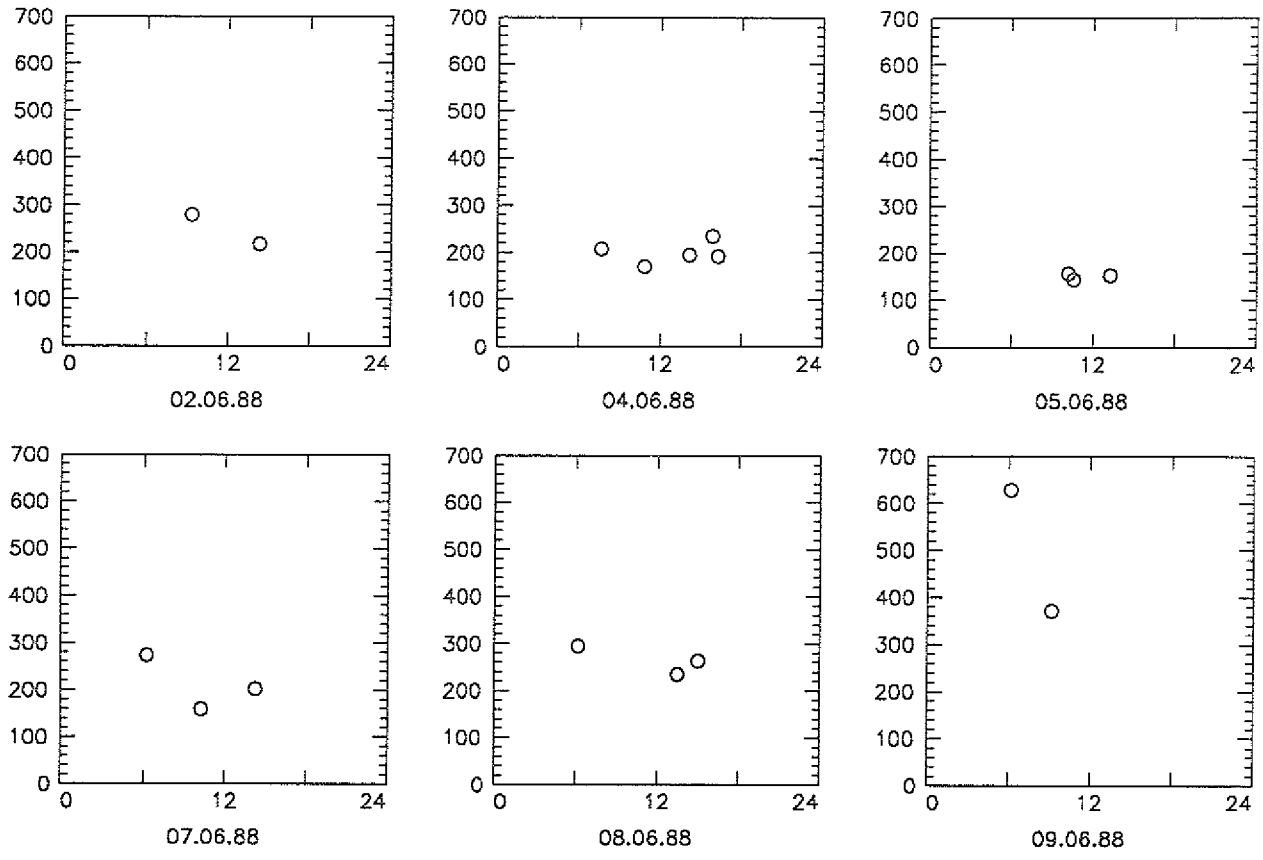

CO (grab sample) / ppb *File: CO_BHLTR ENZ880HJ*

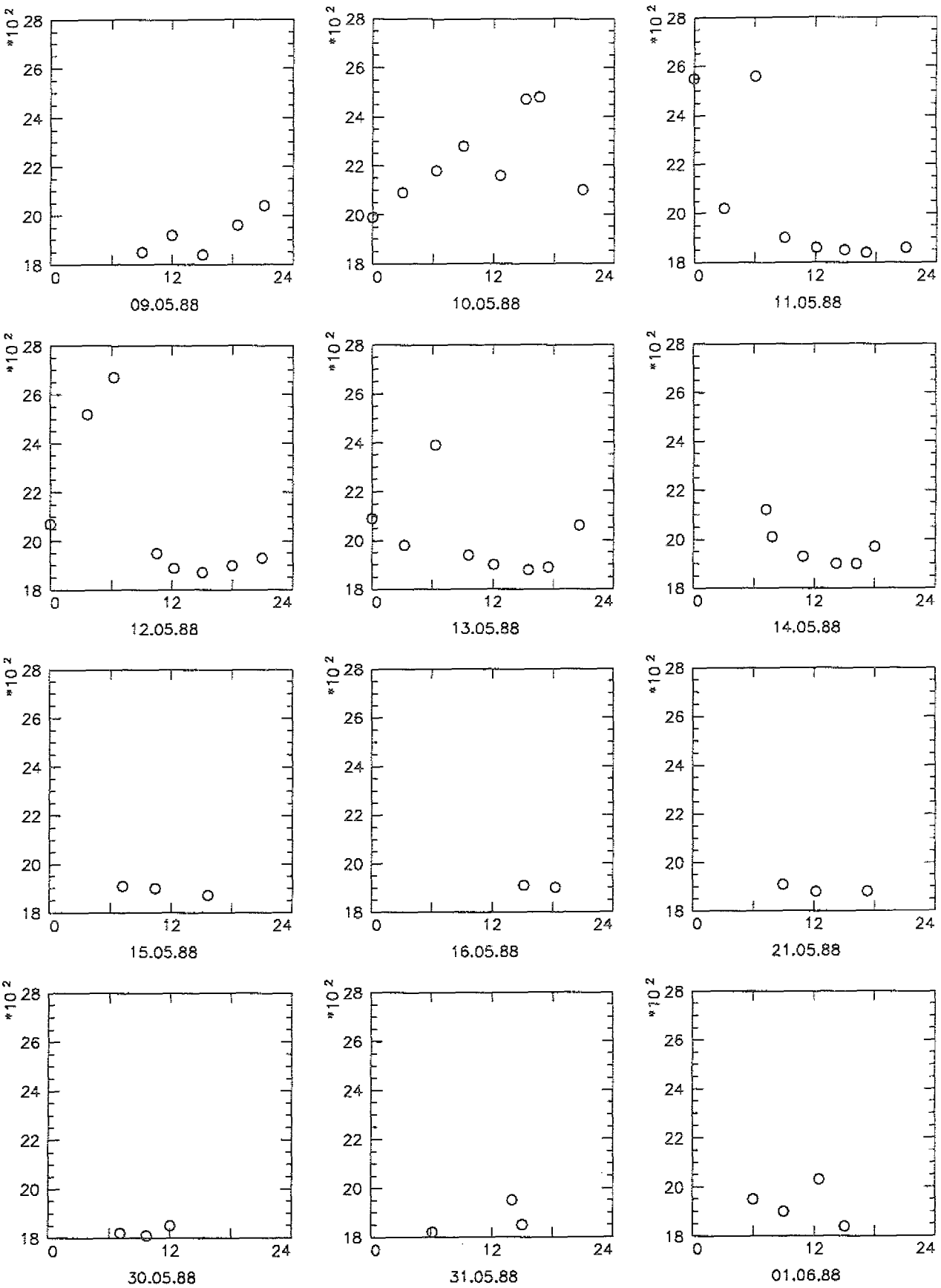

methane / ppb *File: CH4 ENZ880HJ*

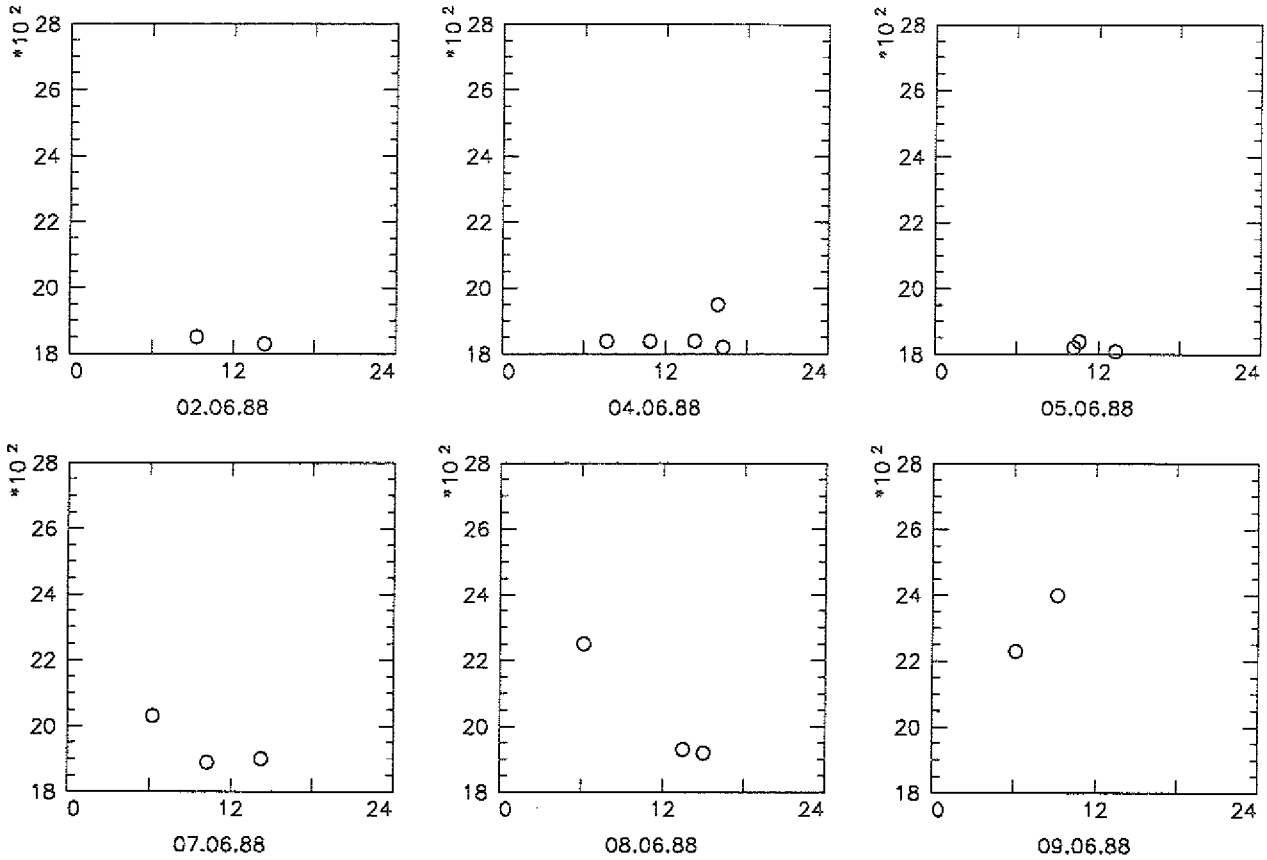

methane / ppb *File: CH4 ENZ880HJ*

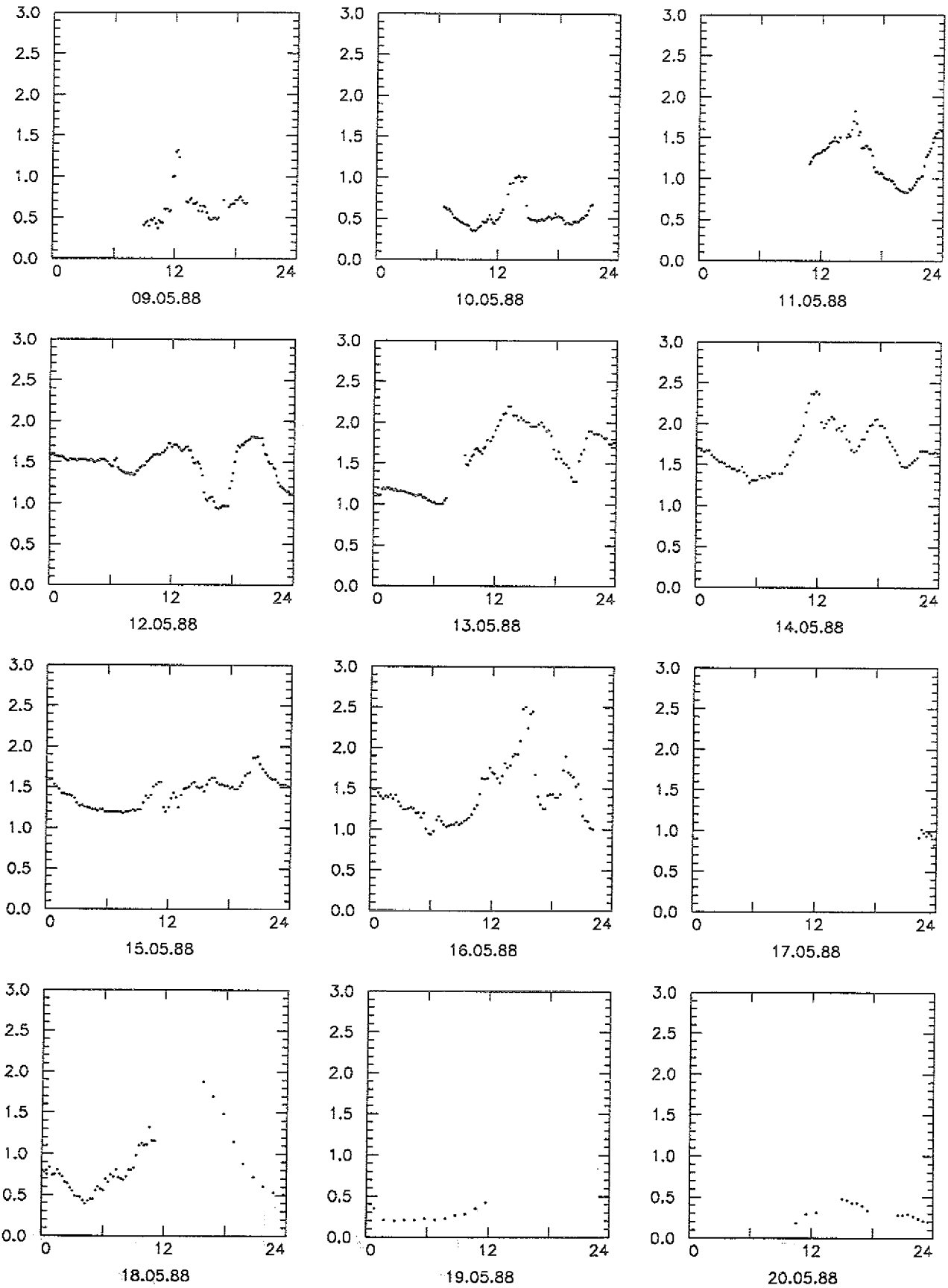

PAN / ppb

File: PAN ENZ880HJ

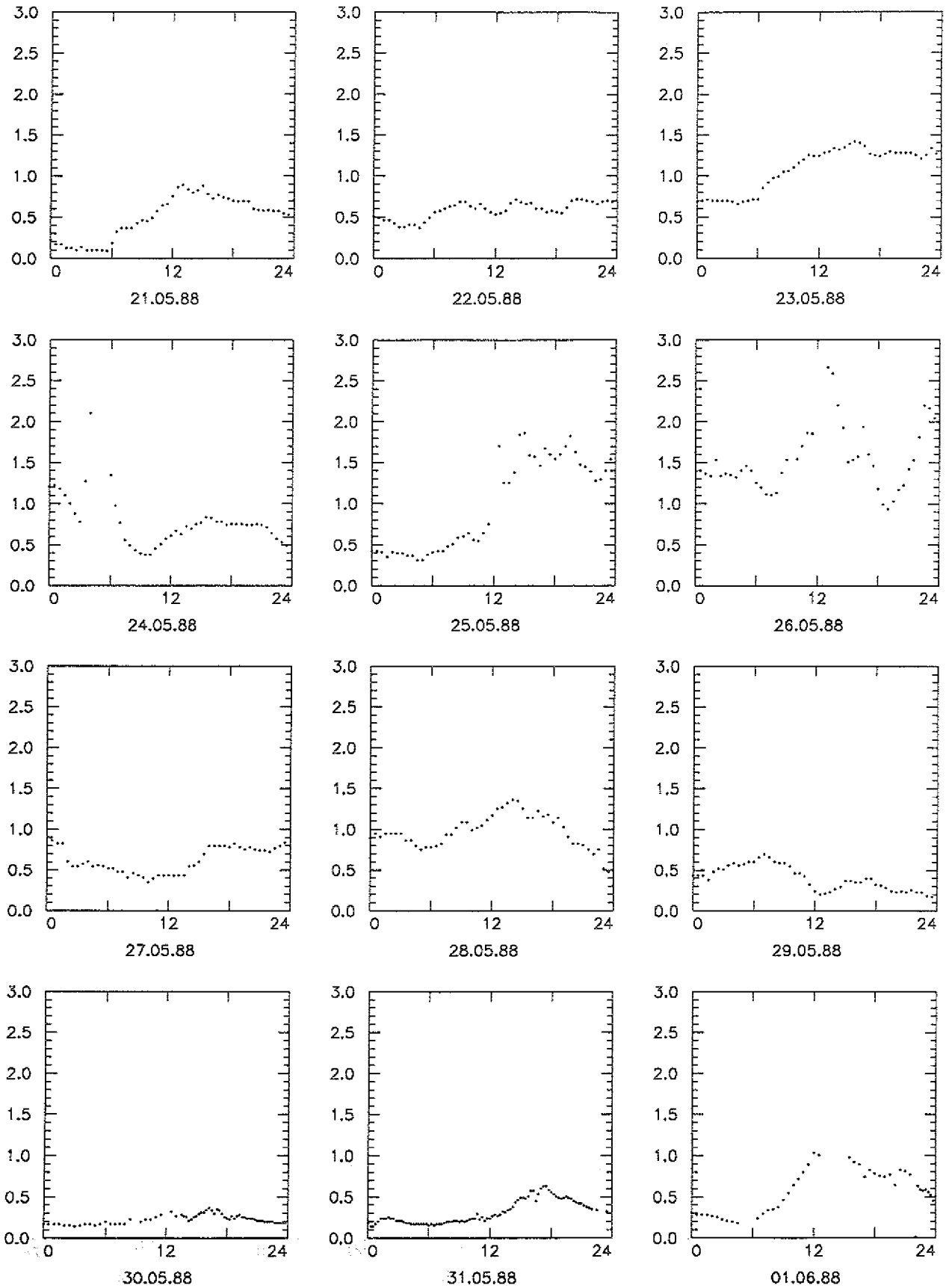

PAN / ppb *File: PAN ENZ880HJ*

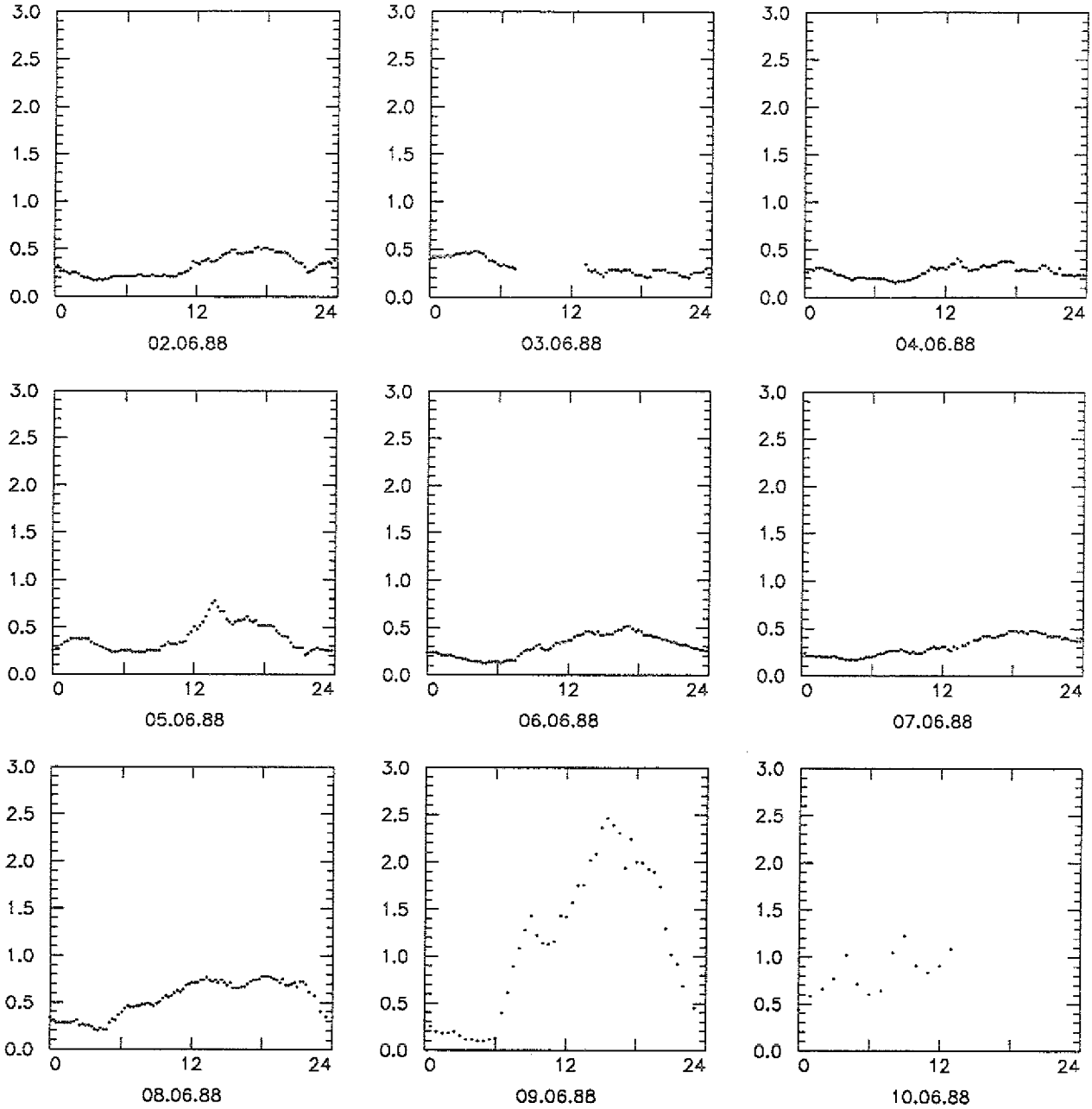

PAN / ppb *File: PAN ENZ880HJ*

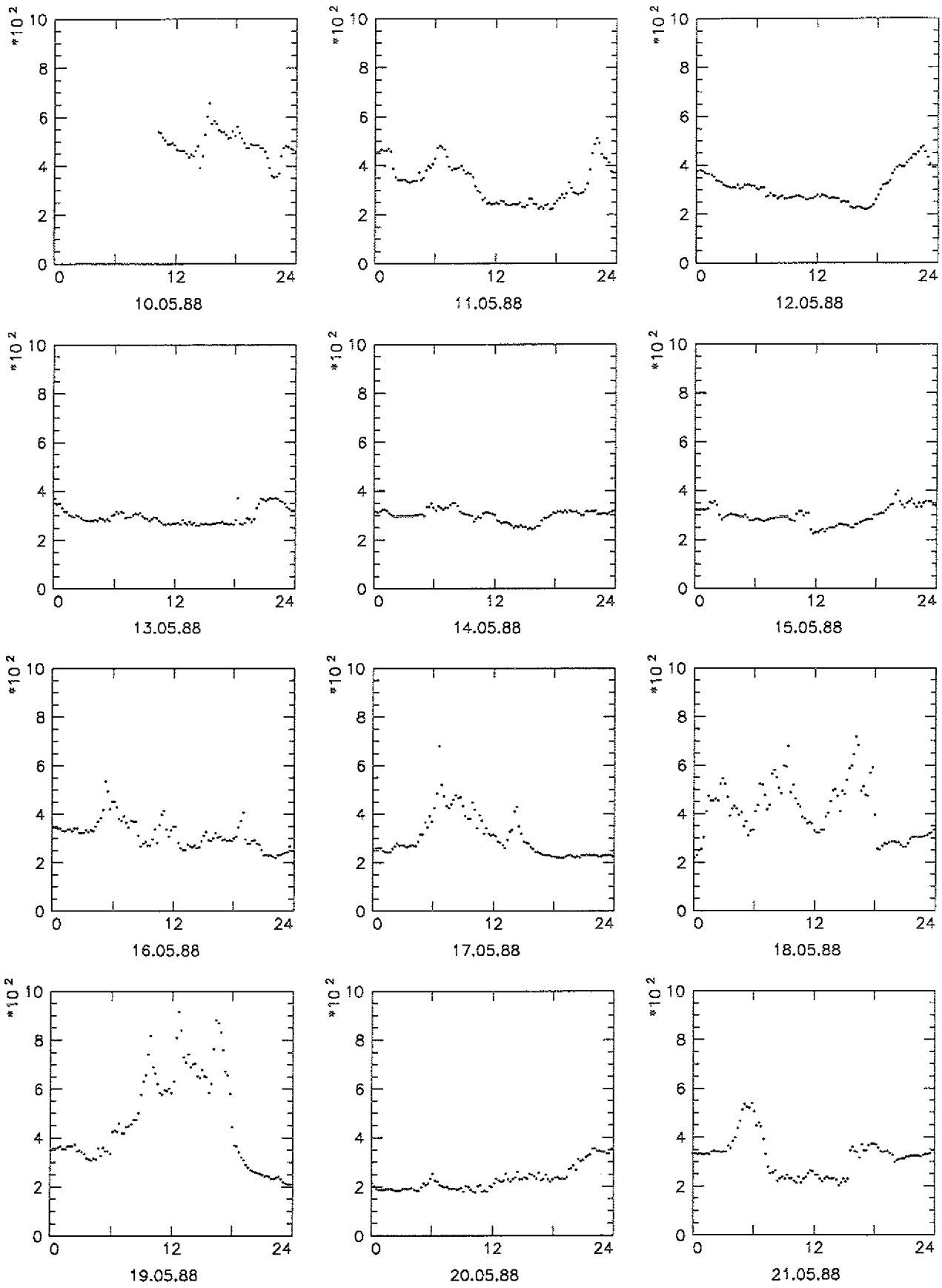

CO (in situ) / ppb *File: COINSIK ENZ880HJ*

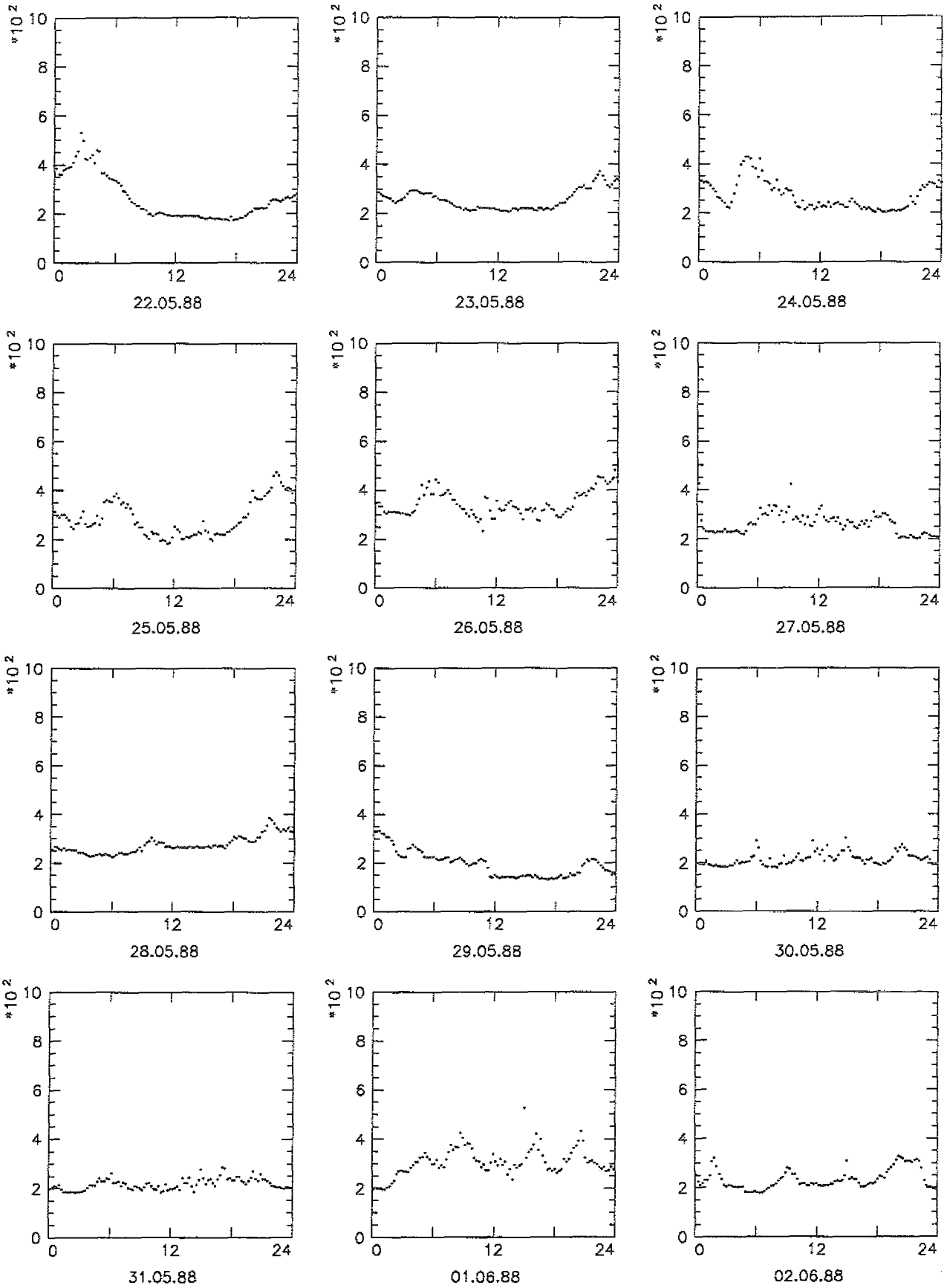

CO (in situ) / ppb *File: COINSIK ENZ880HJ*

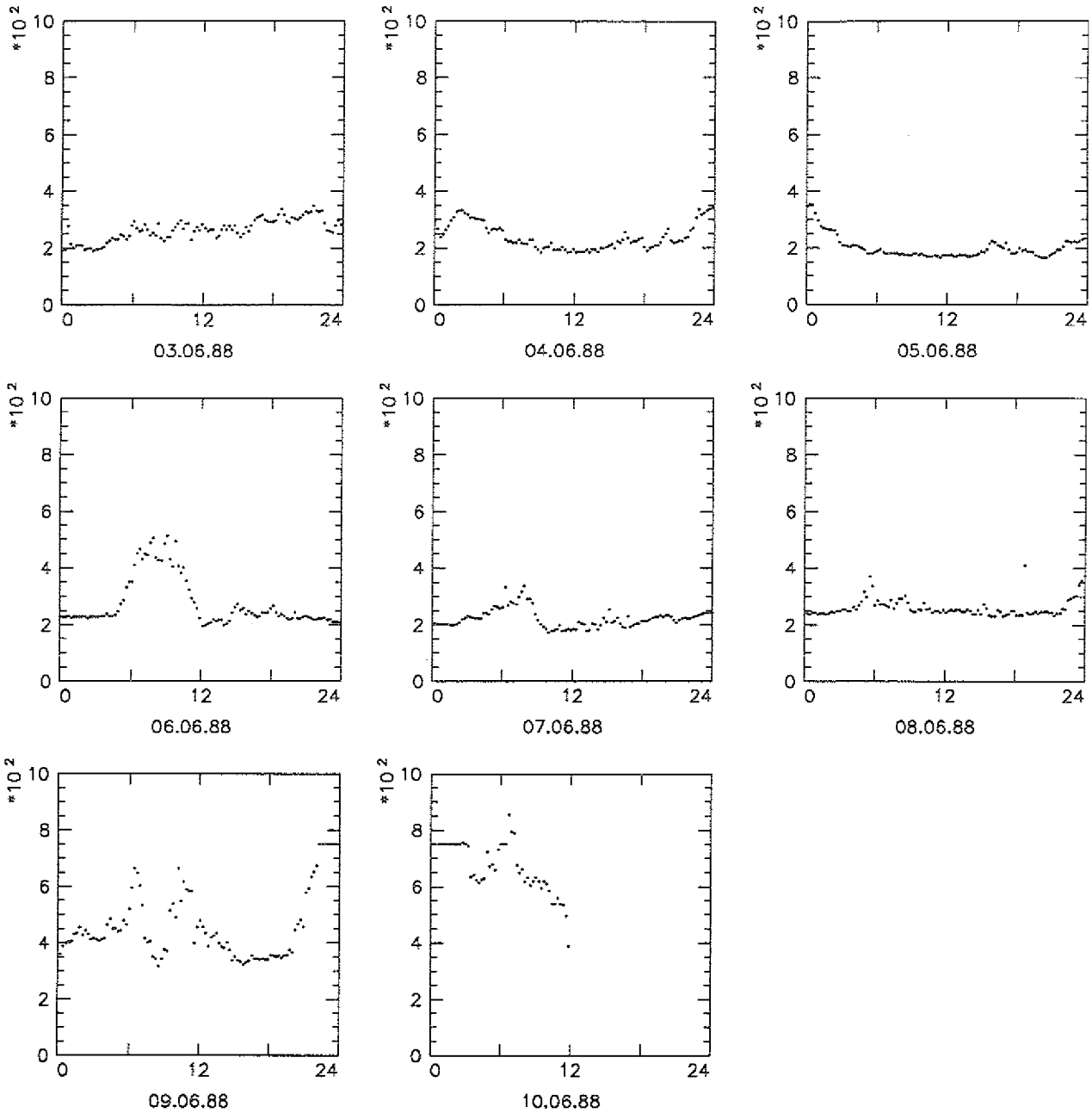

CO (in situ) / ppb *File: COINSIK ENZ880HJ*

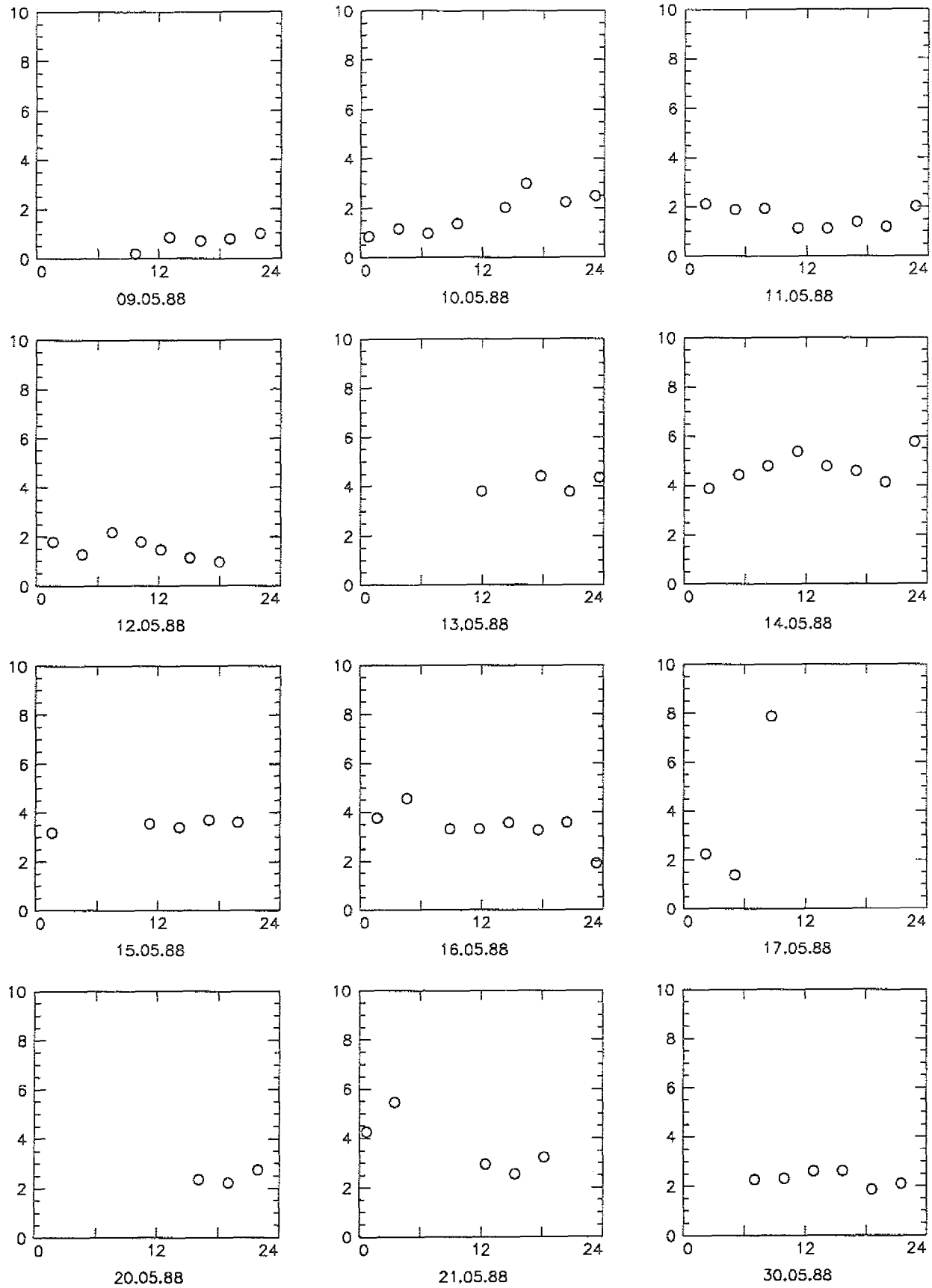

ethane / ppb

File: ETHAN ENZ880HJ

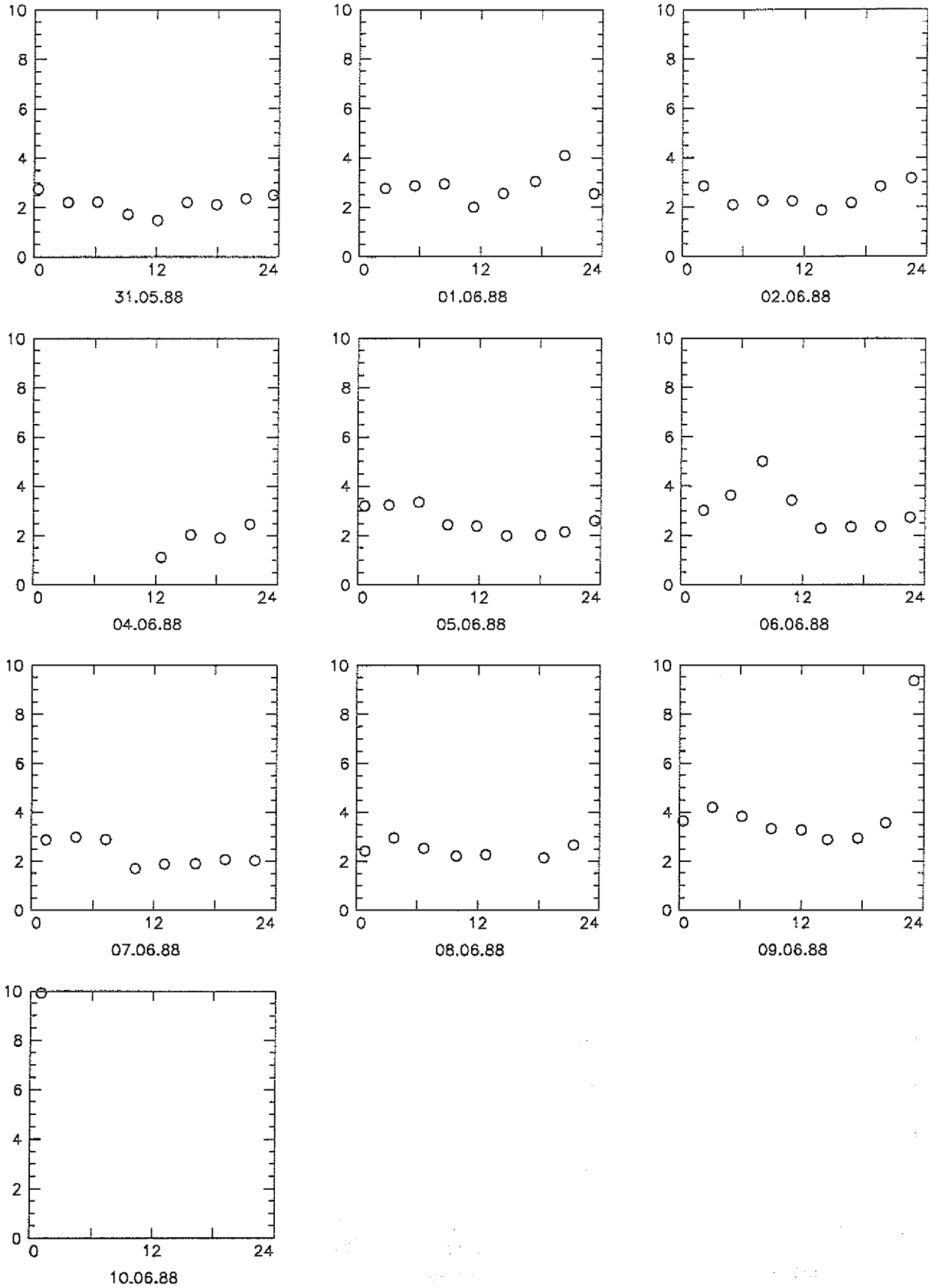

ethane / ppb *File: ETHAN ENZ880HJ*

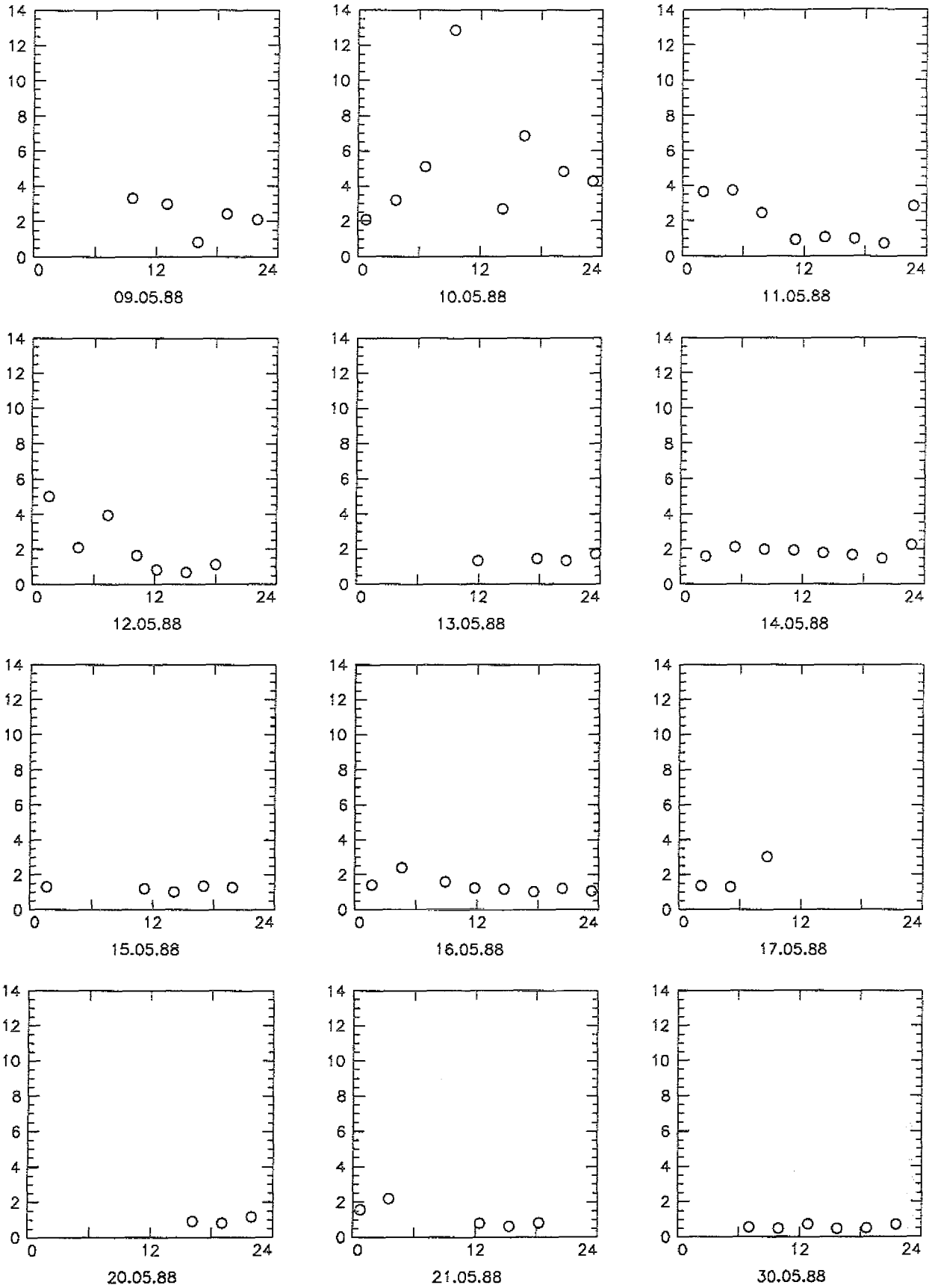

propane / ppb *File: PROPAN ENZ880HJ*

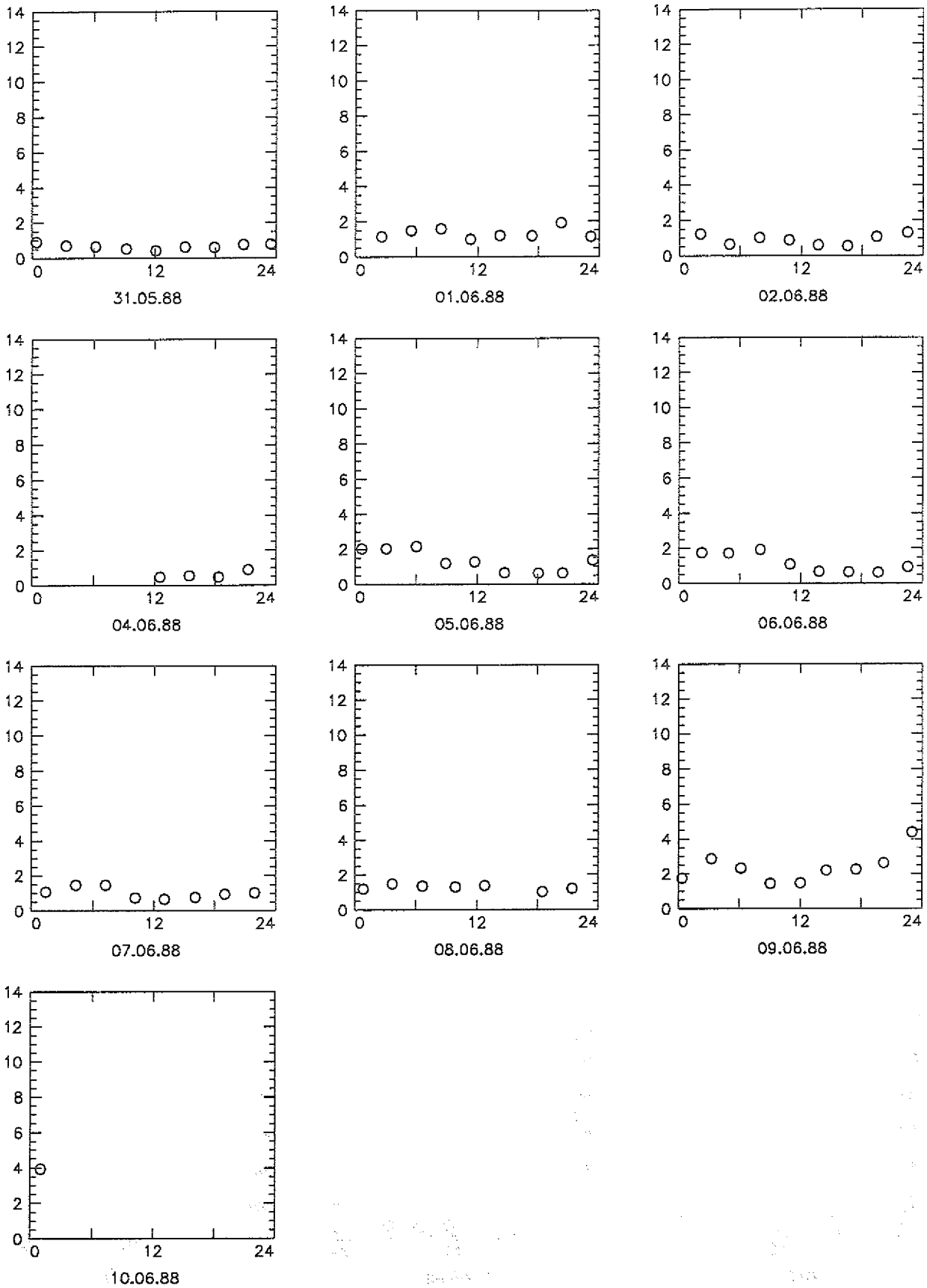

propane / ppb *File: PROPAN ENZ880HJ*

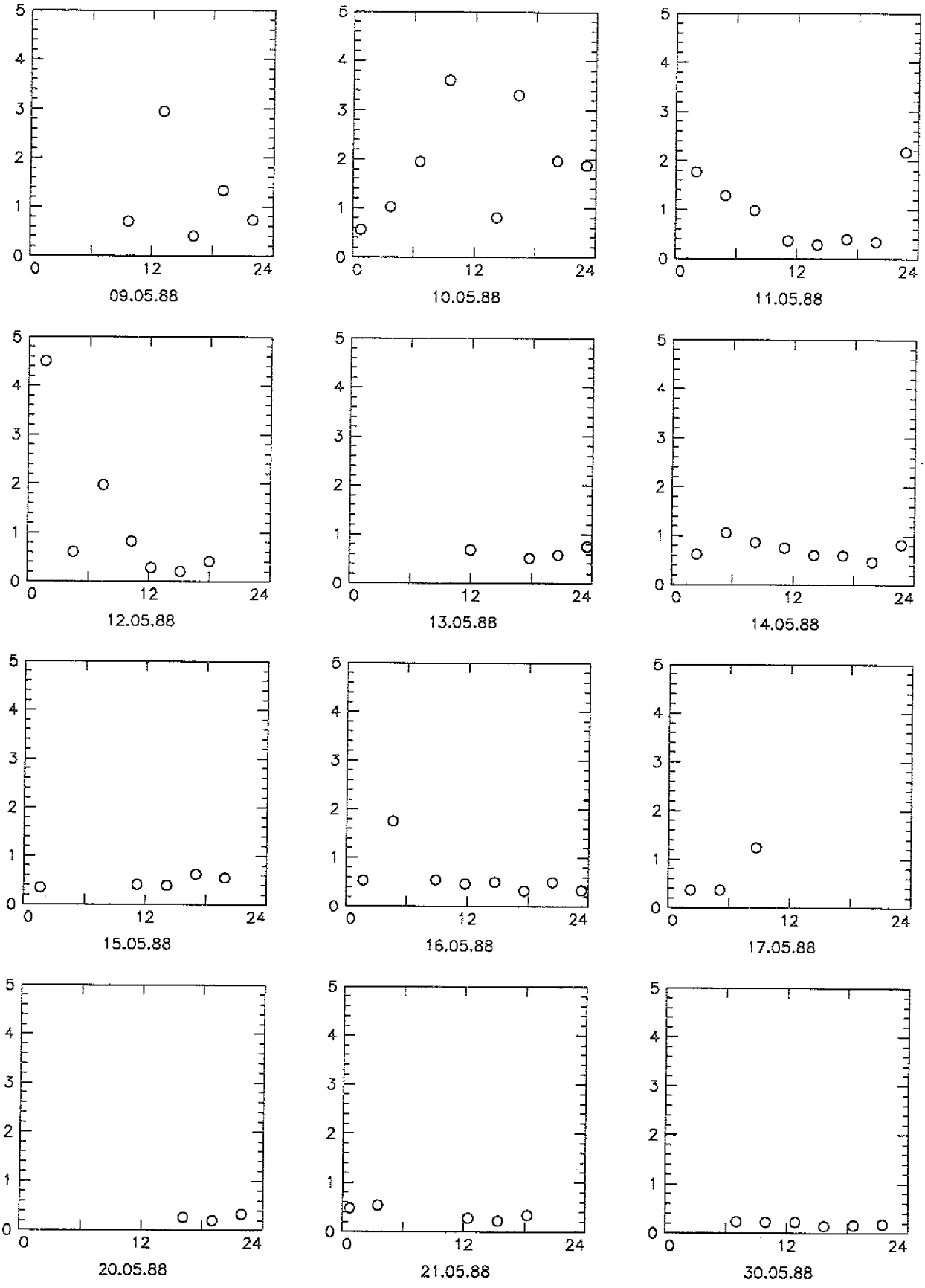

i–butane / ppb

File: I–BUTAN ENZ880HJ

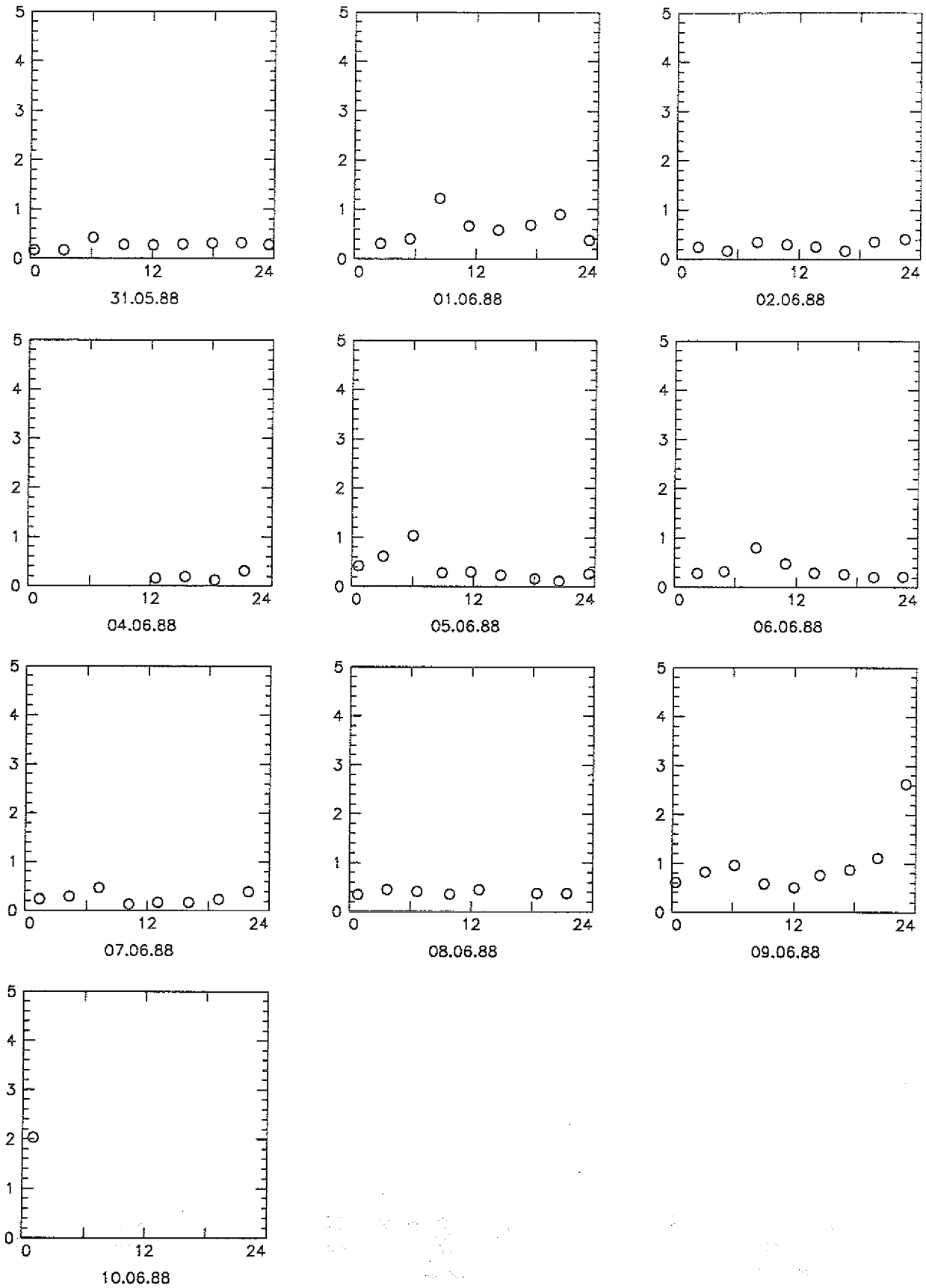

i–butane / ppb

File: I–BUTAN ENZ880HJ

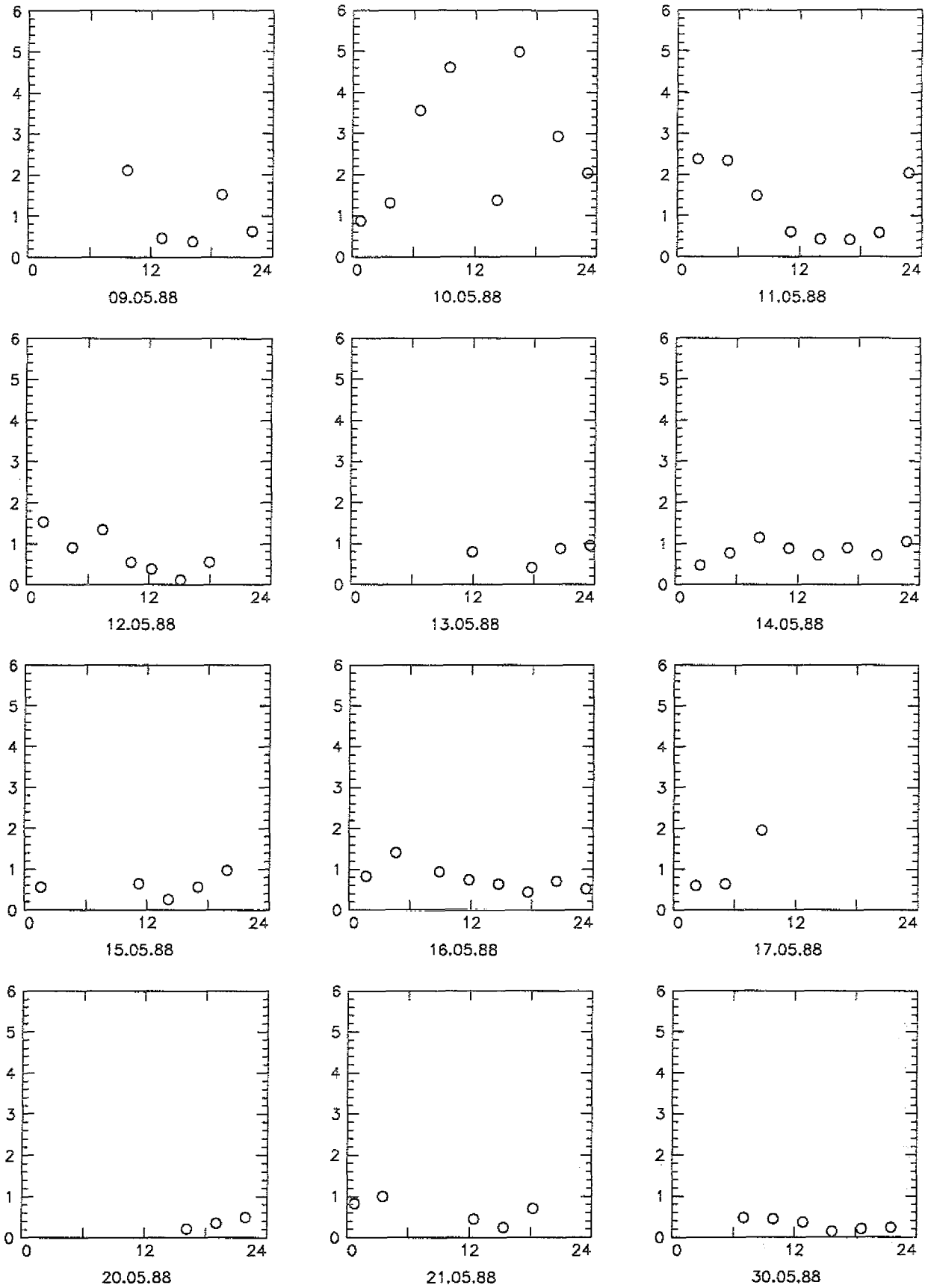

n–butane / ppb

File: N–BUTAN ENZ880HJ

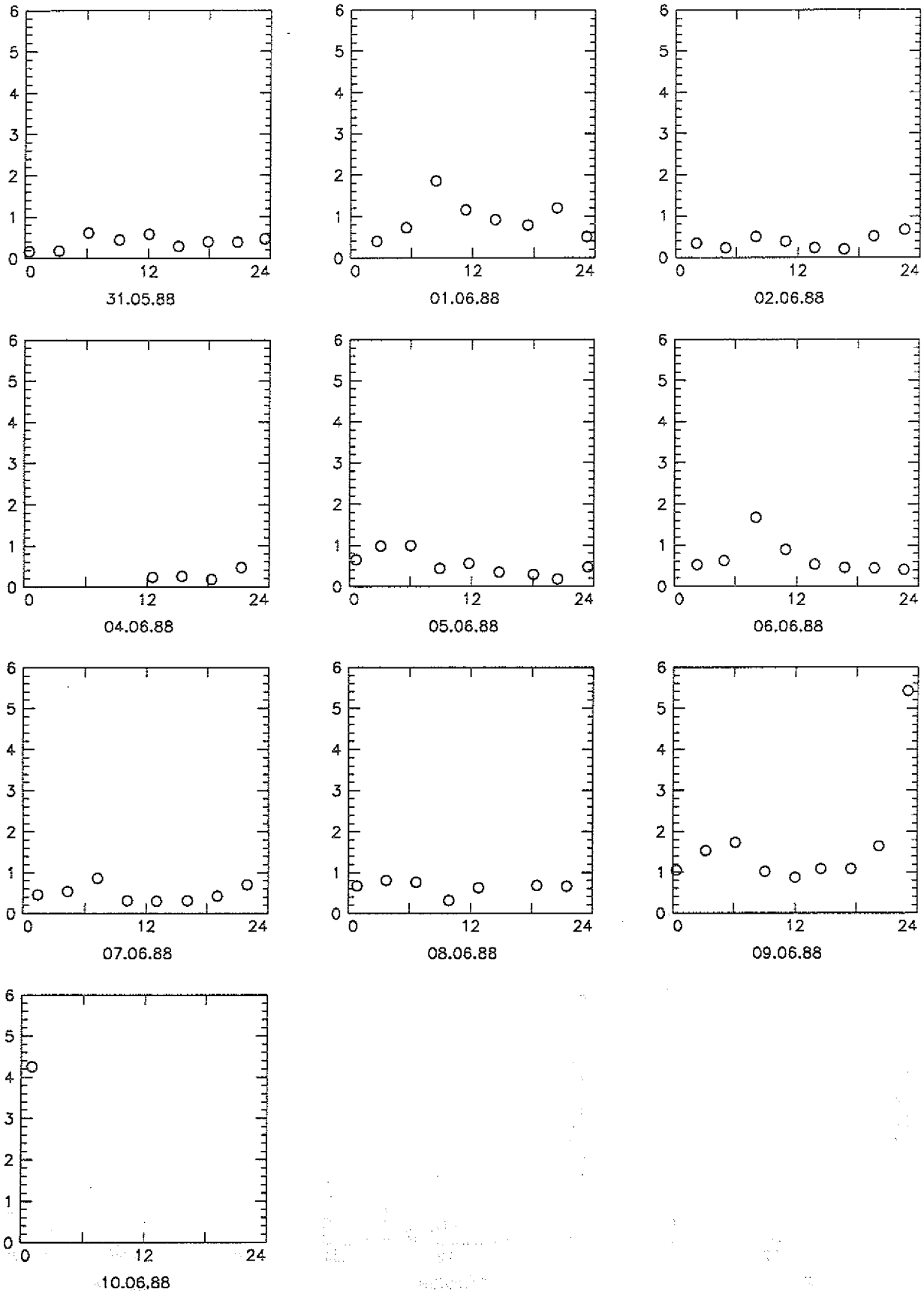

n-butane / ppb

File: N-BUTAN ENZ880HJ

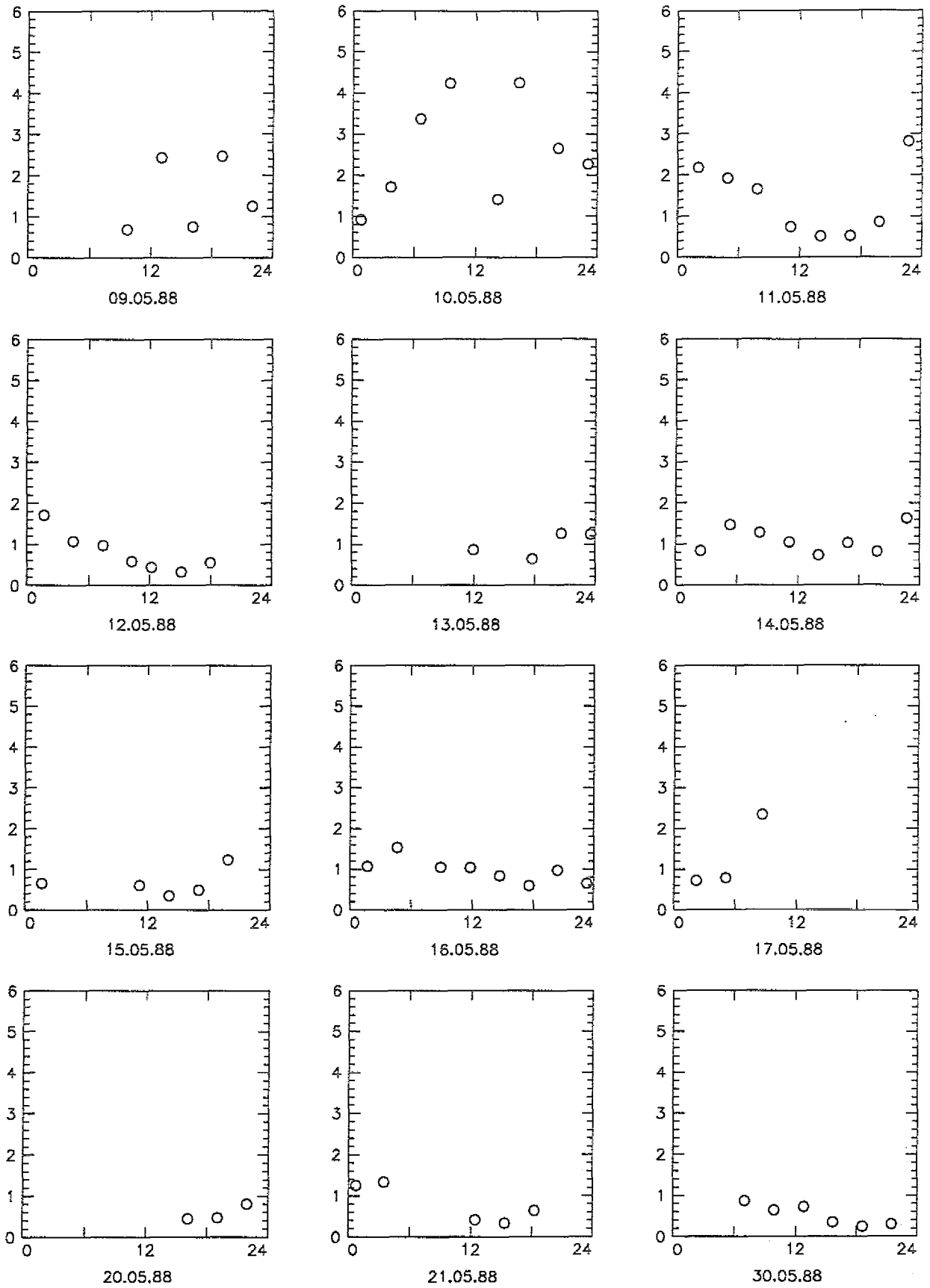

i–pentane / ppb

File: I–PENTAN ENZ880HJ

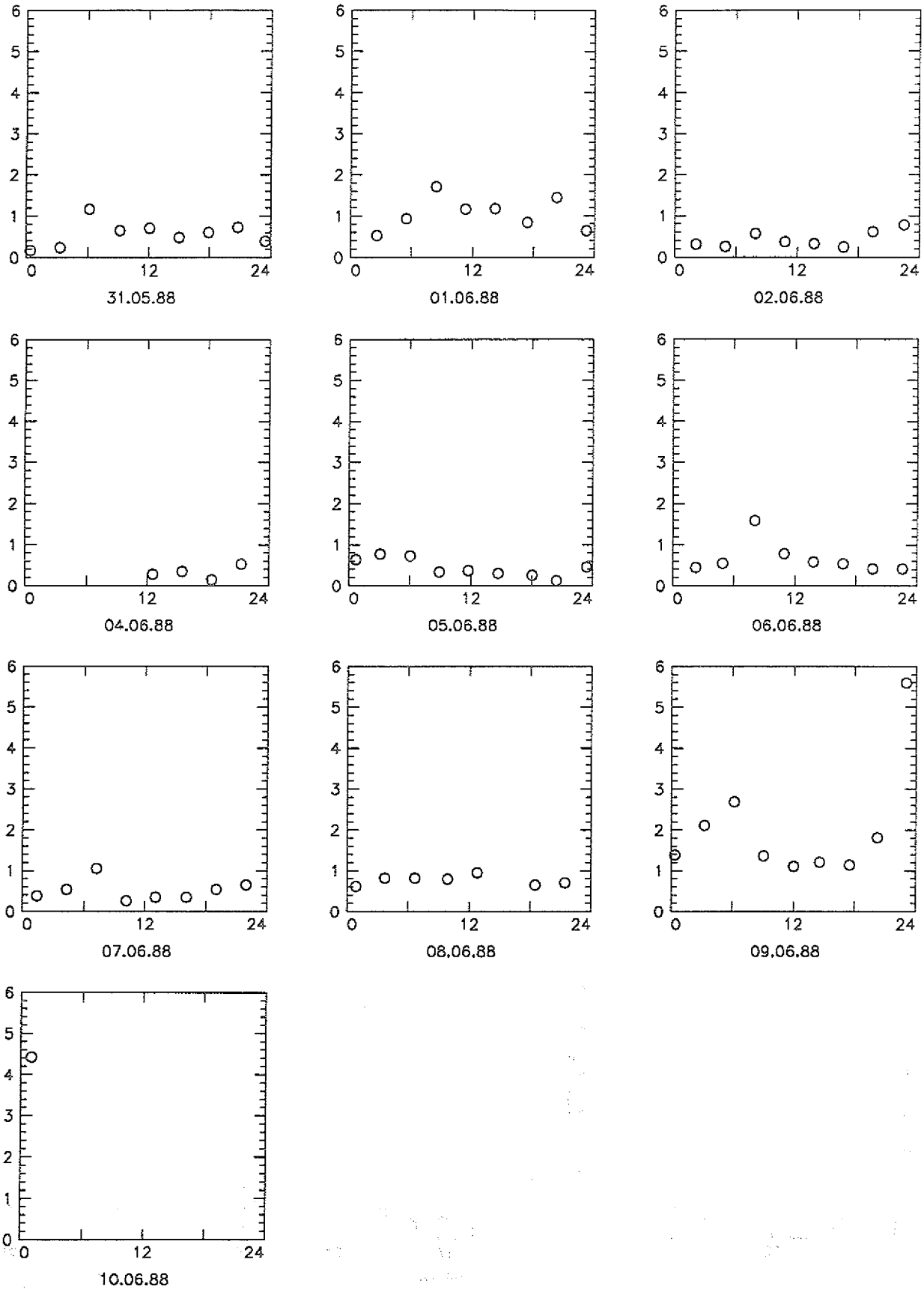

i-pentane / ppb

File: I-PENTAN ENZ880HJ

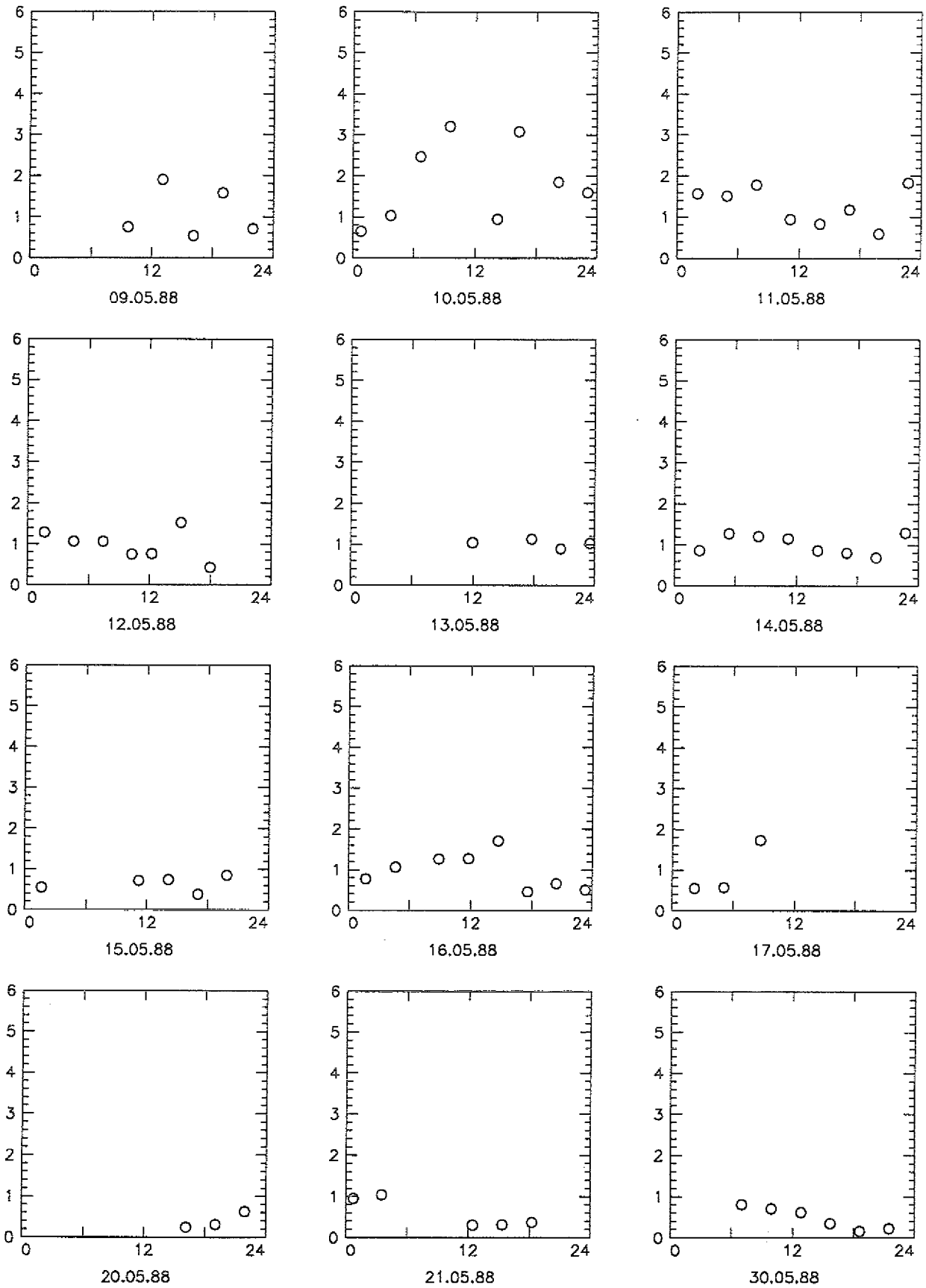

n–pentane / ppb

File: N–PENTAN ENZ880HJ

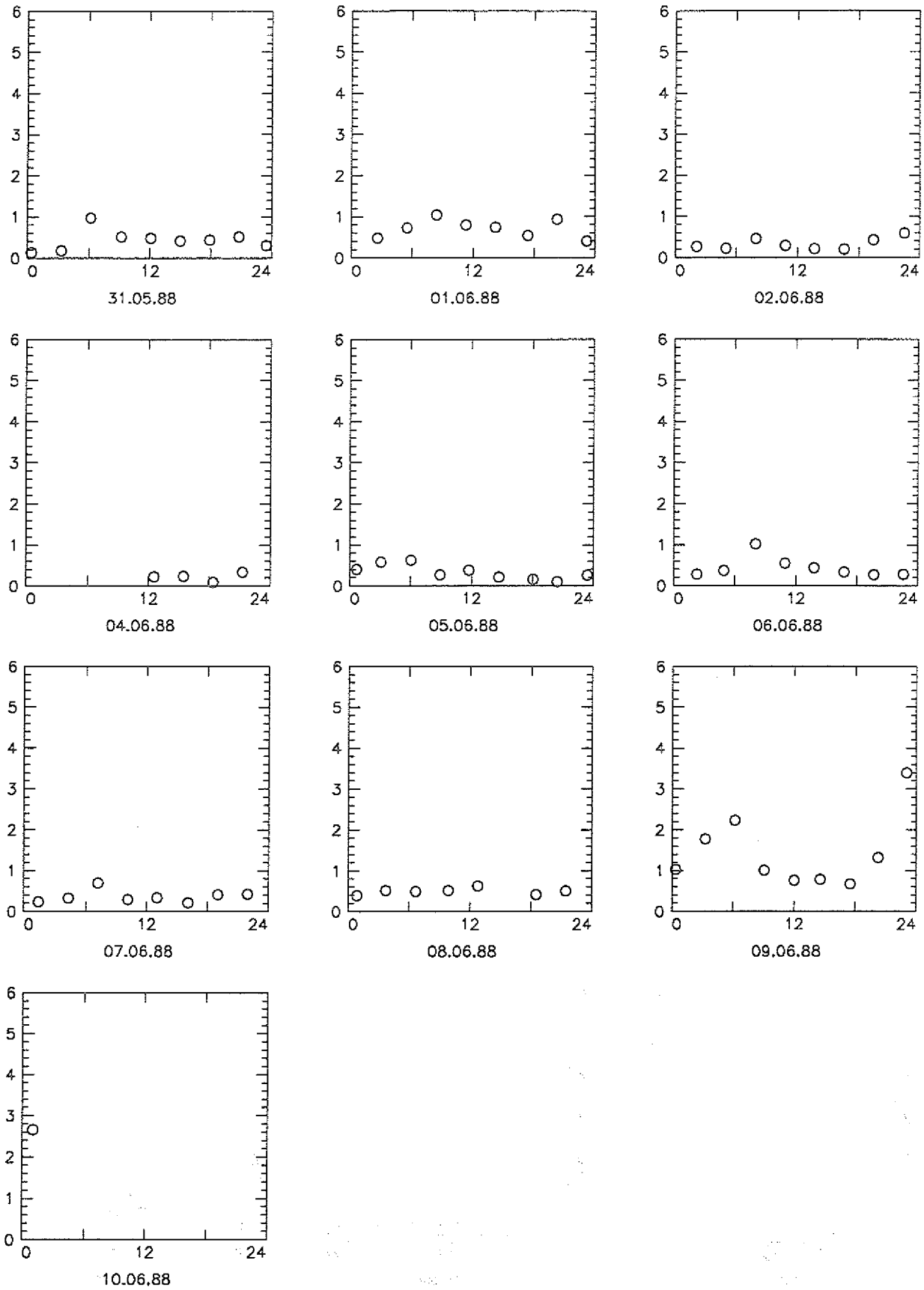

n-pentane / ppb

File: N-PENTAN ENZ880HJ

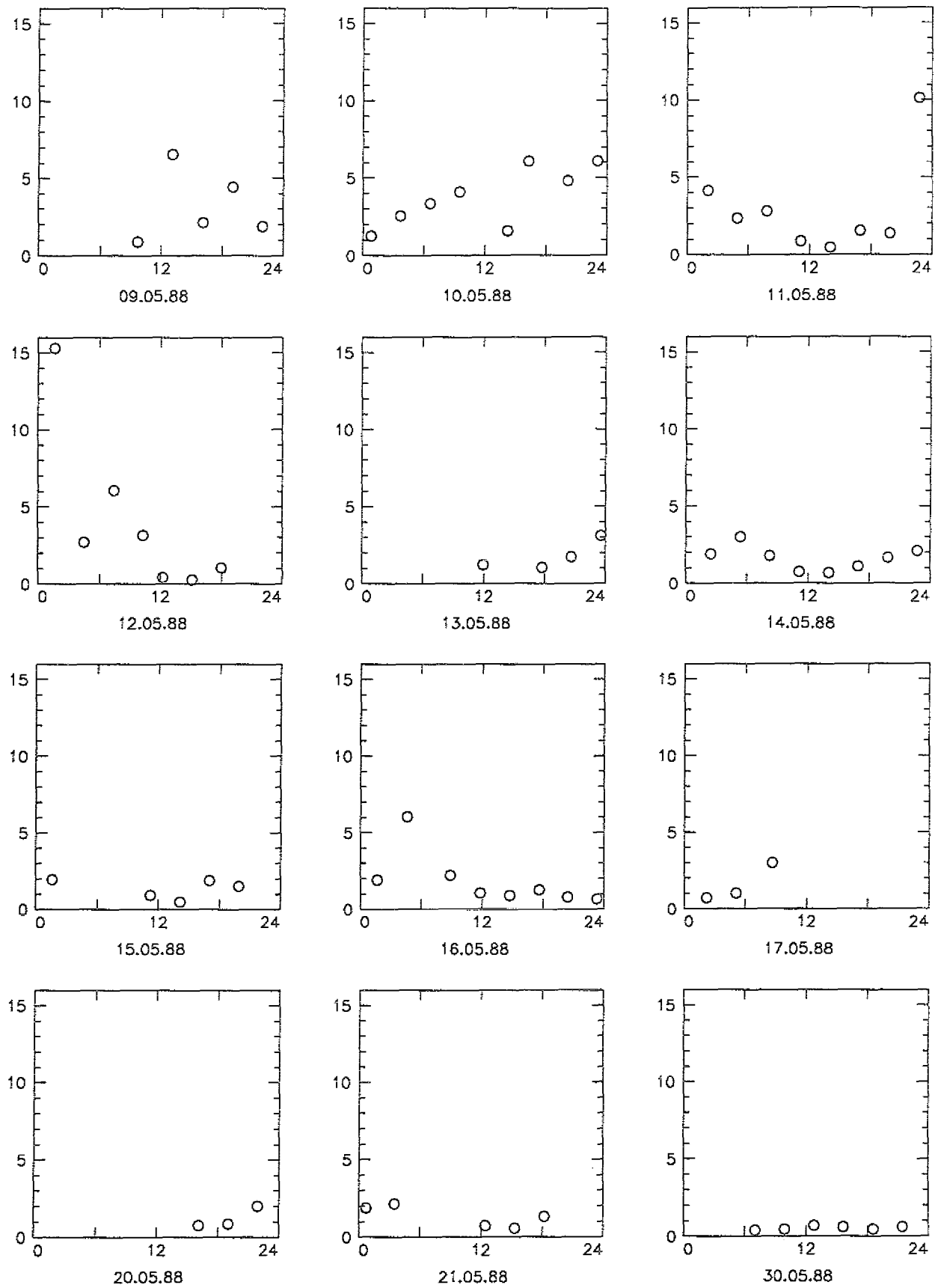

ethene / ppb *File: ETHEN ENZ880HJ*

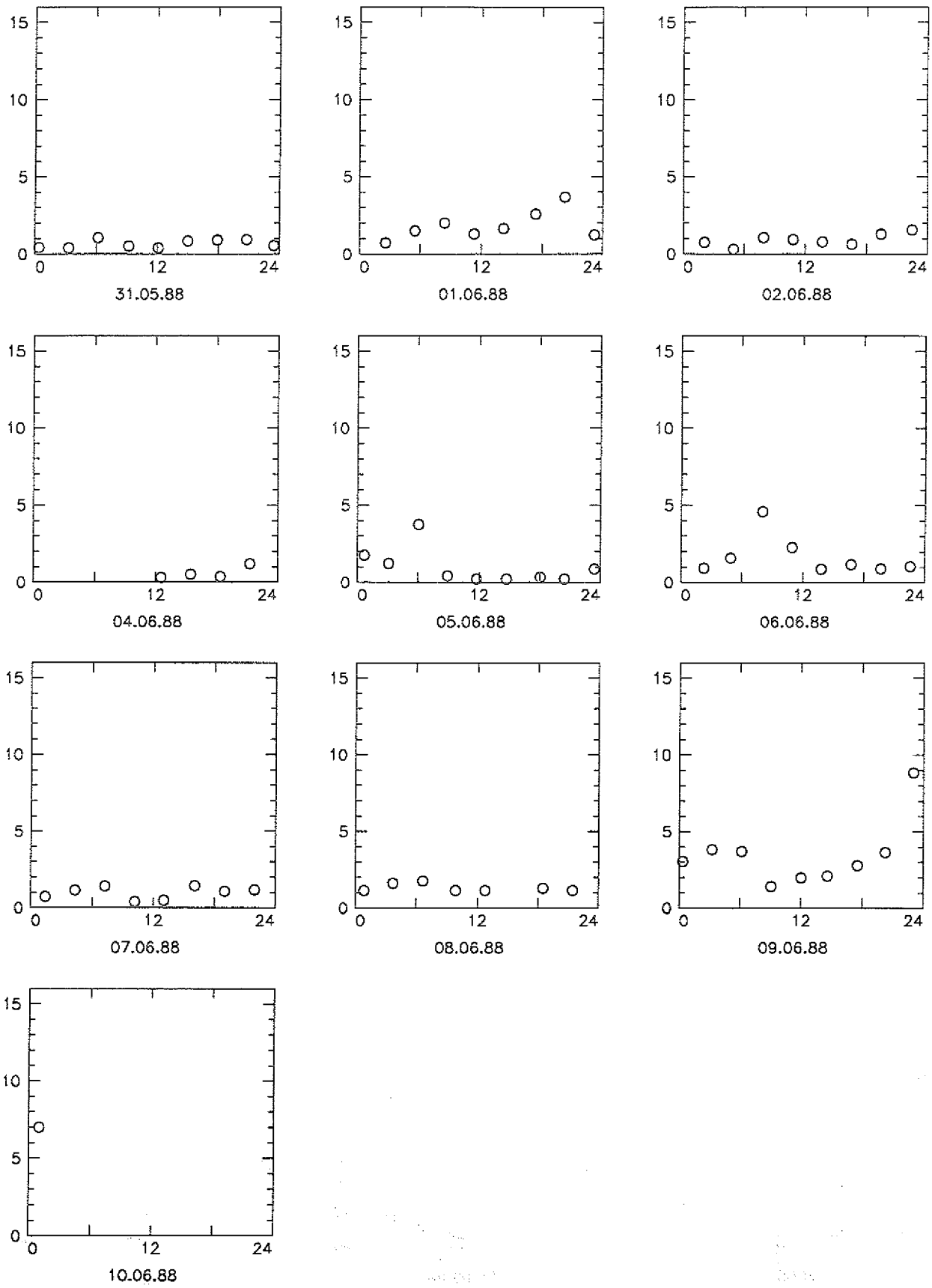

ethene / ppb *File: ETHEN ENZ880HJ*

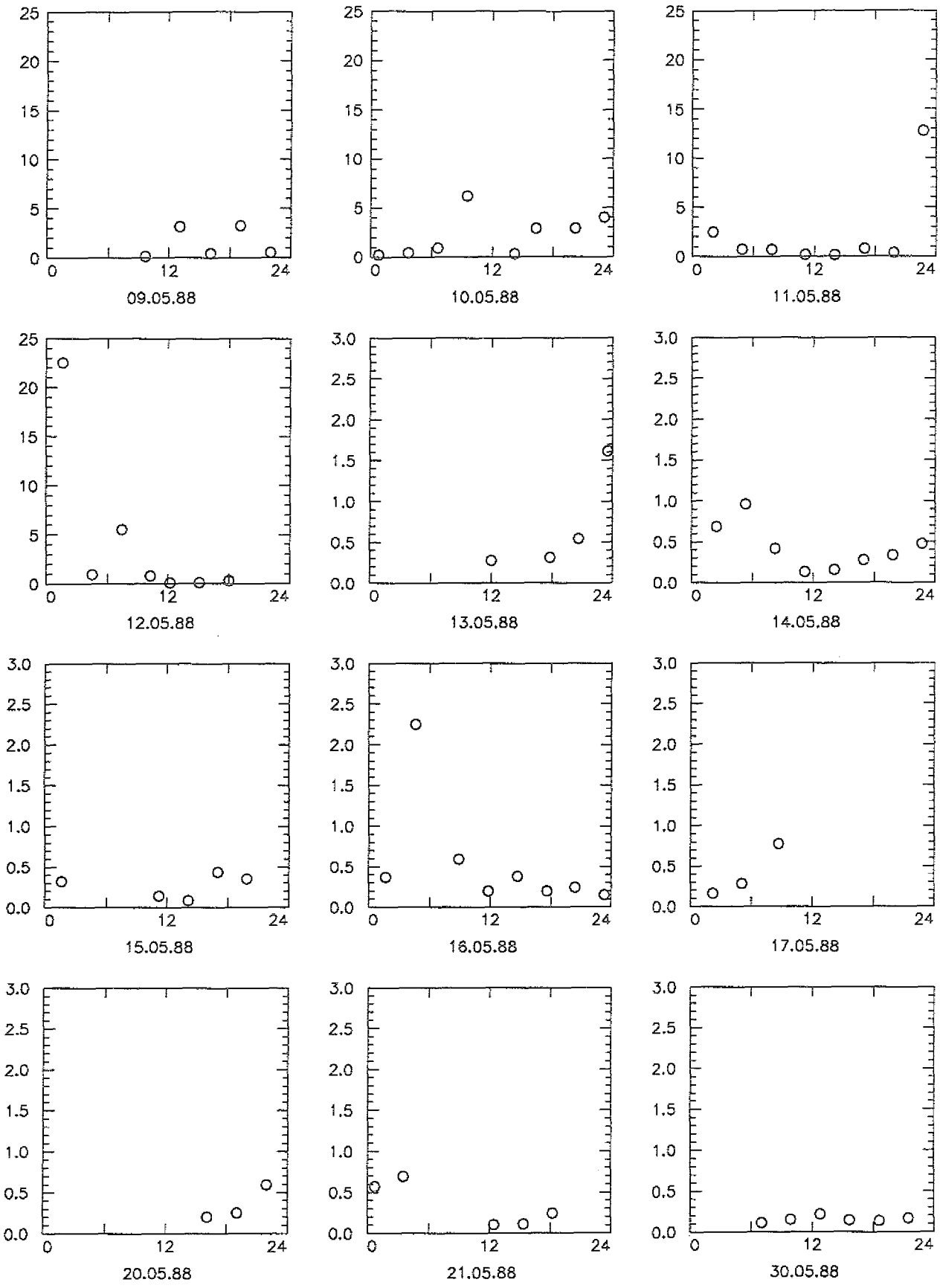

propene / ppb

File: PROPEN ENZ880HJ

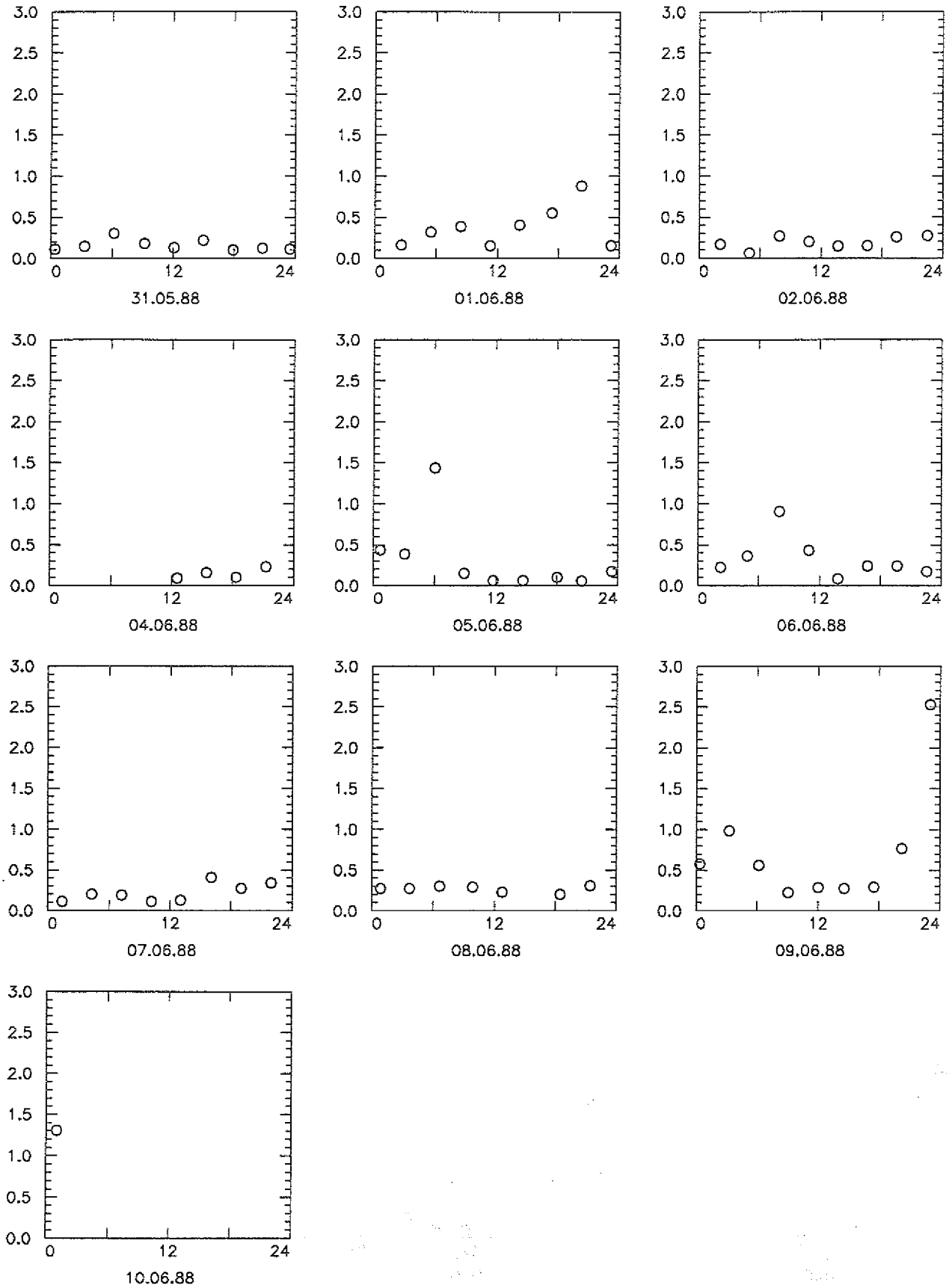

propene / ppb *File: PROPEN ENZ880HJ*

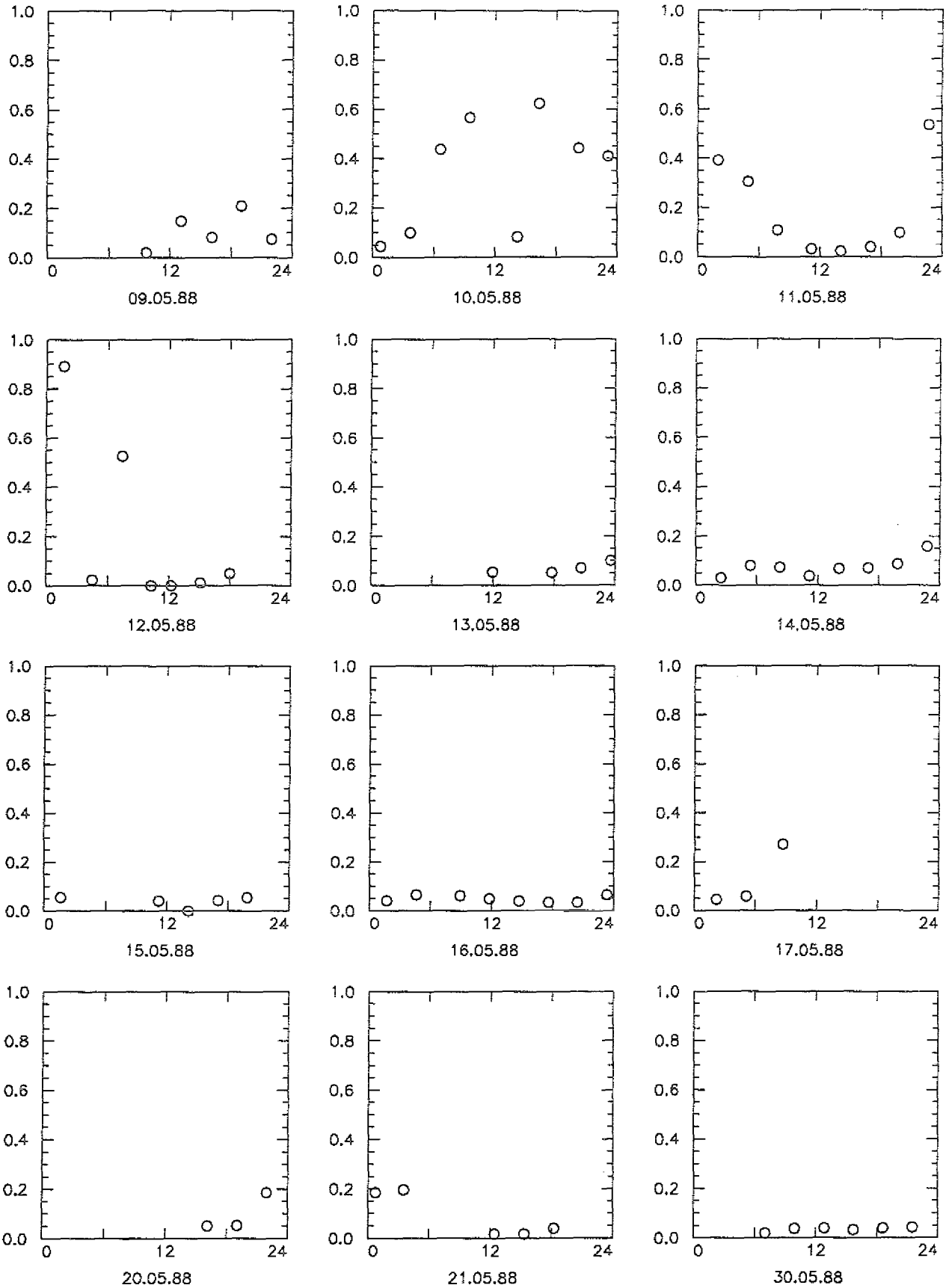

1-butene / ppb

File: 1-BUTEN ENZ880HJ

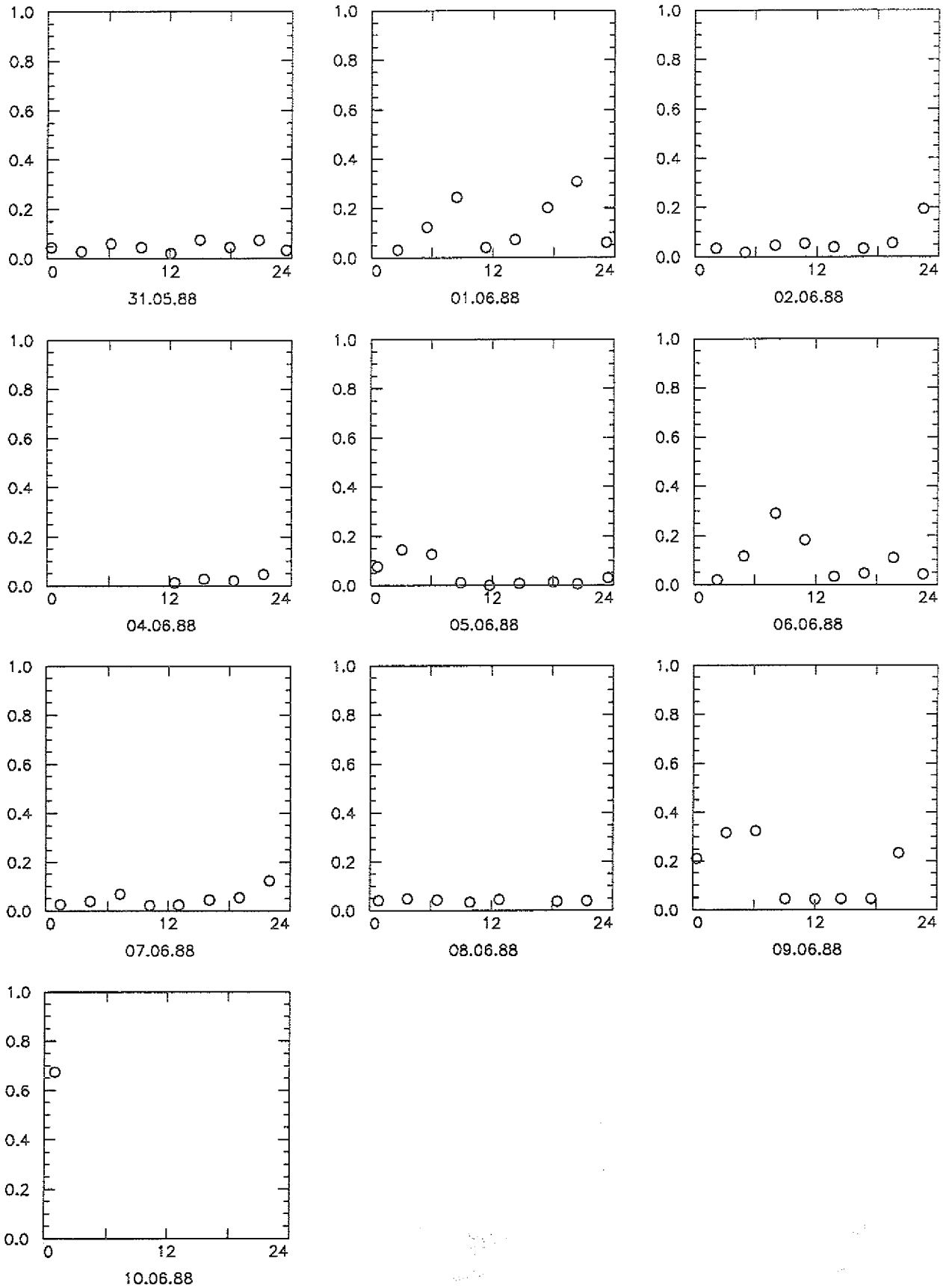

1-butene / ppb

File: 1-BUTEN ENZ880HJ

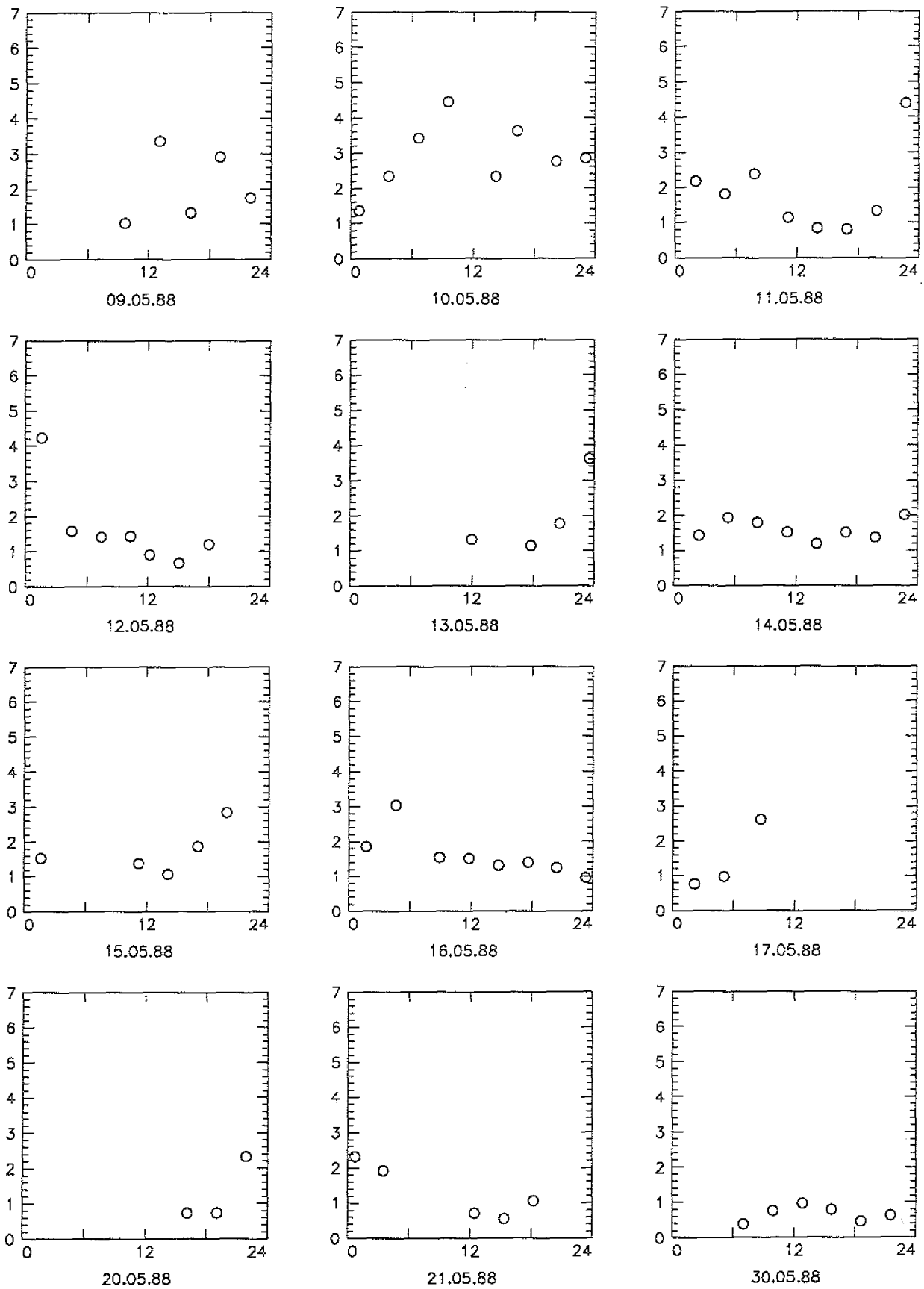

acetylene / ppb

File: ACETYLEN ENZ880HJ

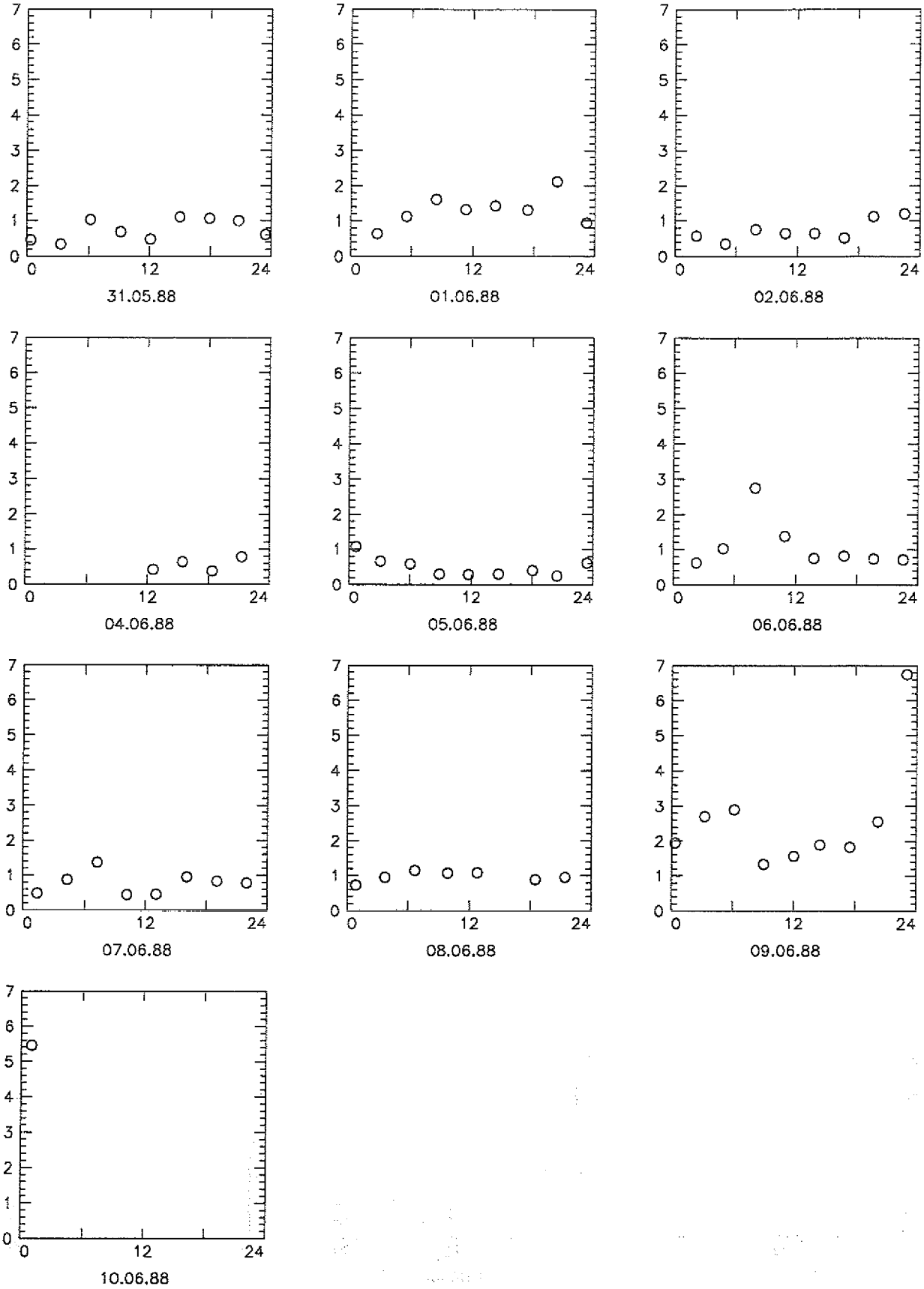

acetylene / ppb

File: ACETYLEN ENZ880HJ

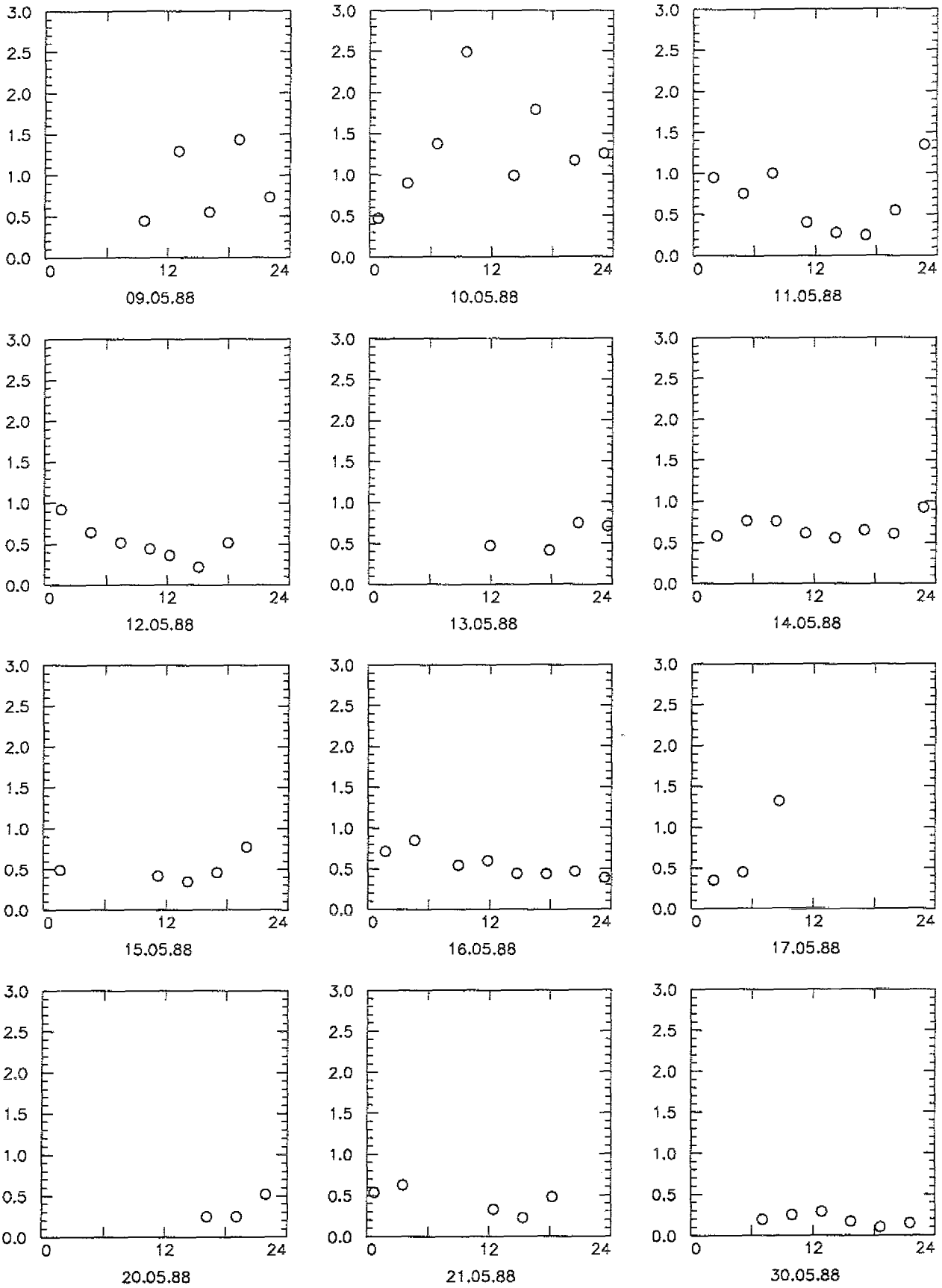

benzene / ppb

File: BENZOL ENZ880HJ

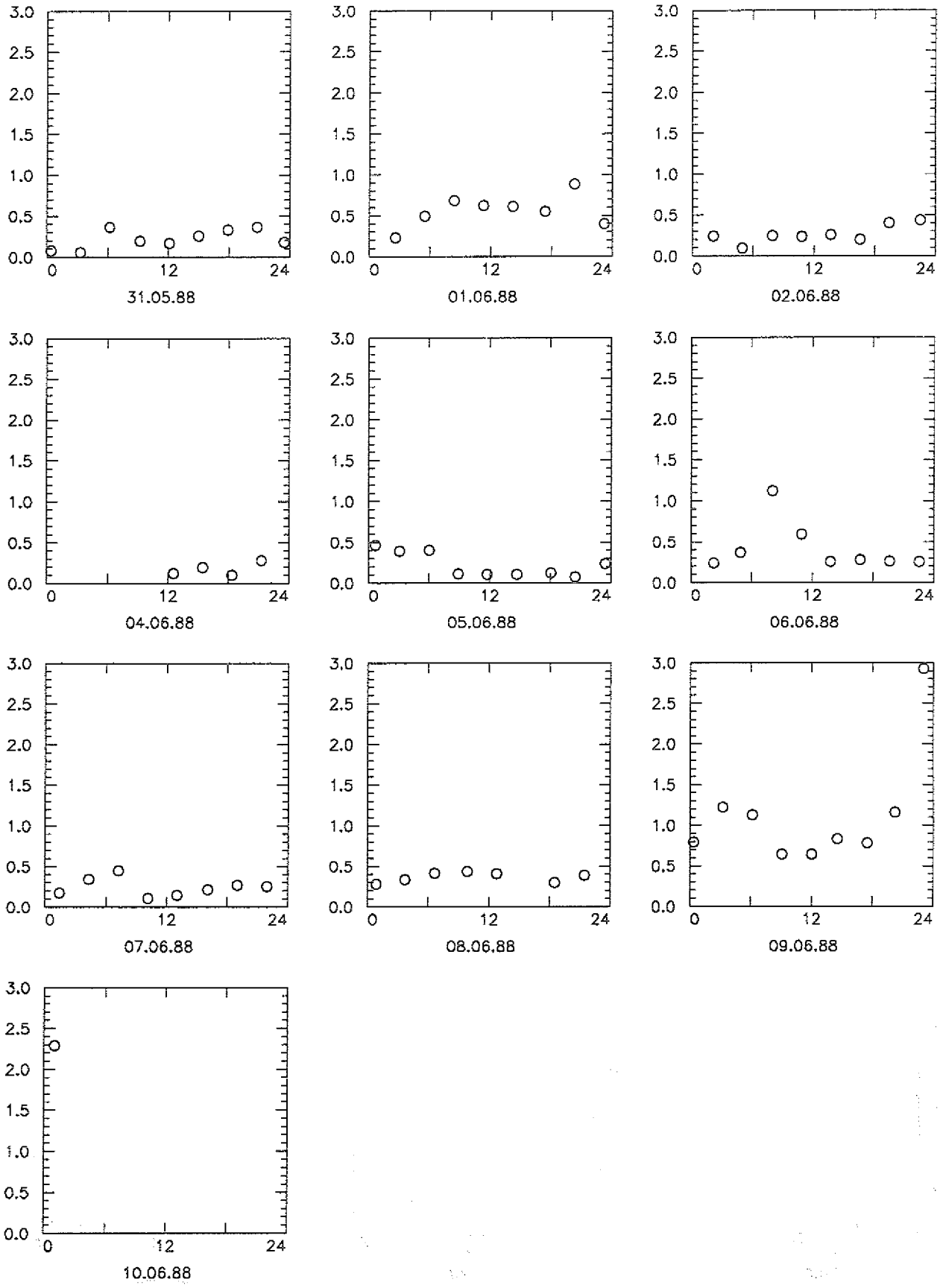

benzene / ppb *File: BENZOL ENZ880HJ*

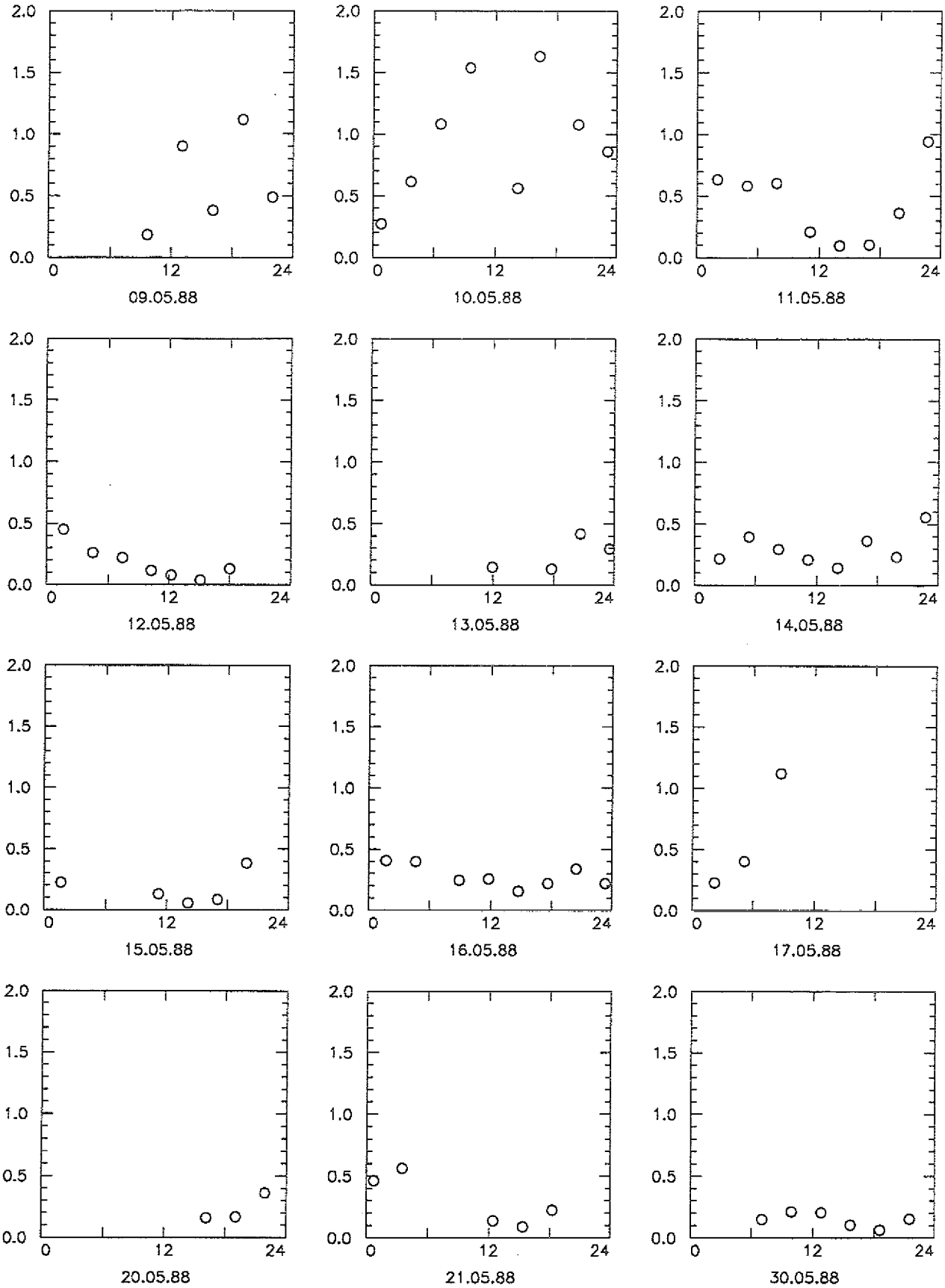

toluene / ppb

File: TOLUOL ENZ880HJ

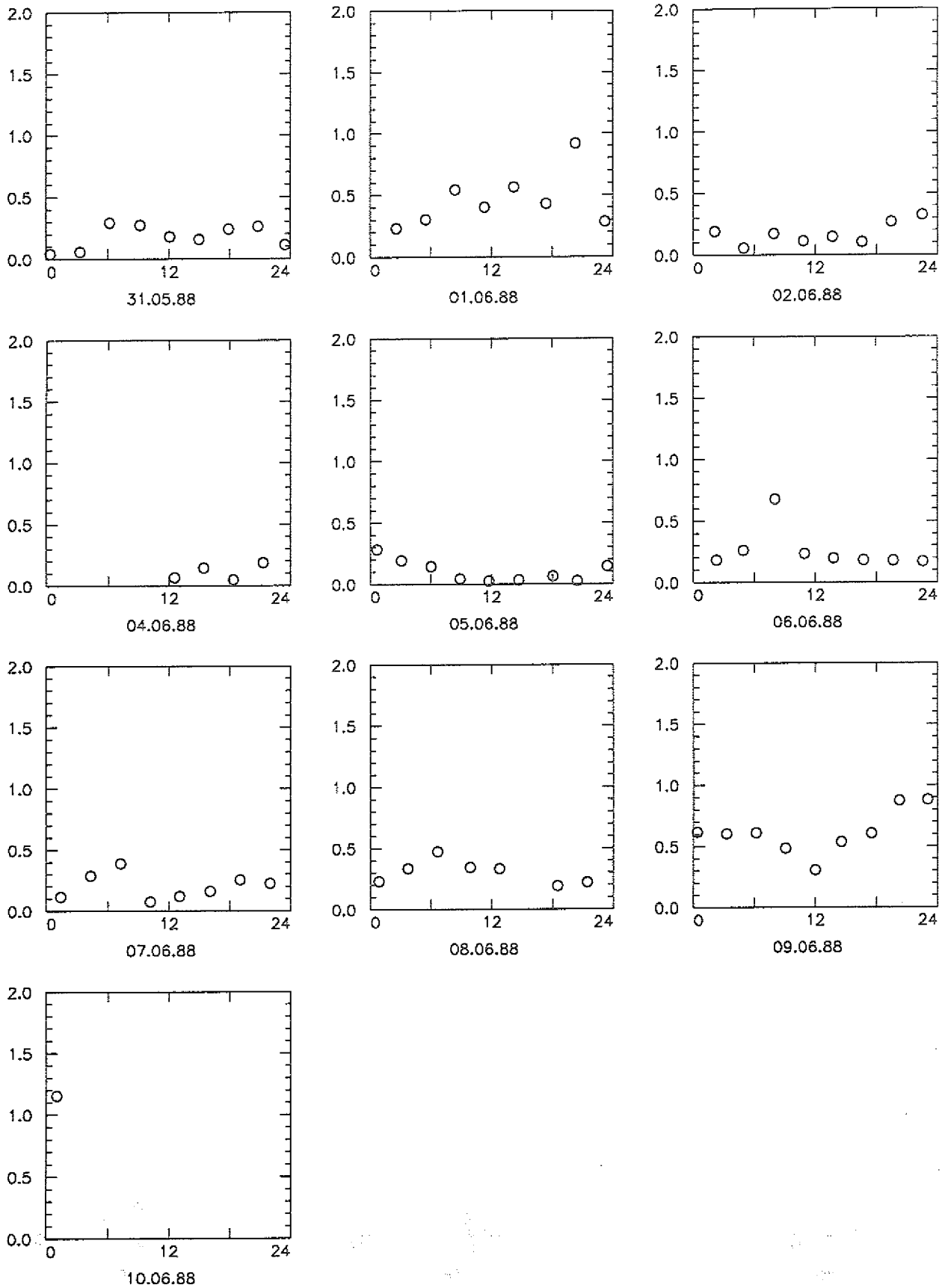

toluene / ppb

File: TOLUOL ENZ880HJ

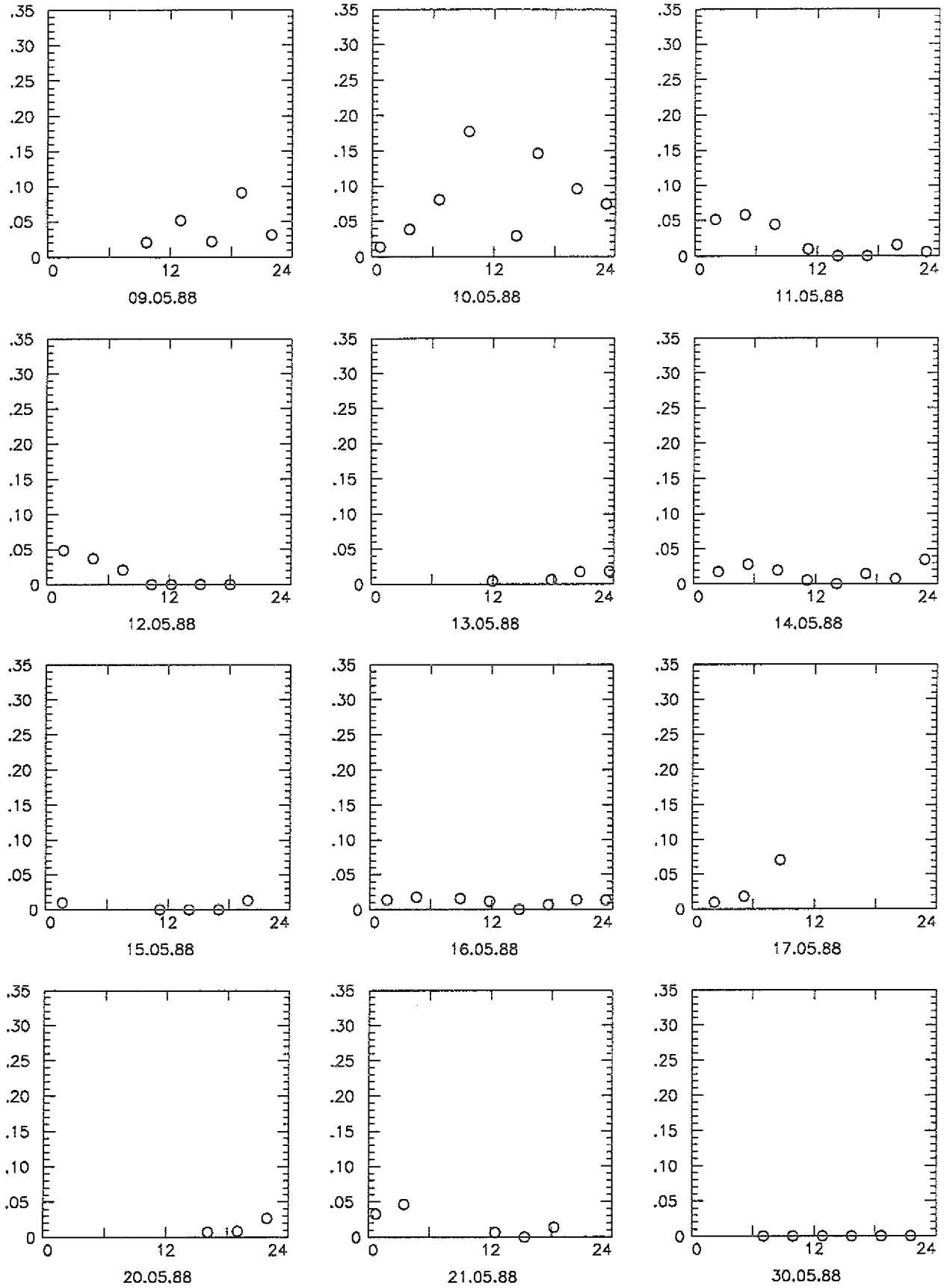

o-xylene / ppb

File: O-XYLOL ENZ880HJ

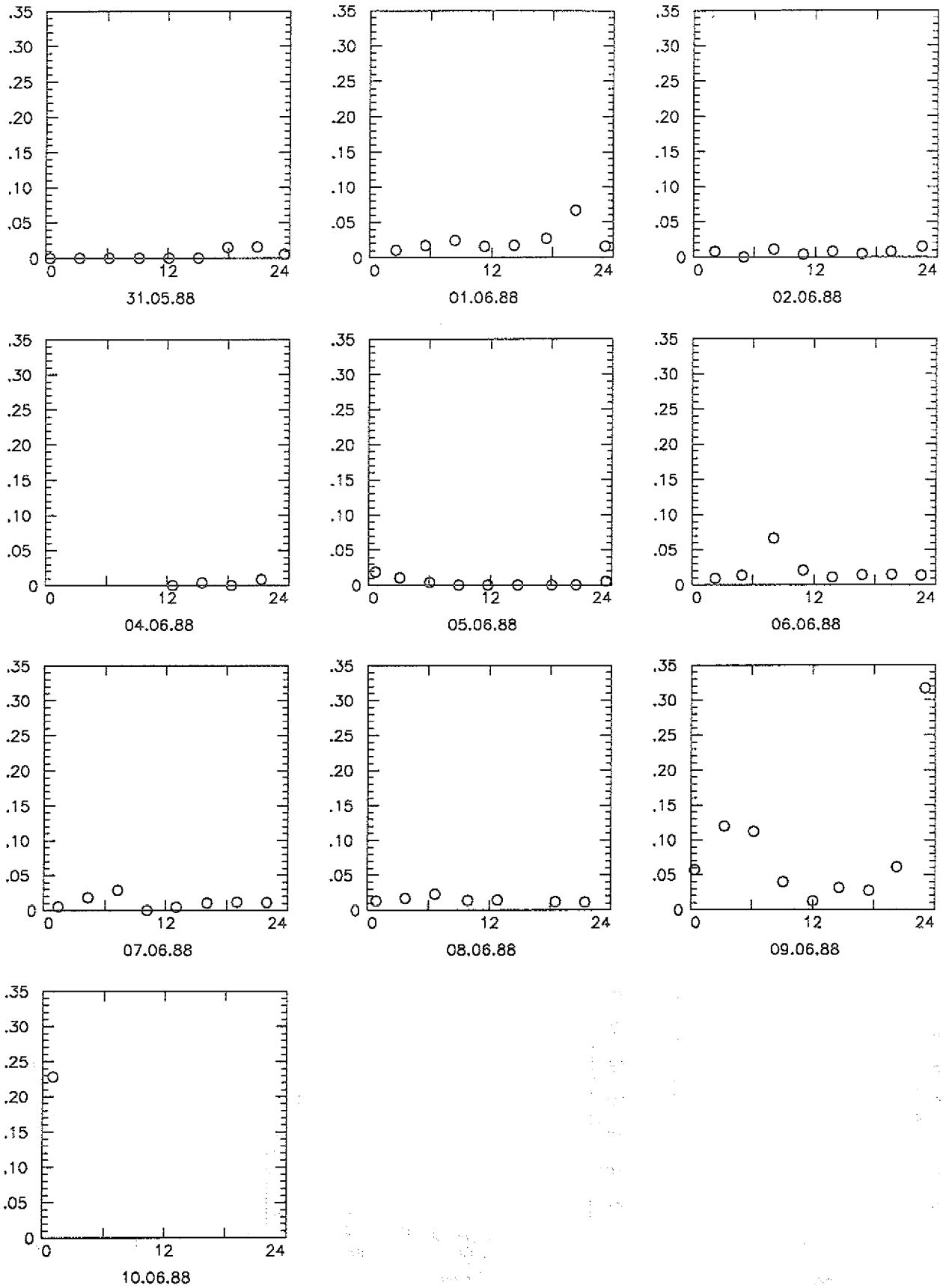

o-xylene / ppb

File: O-XYLOL ENZ880HJ

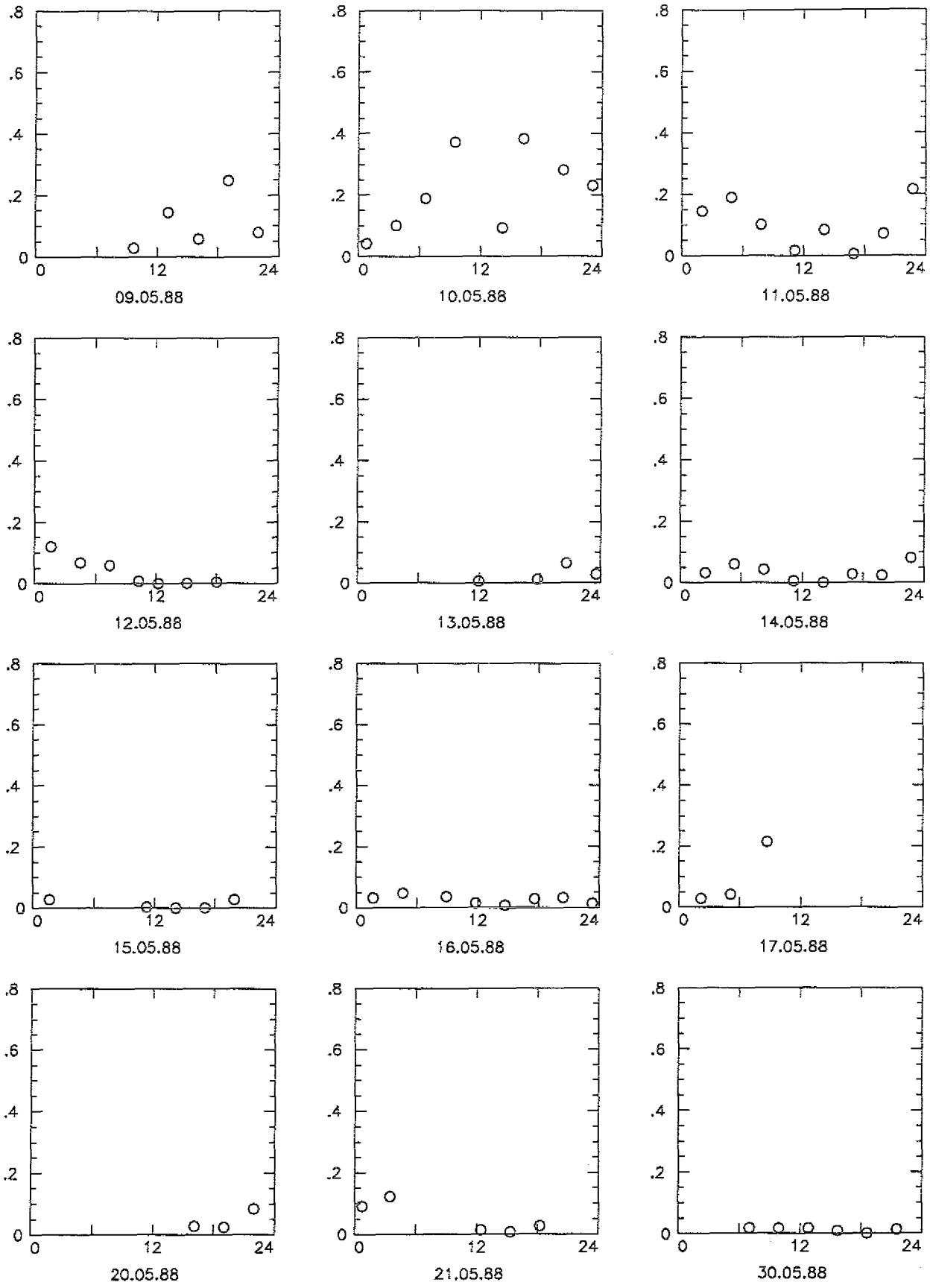

p+m-xylene / ppb

File: PM-XYLOL ENZ880HJ

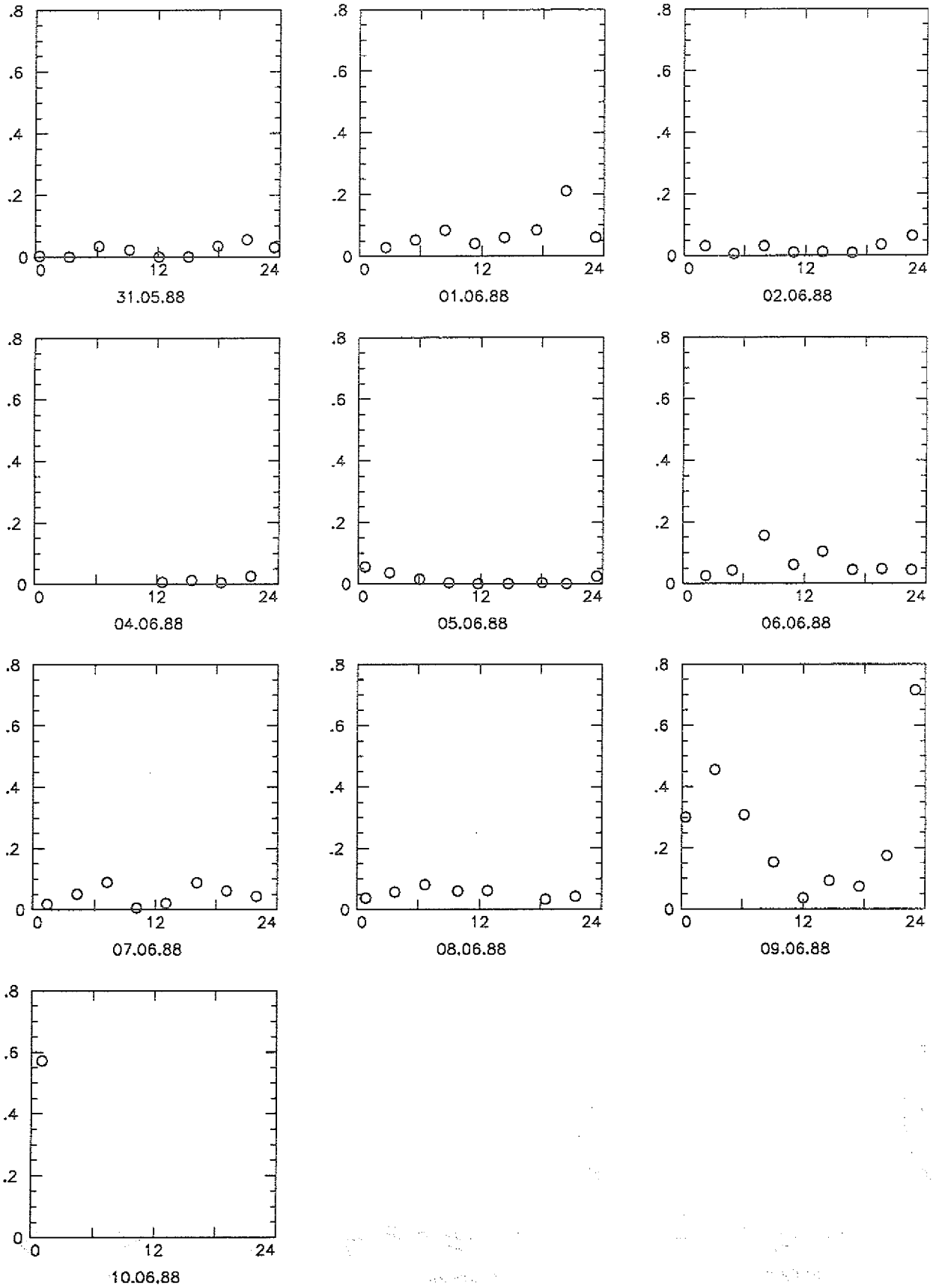

p+m-xylene / ppb

File: PM-XYLOL ENZ880HJ

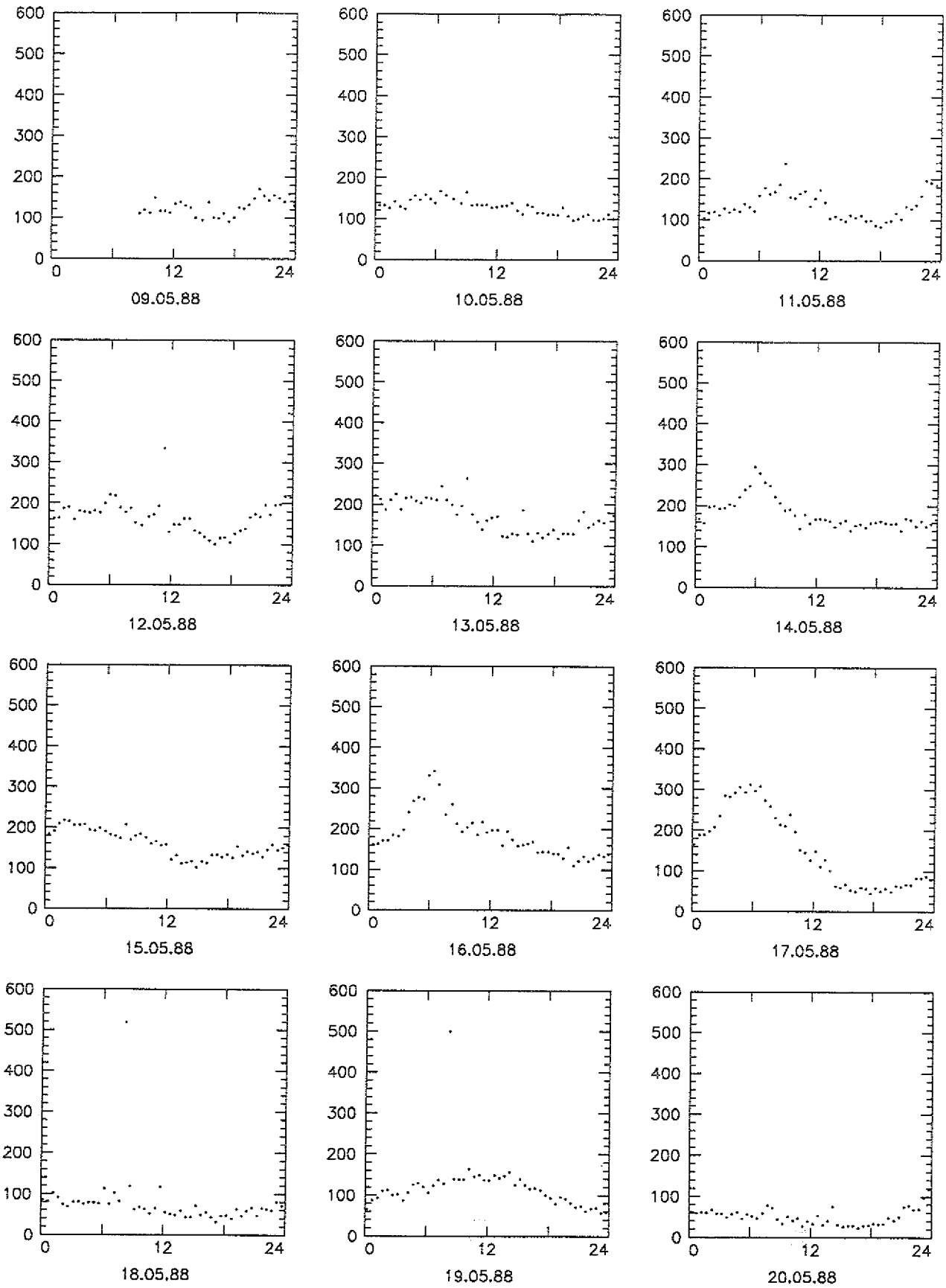

radon activity / rel. units *File: RADON ENZ880HJ*

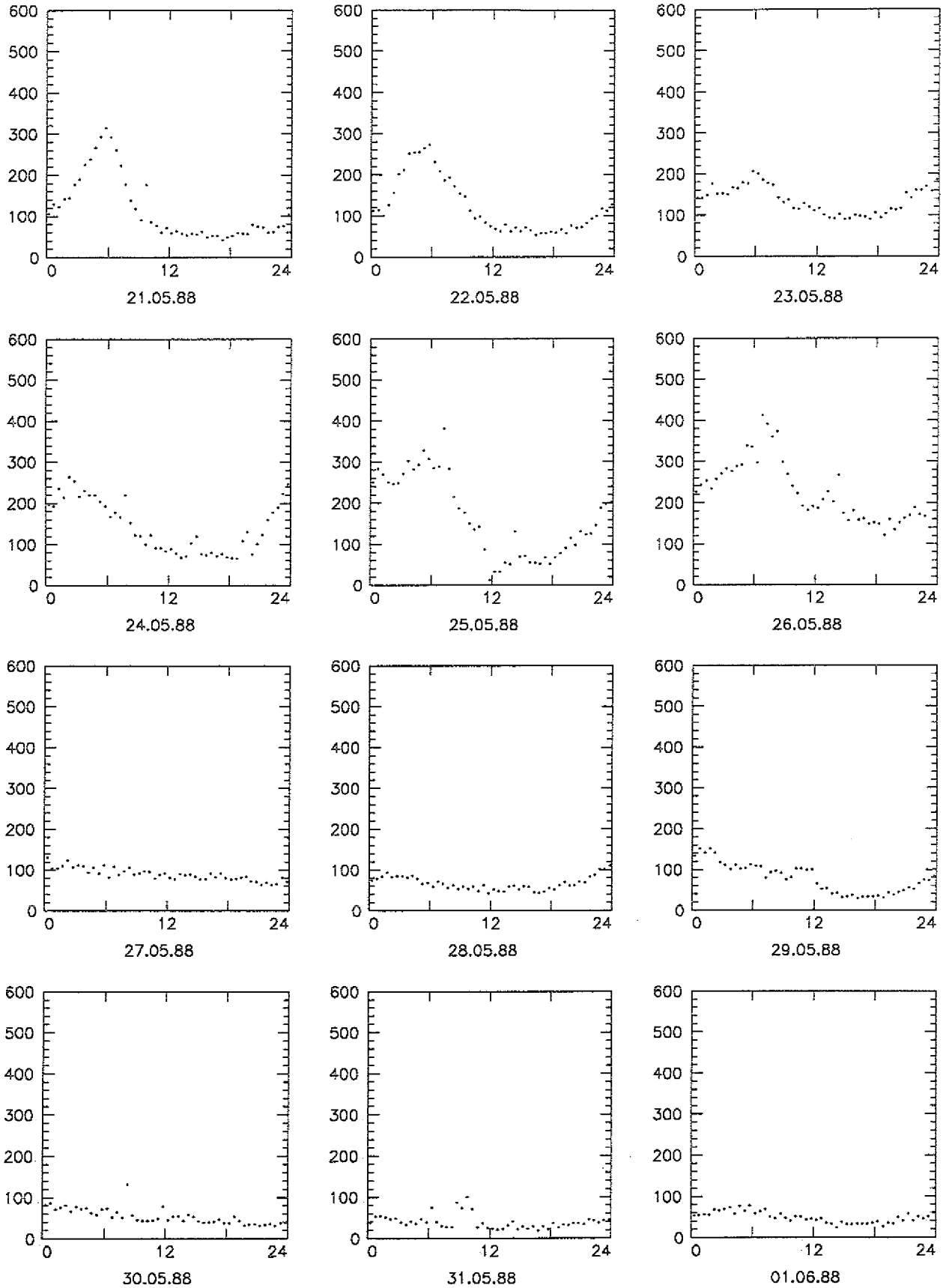

radon activity / rel. units *File: RADON ENZ880HJ*

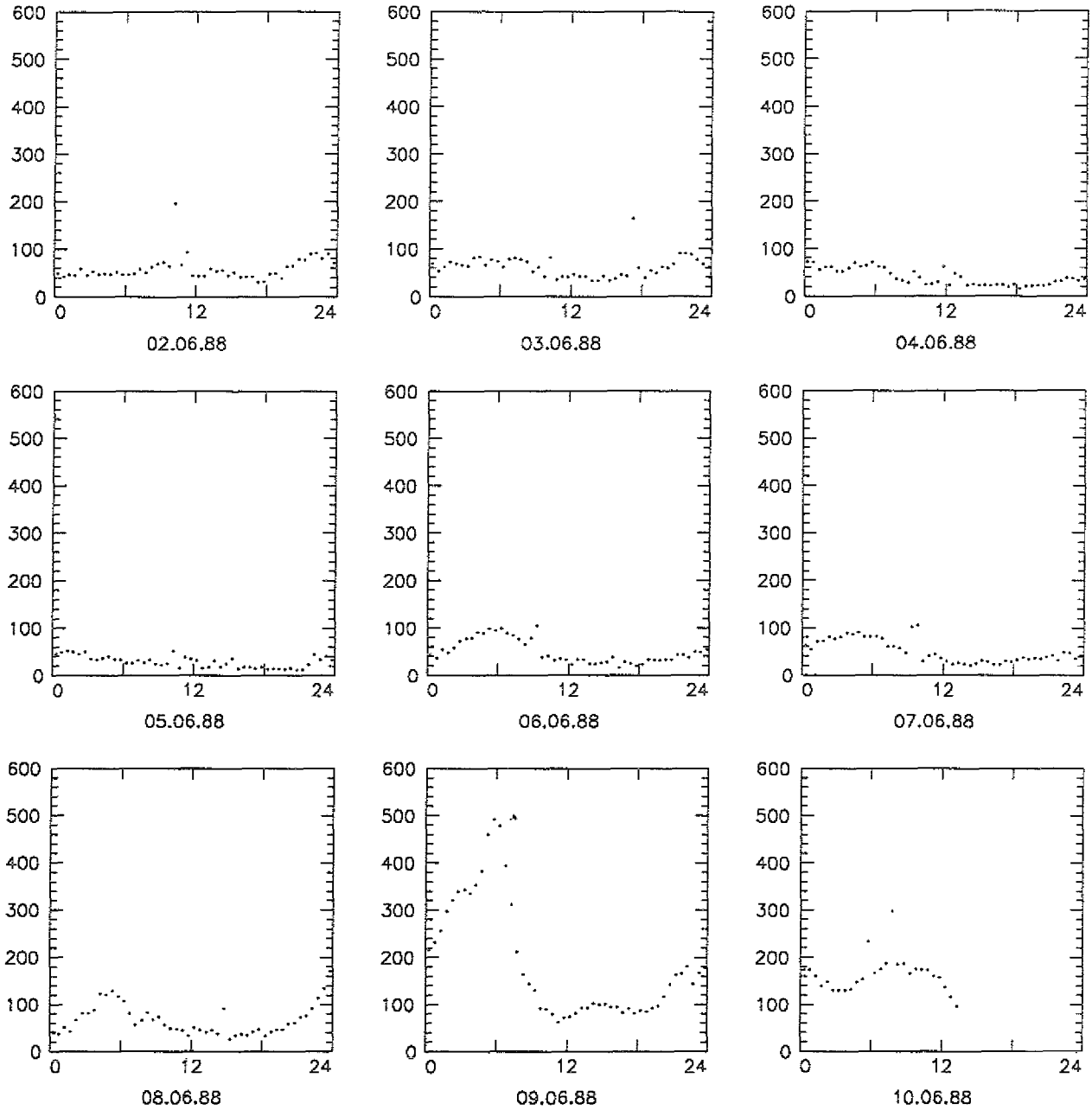

radon activity / rel. units *File: RADON ENZ880HJ*

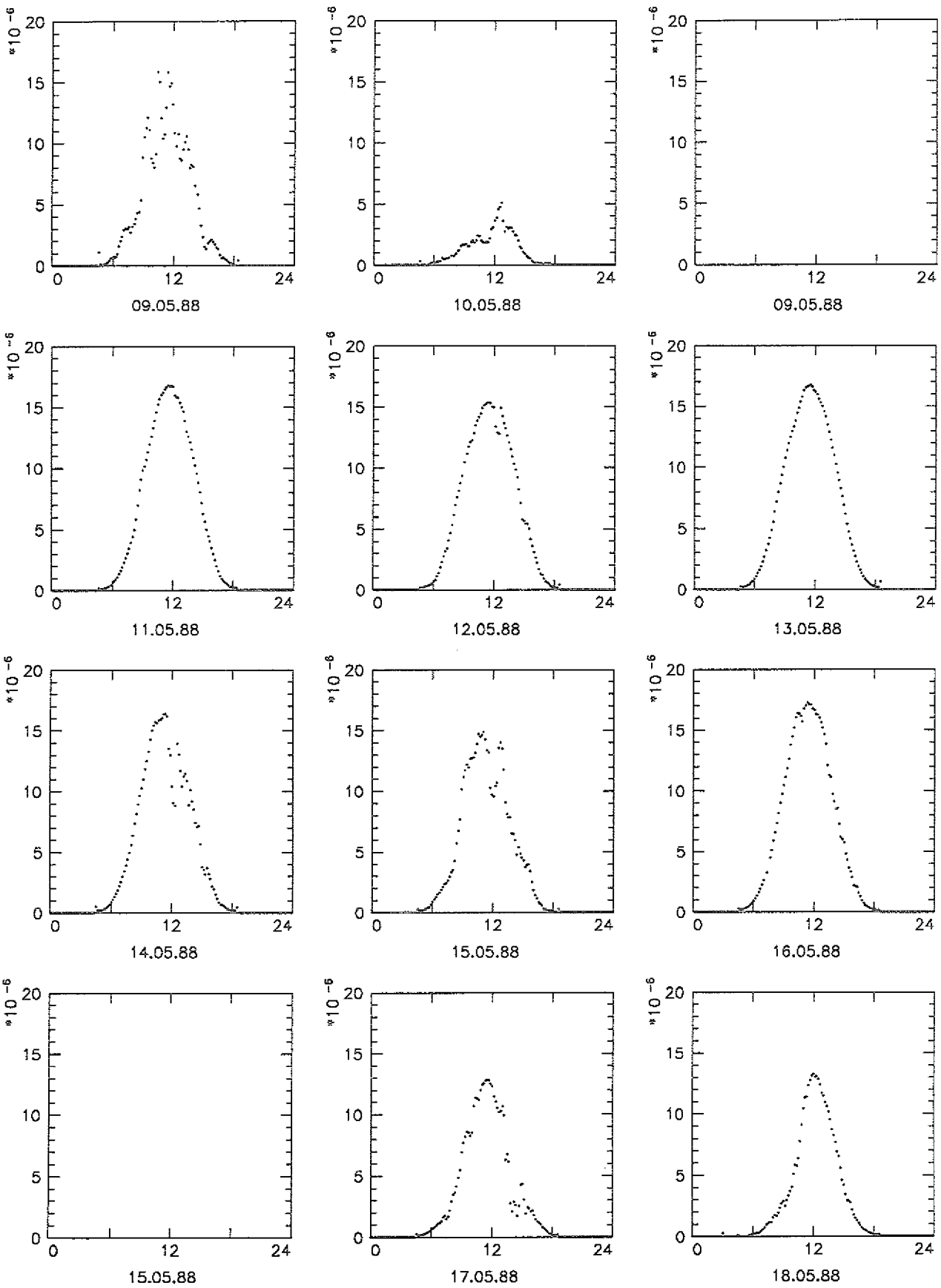

$j(O_3)$ / s^{-1}

File: JO3CALC ENZ880HJ

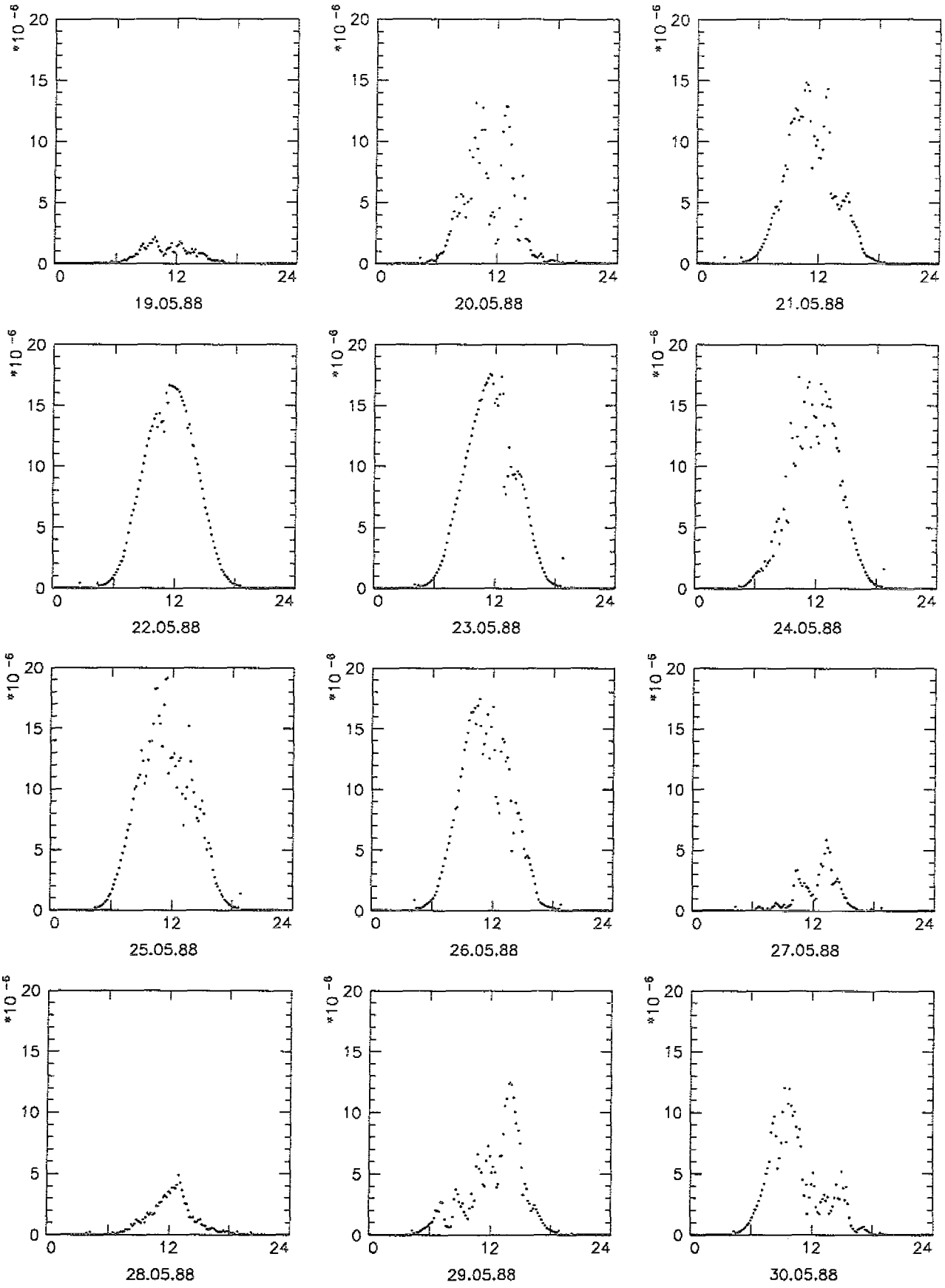

$j(O_3)$ / s^{-1}

File: JO3CALC ENZ880HJ

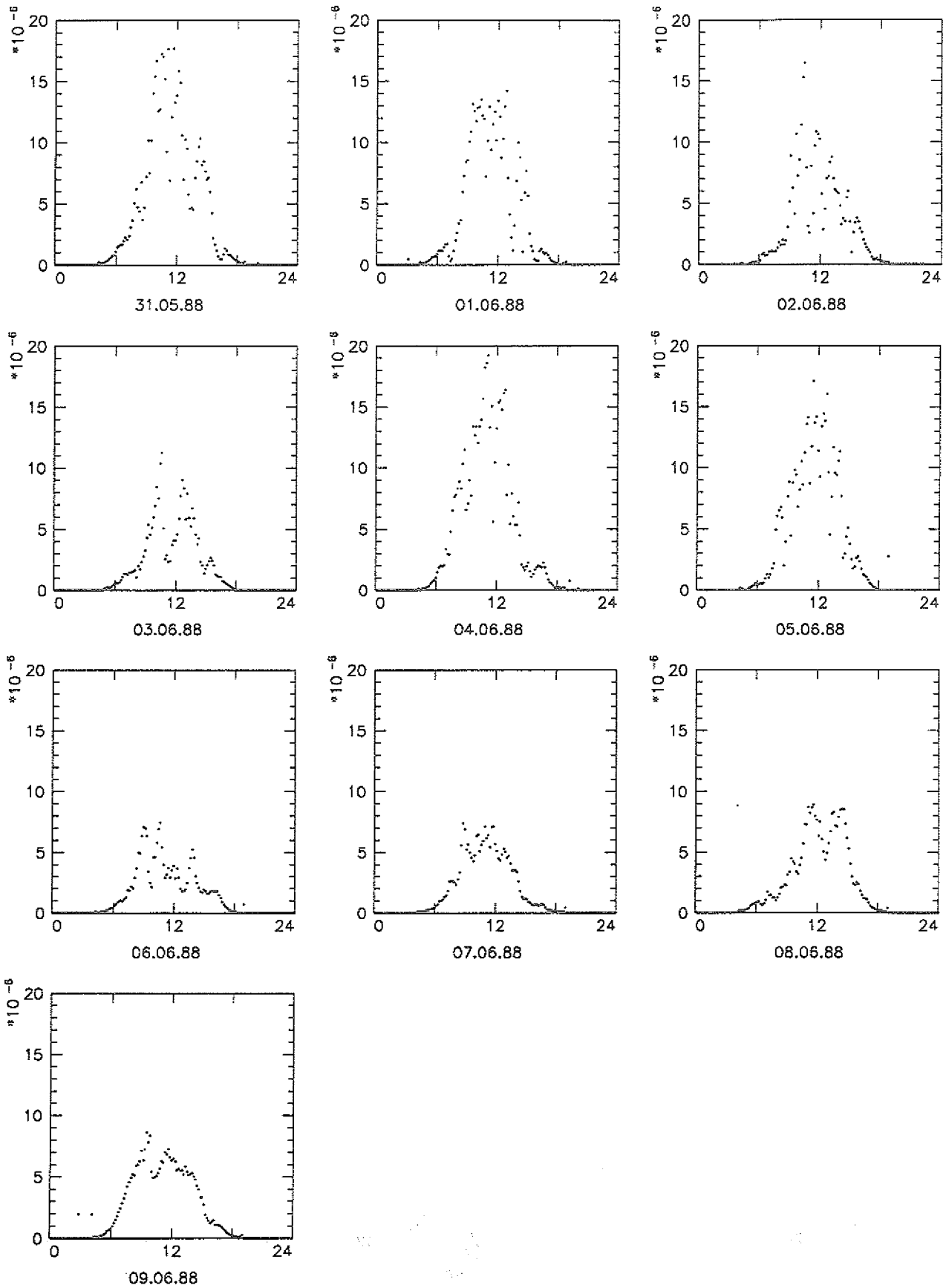

$j(O_3)$ / s^{-1}

File: JO3CALC ENZ880HJ

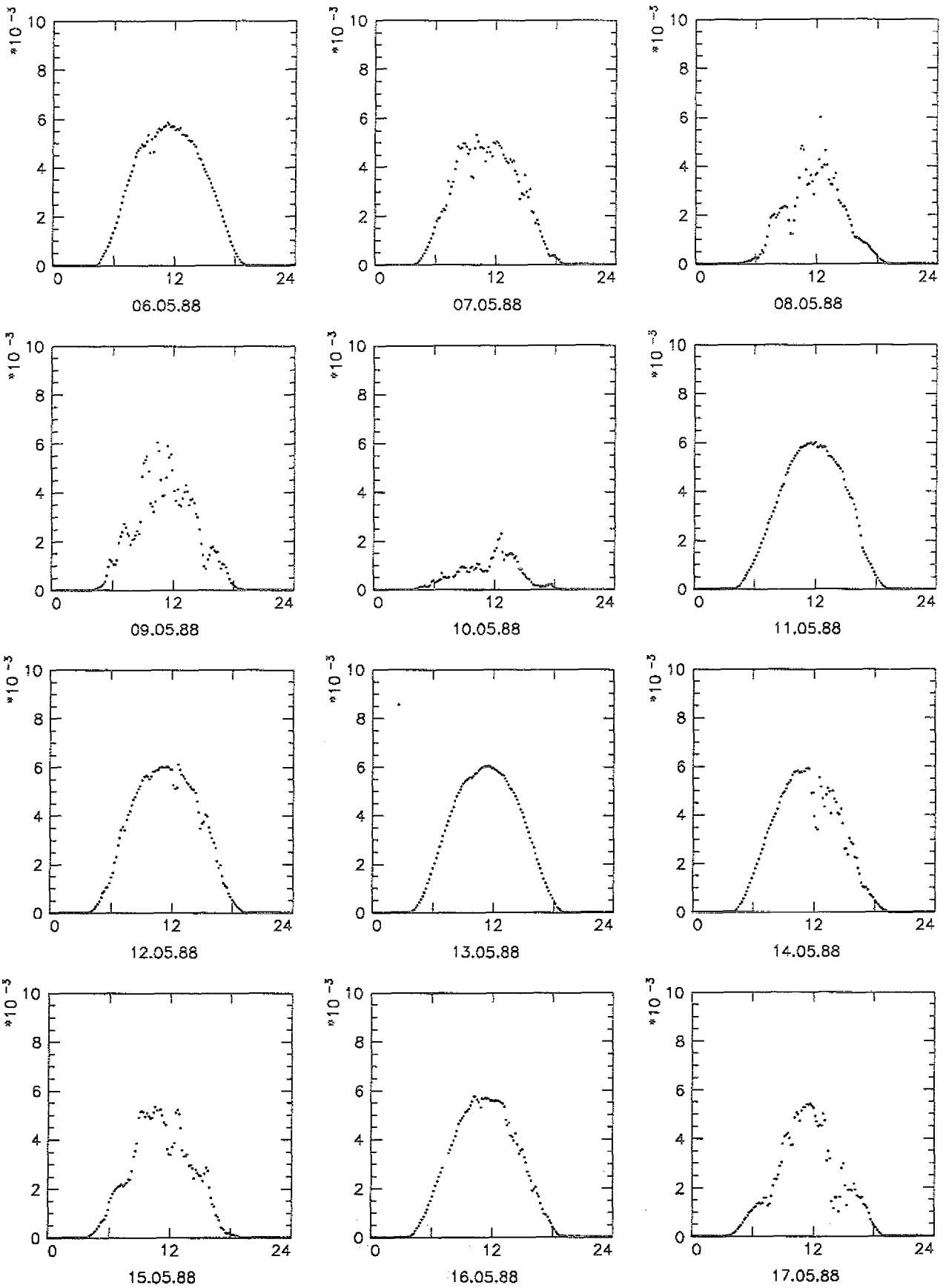

$j(NO_2)$ / s^{-1}

File: JNO2_MET ENZ880HJ

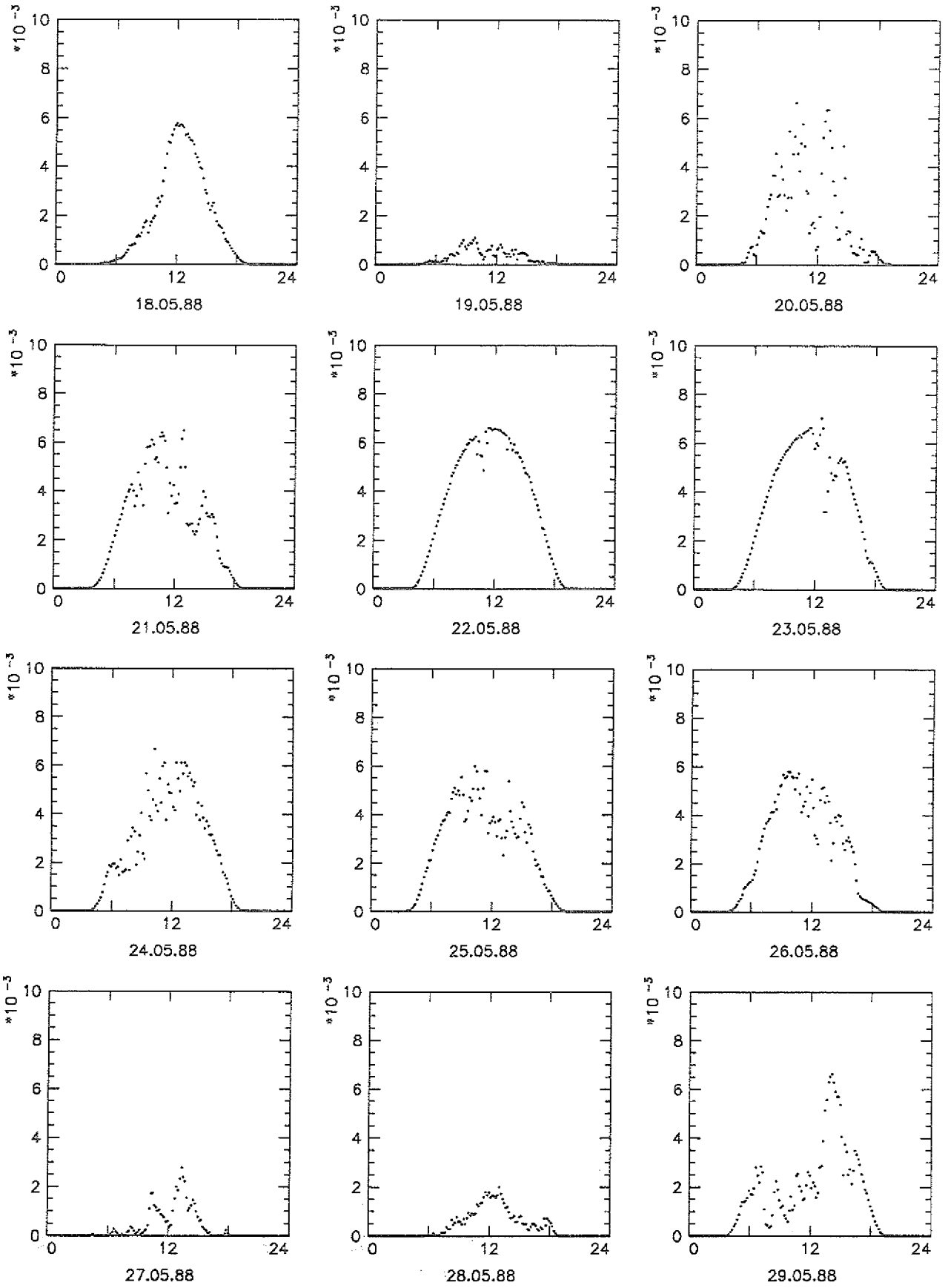

$j(NO_2)$ / s^{-1}

File: JNO2_MET ENZ880HJ

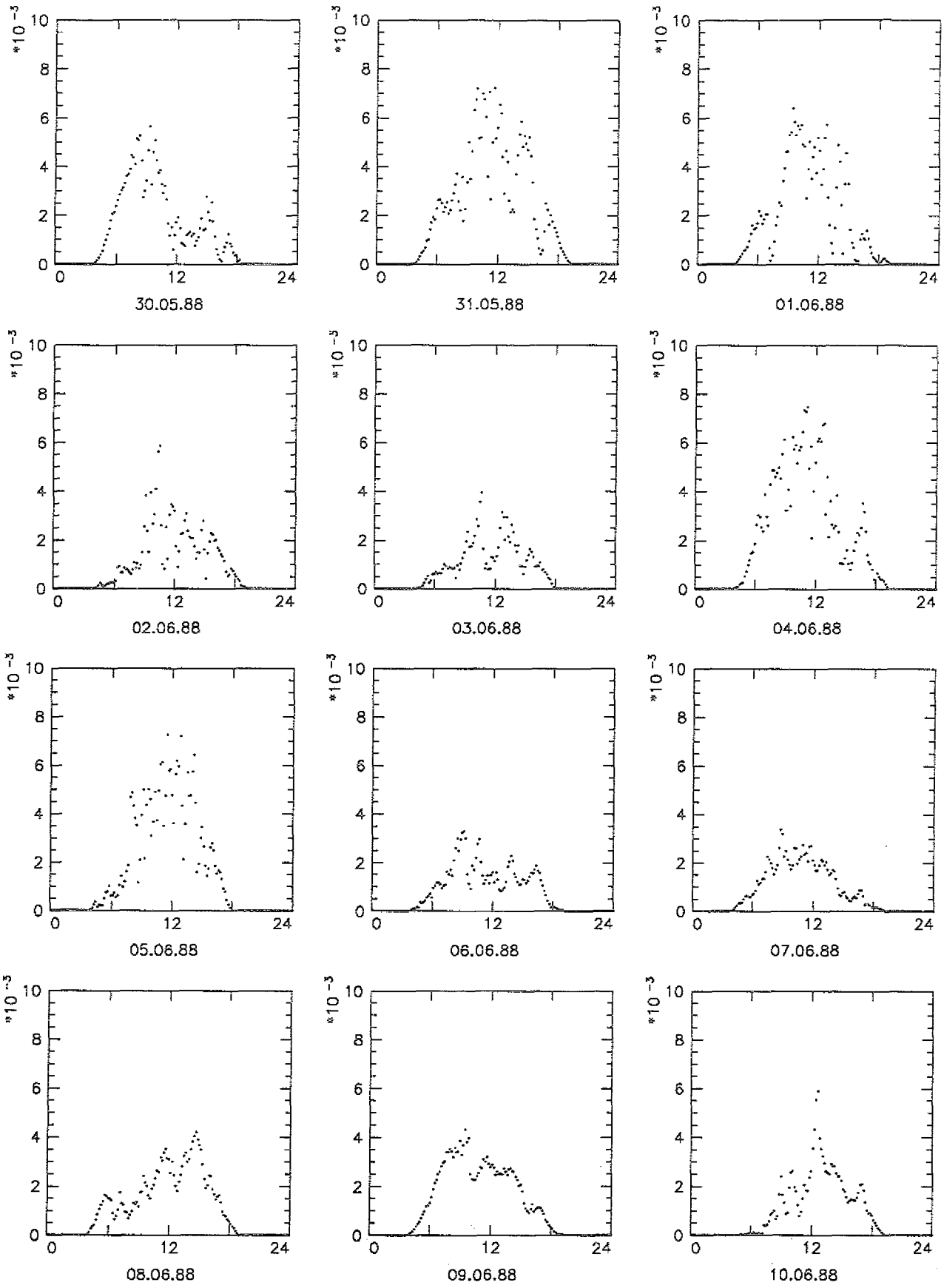

$j(NO_2)$ / s^{-1}

File: JNO2_MET ENZ880HJ

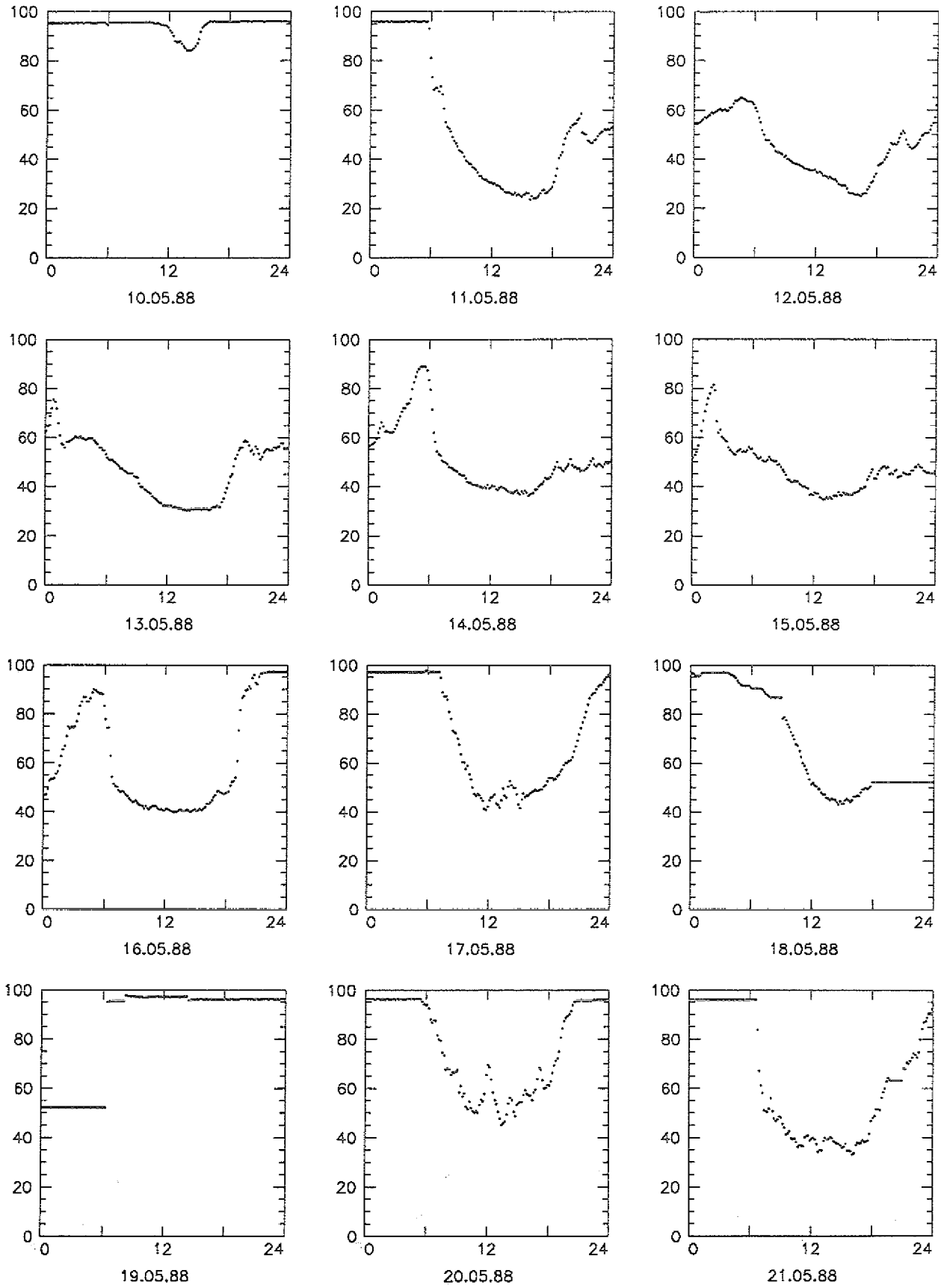

relative humidity / %

File: H20MT02 ENZ880HJ

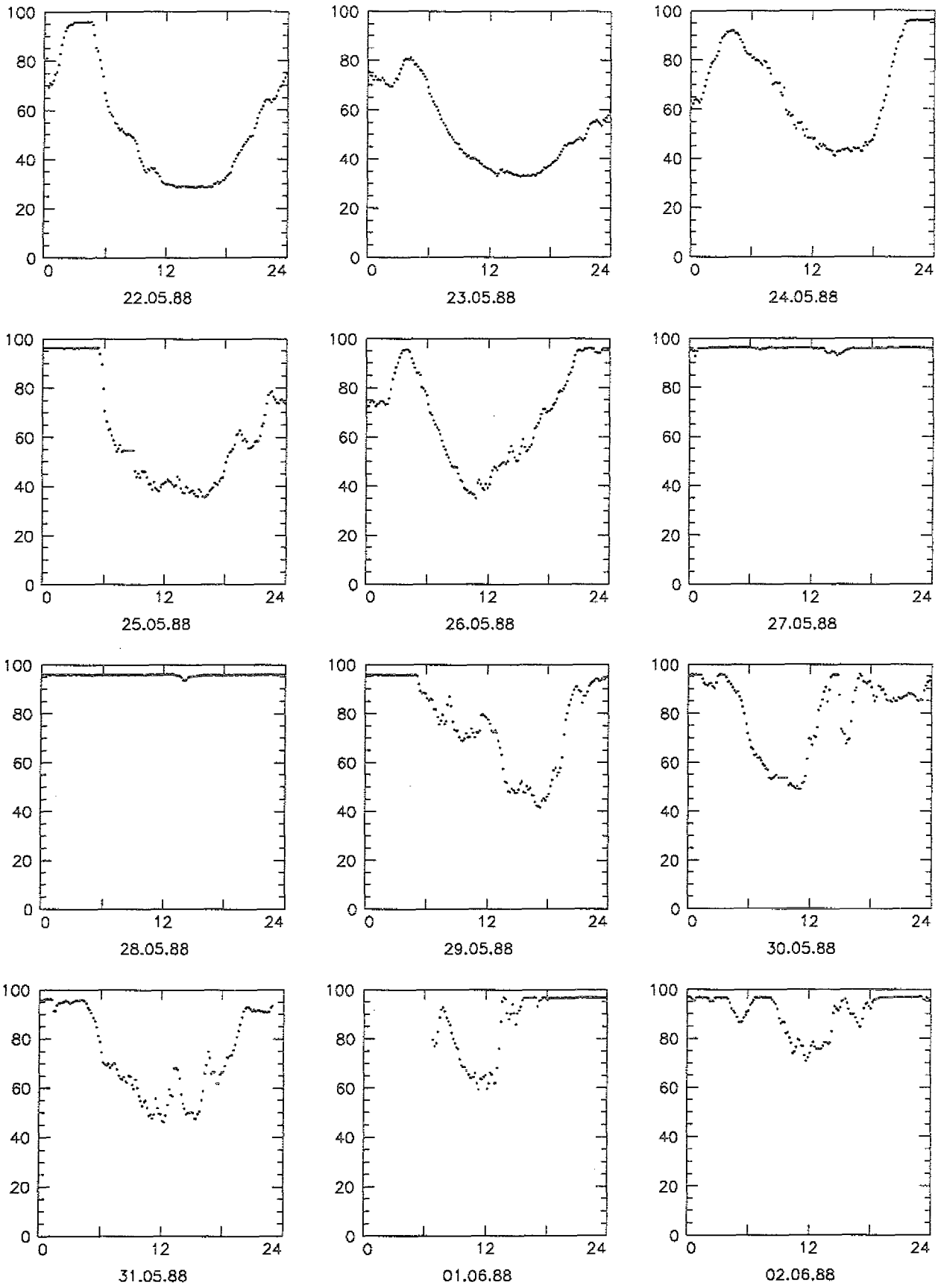

relative humidity / %

File: H20MT02 ENZ880HJ

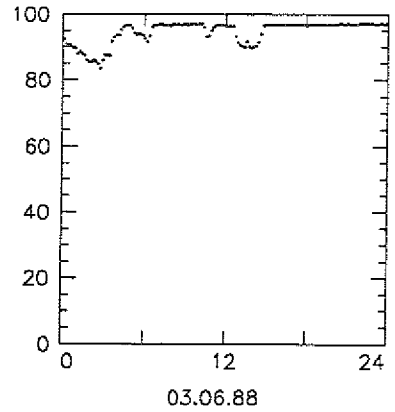

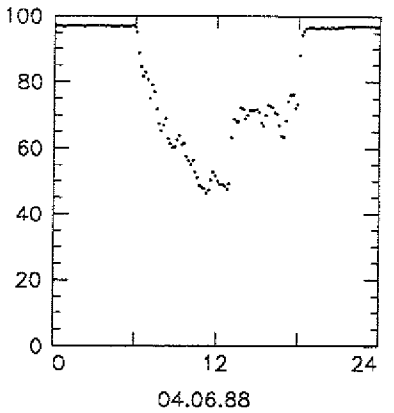

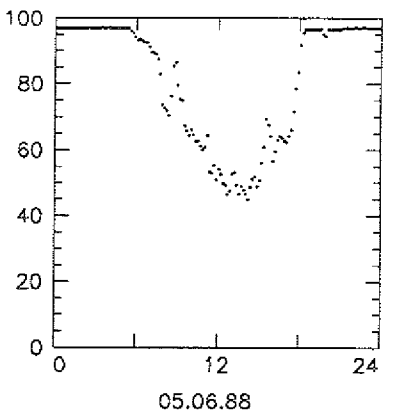

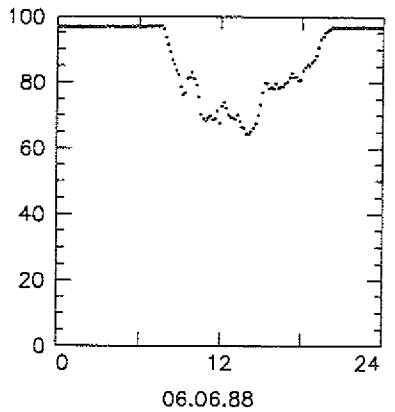

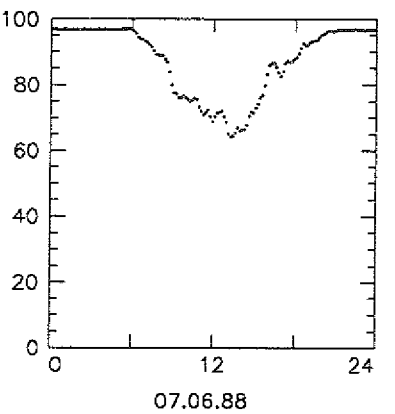

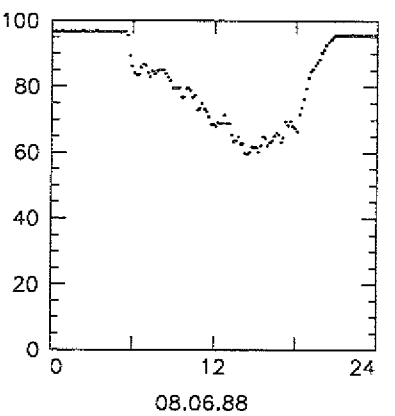

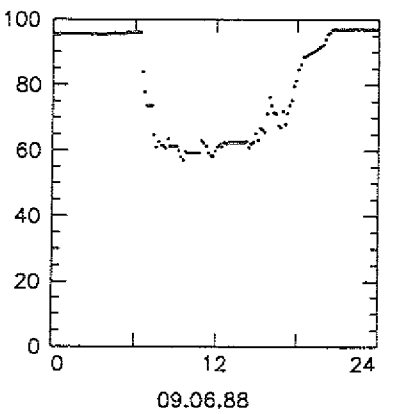

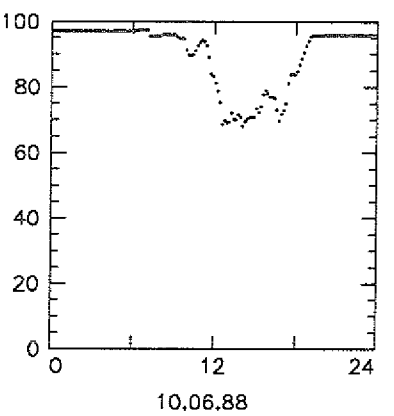

relative humidity / %

File: H20MT02 ENZ880HJ

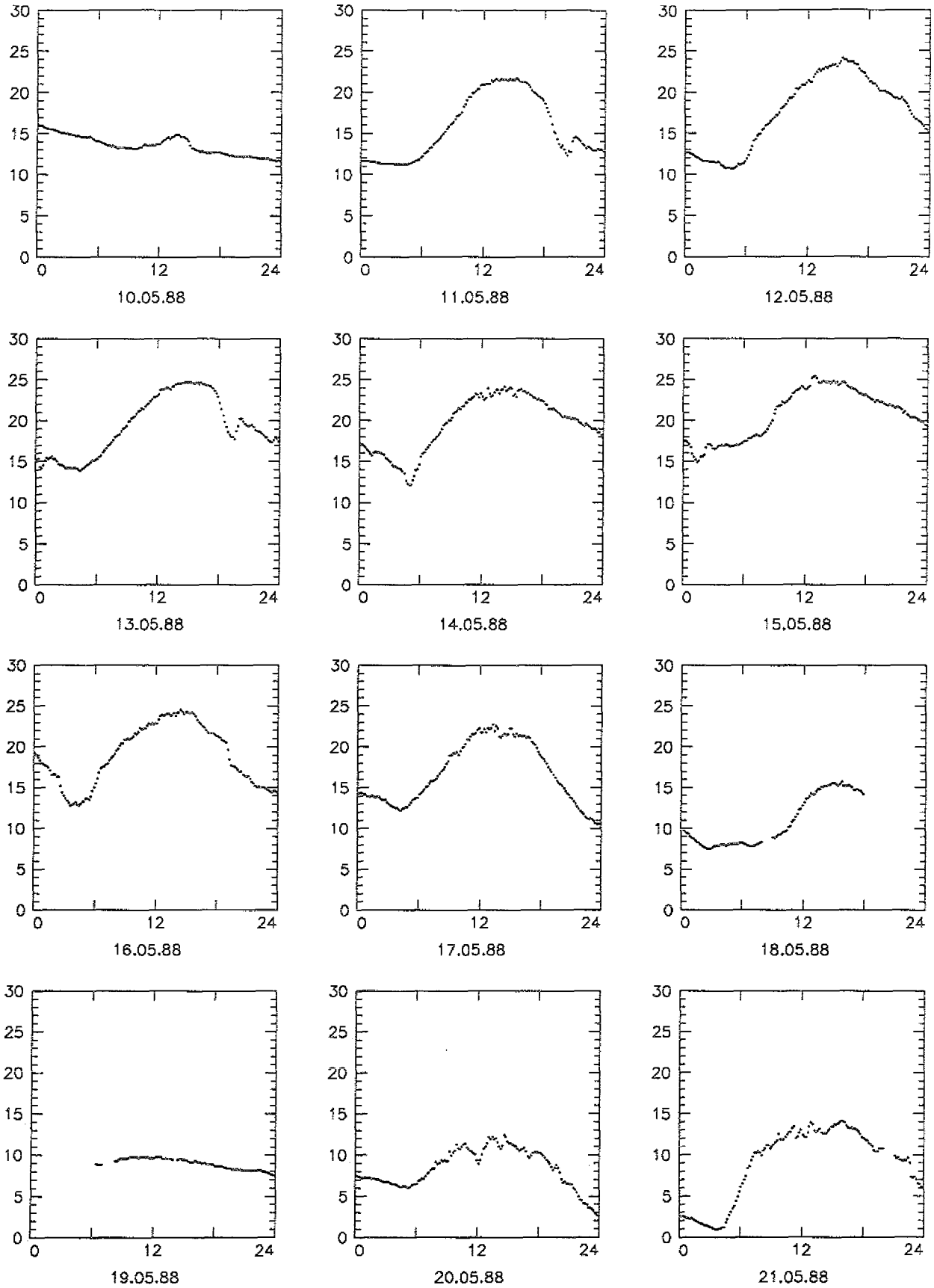

temperature (10 m) / ° C *File: TEMPMT10 ENZ880HJ*

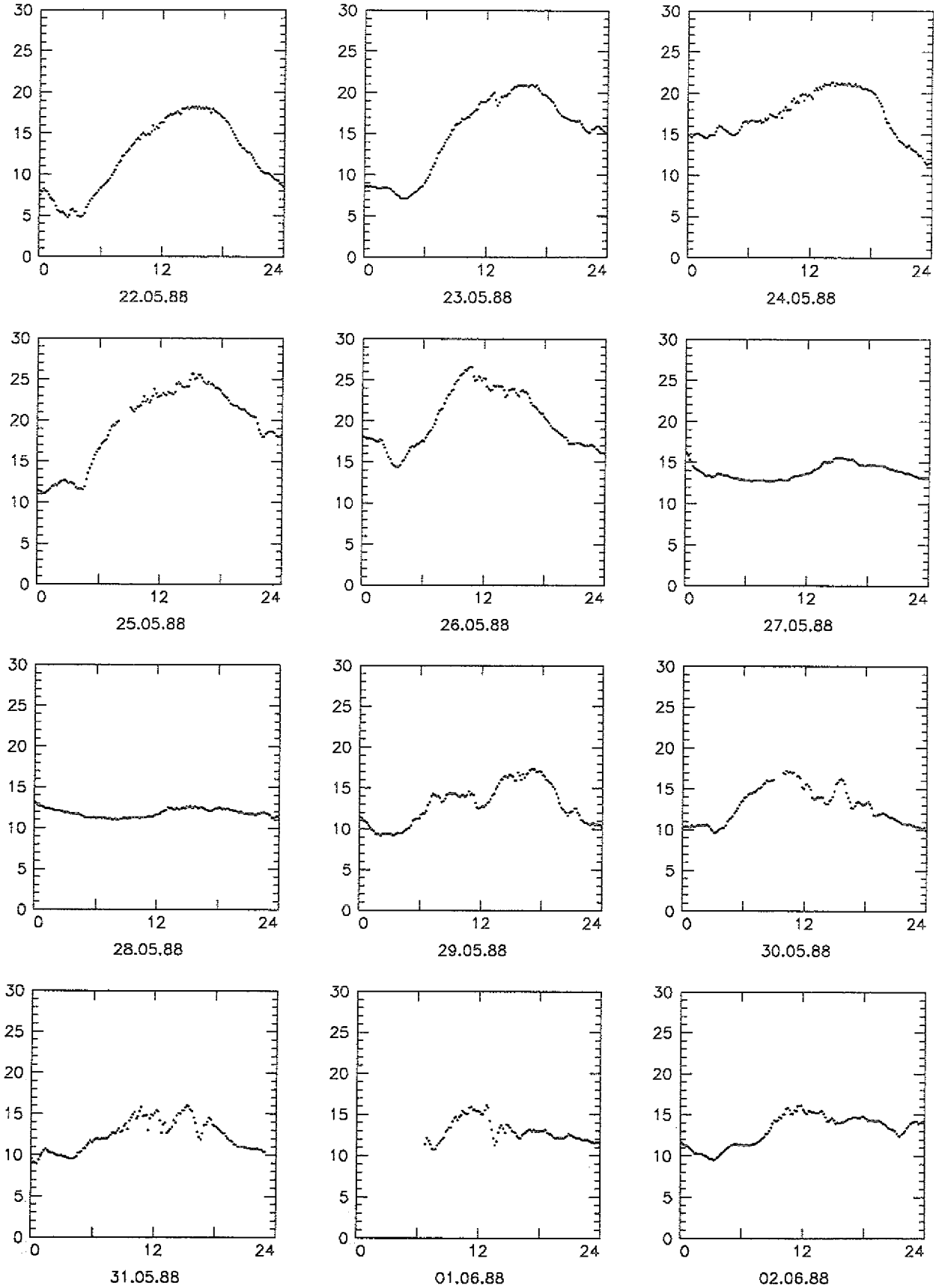

temperature (10 m) / ° C *File: TEMPMT10 ENZ880HJ*

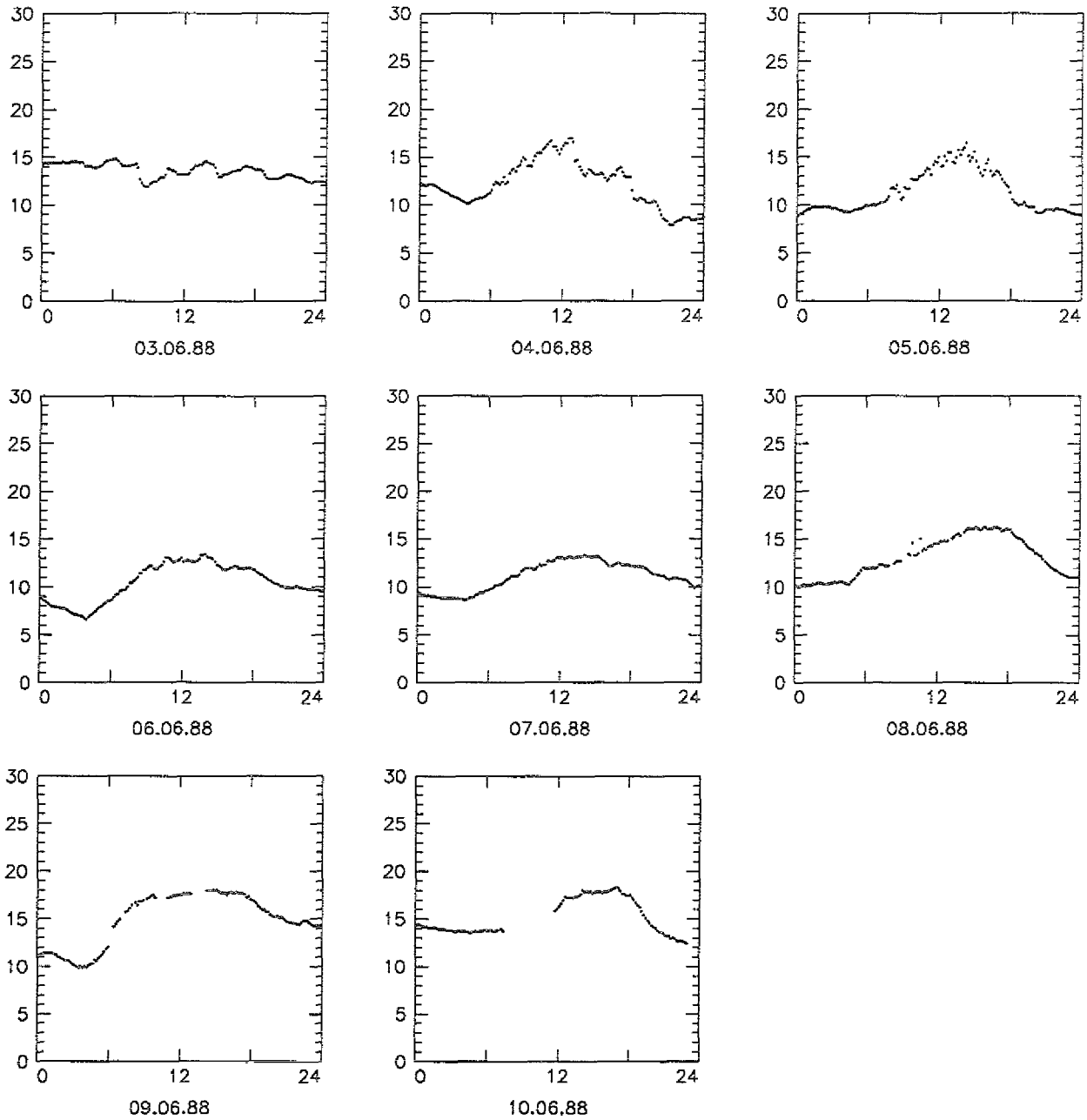

temperature (10 m) / ° C

File: TEMPMT10 ENZ880HJ

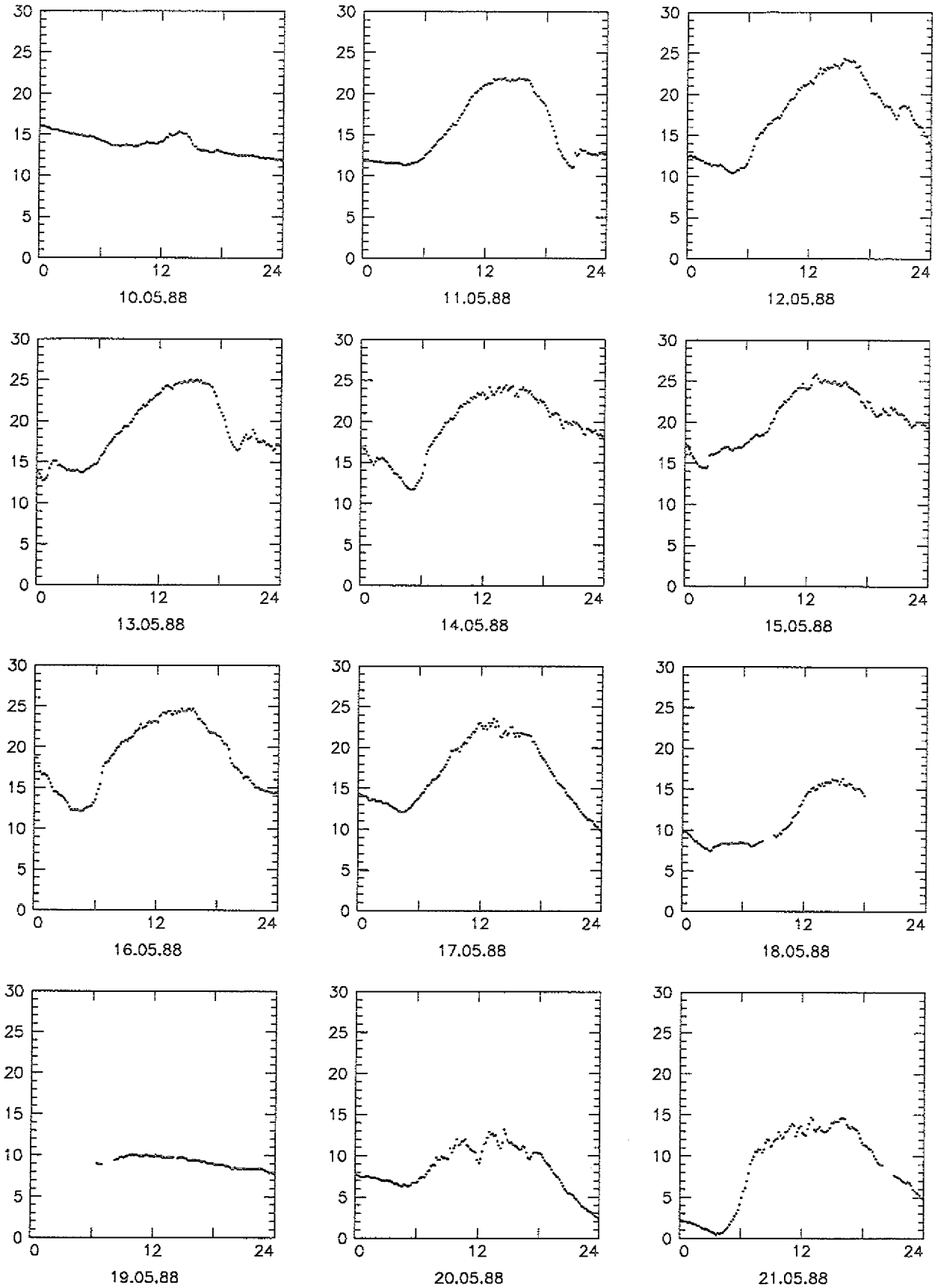

temperature (2 m) / ° C *File: TEMPMT02 ENZ880HJ*

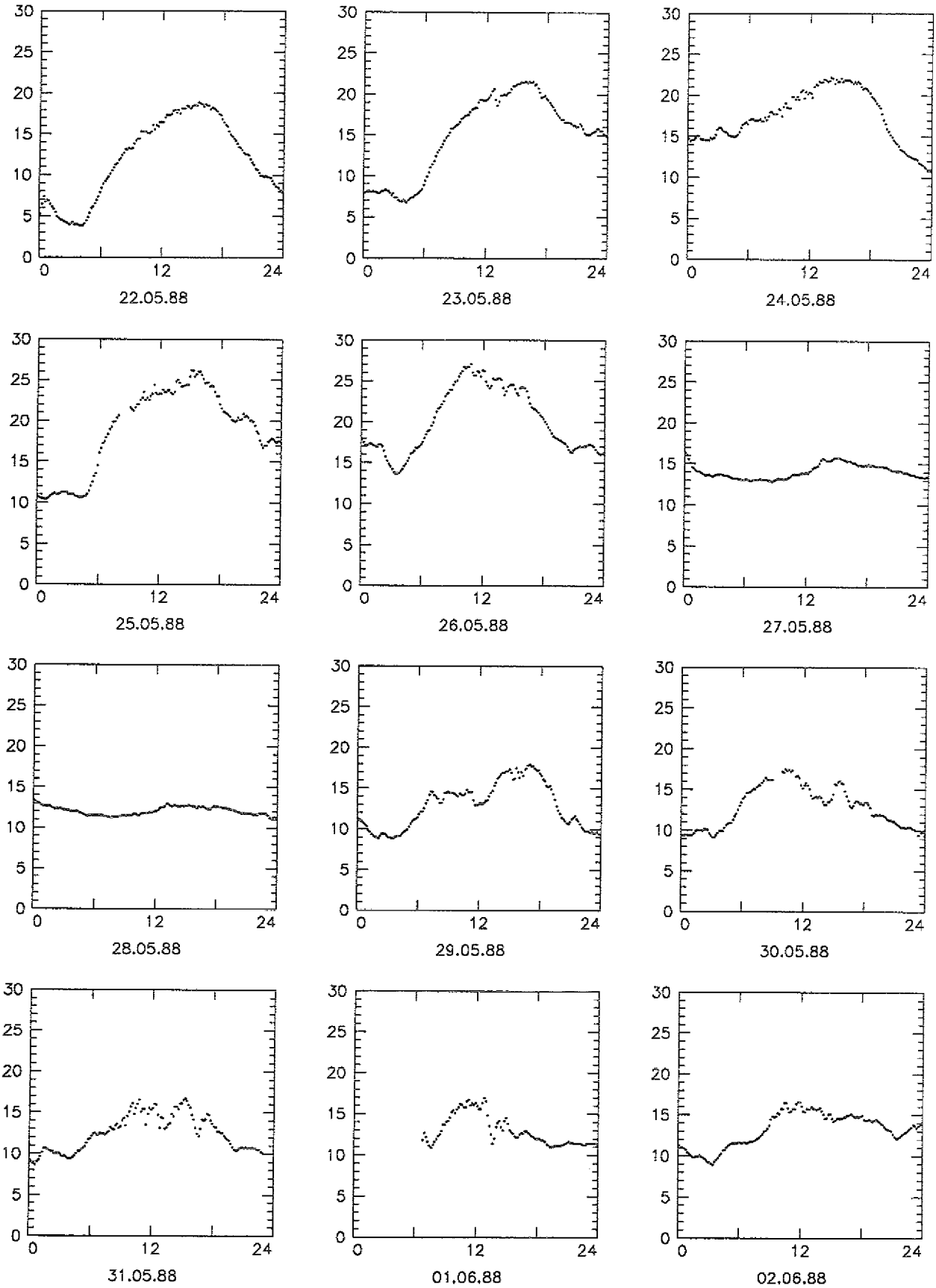

temperature (2 m) / ° C

File: TEMPMT02 ENZ880HJ

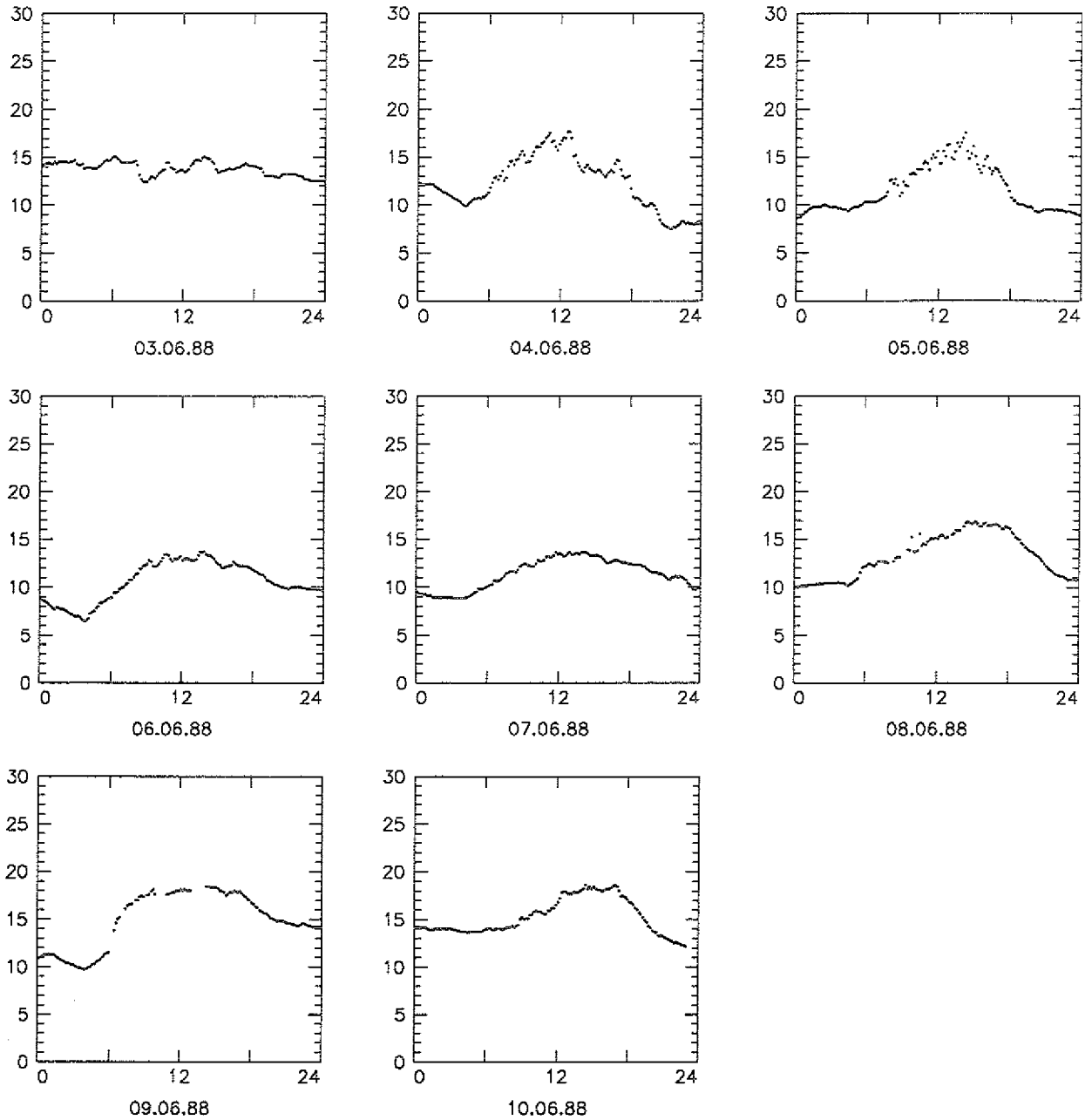

temperature (2 m) / ° C *File: TEMPMT02 ENZ880HJ*

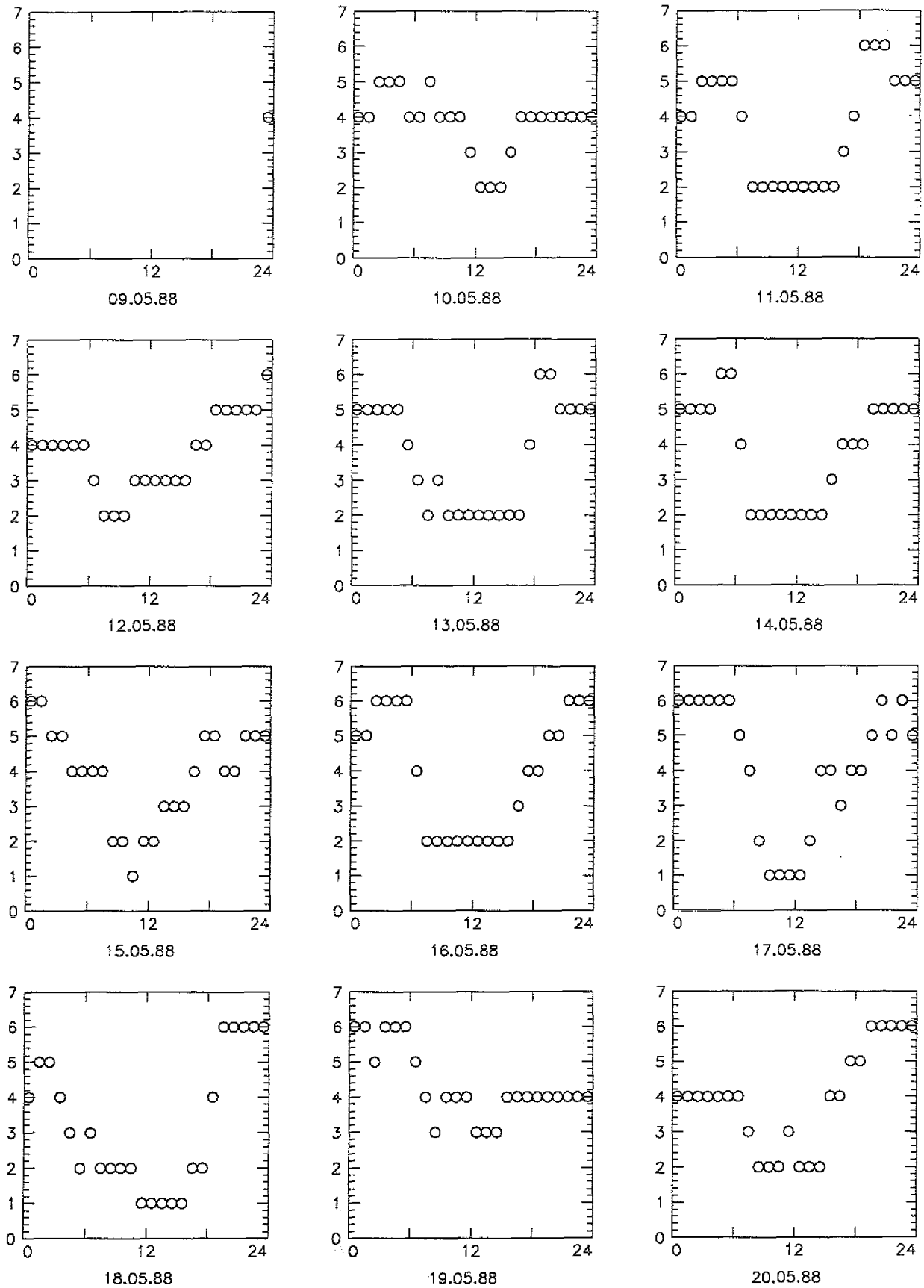

stability class *File: DIFK ENZ880HJ*

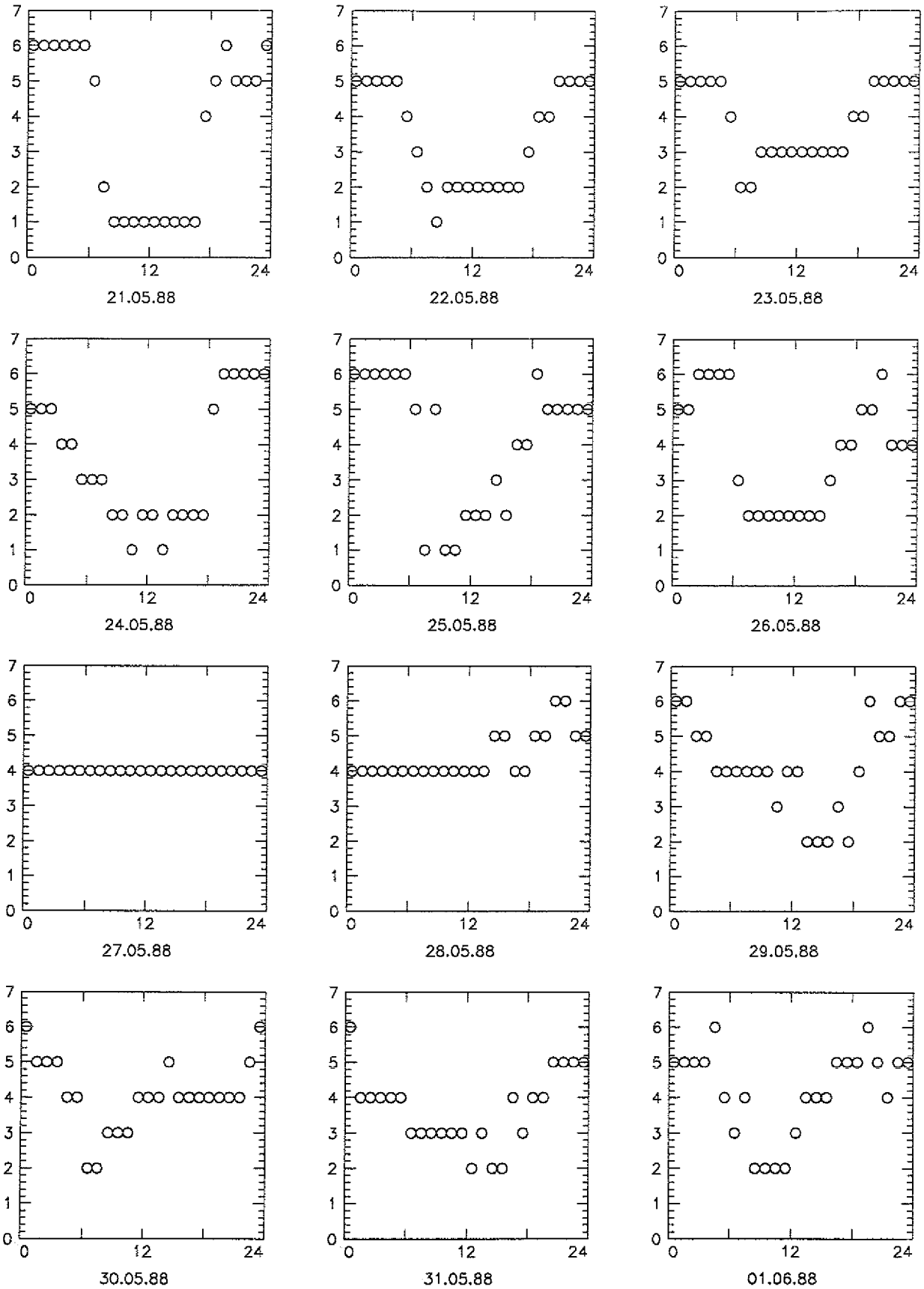

stability class *File: DIFK ENZ880HJ*

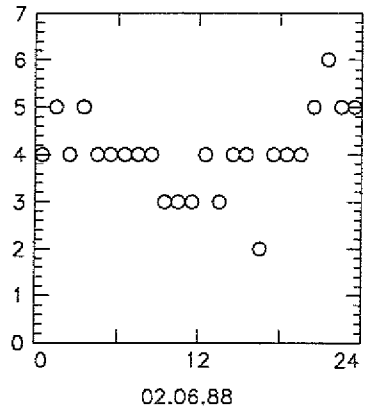

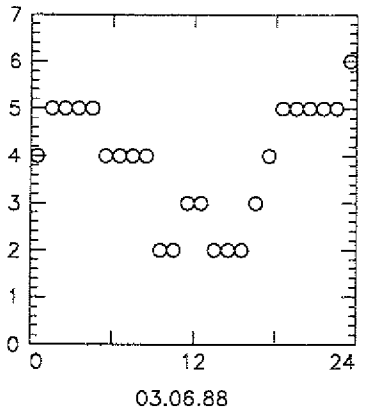

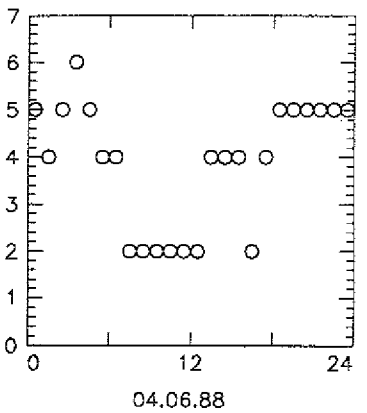

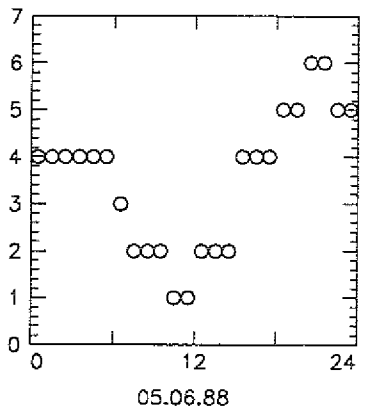

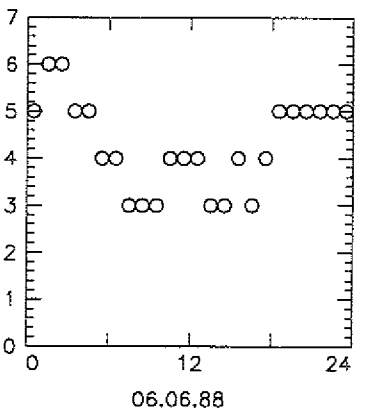

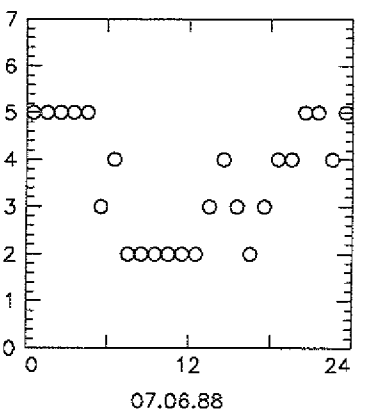

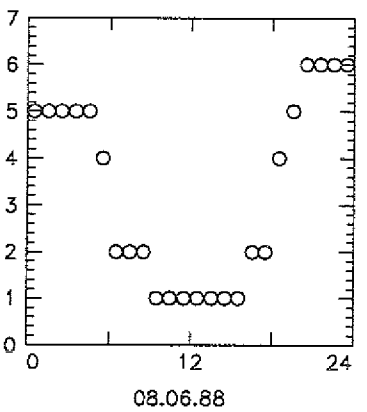

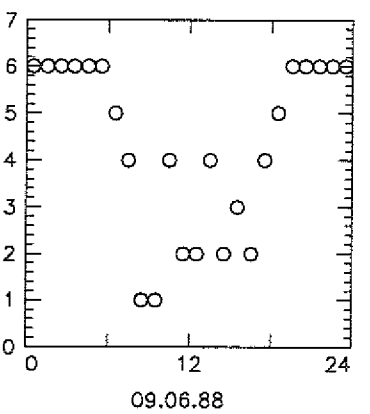

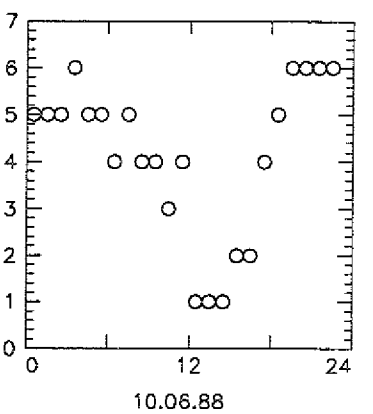

stability class *File: DIFK ENZ880HJ*

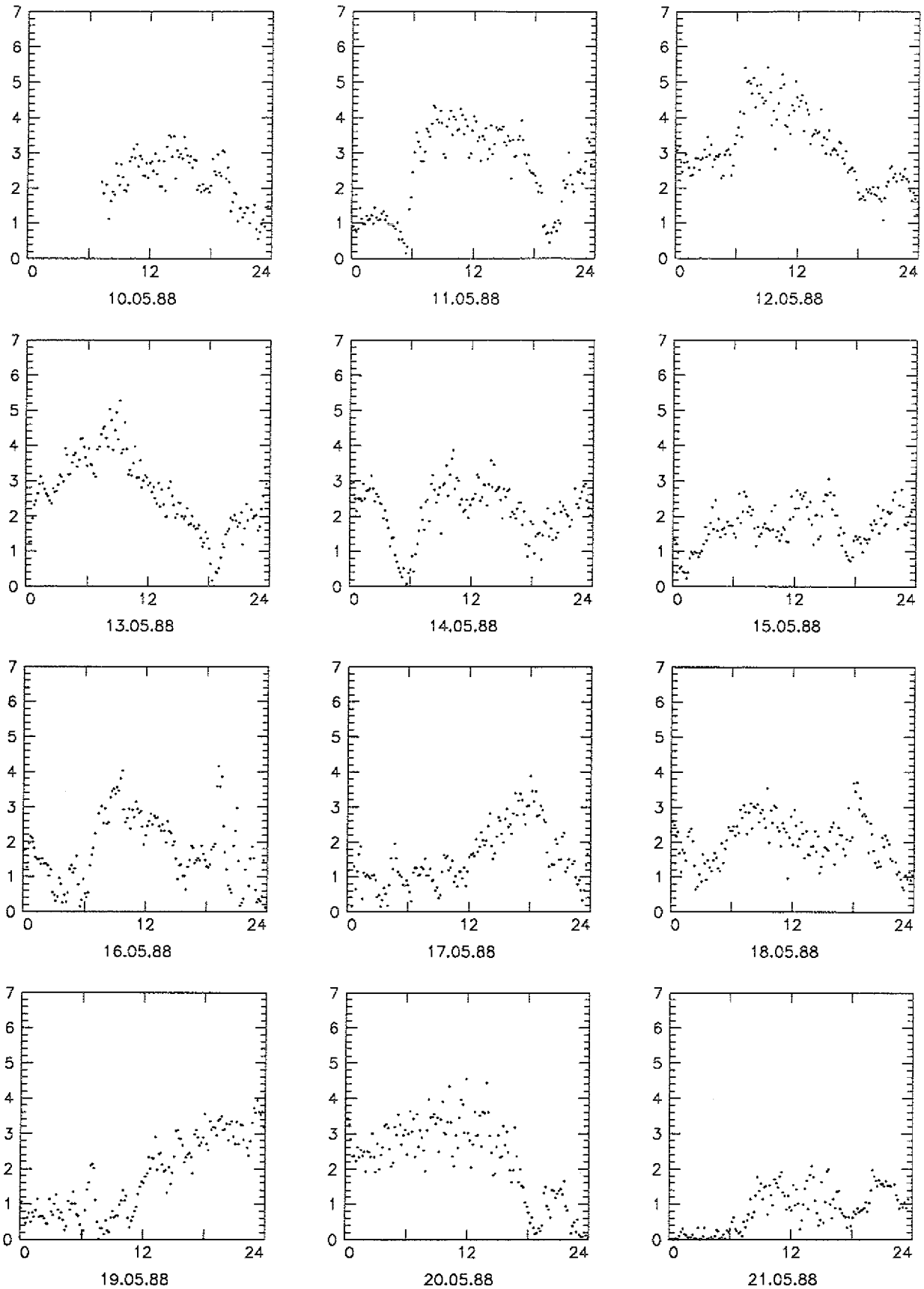

wind speed / m s^{-1}

File: WINDGSCH ENZ880HJ

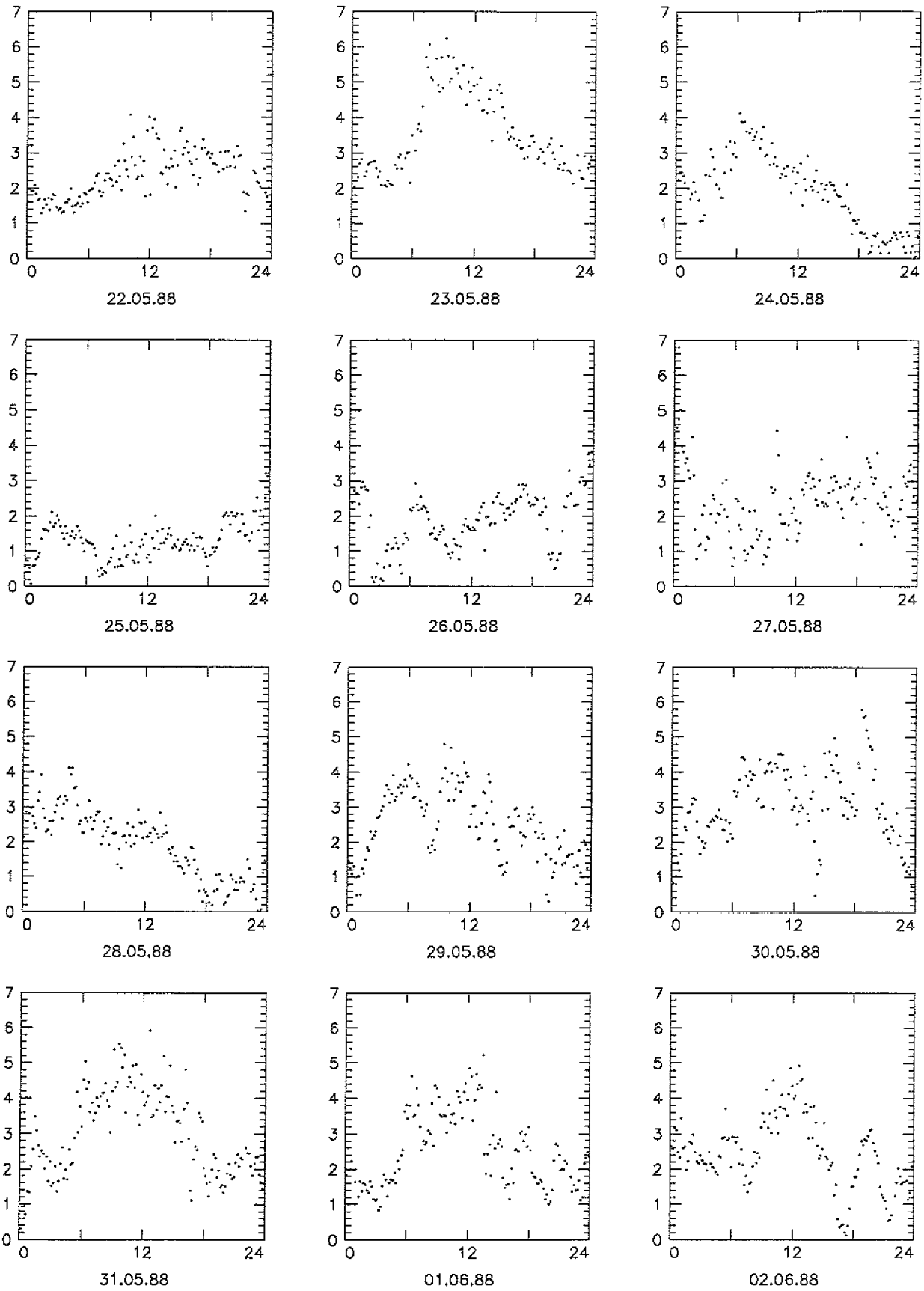

wind speed / m s^{-1}

File: WINDGSCH ENZ880HJ

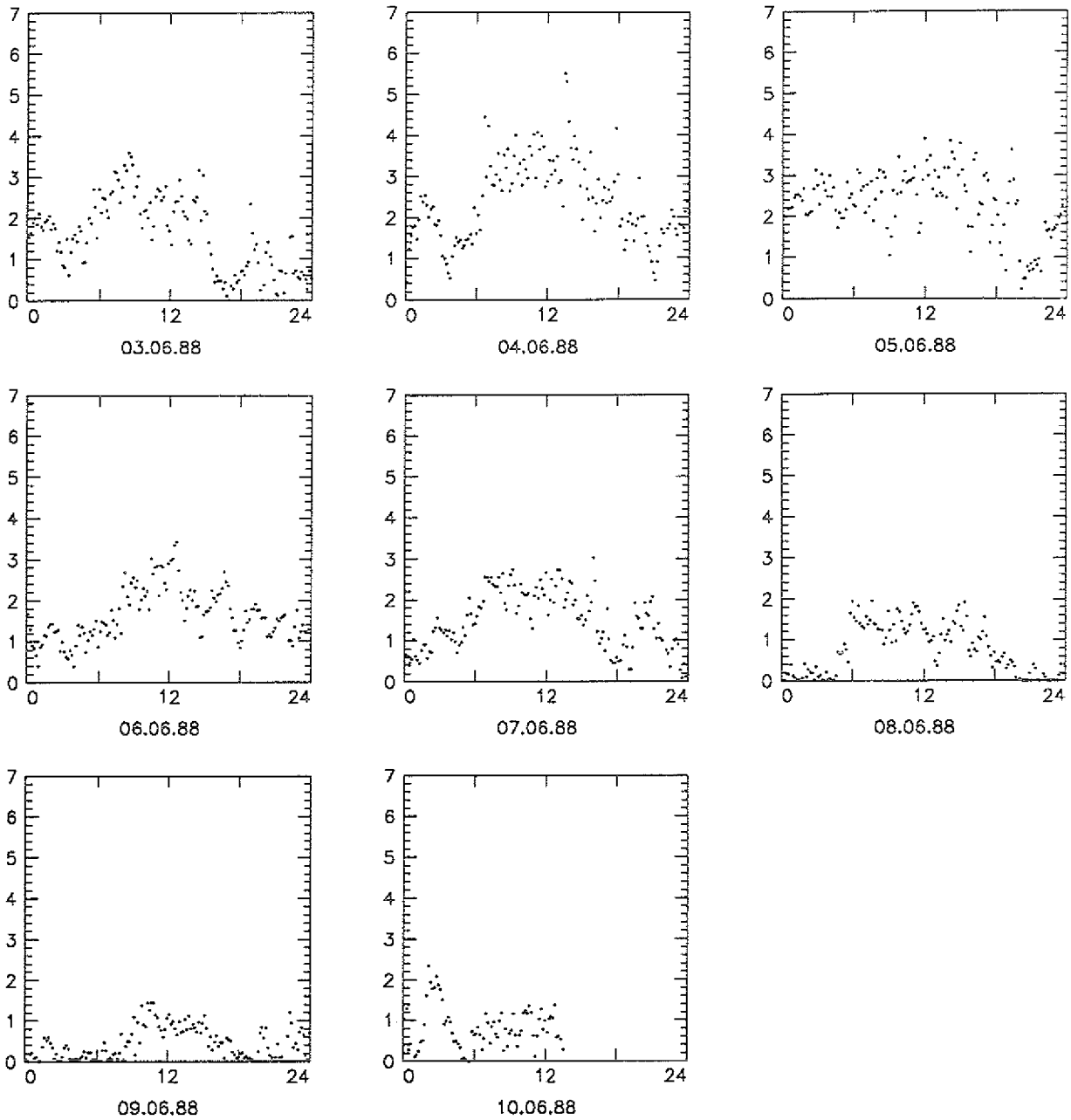

wind speed / m s^{-1}

File: WINDGSCH ENZ880HJ

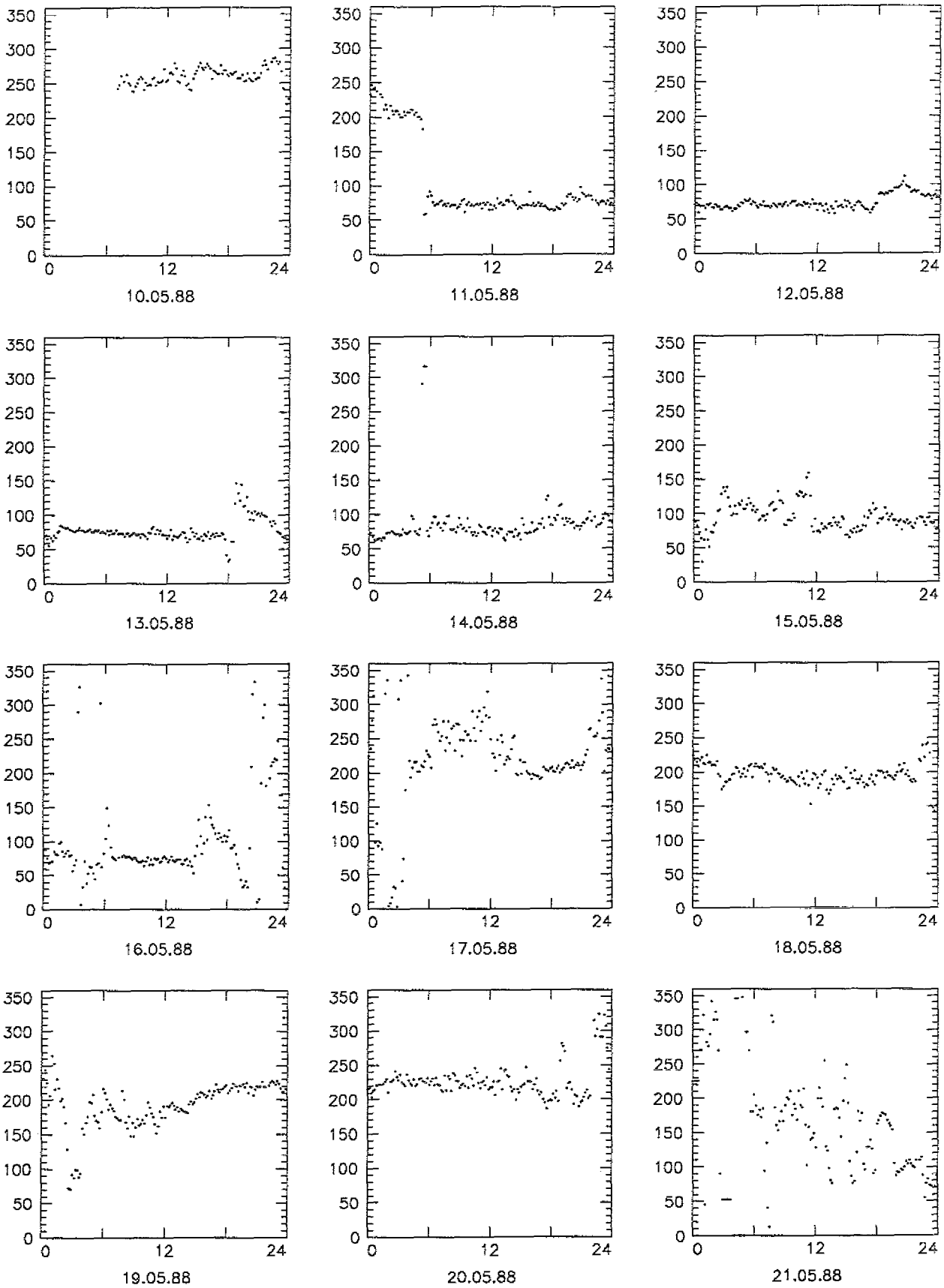

wind direction / °

File: WINDRICH ENZ880HJ

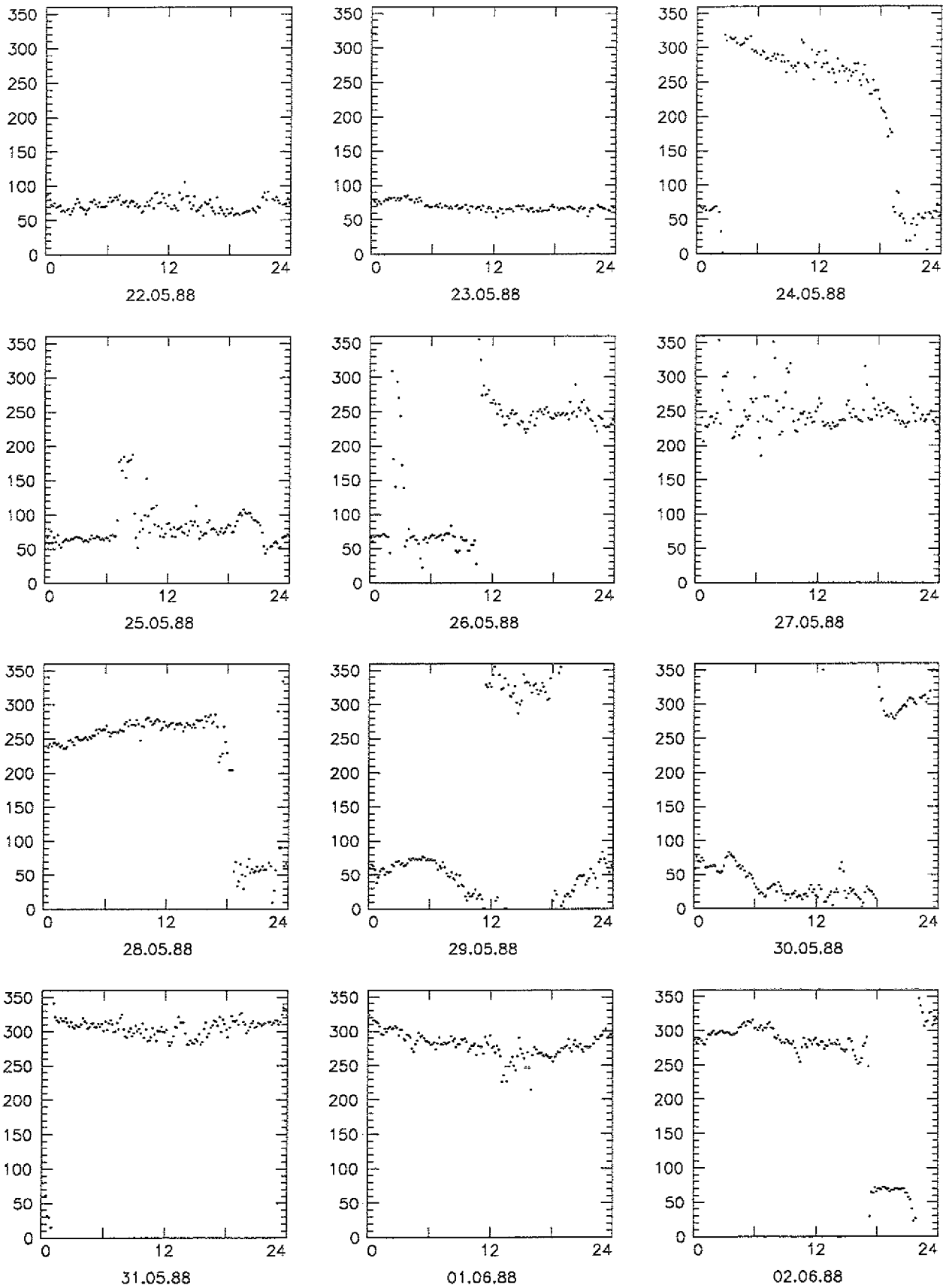

wind direction / °

File: WINDRICH ENZ880HJ

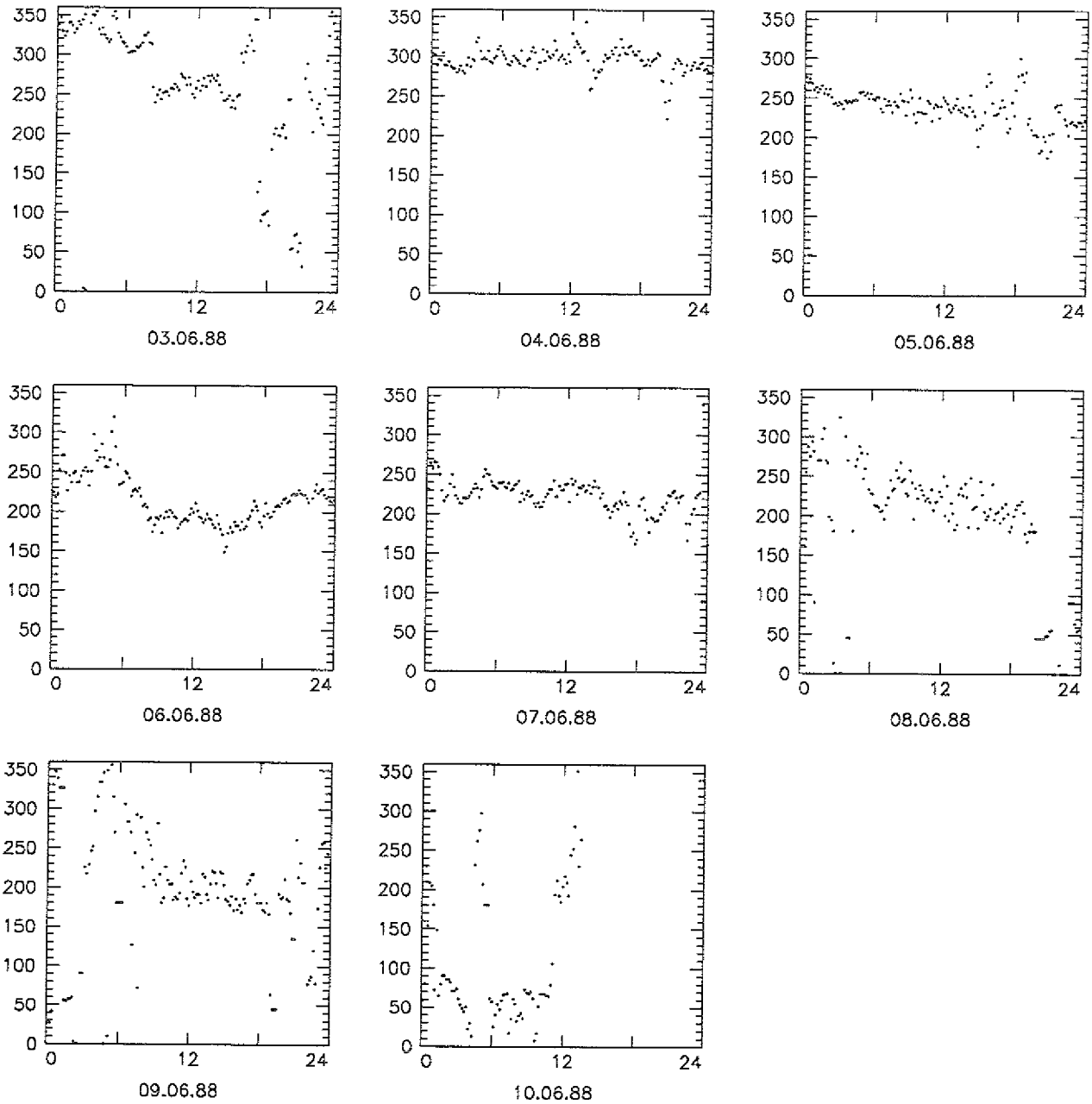

wind direction / °

File: WINDRICH ENZ880HJ

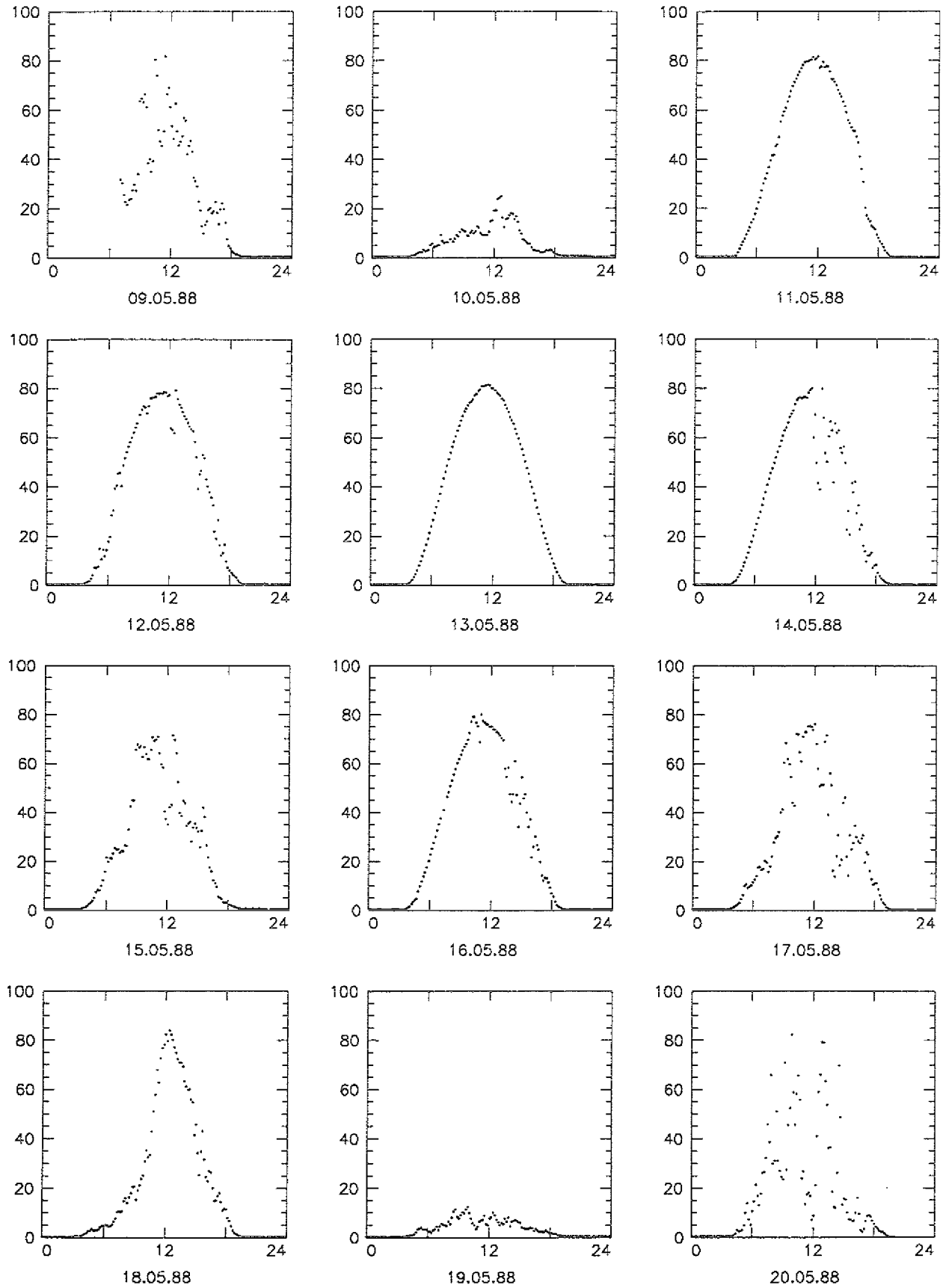

total radiation / mW cm^{-2} *File: GSTRHLNG ENZ880HJ*

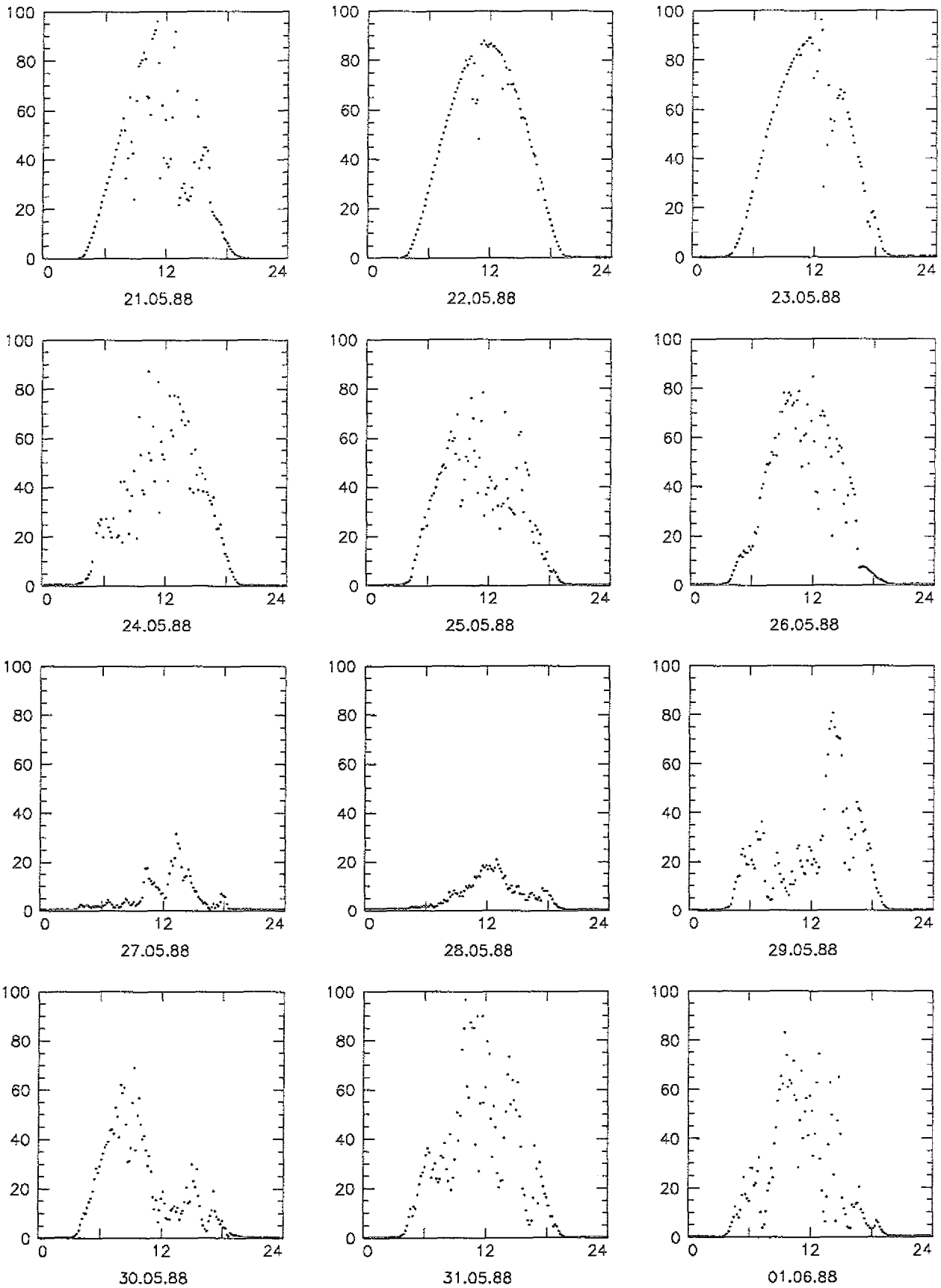

total radiation / mW cm^{-2} *File: GSTRHLNG ENZ880HJ*

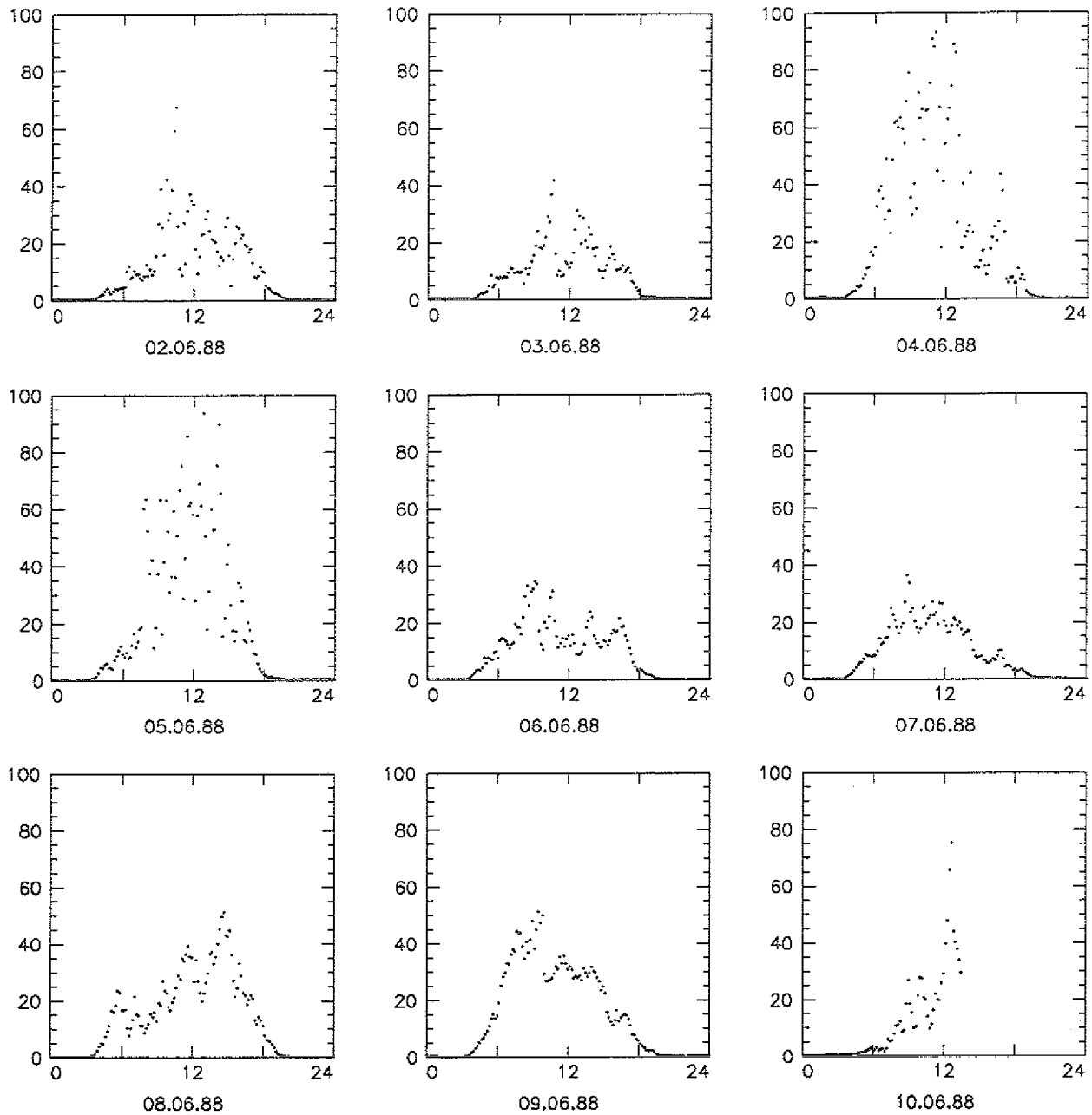

total radiation / mW cm^{-2} *File: GSTRHLNG ENZ880HJ*

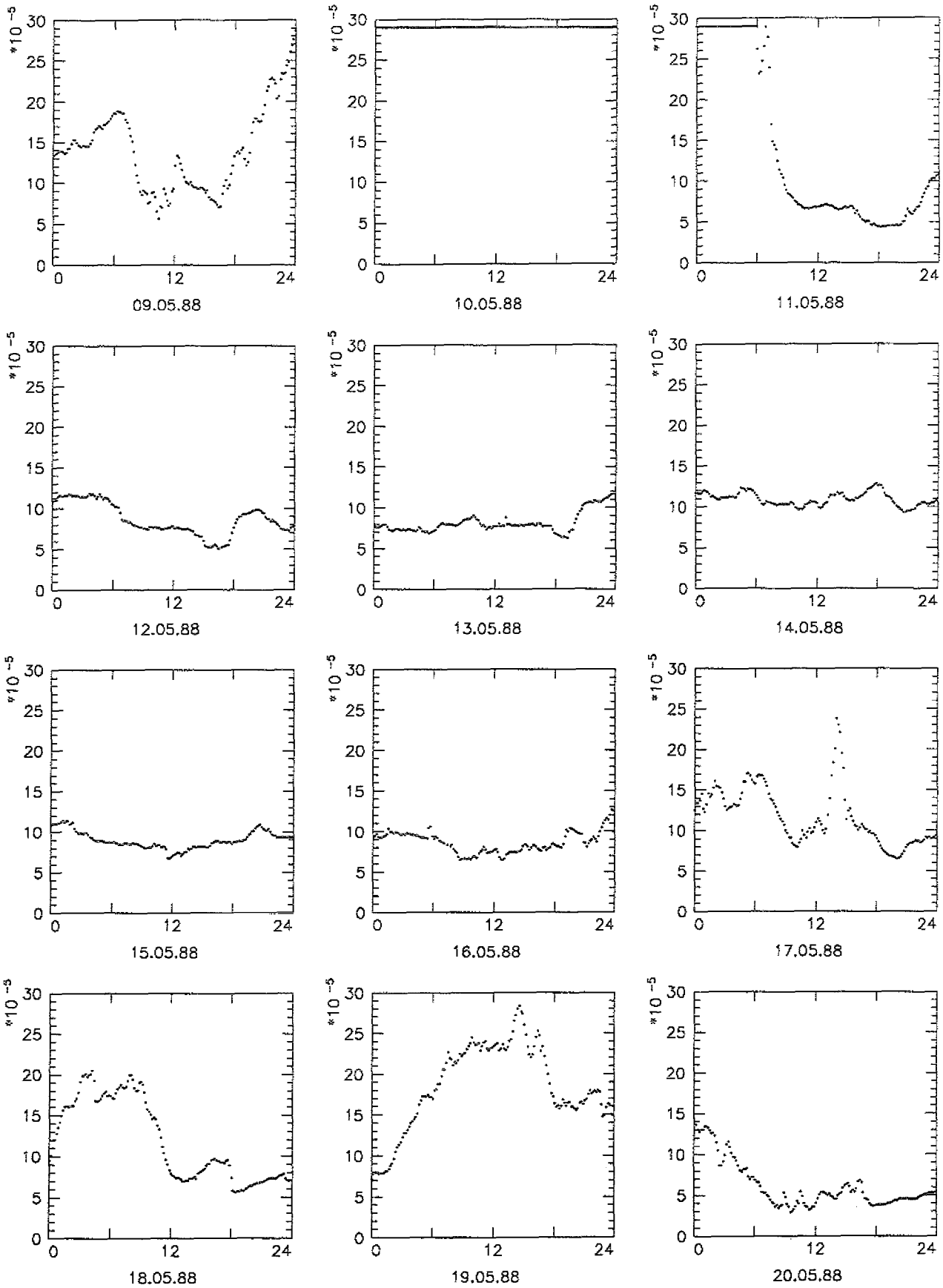

scattering coefficient / m^{-1} *File: STREU ENZ880HJ*

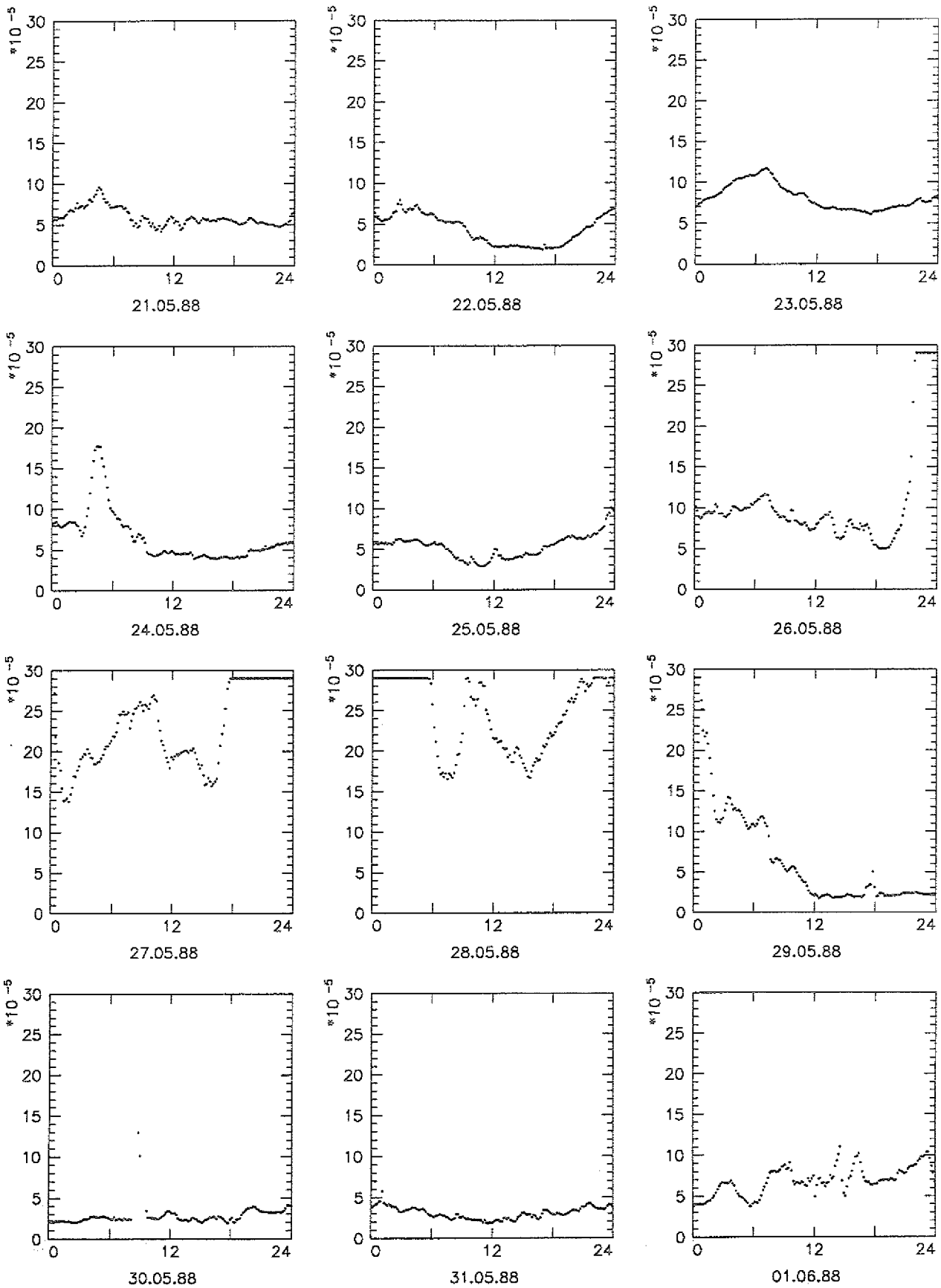

scattering coefficient / m^{-1} *File: STREU ENZ880HJ*

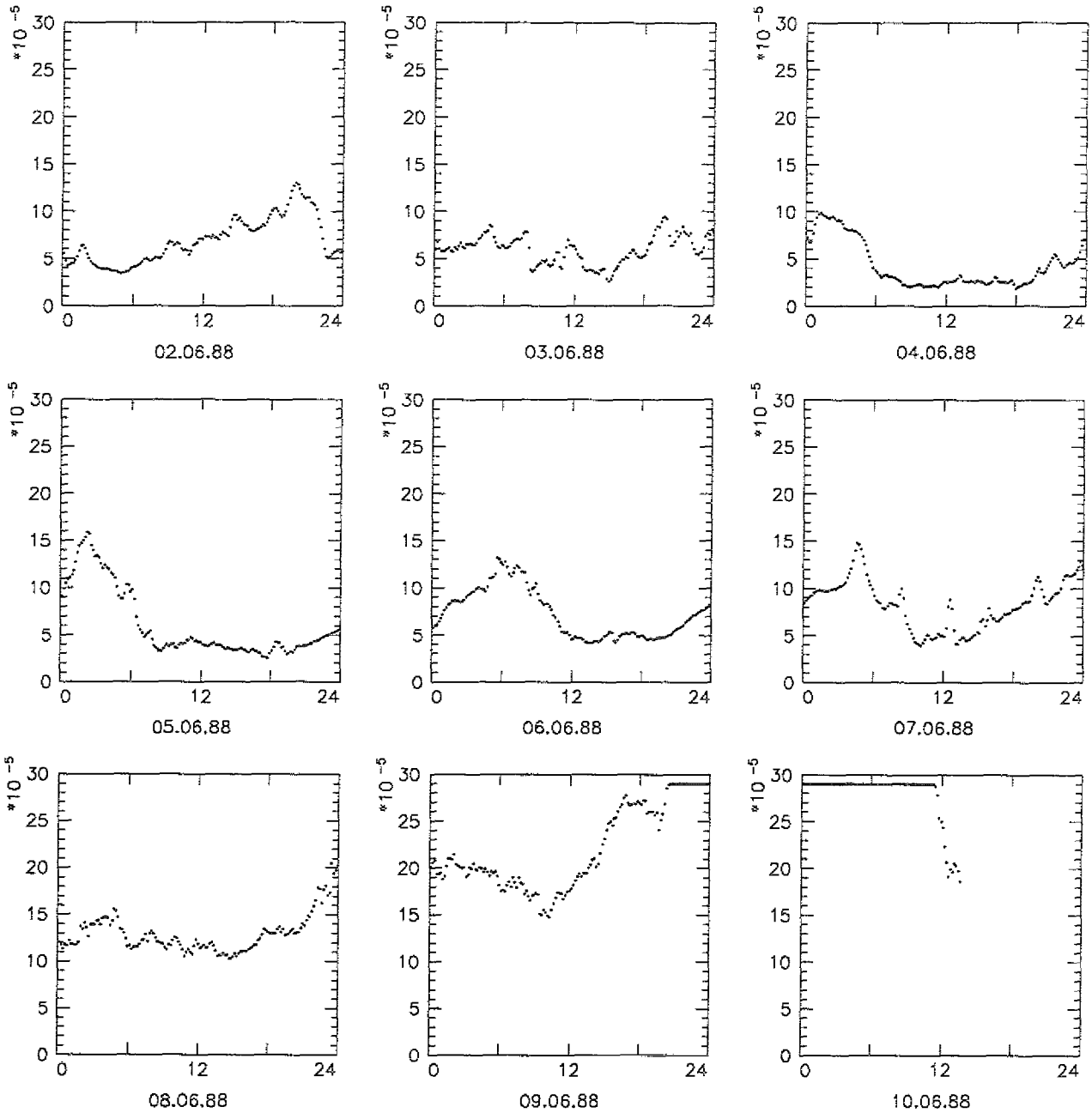

scattering coefficient / m^{-1} *File: STREU ENZ880HJ*

Appendix B Weather Maps for the period May 5 to June 12, 1988

The maps refer to ground level (Boden) at 12 UTC. The charts were kindly provided by the Deutscher Wetterdienst.

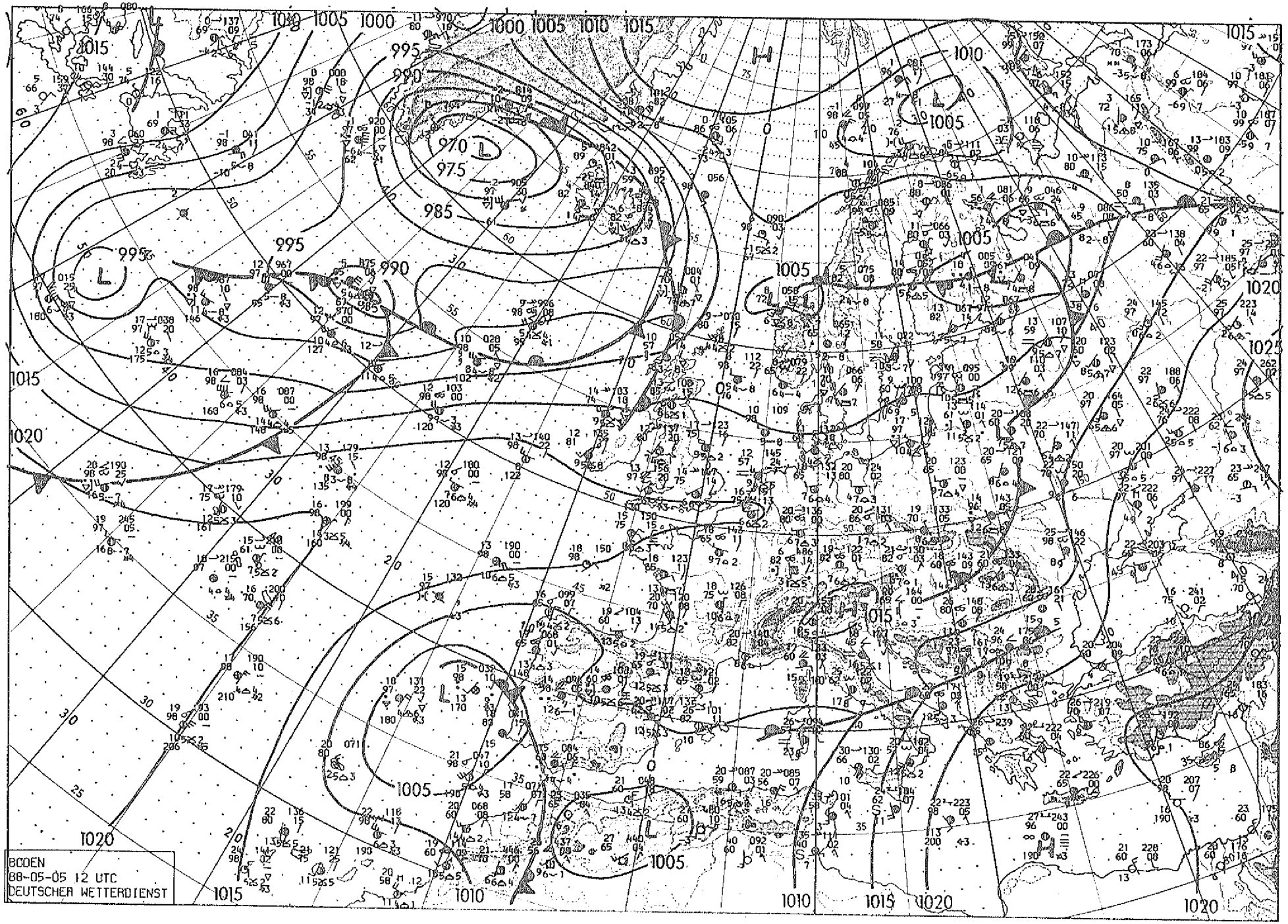
BODEN
88-05-05 12 UTC
DEUTSCHER WETTERDIENST

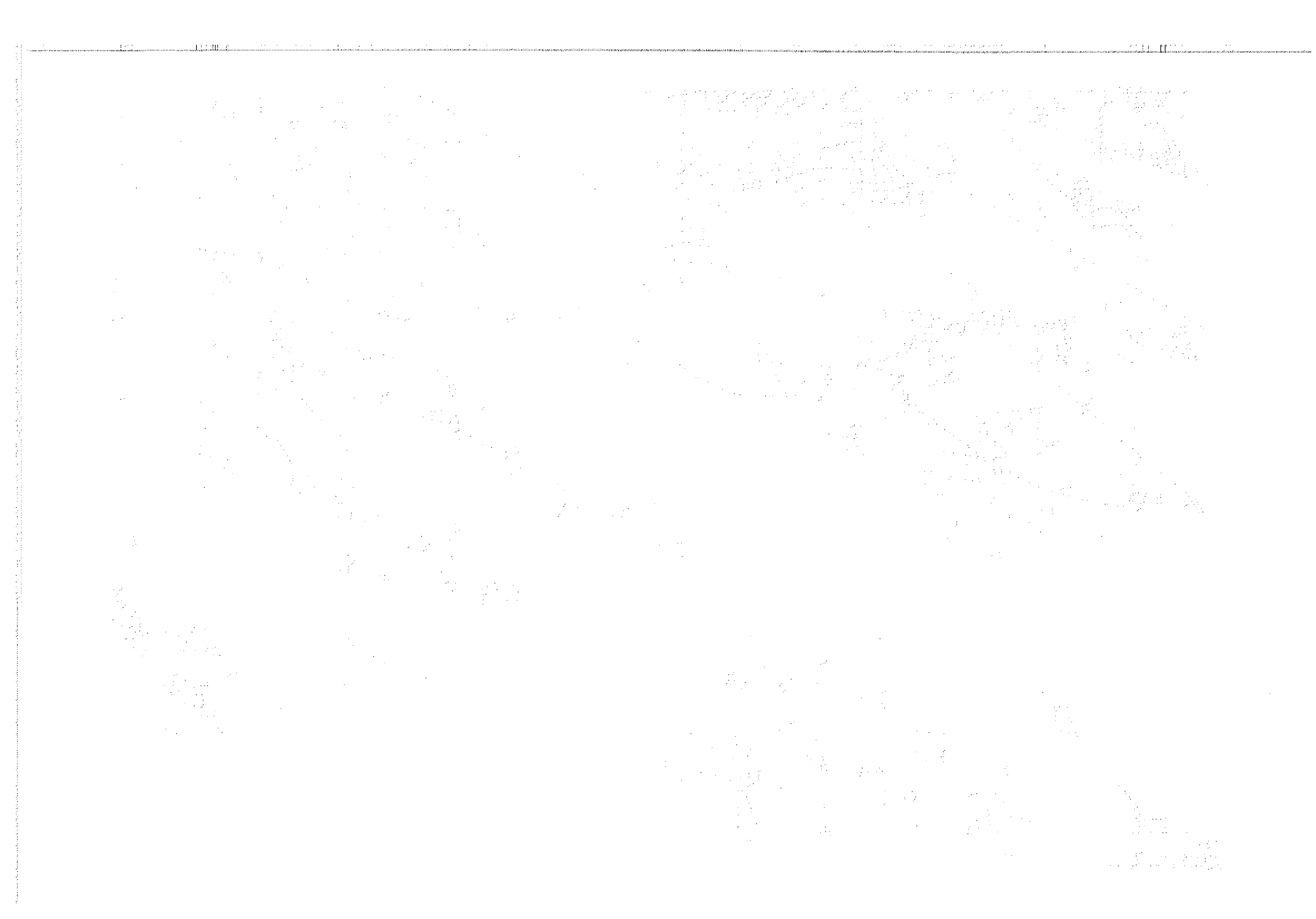

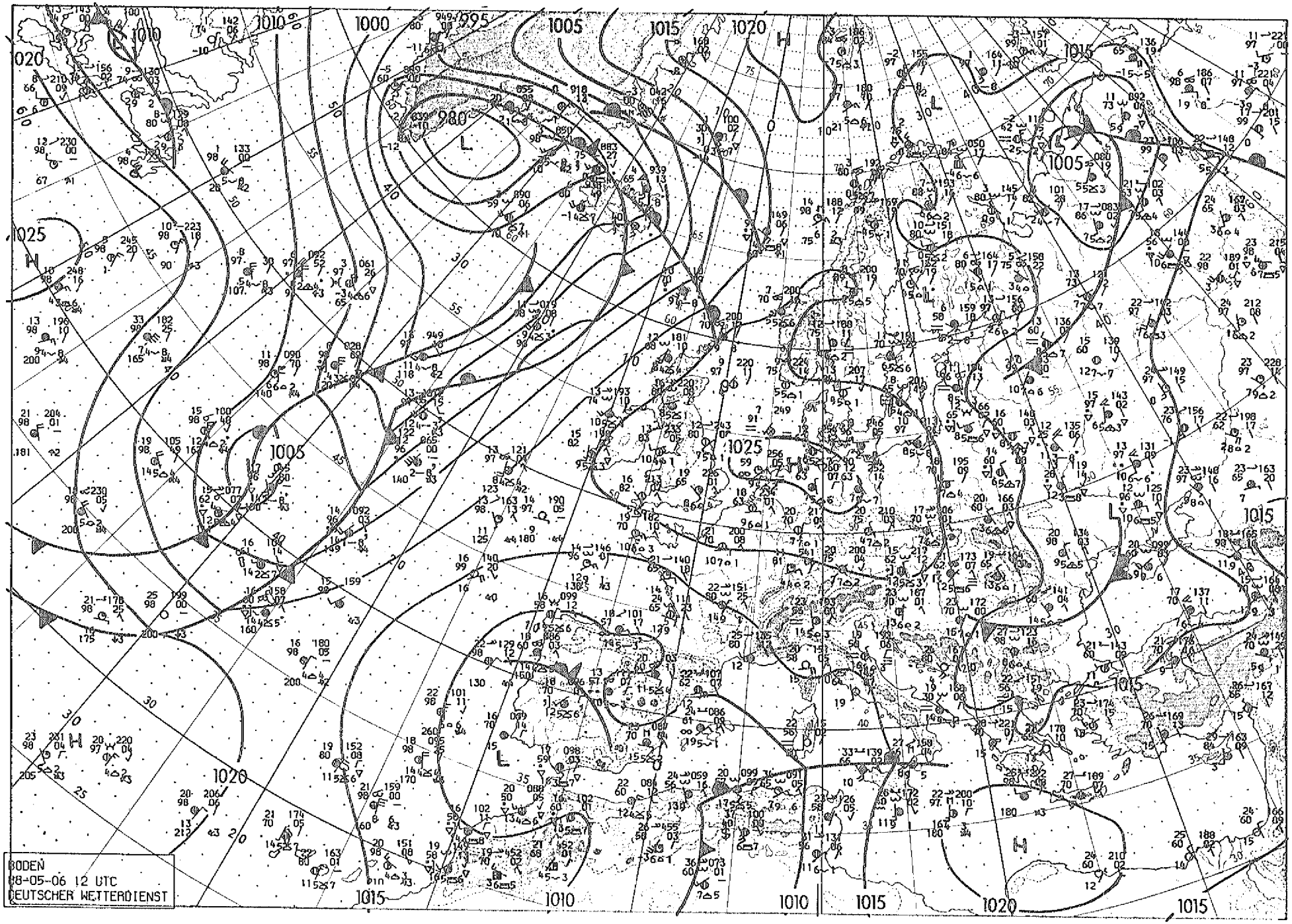
BODEN
08-05-06 12 UTC
DEUTSCHER WETTERDIENST

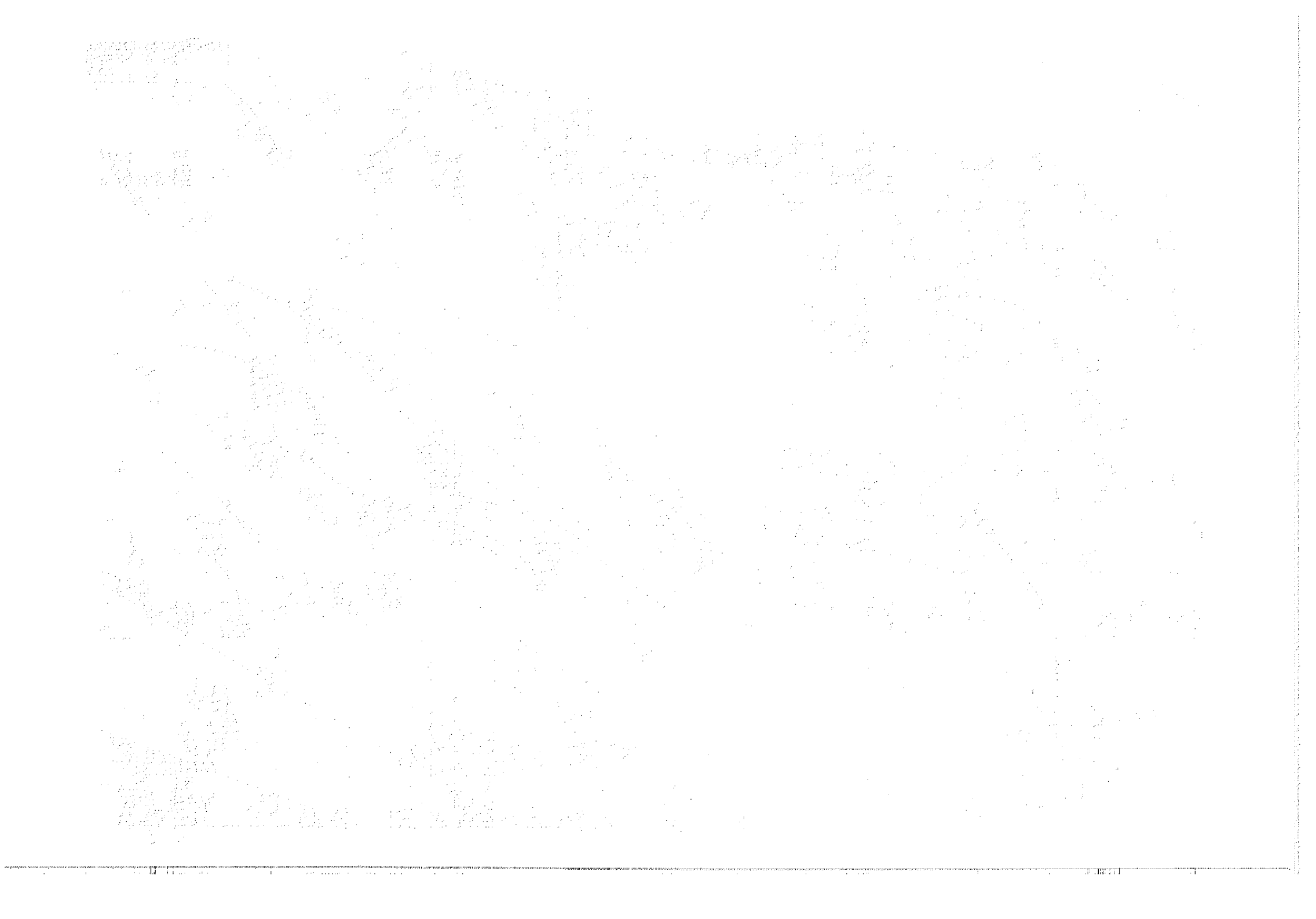

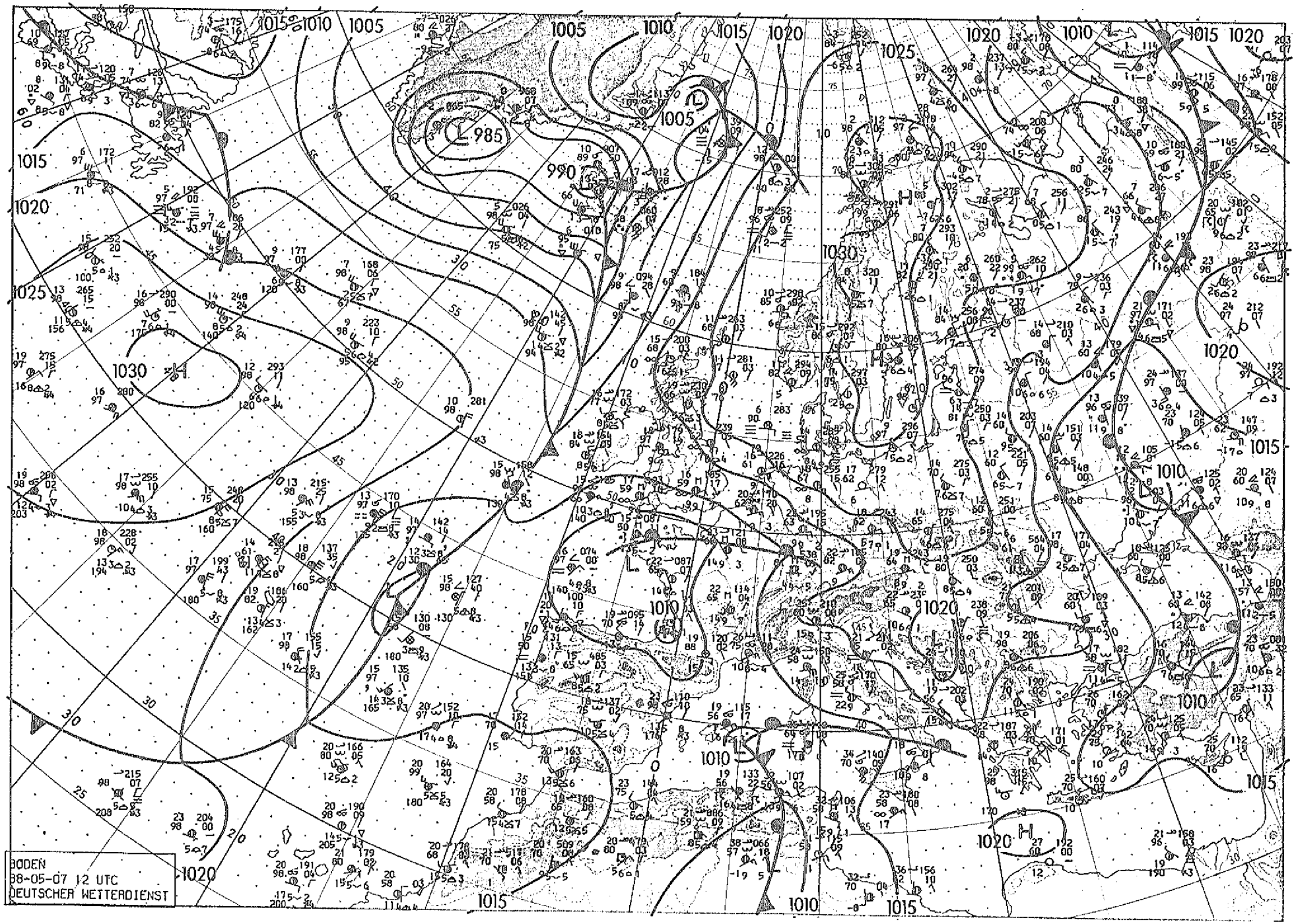
BODEN
88-05-07 12 UTC
DEUTSCHER WETTERDIENST

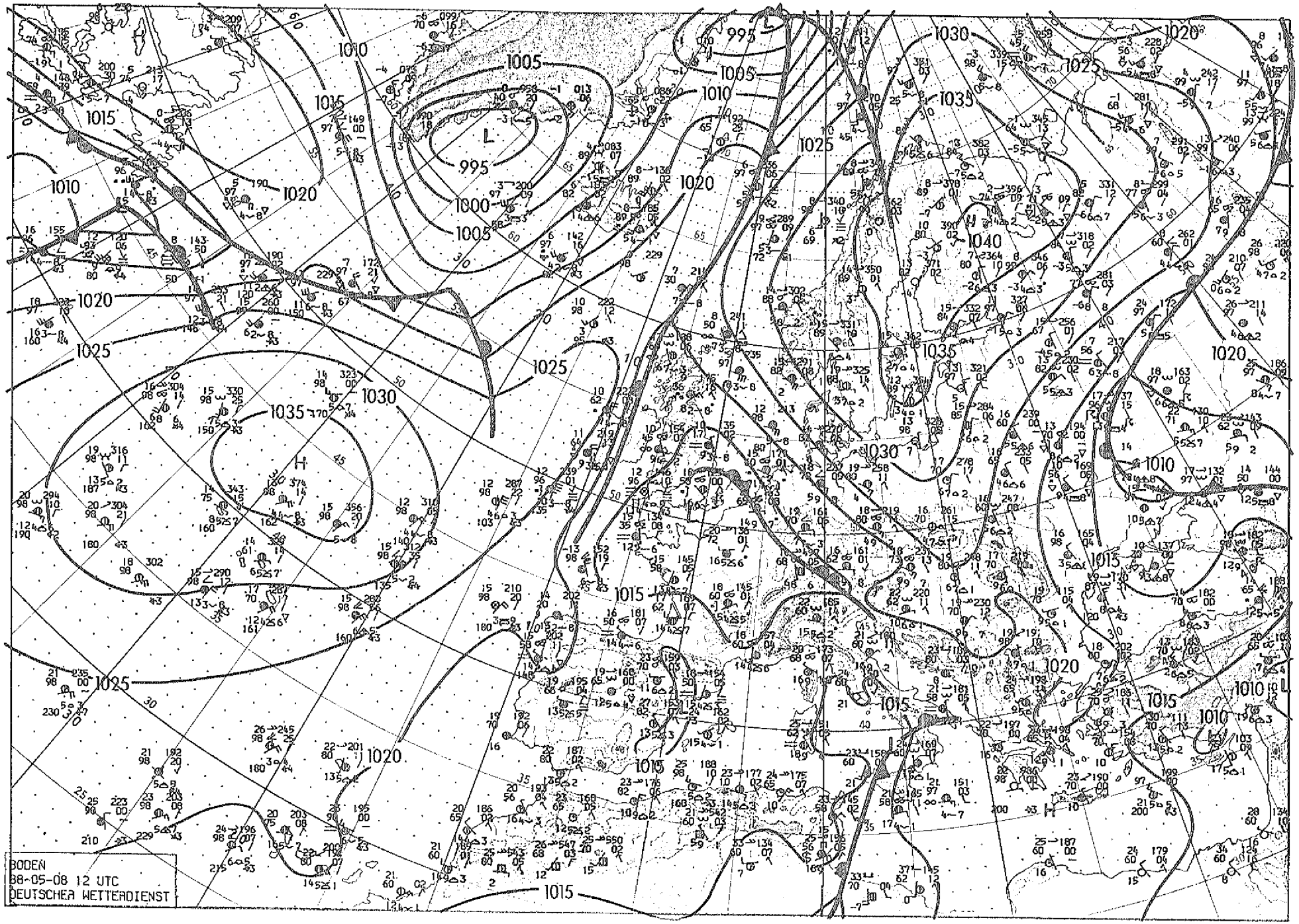
BODEN
88-05-08 12 UTC
DEUTSCHER WETTERDIENST

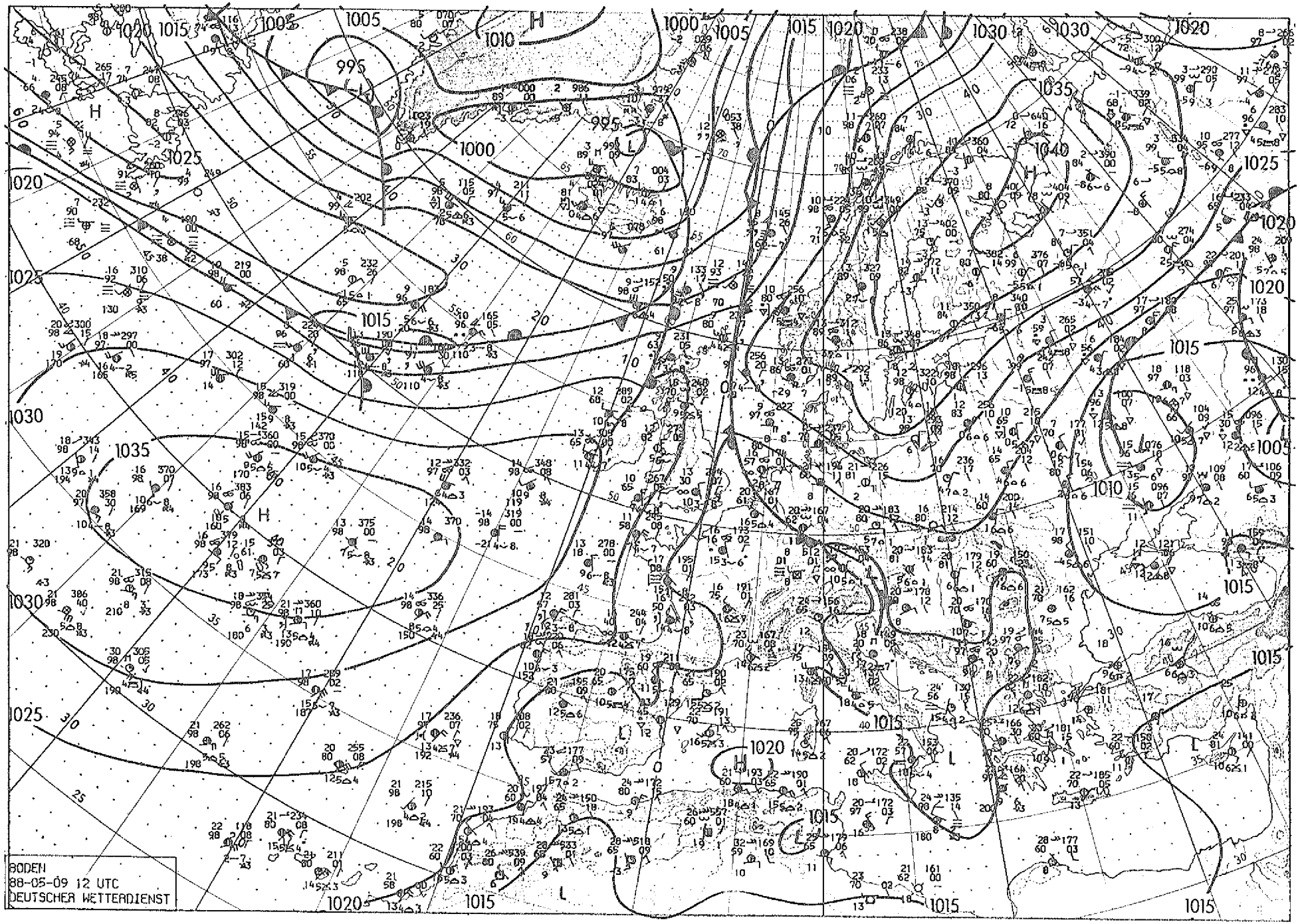
BODEN
88-05-09 12 UTC
DEUTSCHER WETTERDIENST

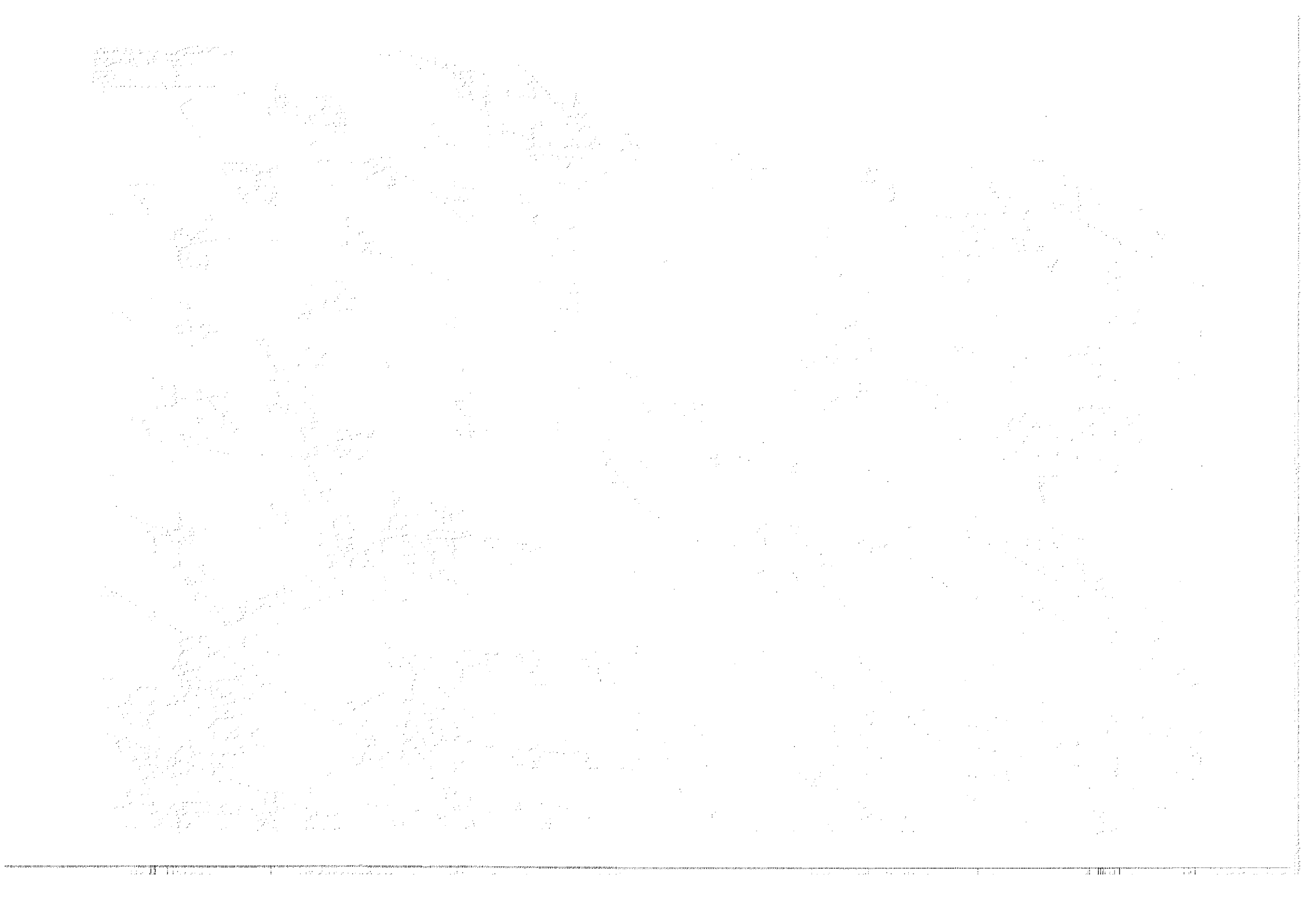

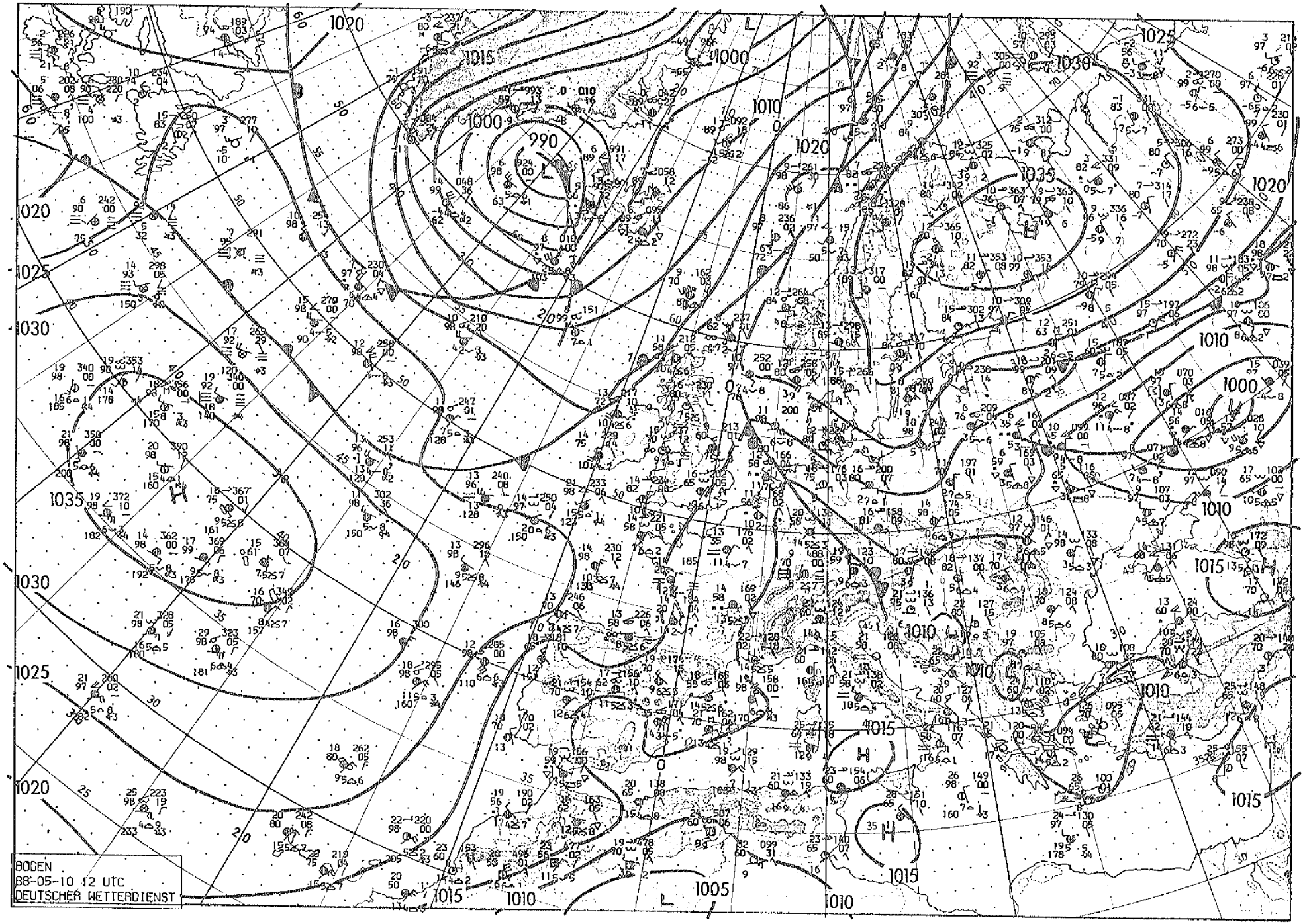
BODEN
88-05-10 12 UTC
DEUTSCHER WETTERDIENST

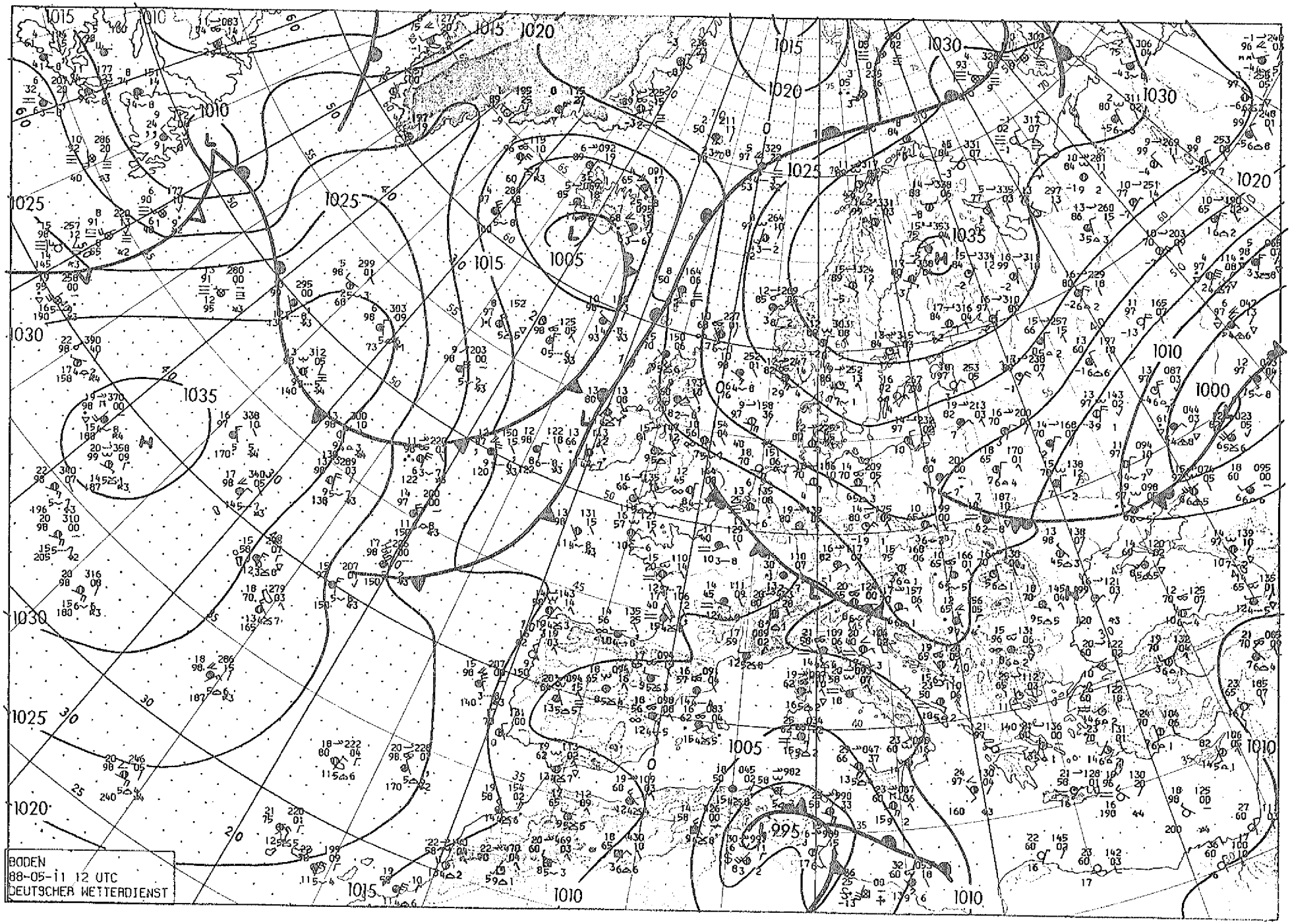
BODEN
88-05-11 12 UTC
DEUTSCHER WETTERDIENST

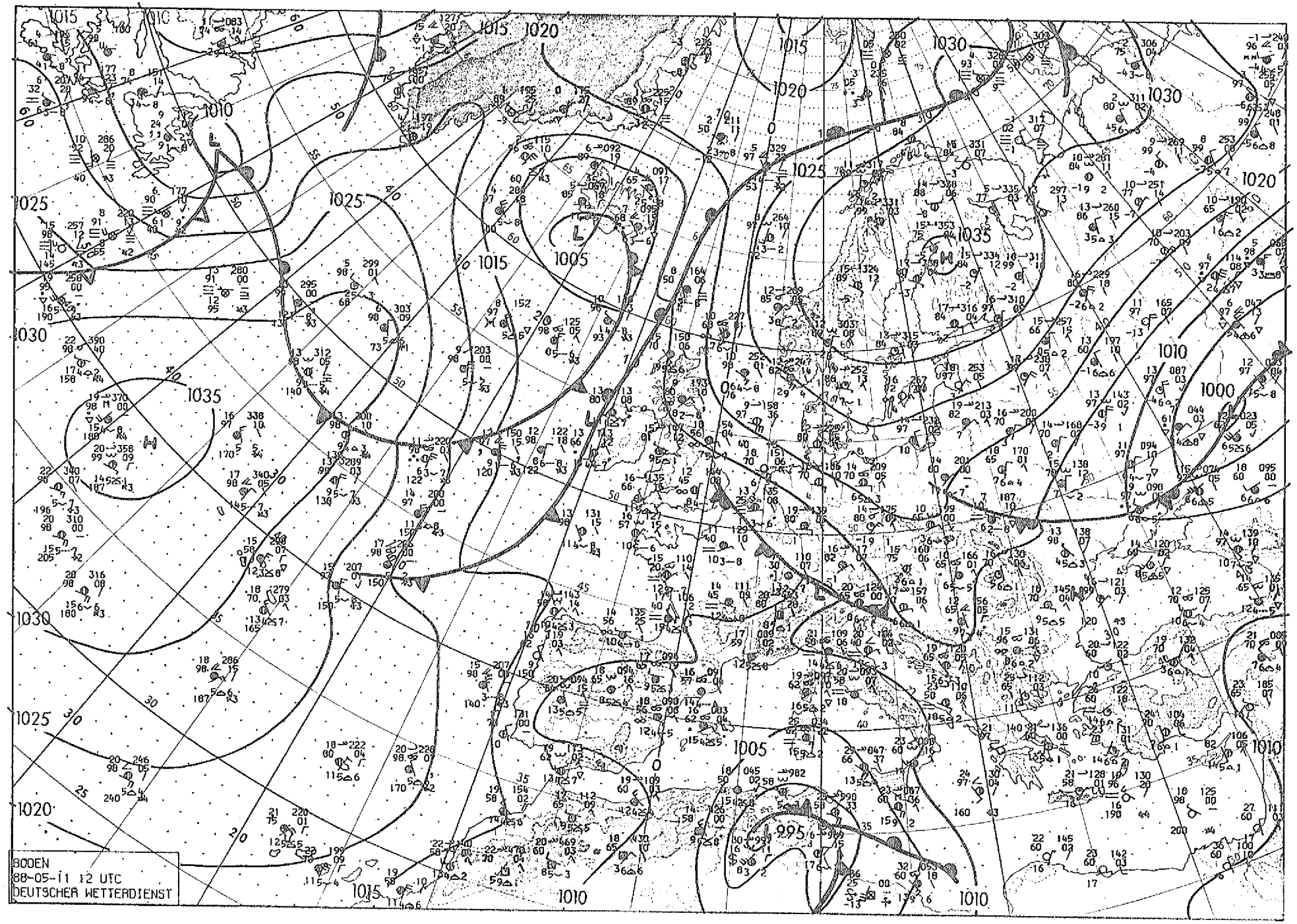
BODEN
88-05-11 12 UTC
DEUTSCHER WETTERDIENST

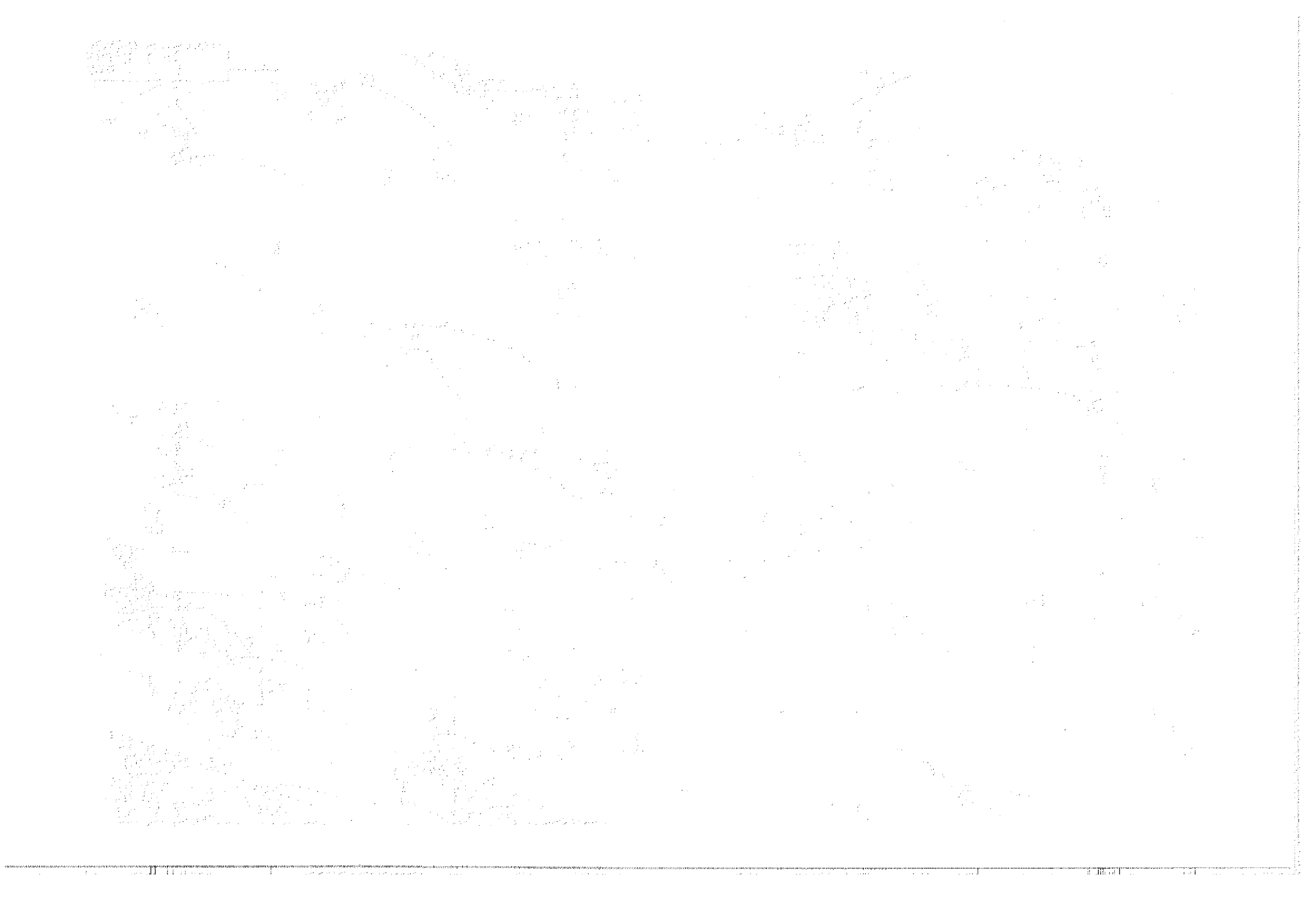

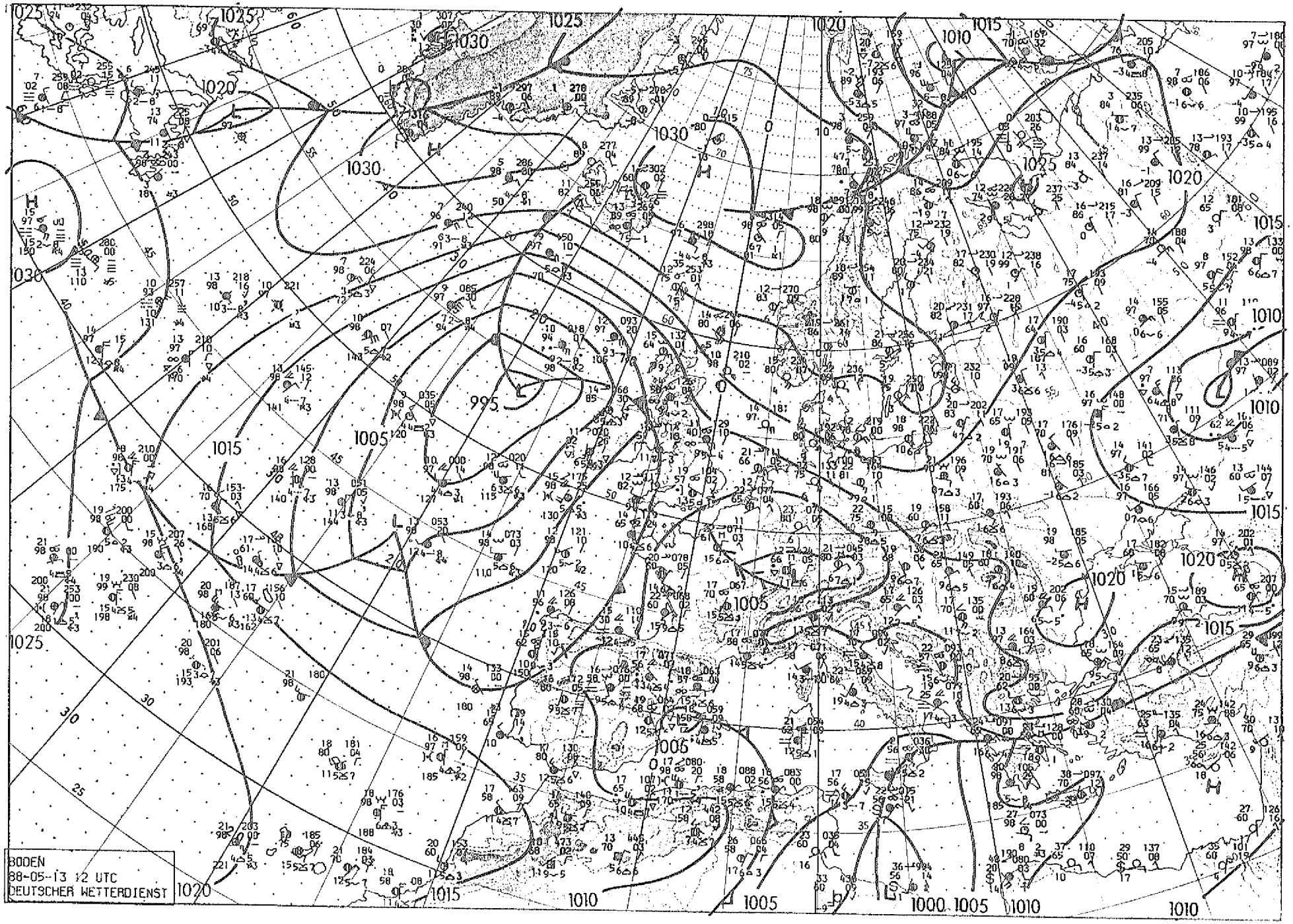
BODEN
88-05-13 12 UTC
DEUTSCHER WETTERDIENST

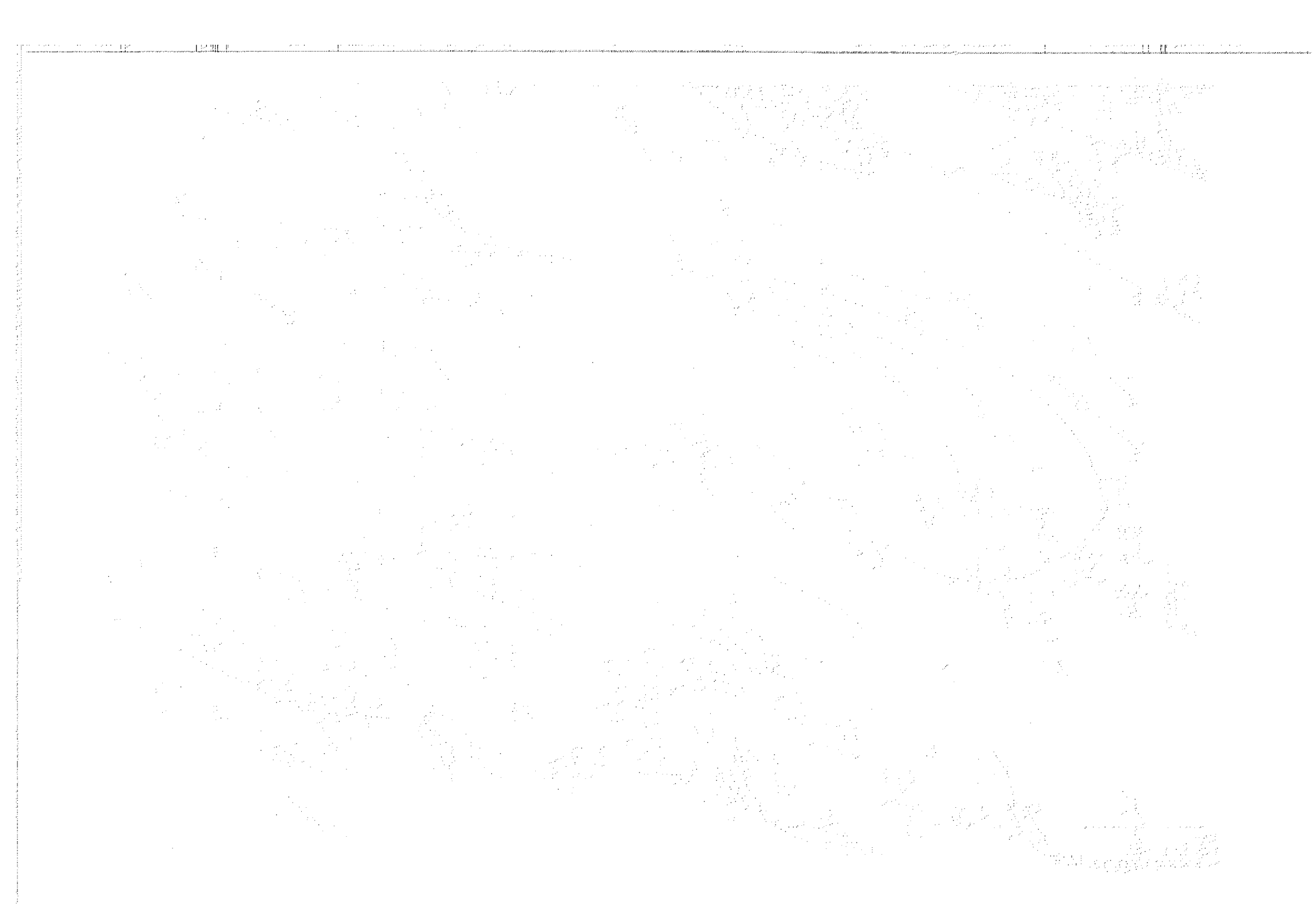

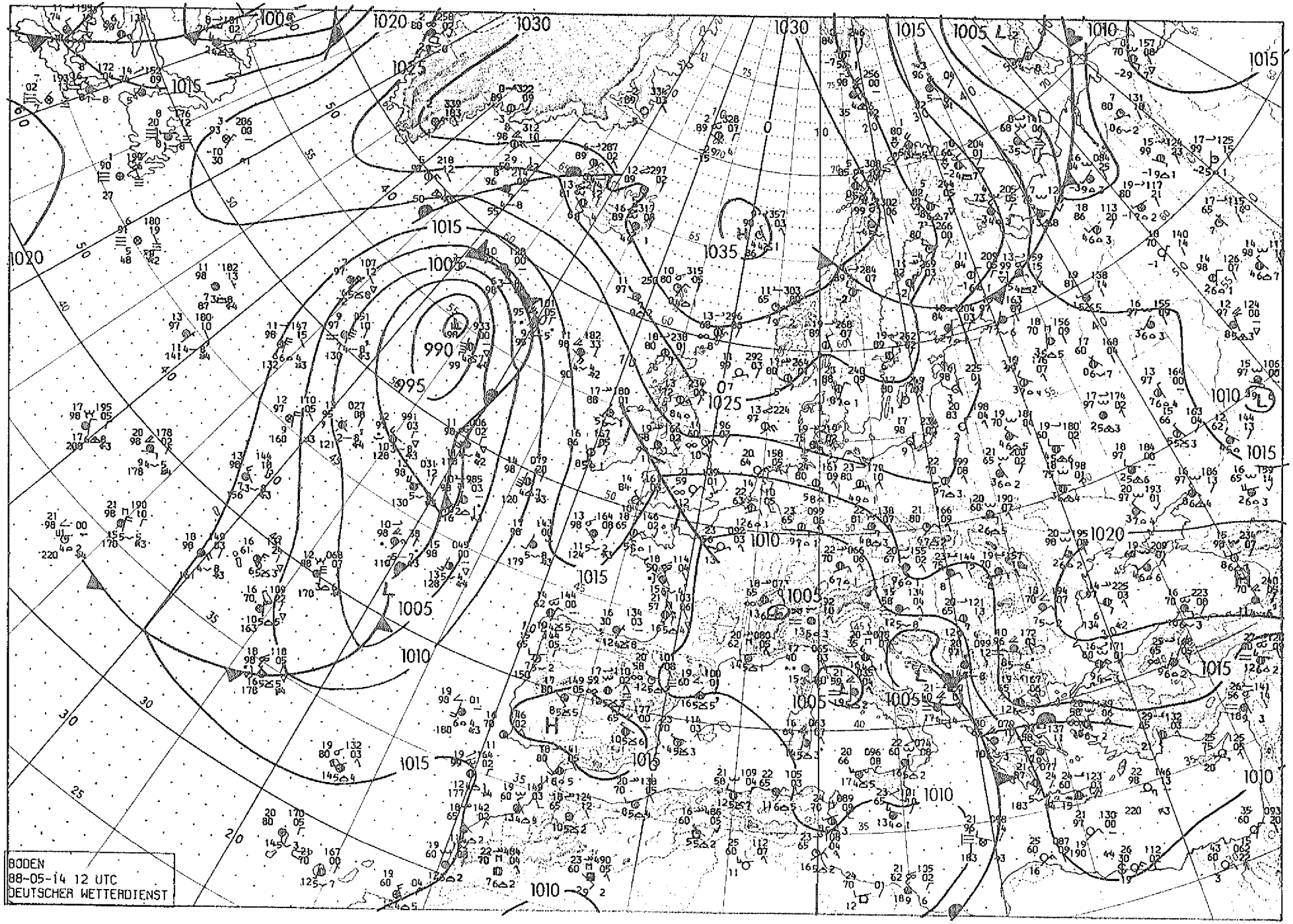
BODEN
88-05-14 12 UTC
DEUTSCHER WETTERDIENST

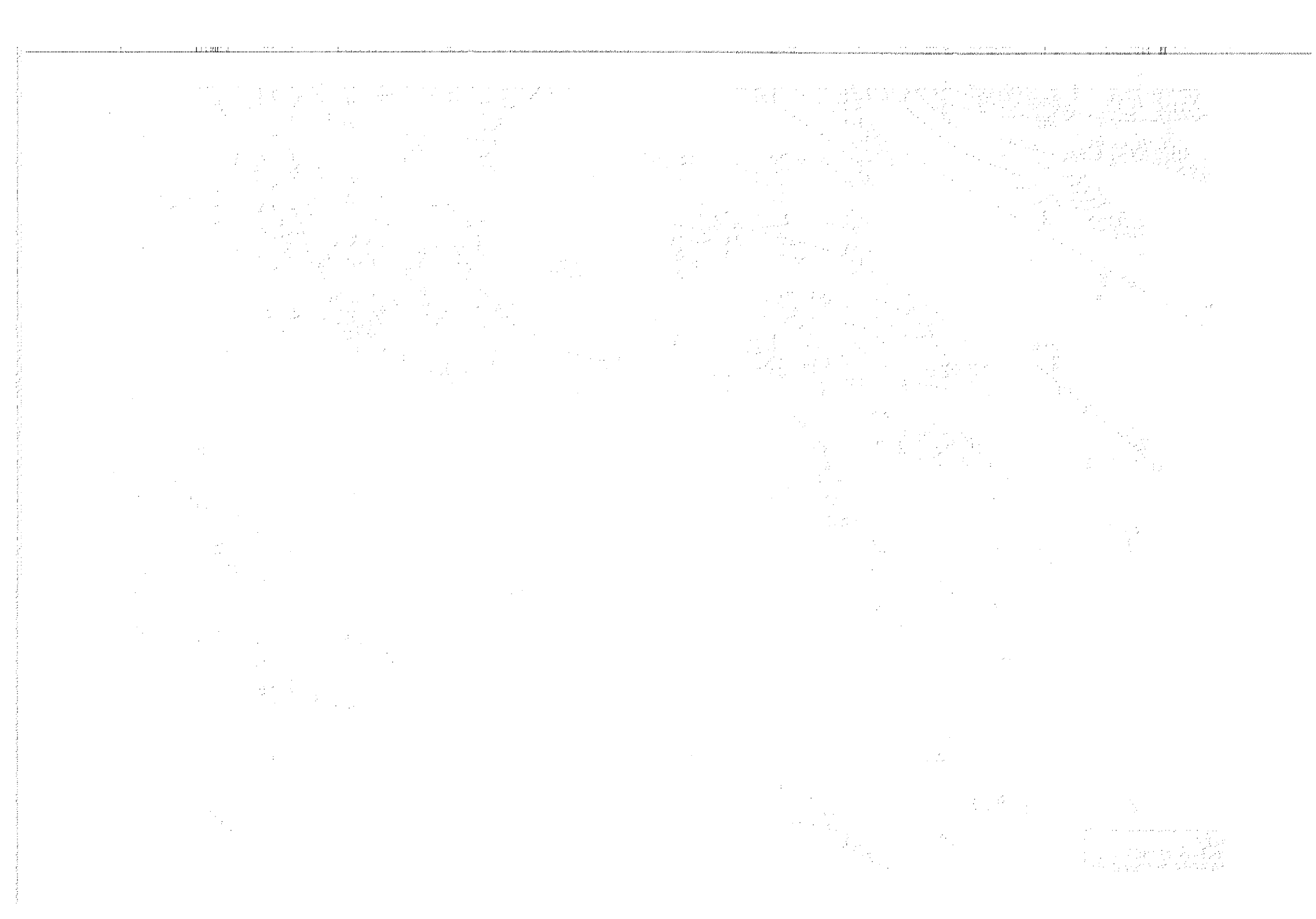

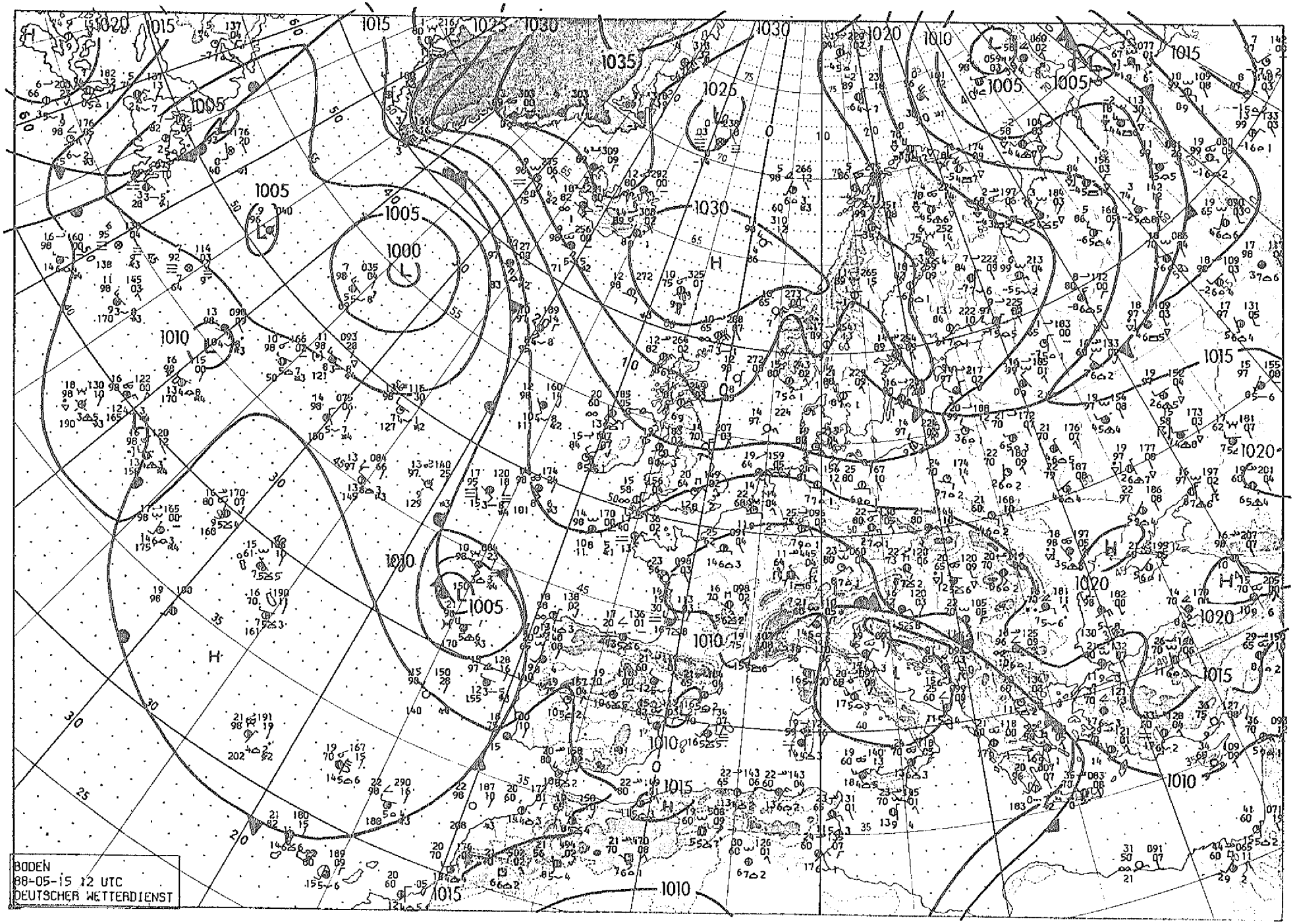
BODEN
88-05-15 12 UTC
DEUTSCHER WETTERDIENST

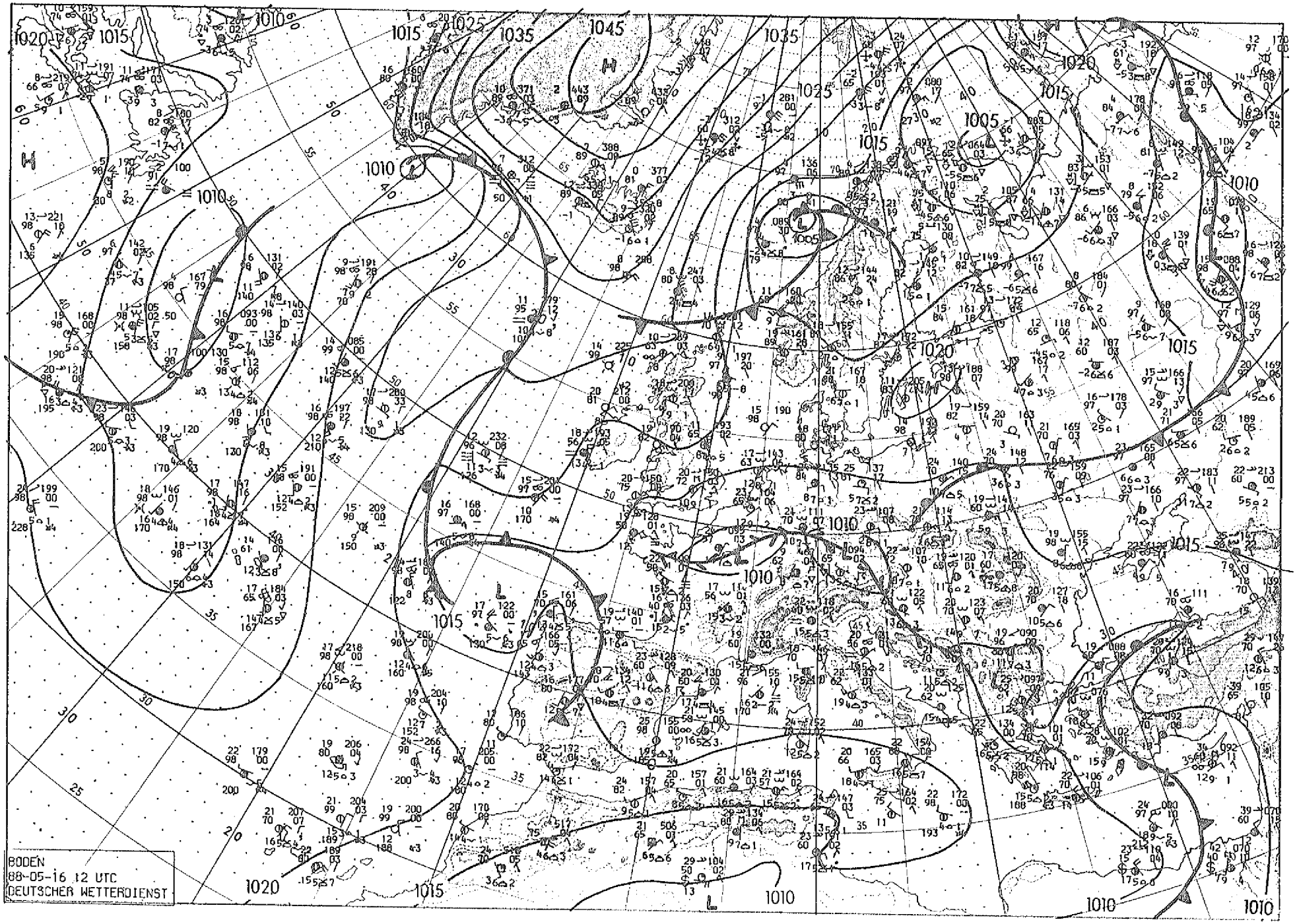
BODEN
88-05-16 12 UTC
DEUTSCHER WETTERDIENST

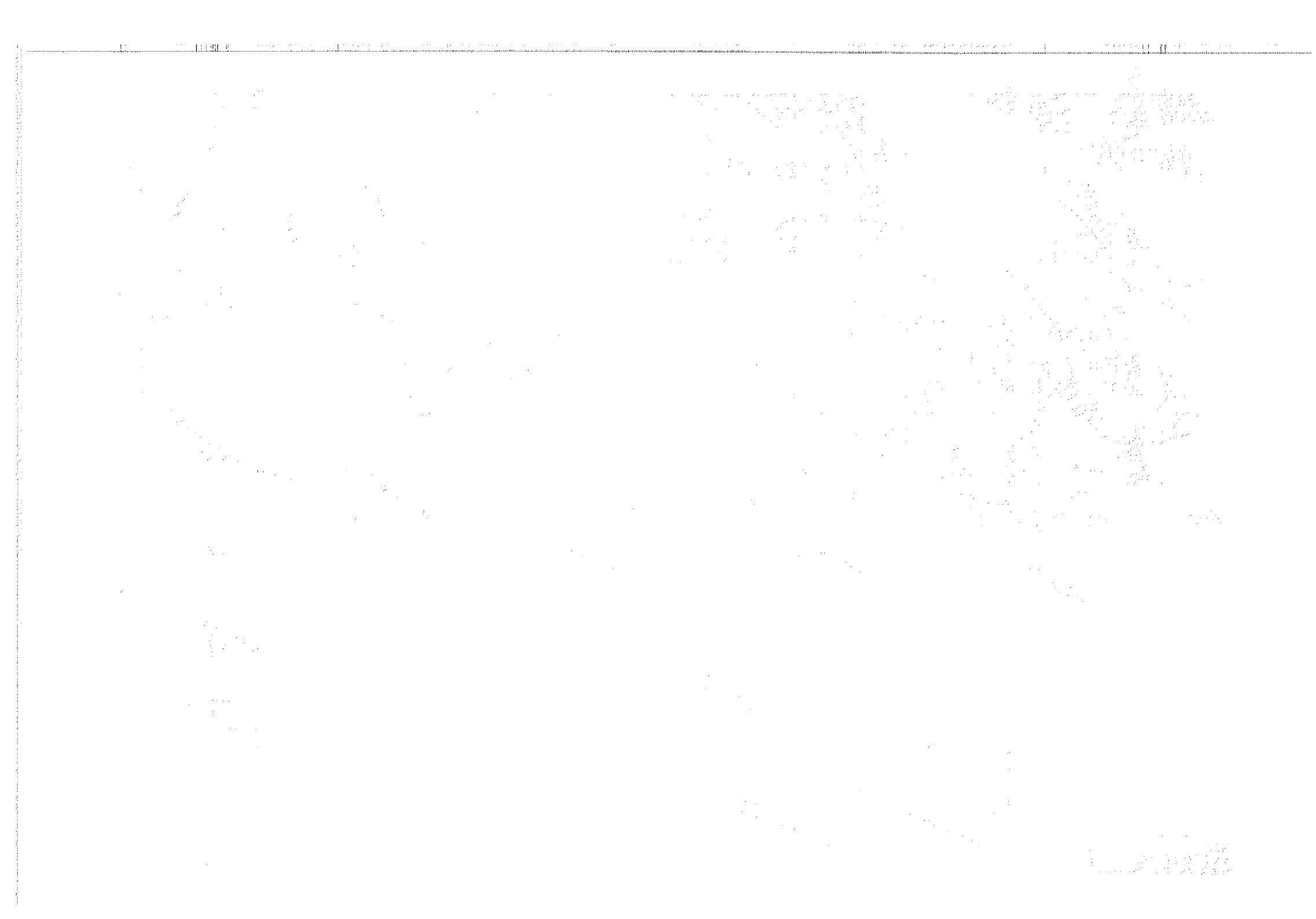

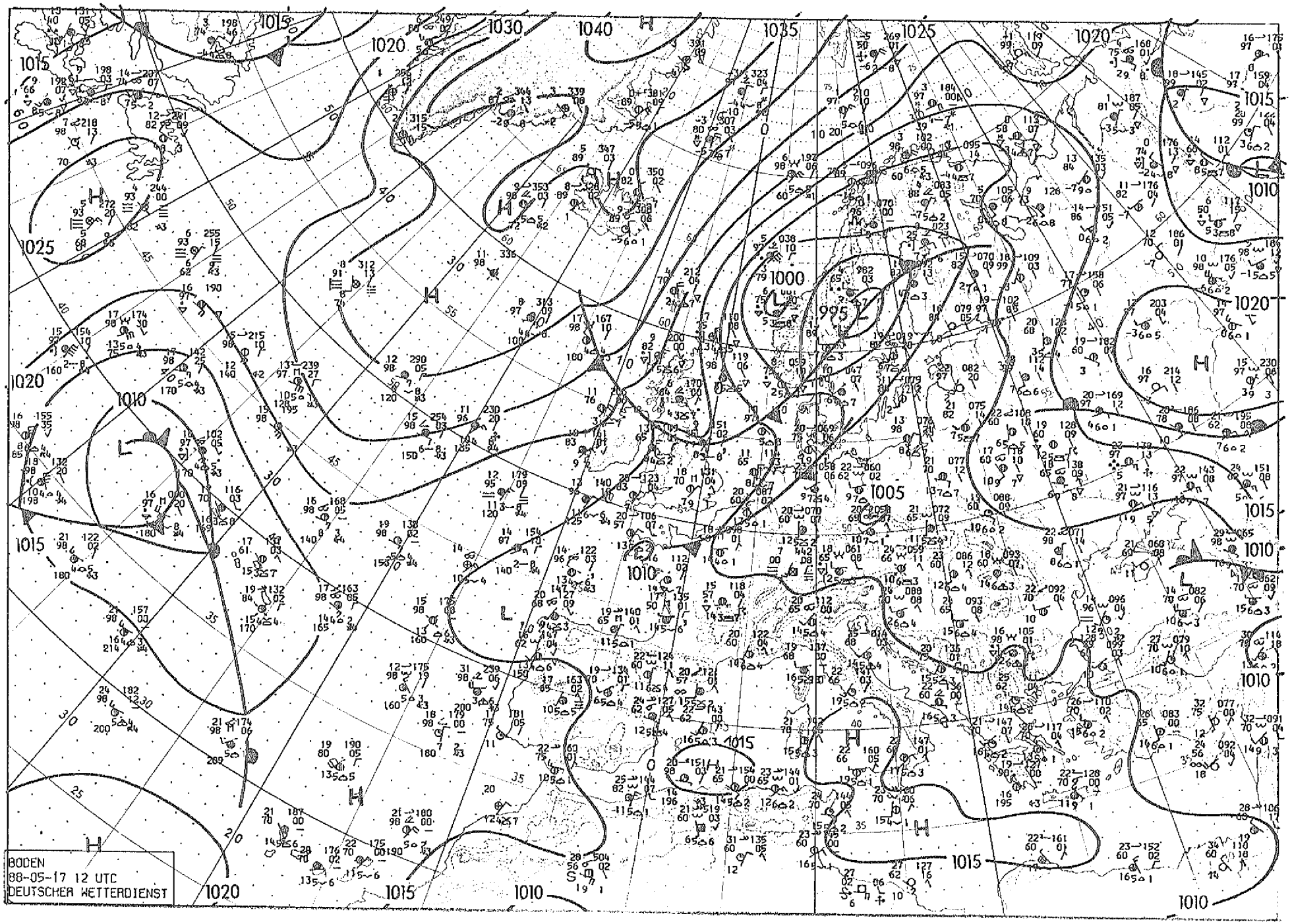
BODEN
88-05-17 12 UTC
DEUTSCHER WETTERDIENST

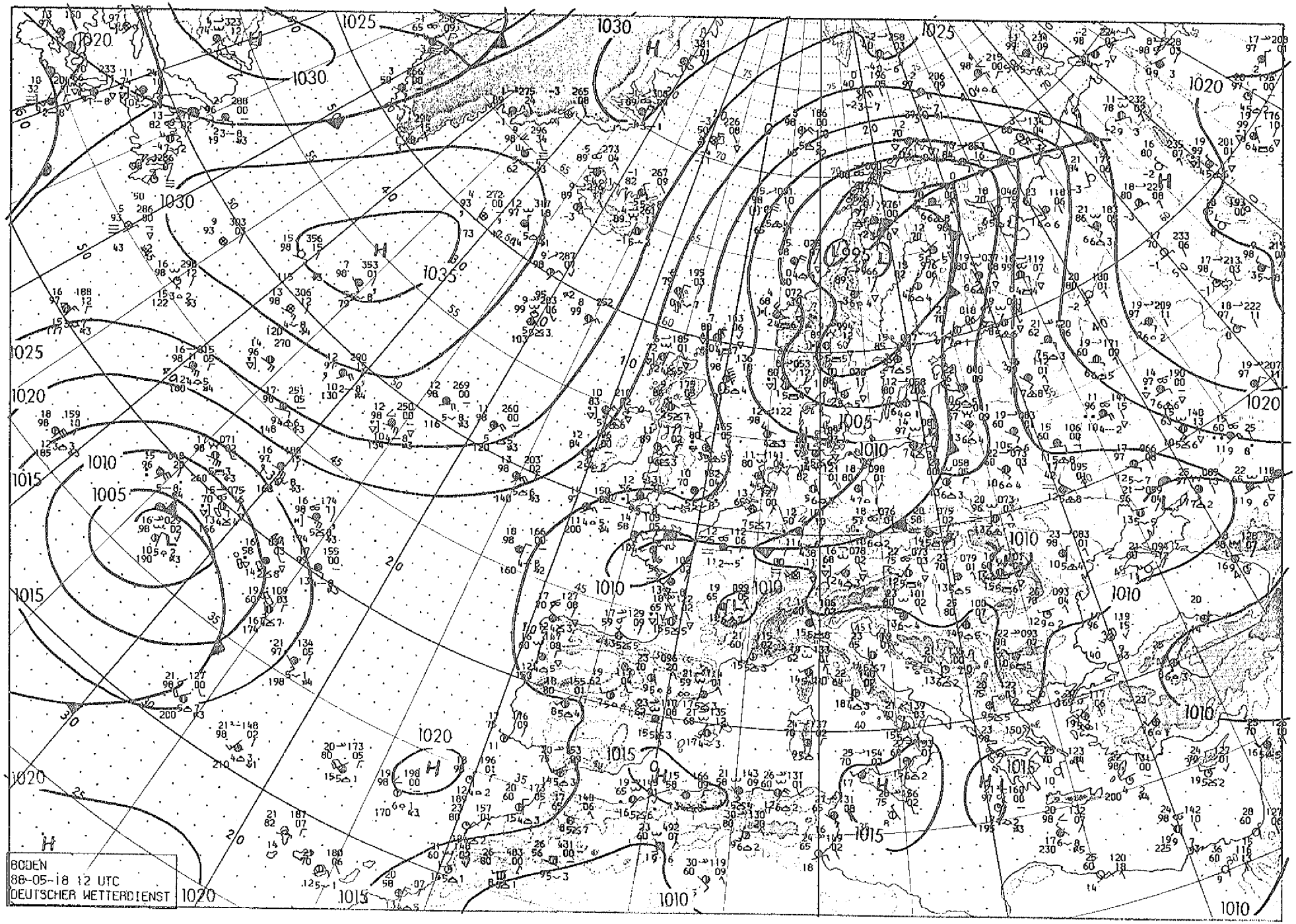
BODEN
88-05-18 12 UTC
DEUTSCHER WETTERDIENST

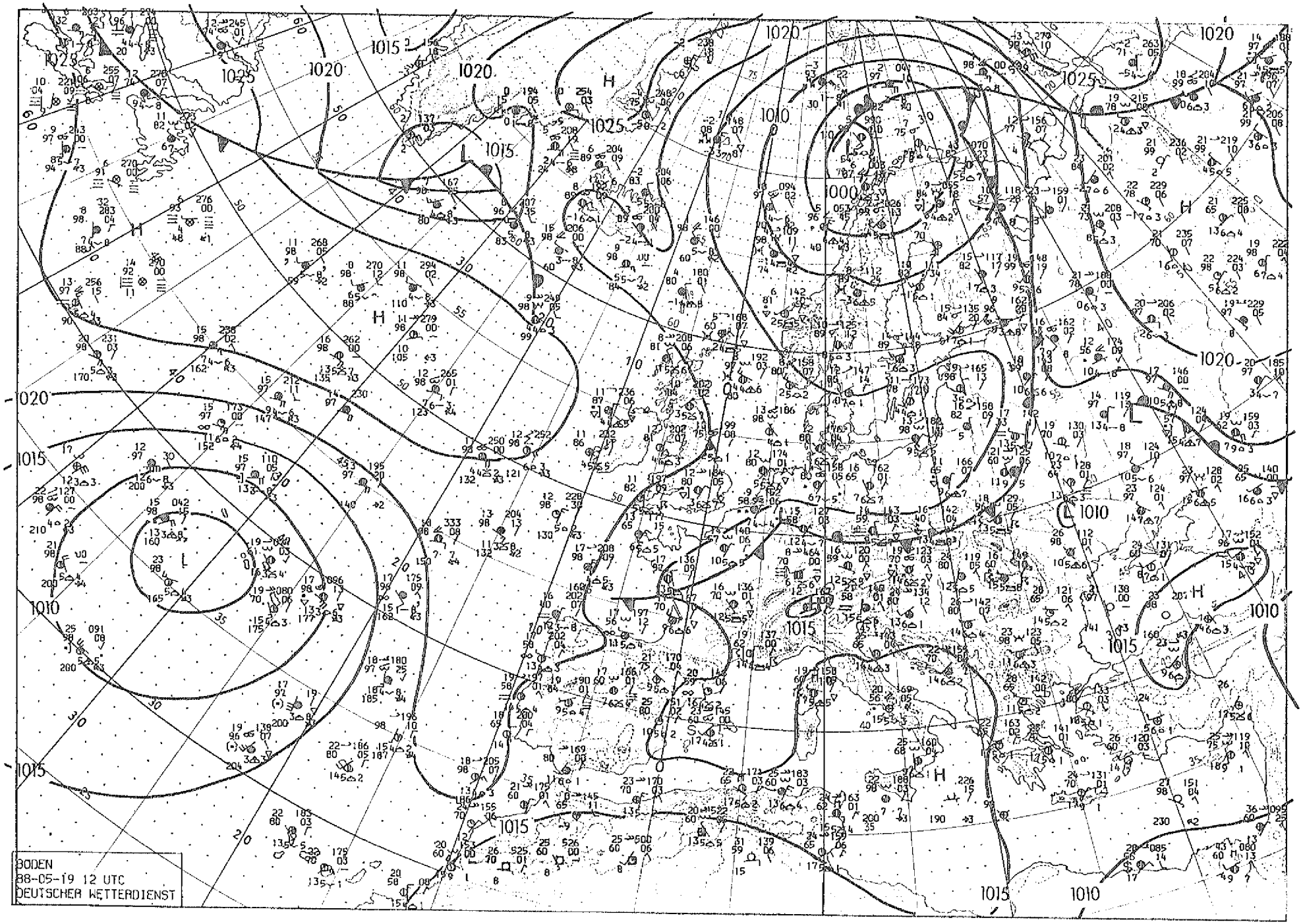
BODEN
88-05-19 12 UTC
DEUTSCHER WETTERDIENST

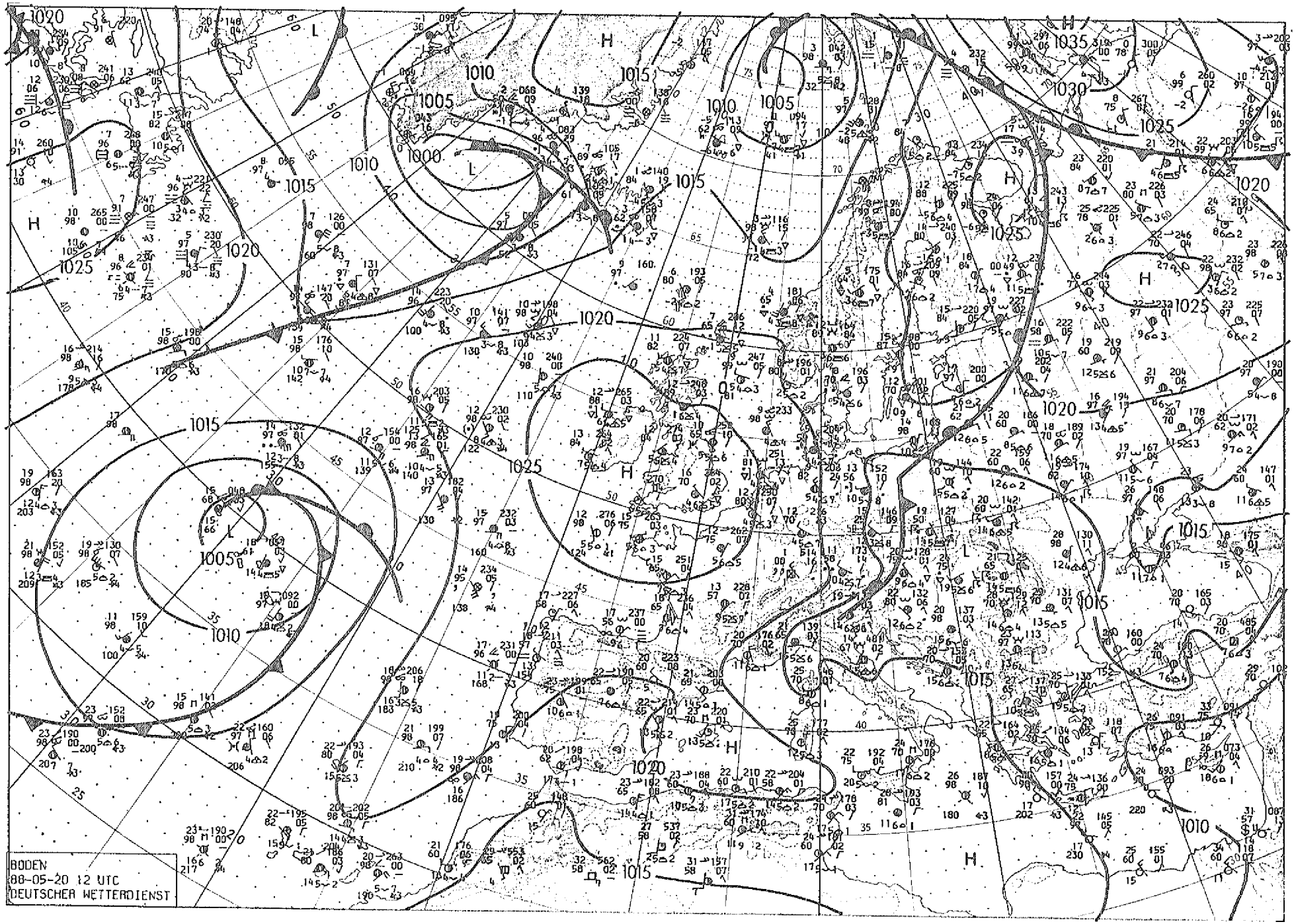
BODEN
88-05-20 12 UTC
DEUTSCHER WETTERDIENST

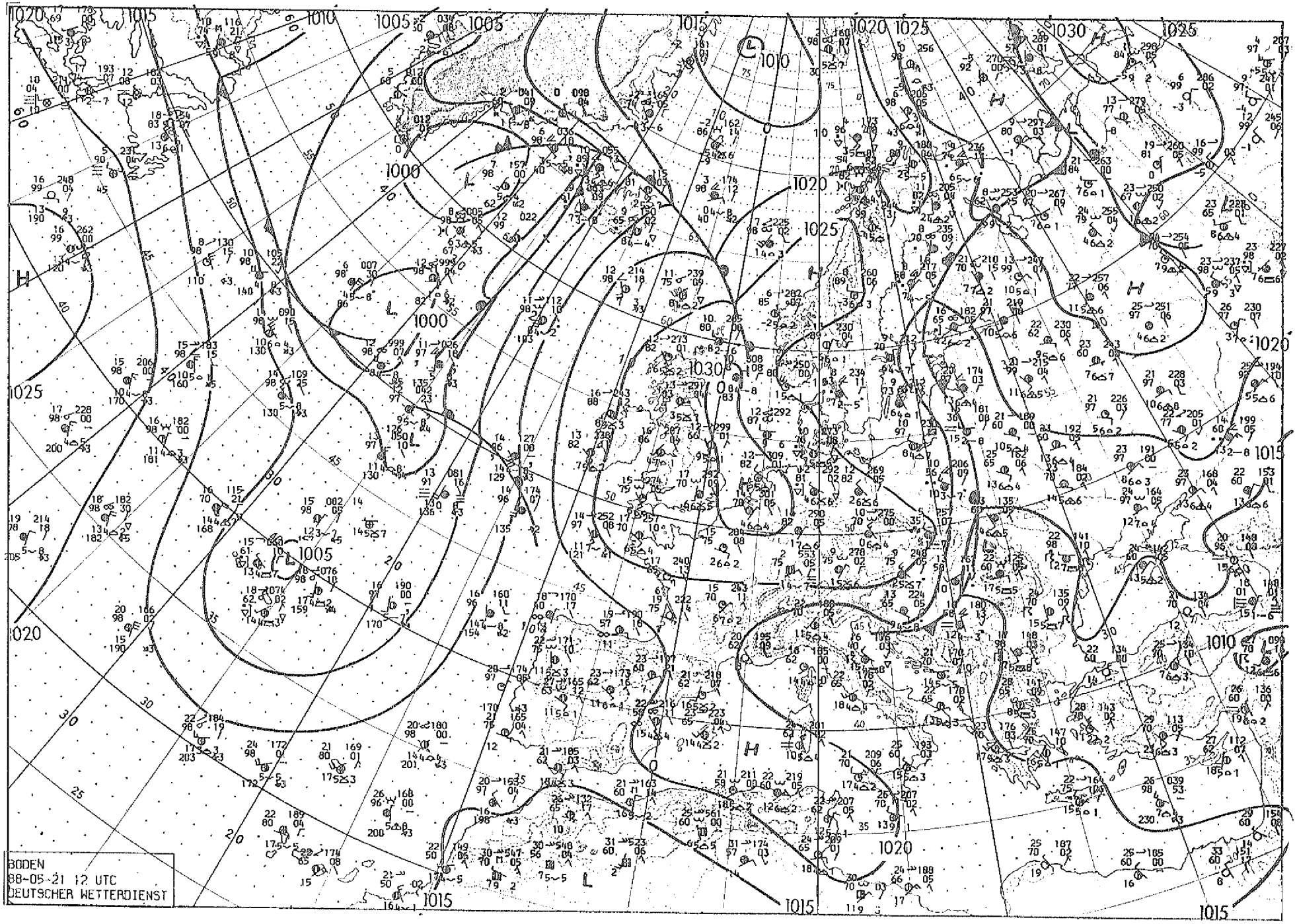
BODEN
88-05-21 12 UTC
DEUTSCHER WETTERDIENST

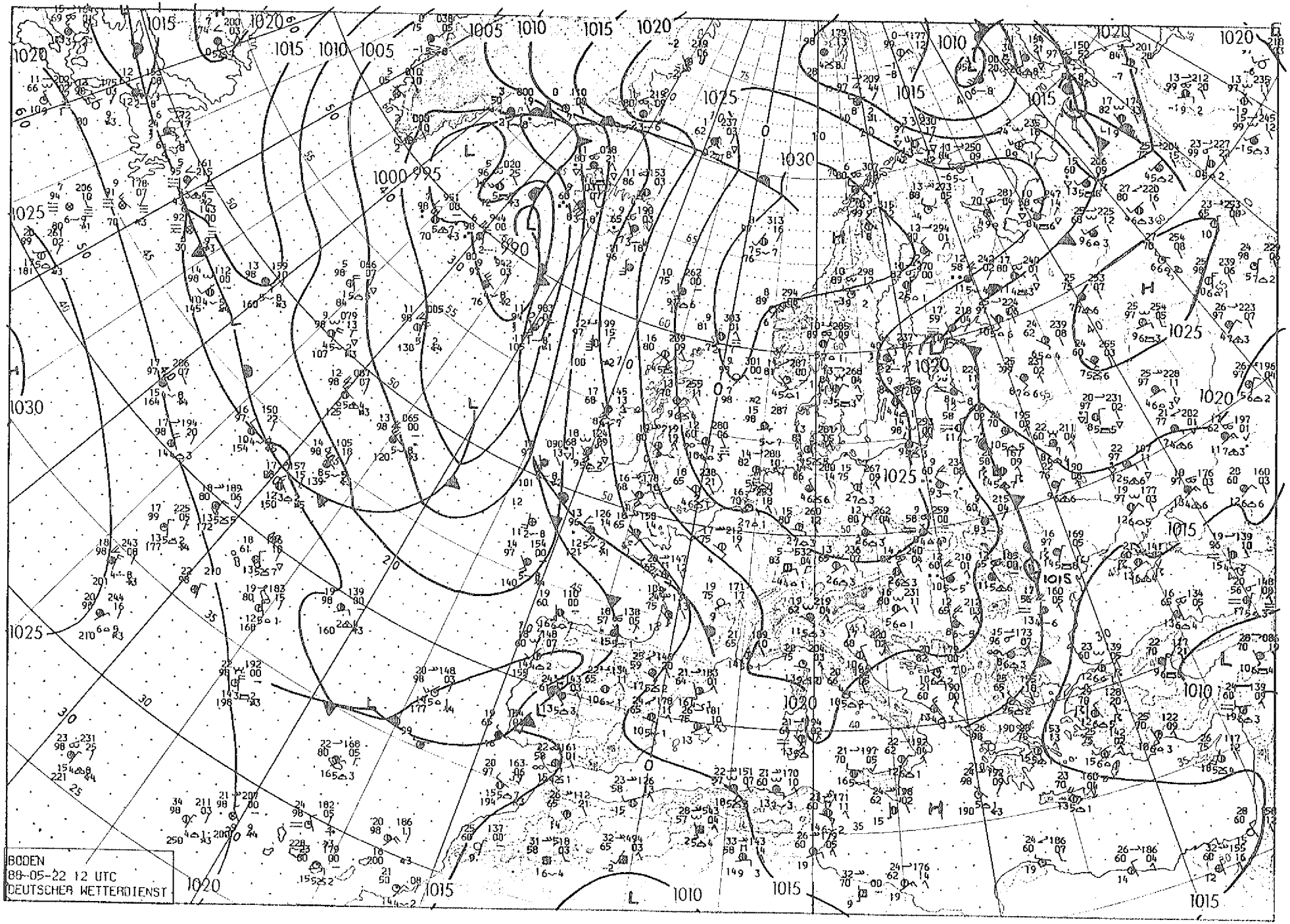
BODEN
88-05-22 12 UTC
DEUTSCHER WETTERDIENST

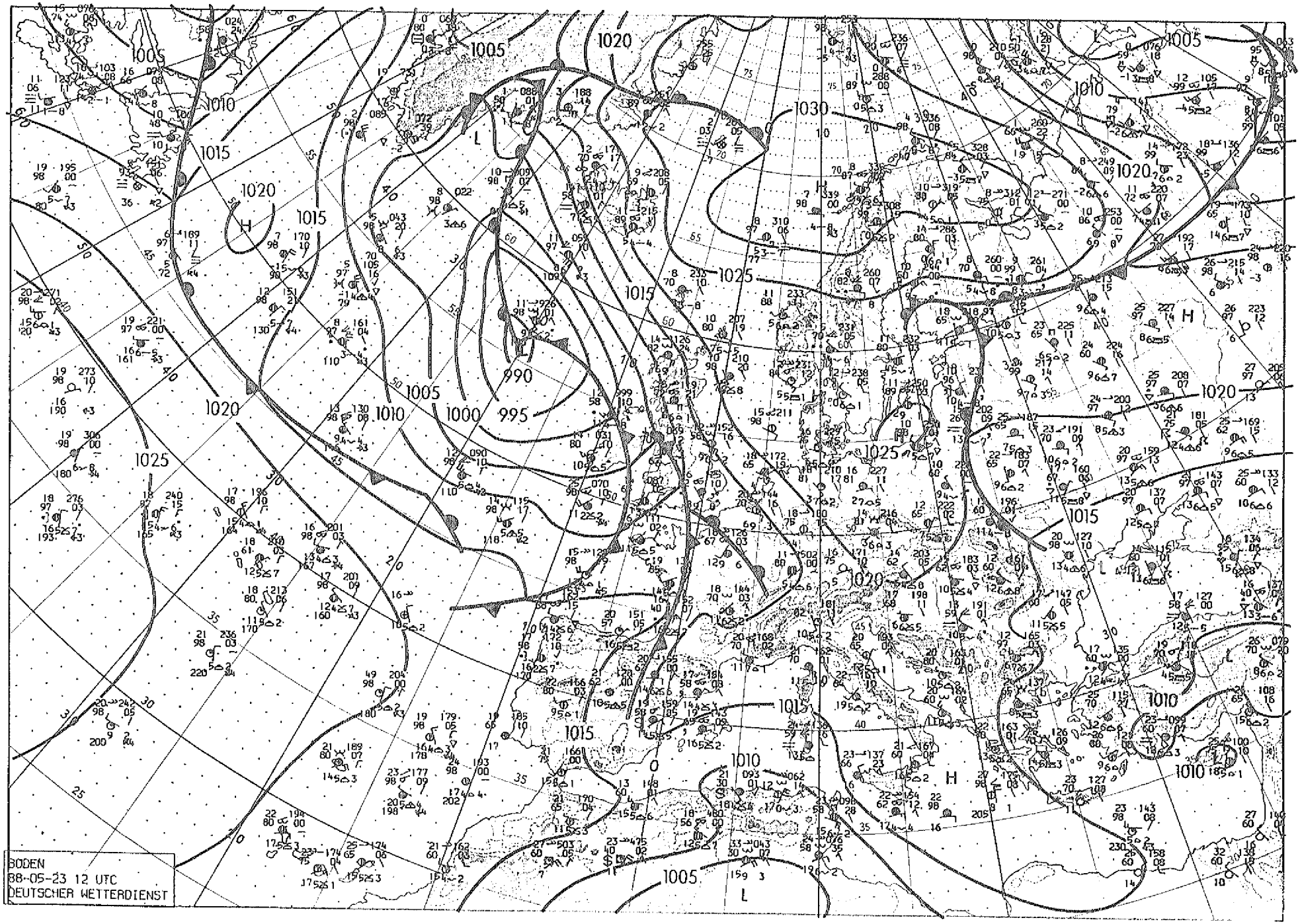
BODEN
88-05-23 12 UTC
DEUTSCHER WETTERDIENST

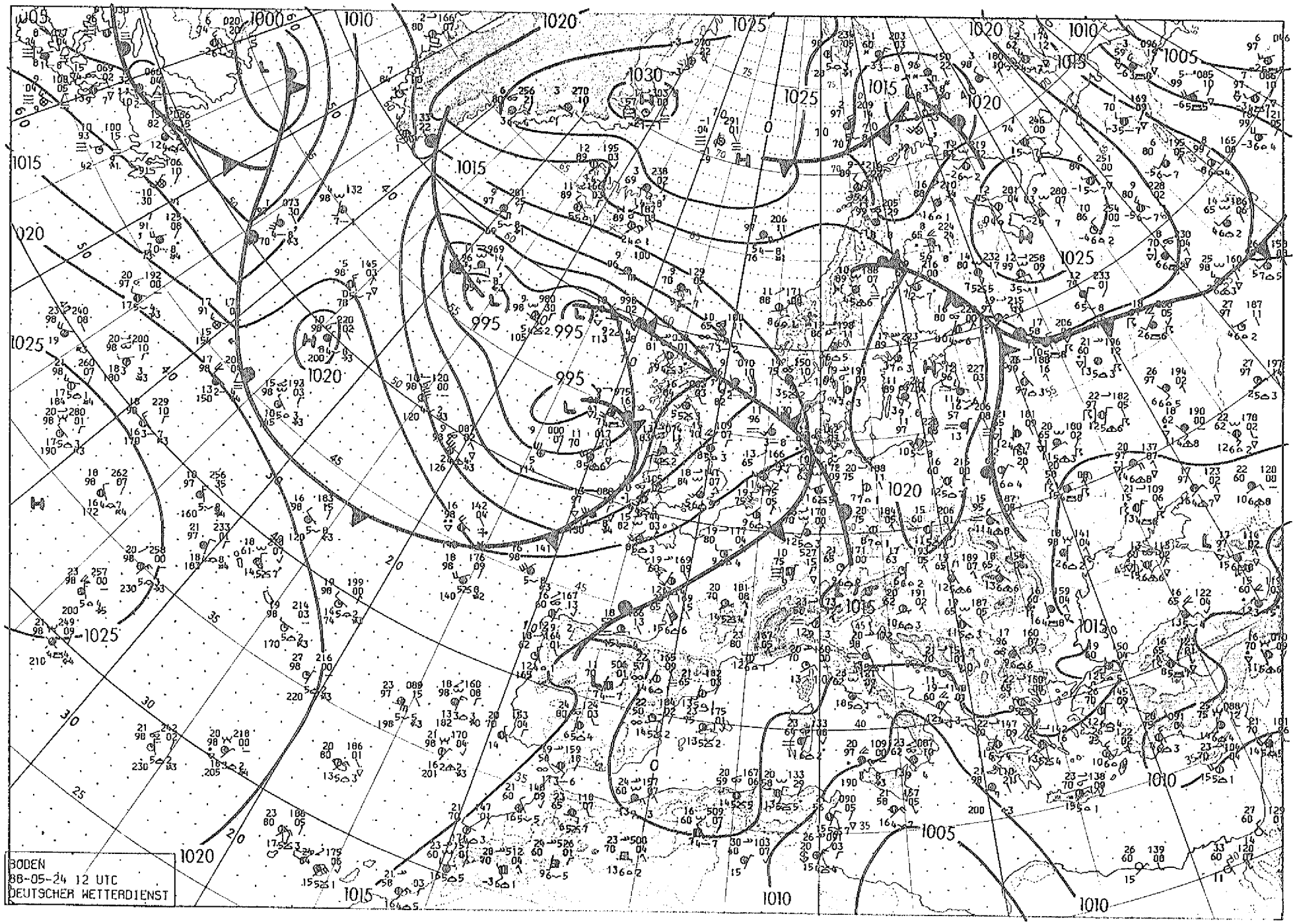
BODEN
88-05-24 12 UTC
DEUTSCHER WETTERDIENST

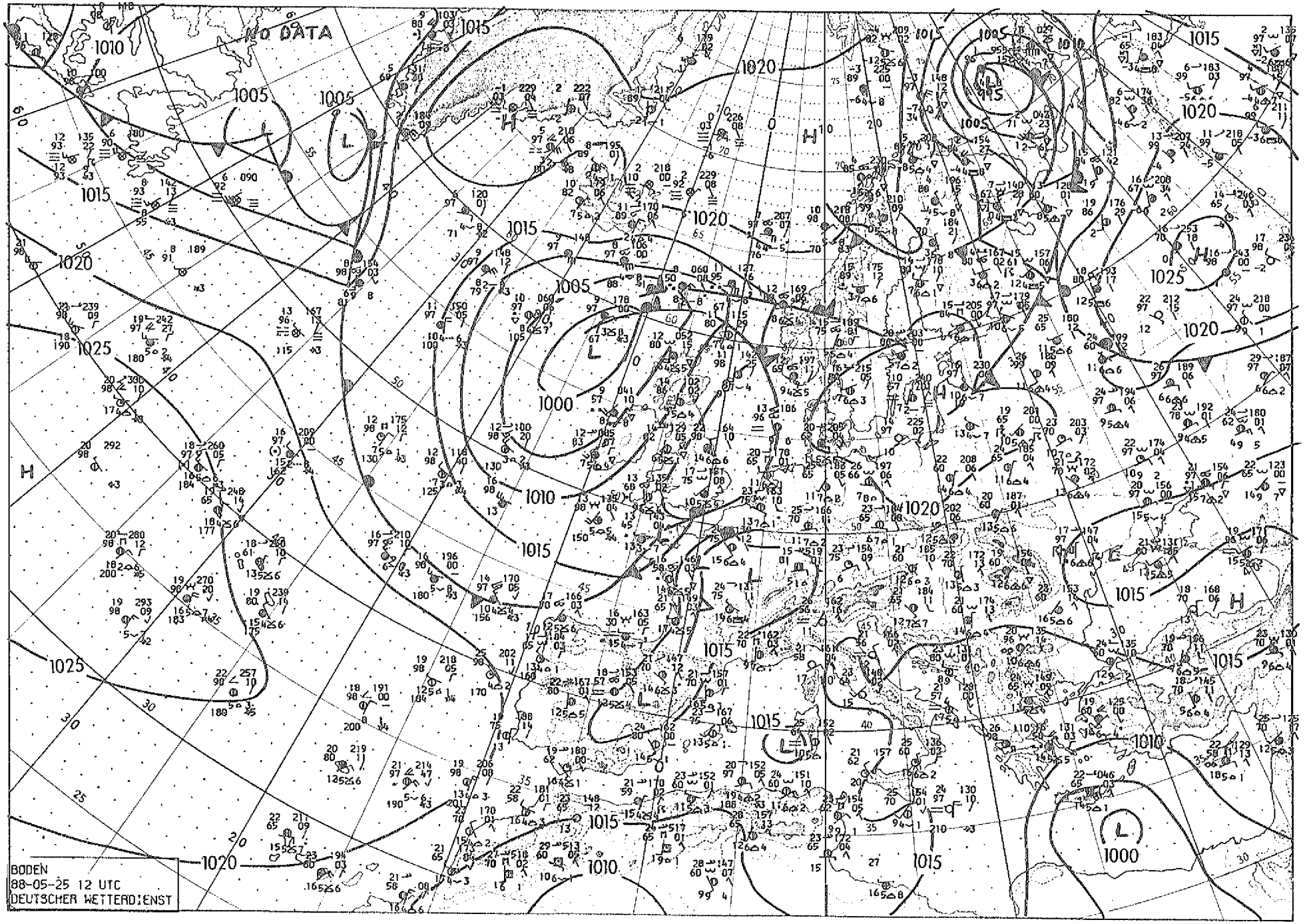
NO DATA
BODEN
88-05-25 12 UTC
DEUTSCHER WETTERDIENST

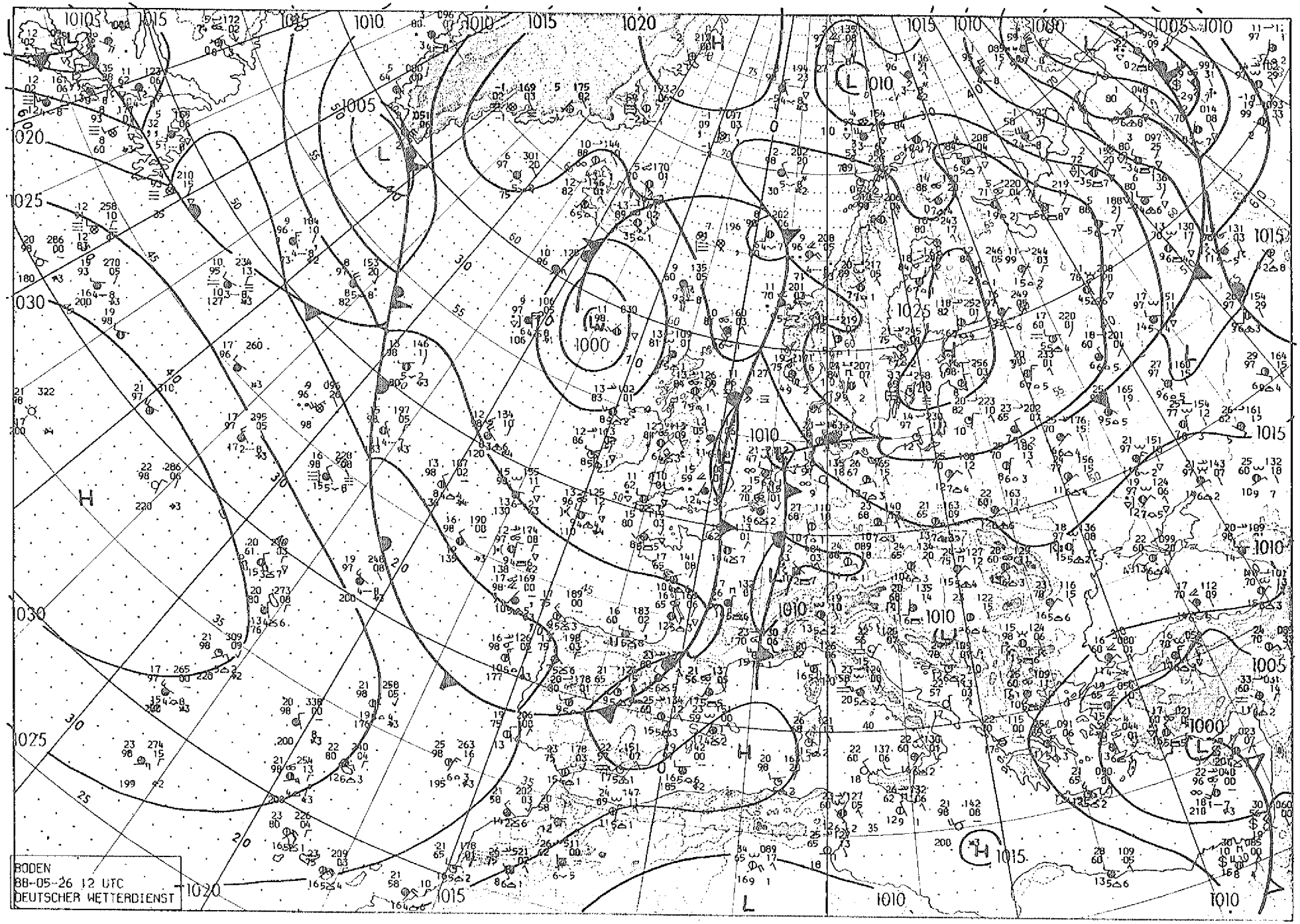
BODEN
88-05-26 12 UTC
DEUTSCHER WETTERDIENST

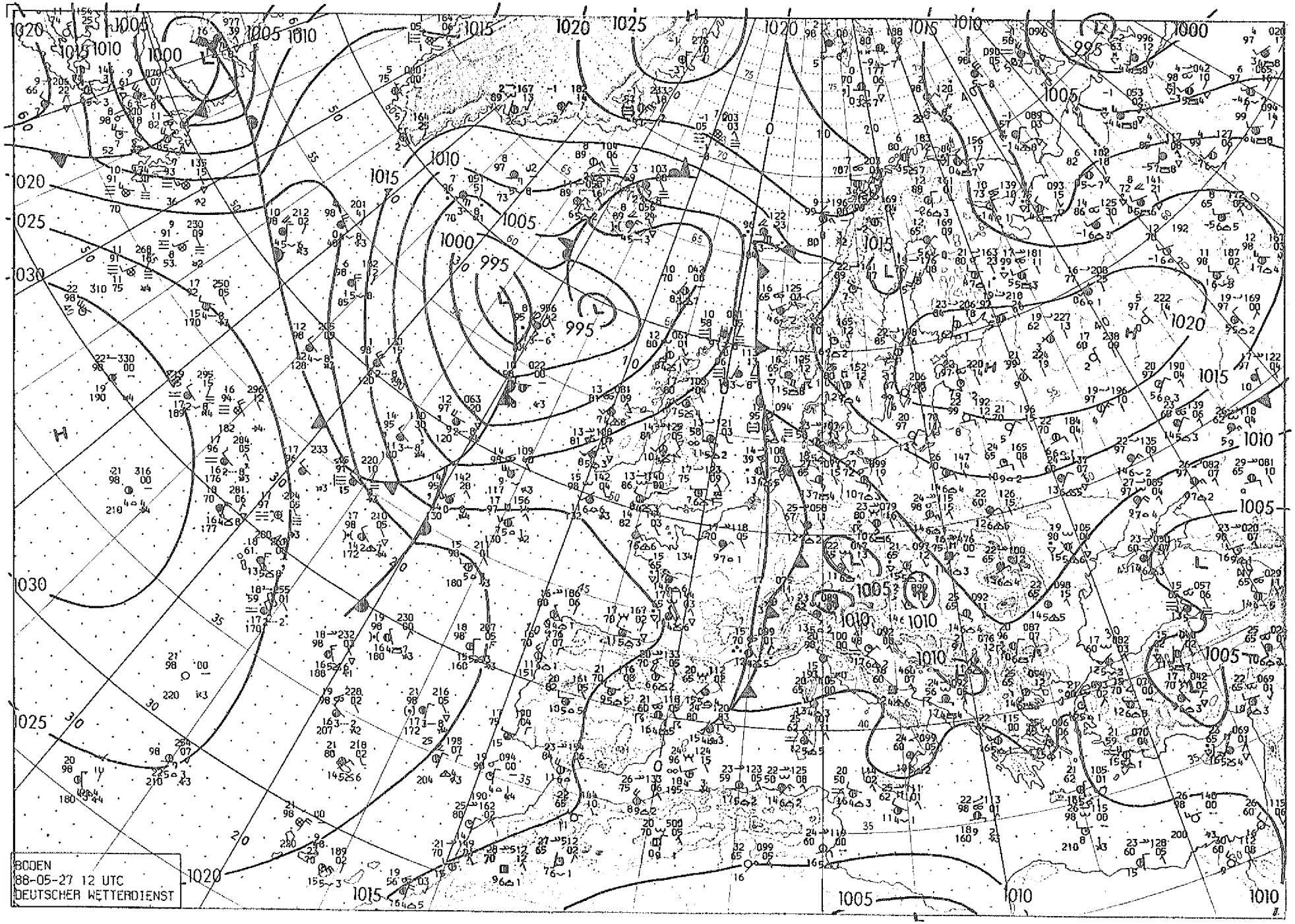
BODEN
88-05-27 12 UTC
DEUTSCHER WETTERDIENST

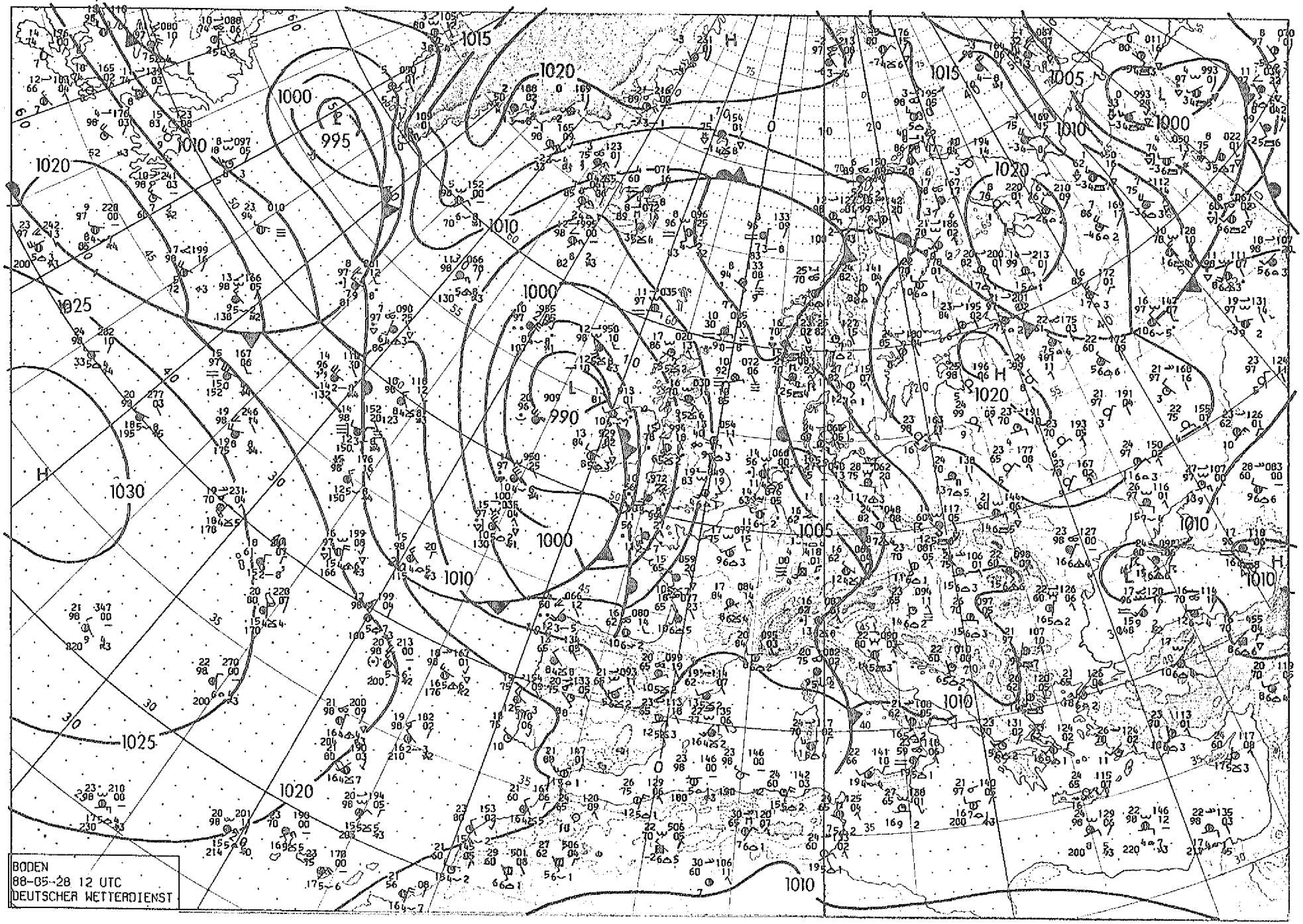
BODEN
88-05-28 12 UTC
DEUTSCHER WETTERDIENST

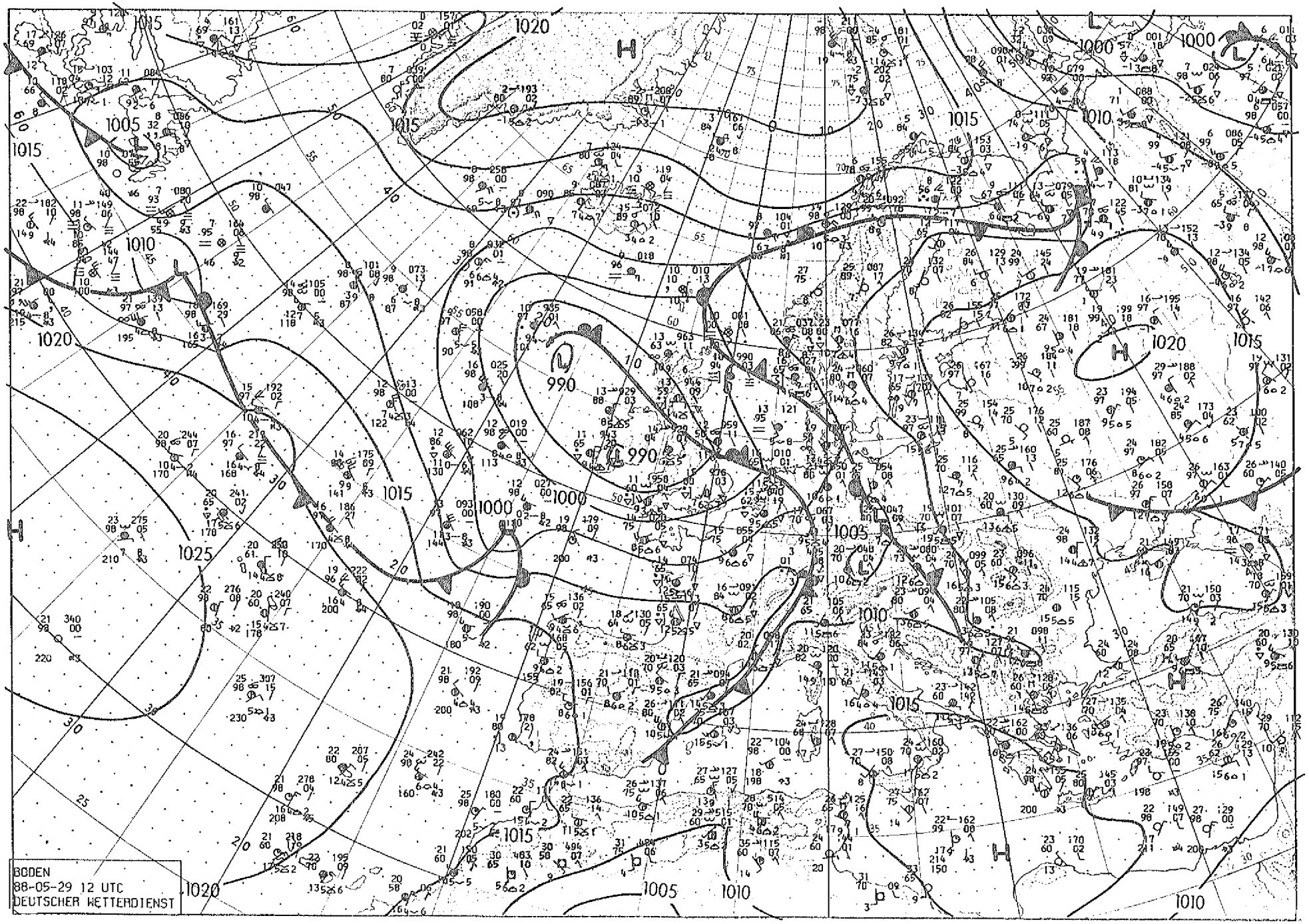
BODEN
88-05-29 12 UTC
DEUTSCHER WETTERDIENST

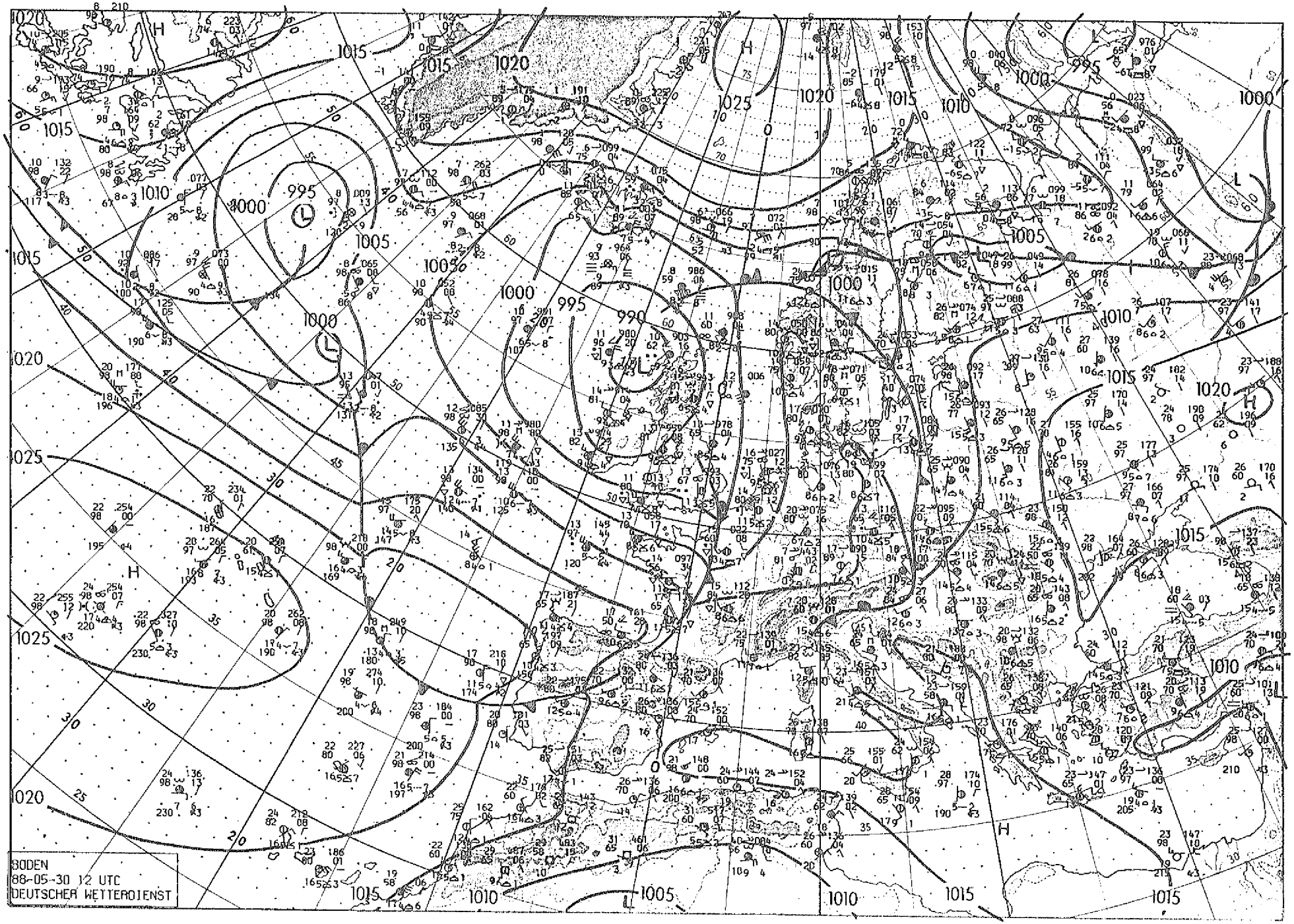
BODEN
88-05-30 12 UTC
DEUTSCHER WETTERDIENST

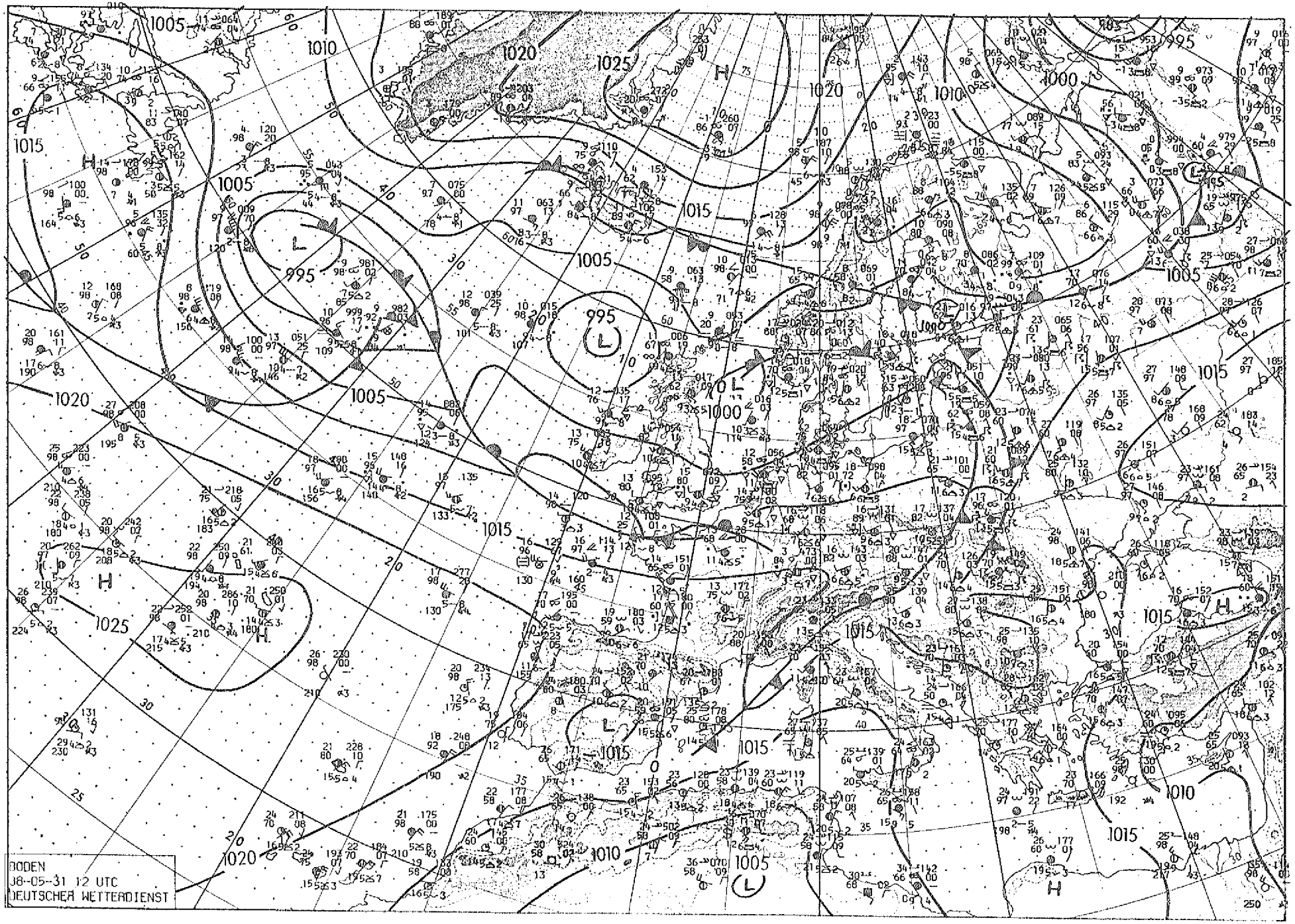
BODEN
38-05-31 12 UTC
DEUTSCHER WETTERDIENST

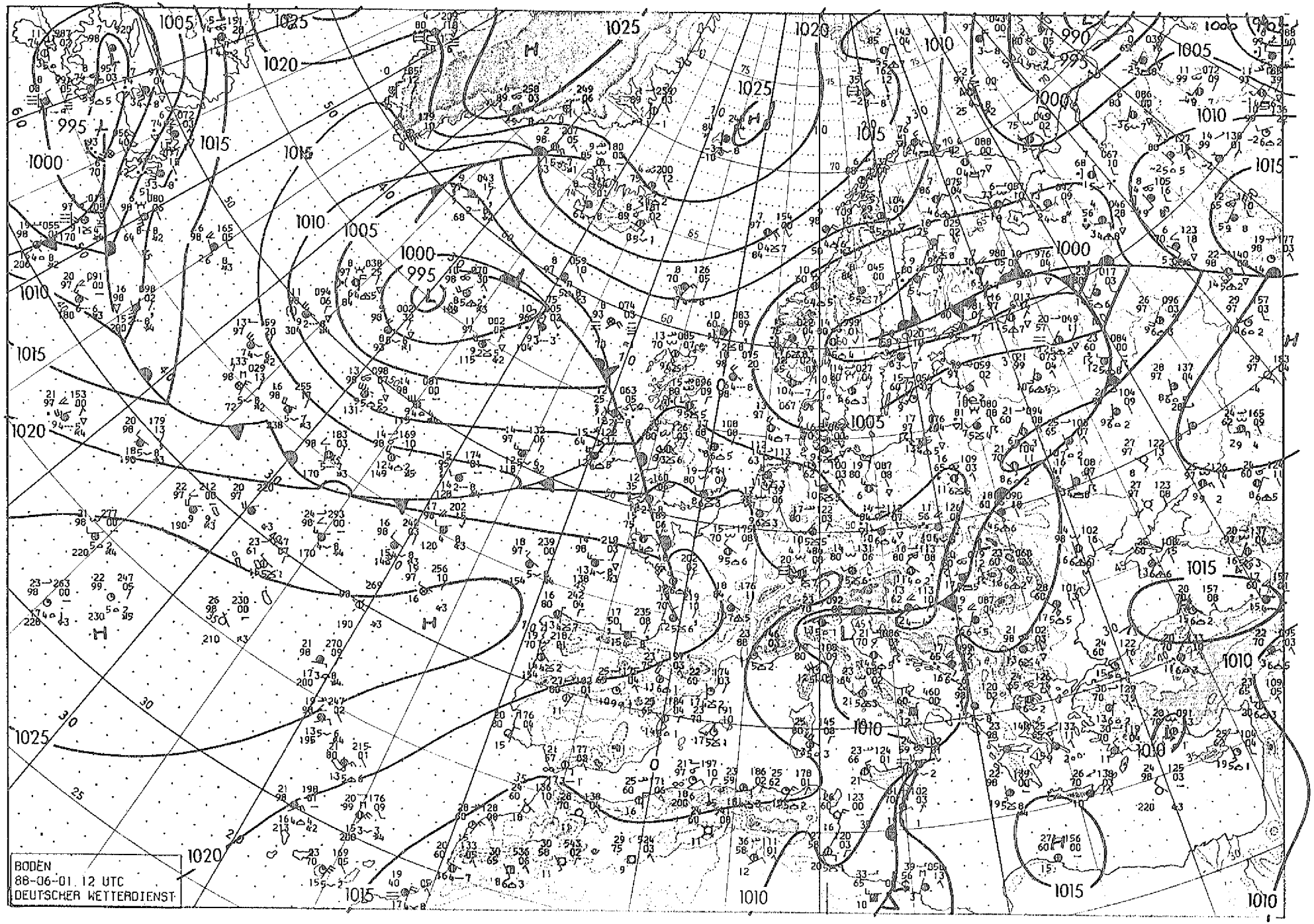
BODEN
88-06-01 12 UTC
DEUTSCHER WETTERDIENST

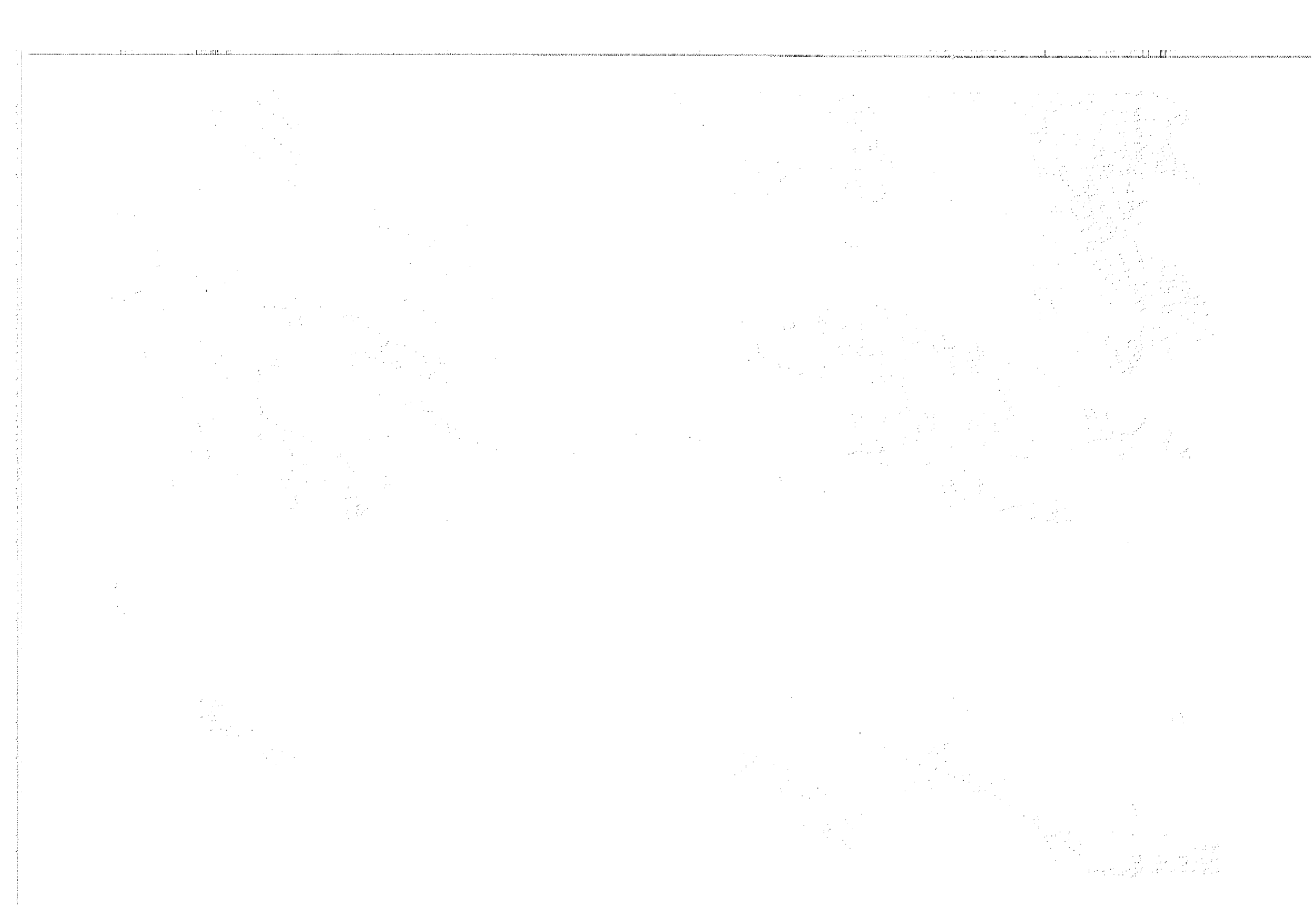

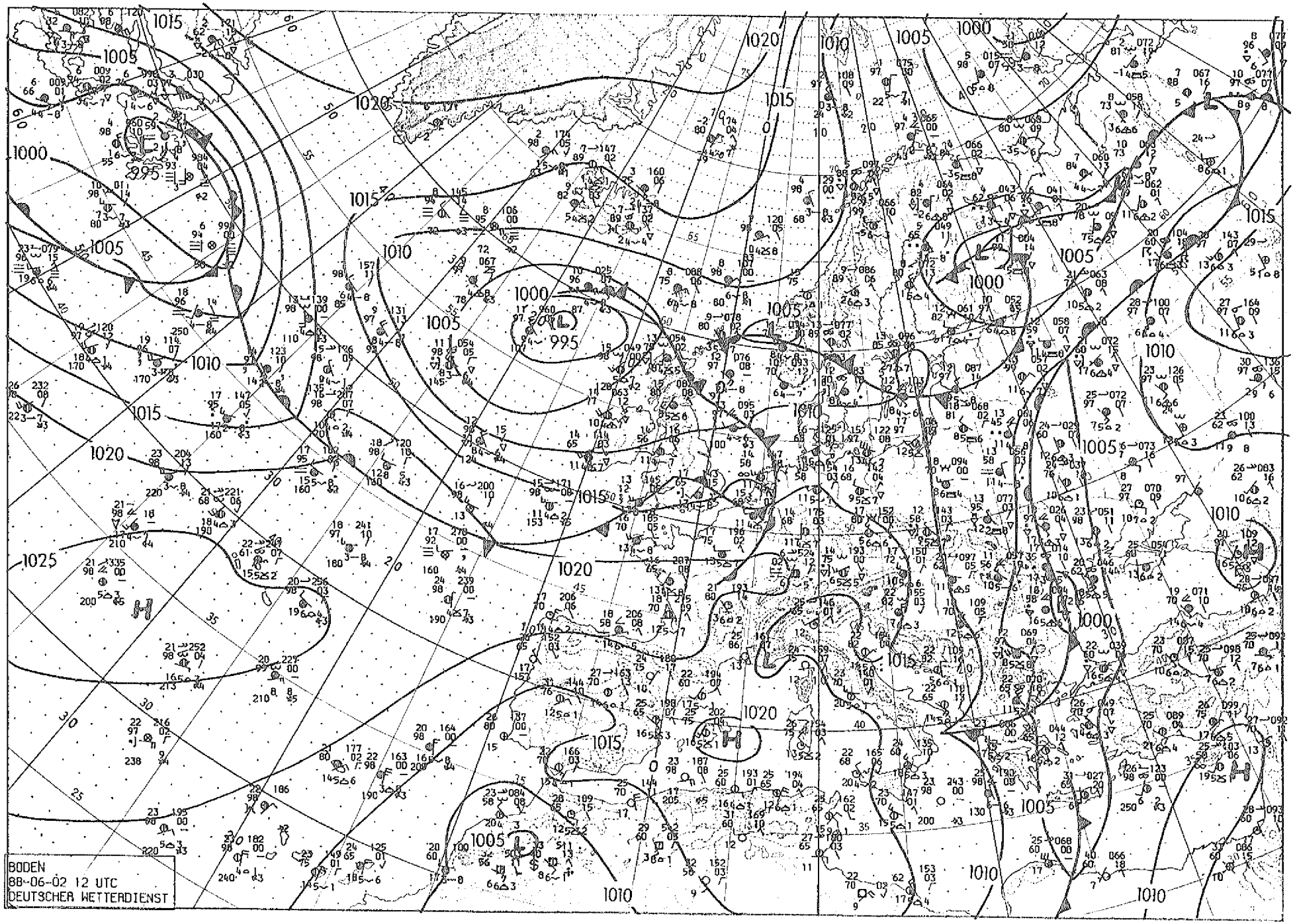
BODEN
88-06-02 12 UTC
DEUTSCHER WETTERDIENST

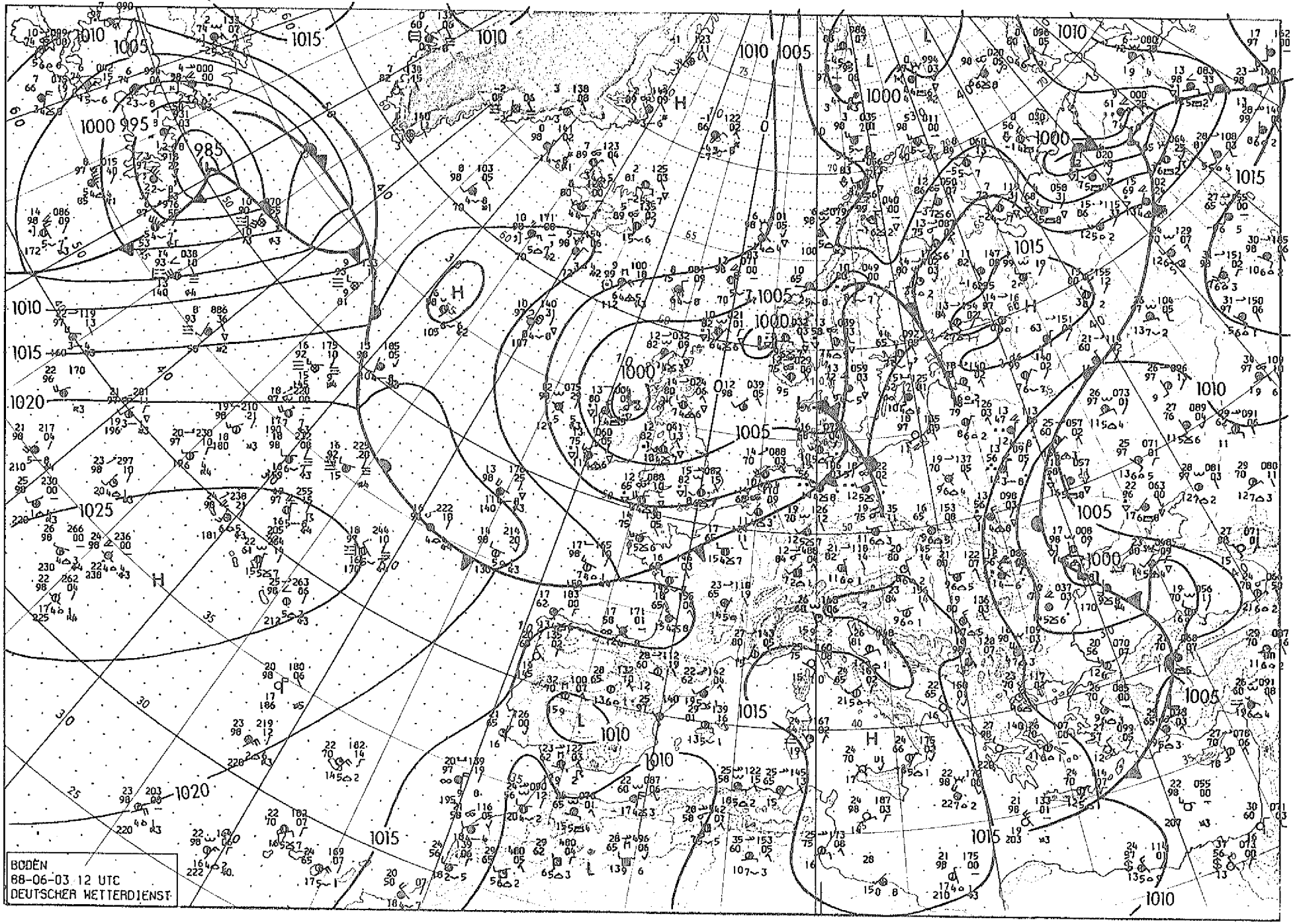
BODEN
88-06-03 12 UTC
DEUTSCHER WETTERDIENST

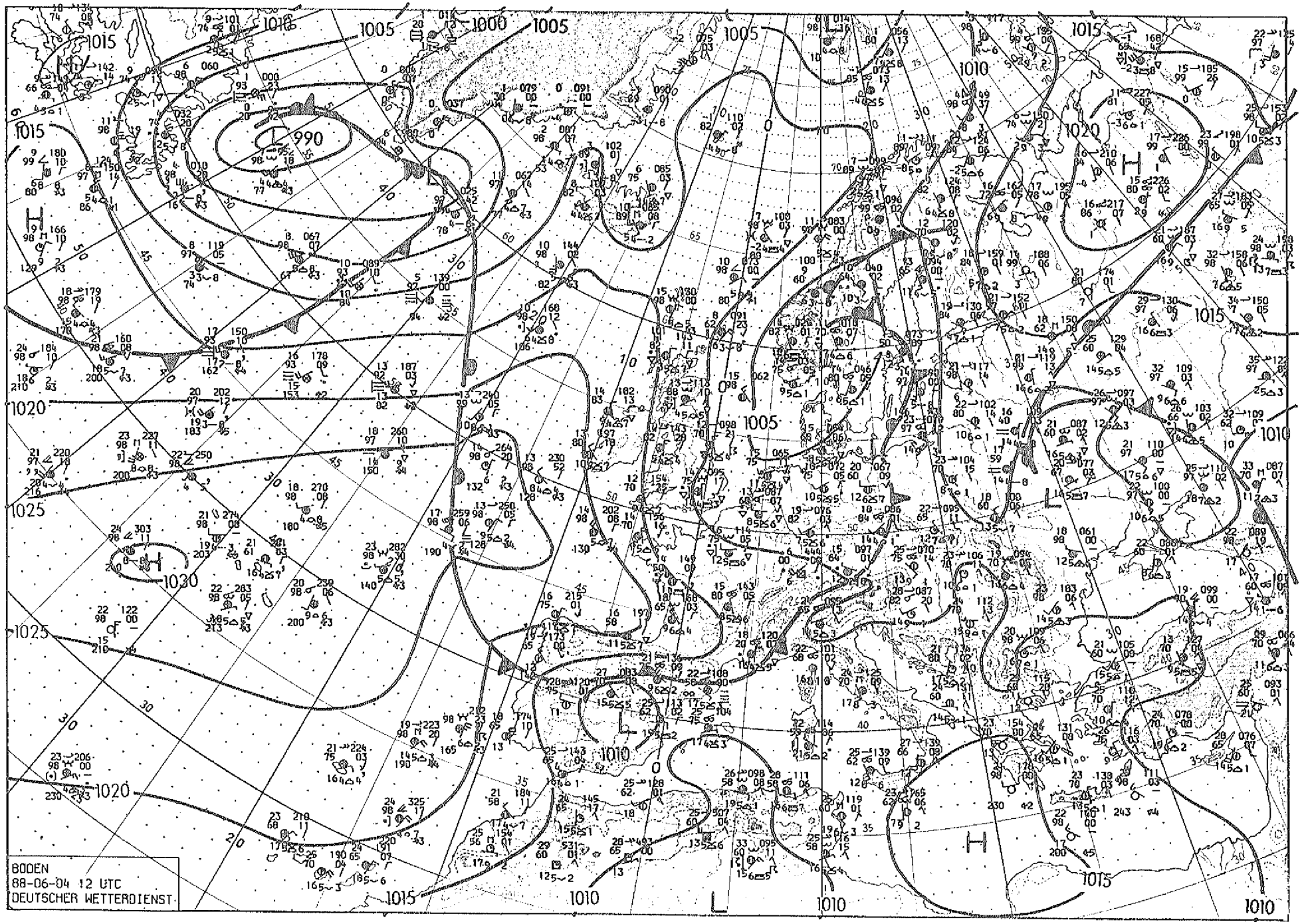
BODEN
88-06-04 12 UTC
DEUTSCHER WETTERDIENST

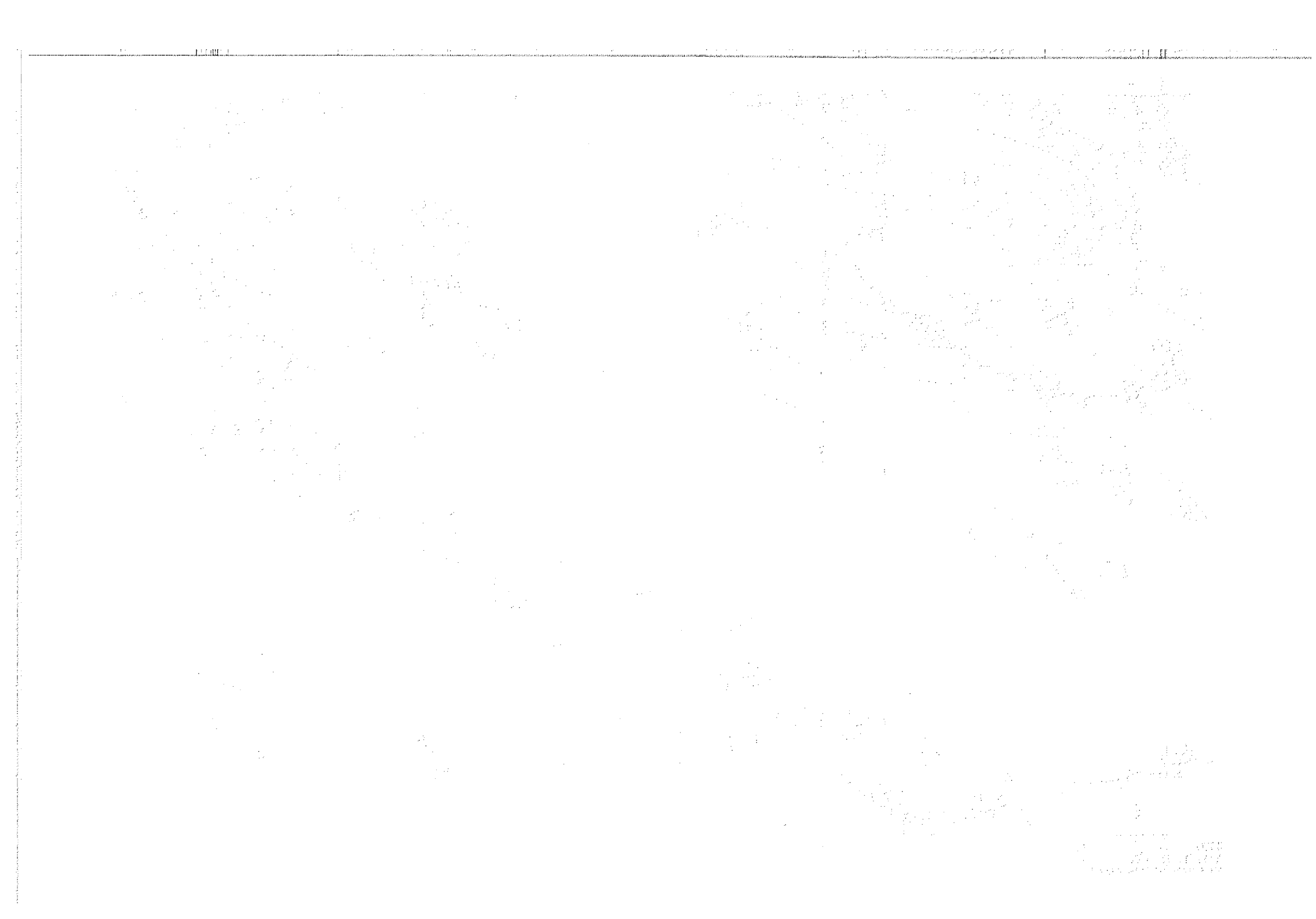

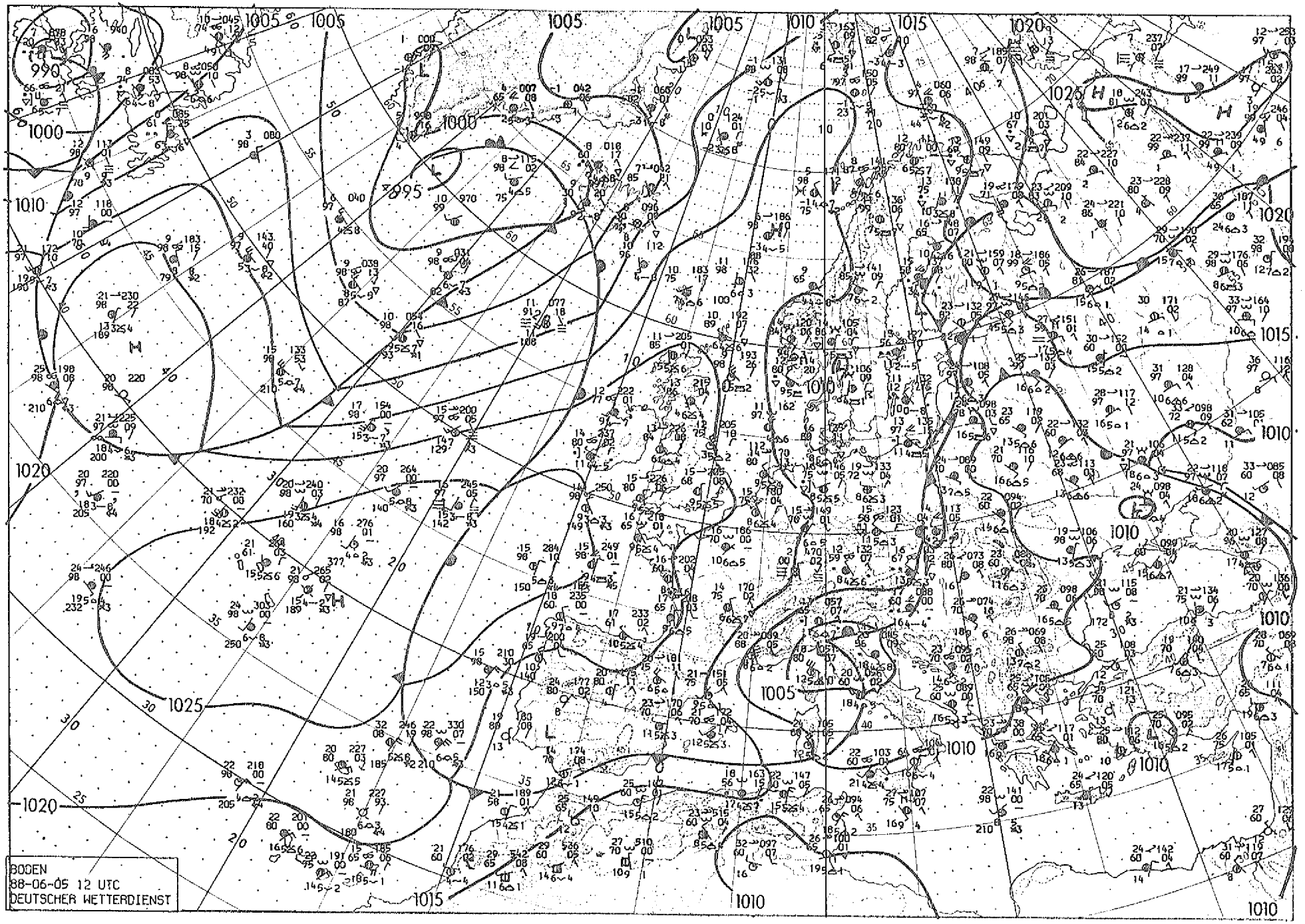
BODEN
88-06-05 12 UTC
DEUTSCHER WETTERDIENST

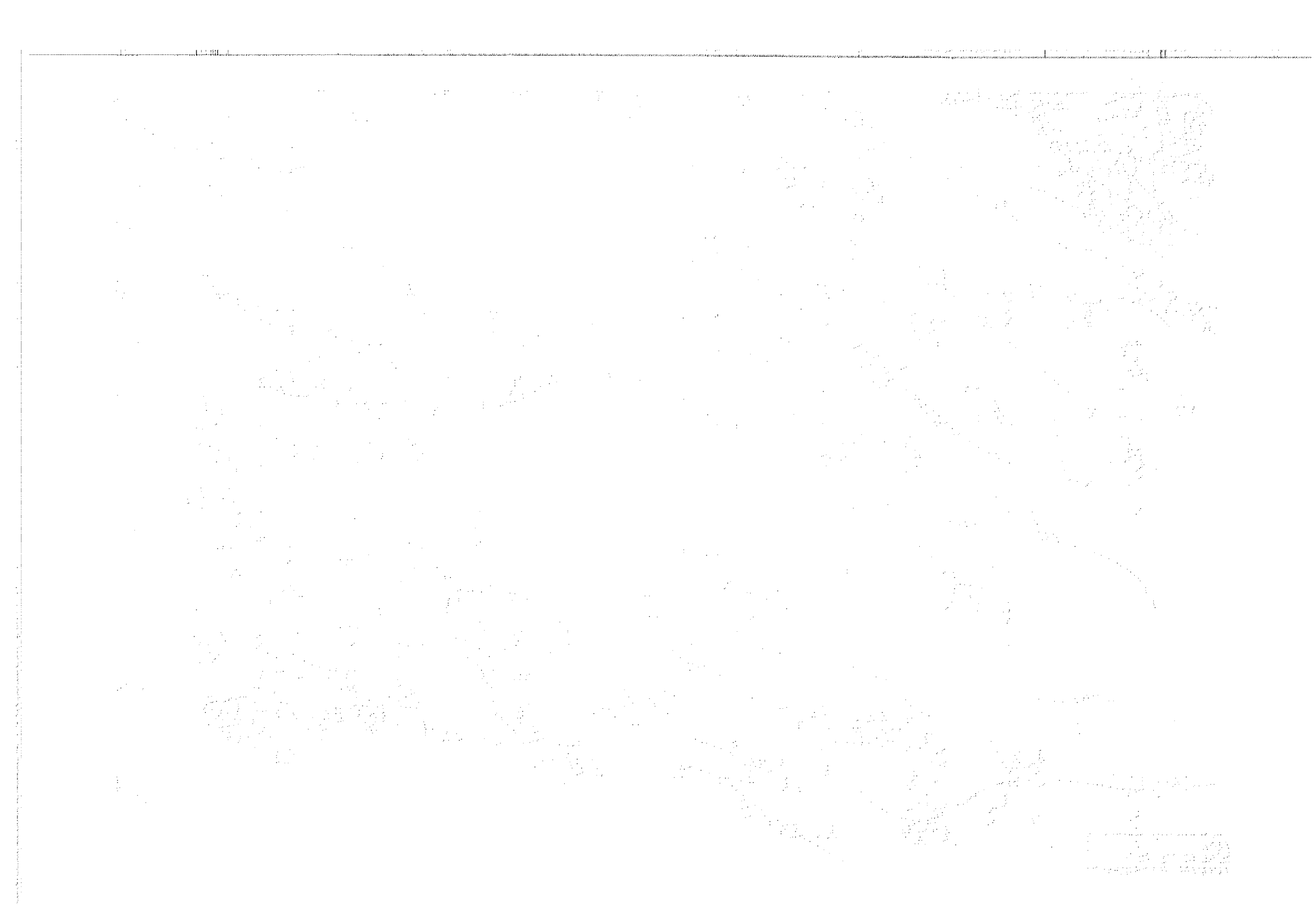

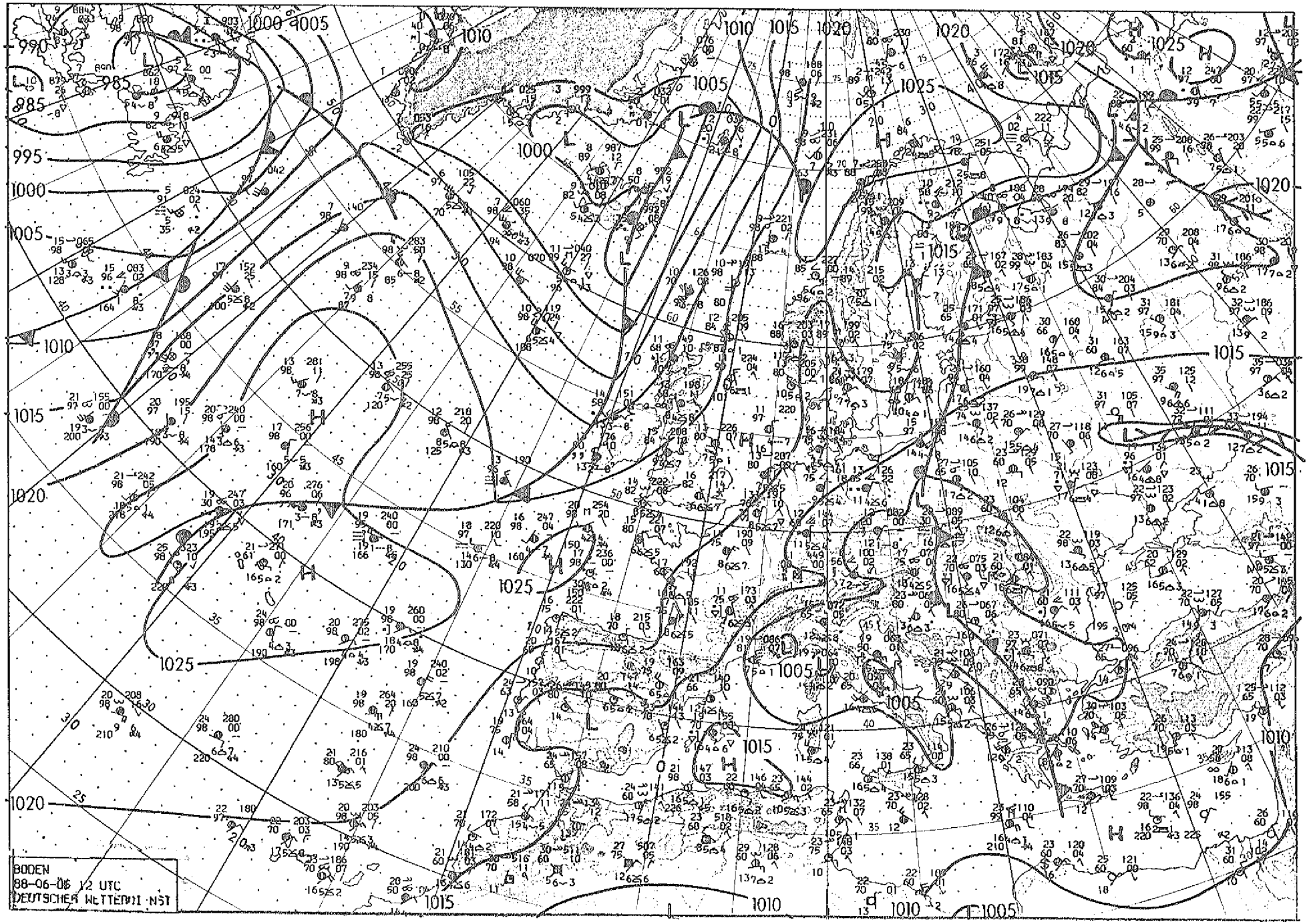
BODEN
88-06-06 12 UTC
DEUTSCHER WETTERDIENST

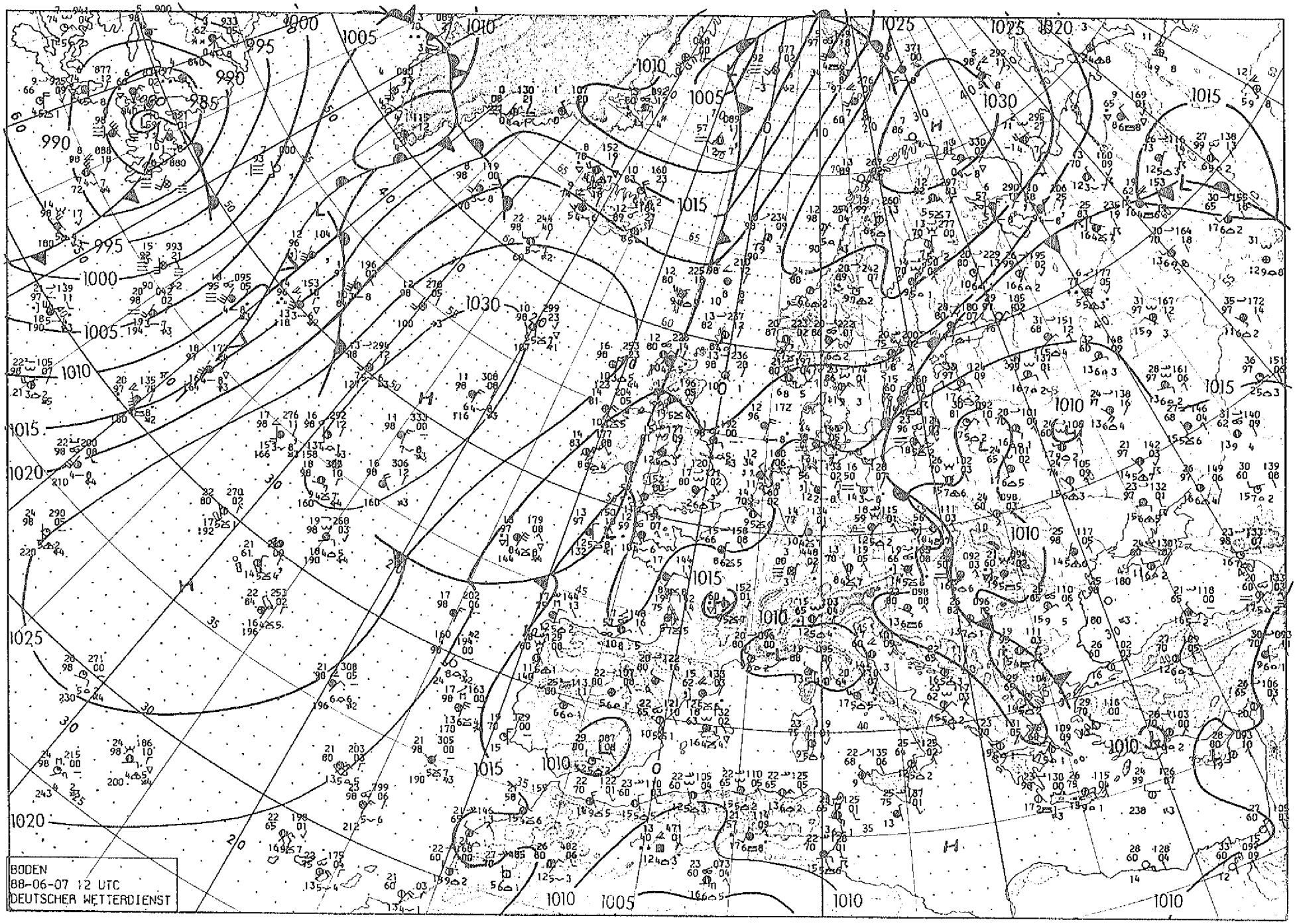
BODEN
88-06-07 12 UTC
DEUTSCHER WETTERDIENST

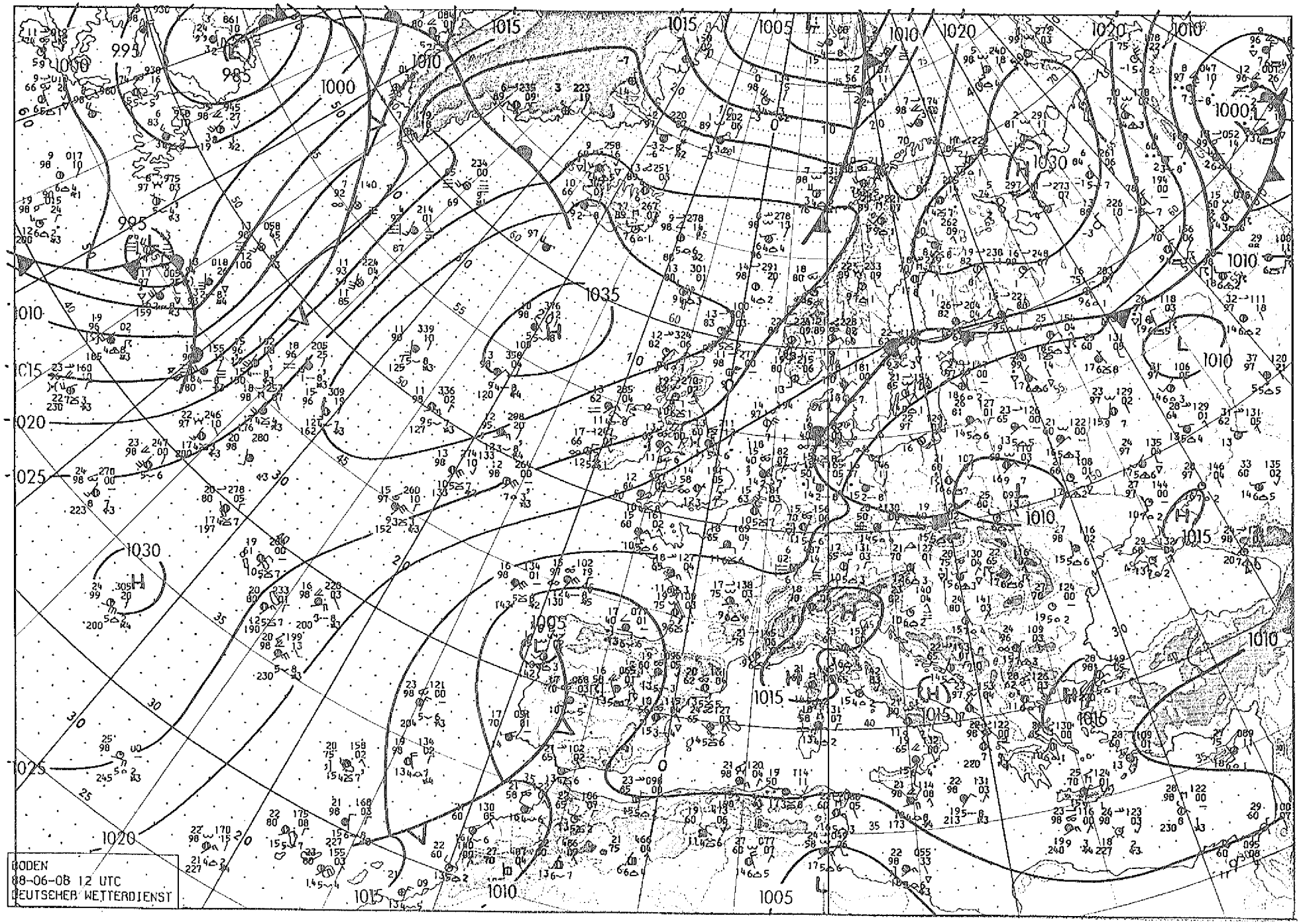
BODEN
88-06-08 12 UTC
DEUTSCHER WETTERDIENST

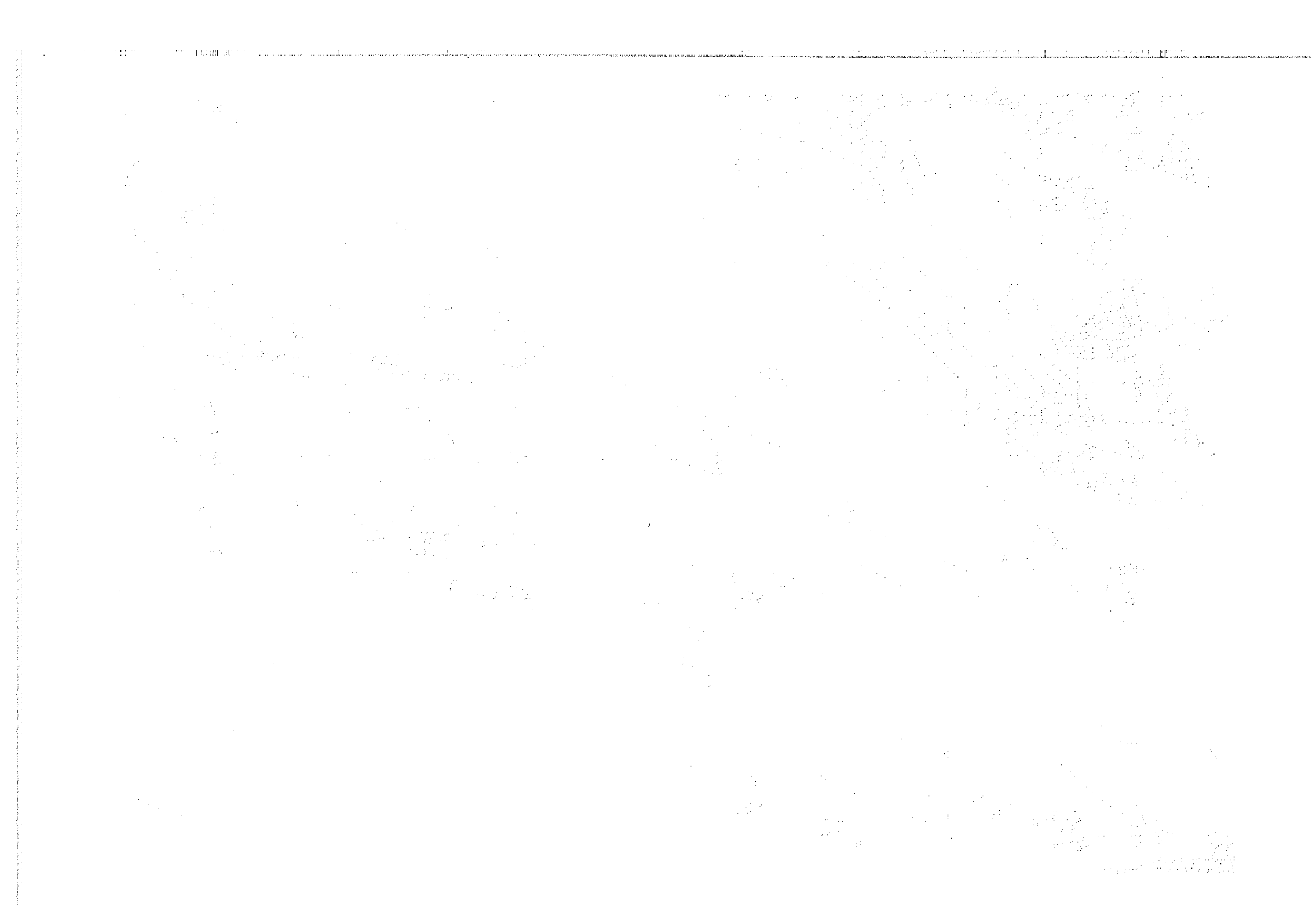

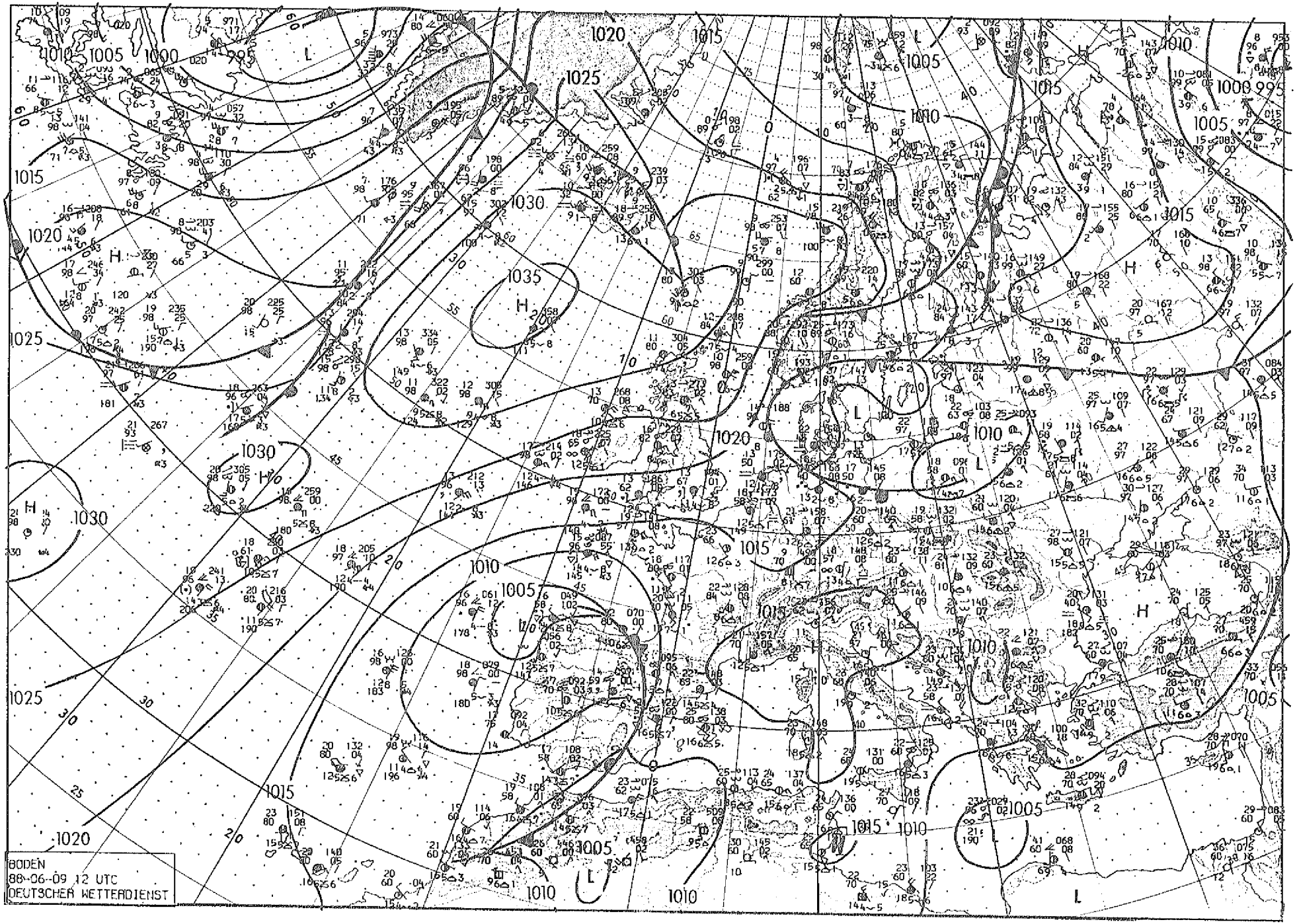
BODEN
88-06-09 12 UTC
DEUTSCHER WETTERDIENST

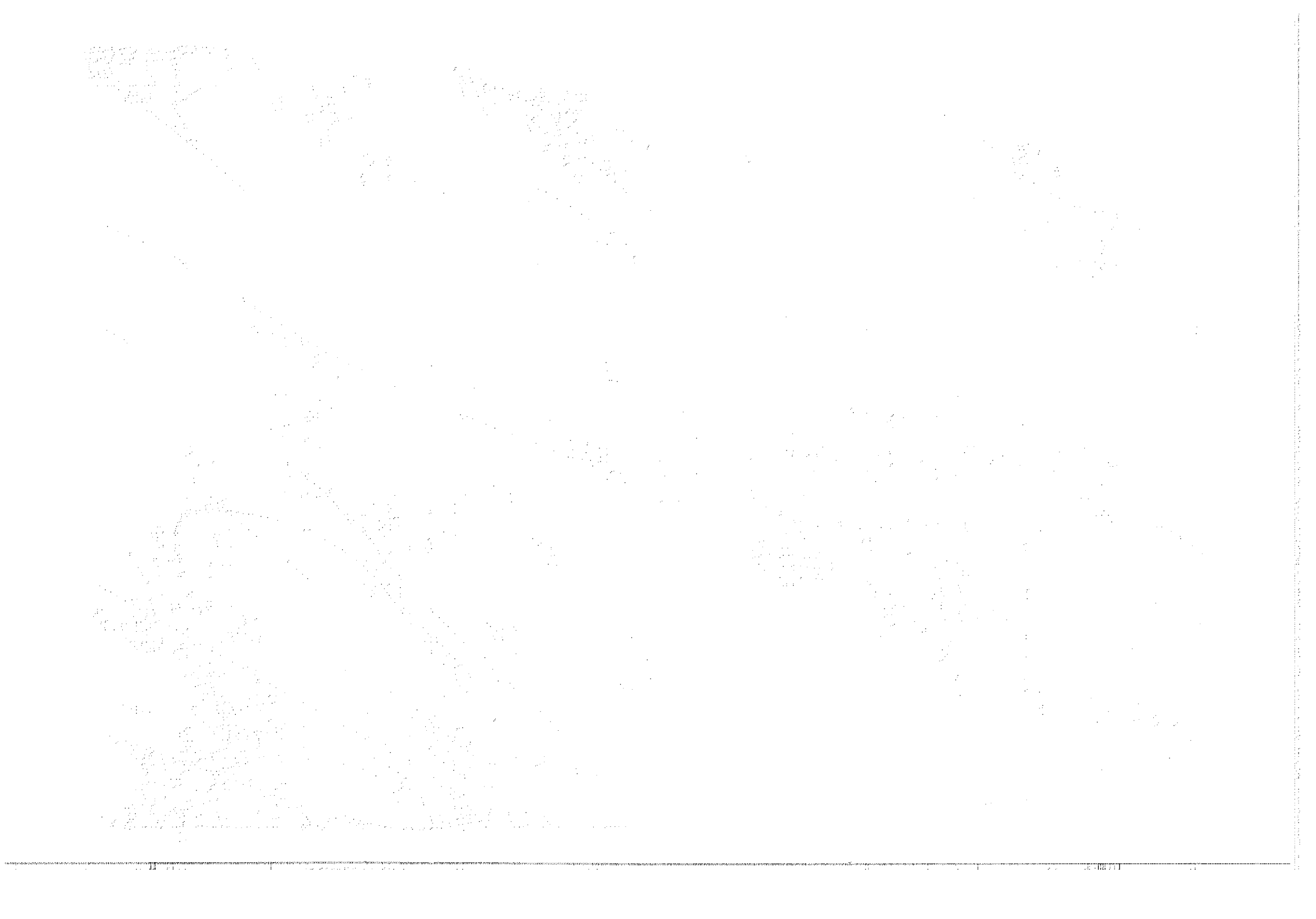

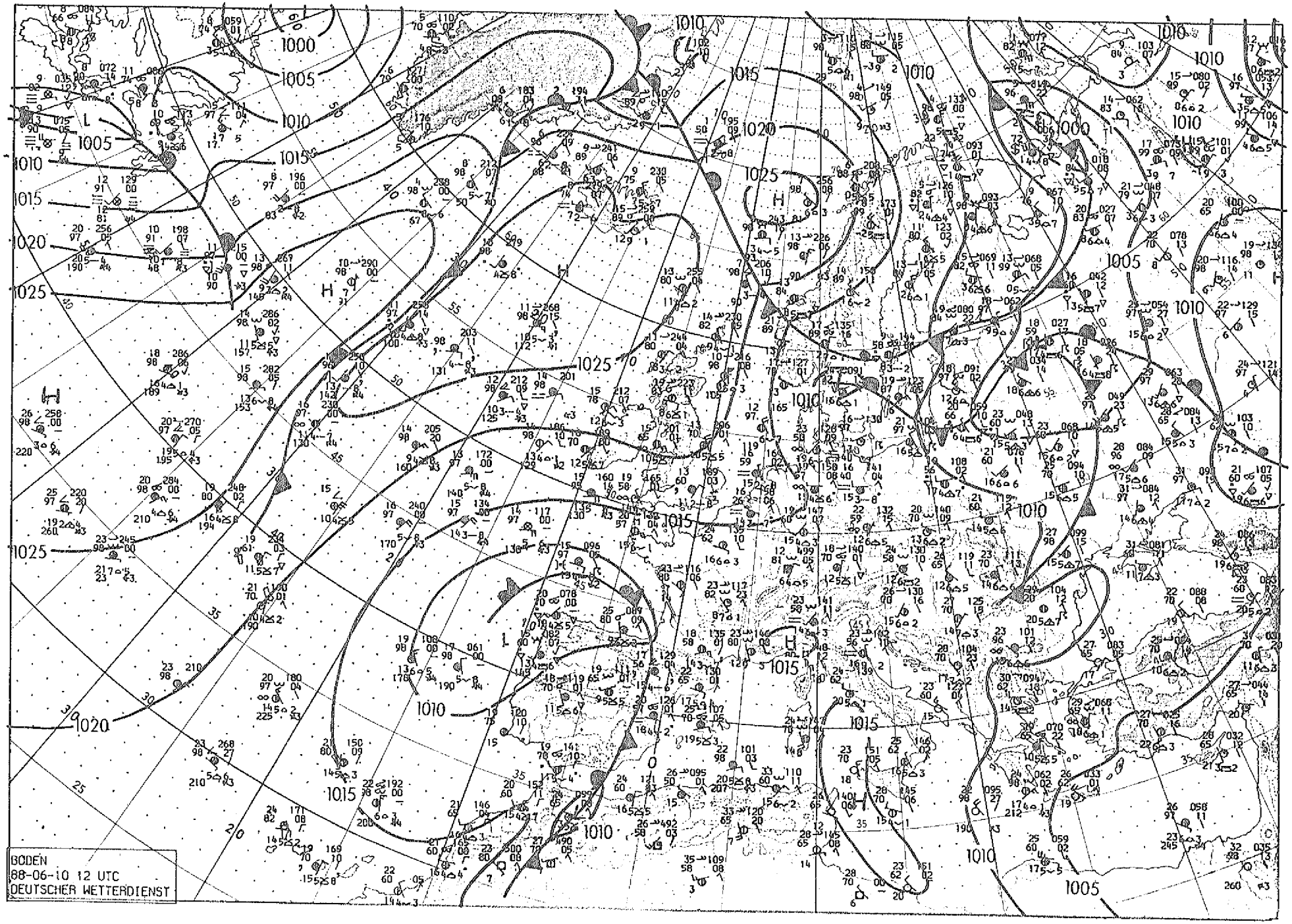
BODEN
88-06-10 12 UTC
DEUTSCHER WETTERDIENST

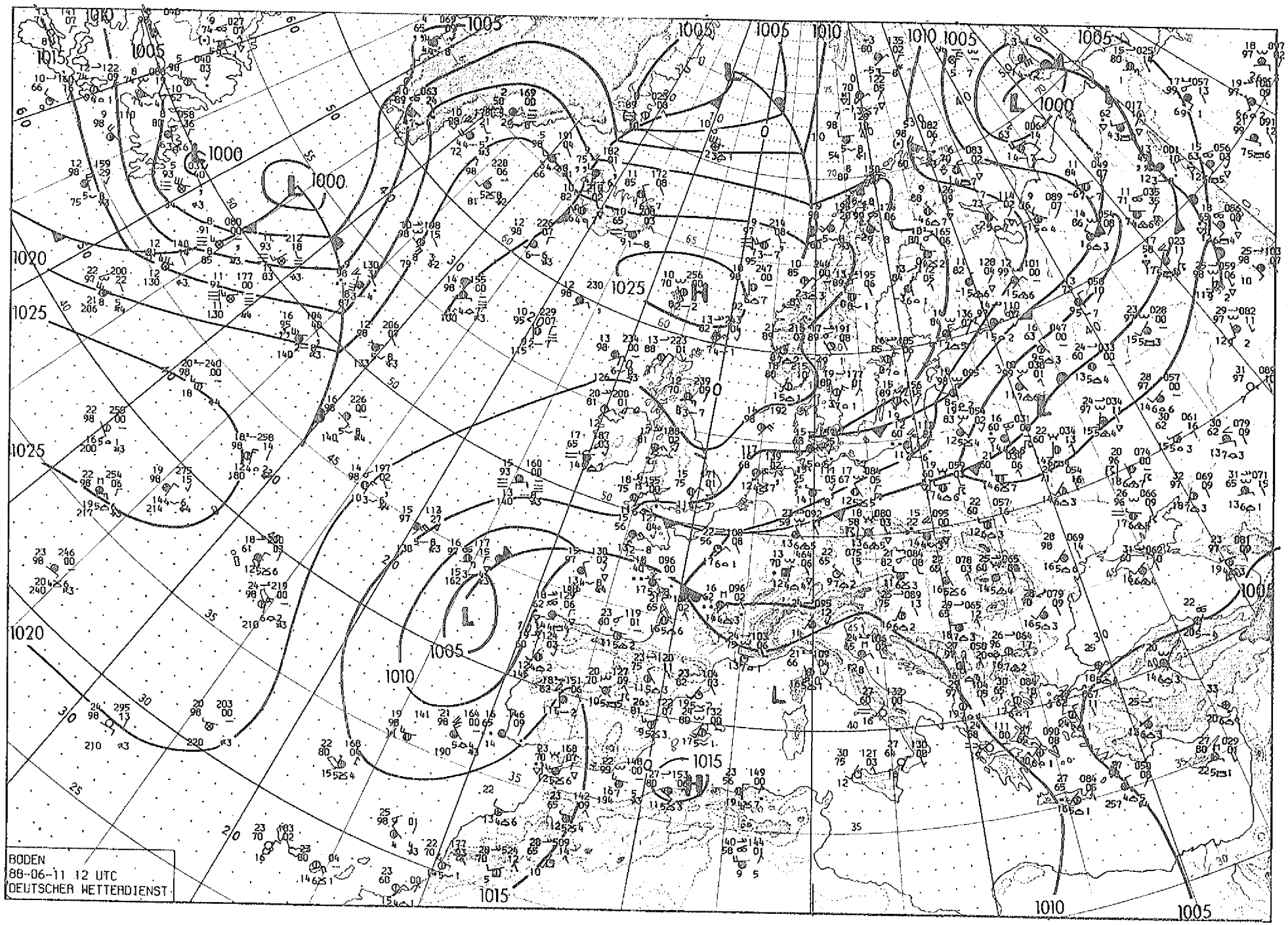
BODEN
88-06-11 12 UTC
DEUTSCHER WETTERDIENST

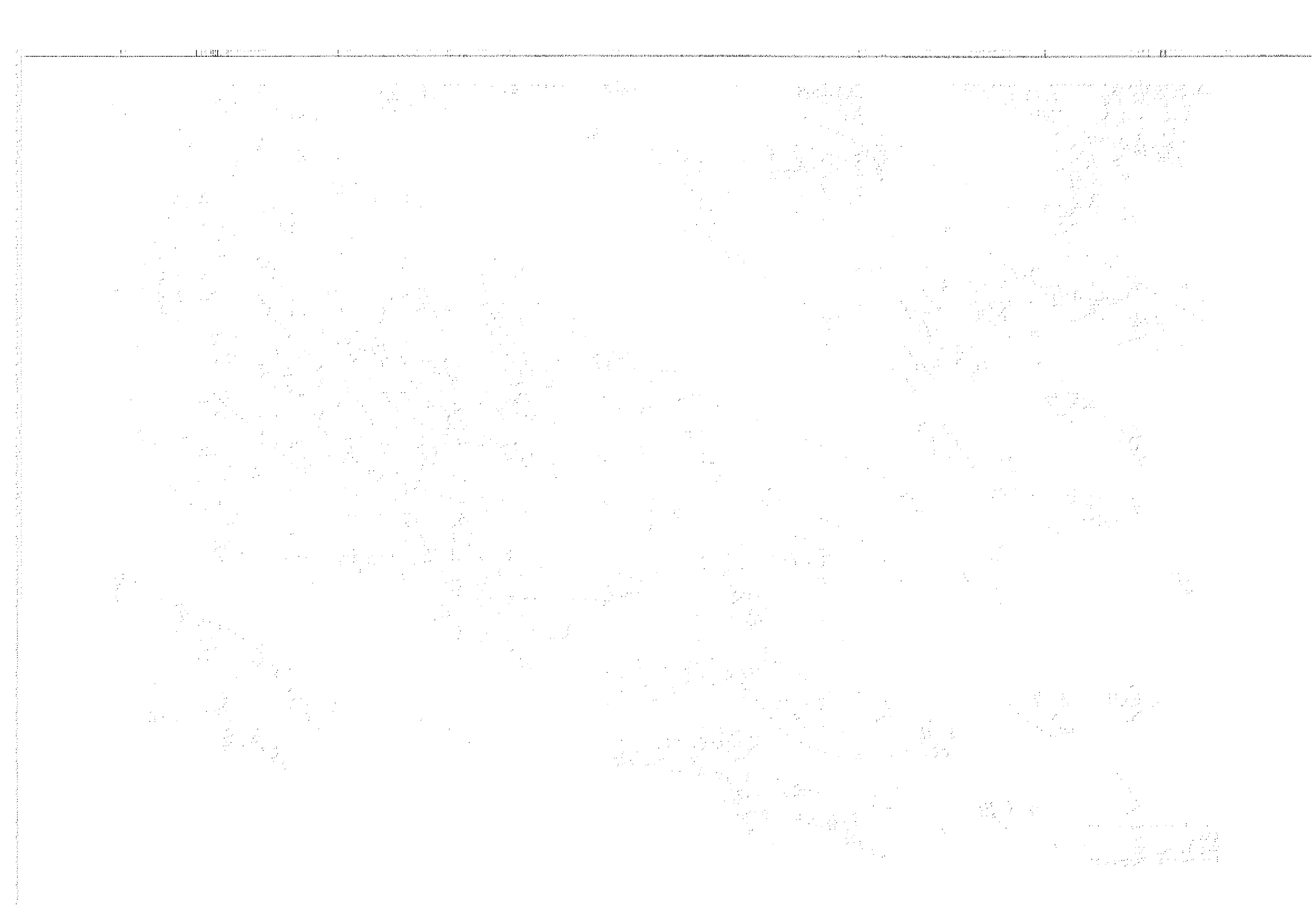

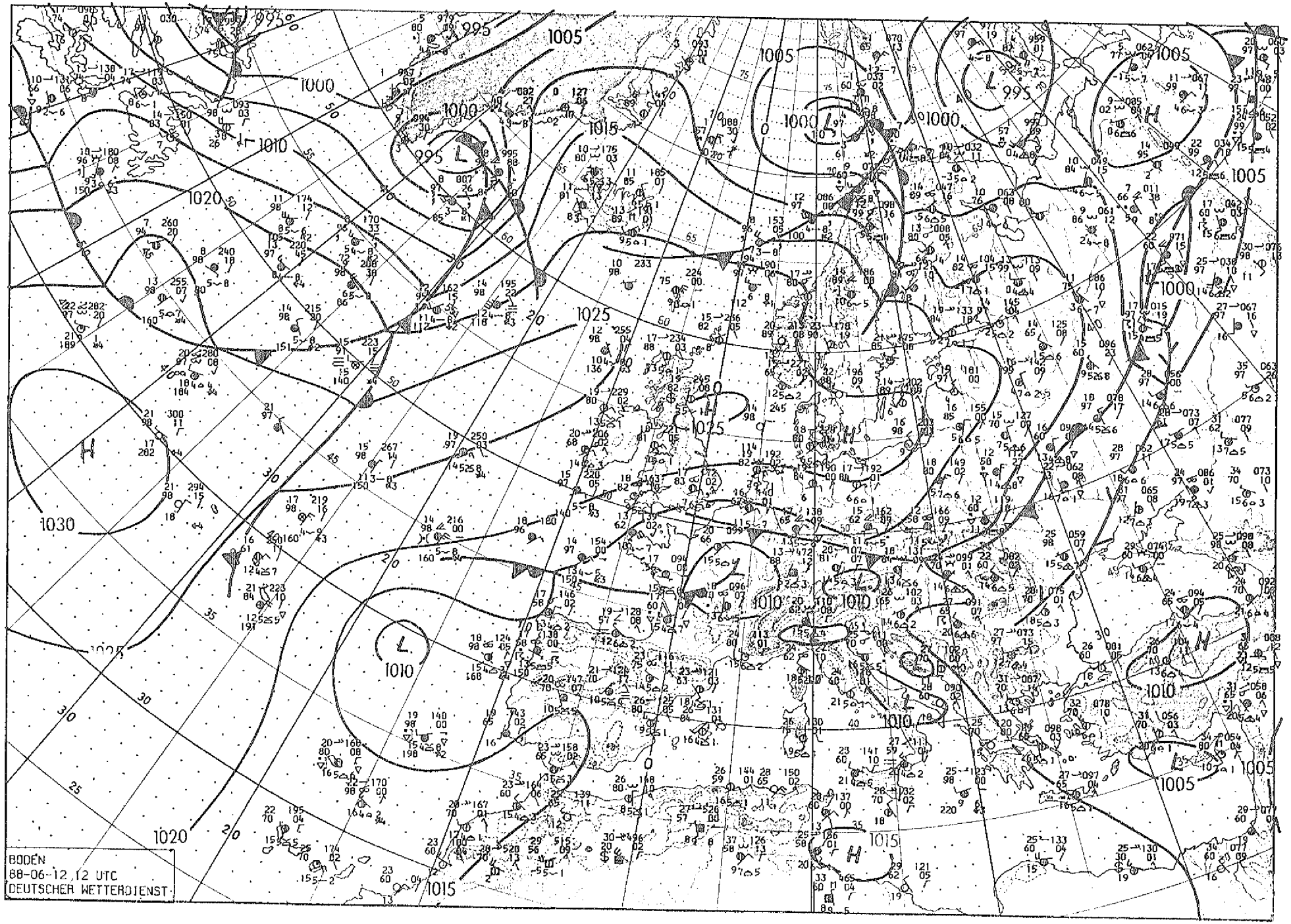
BODEN
88-06-12 12 UTC
DEUTSCHER WETTERDIENST

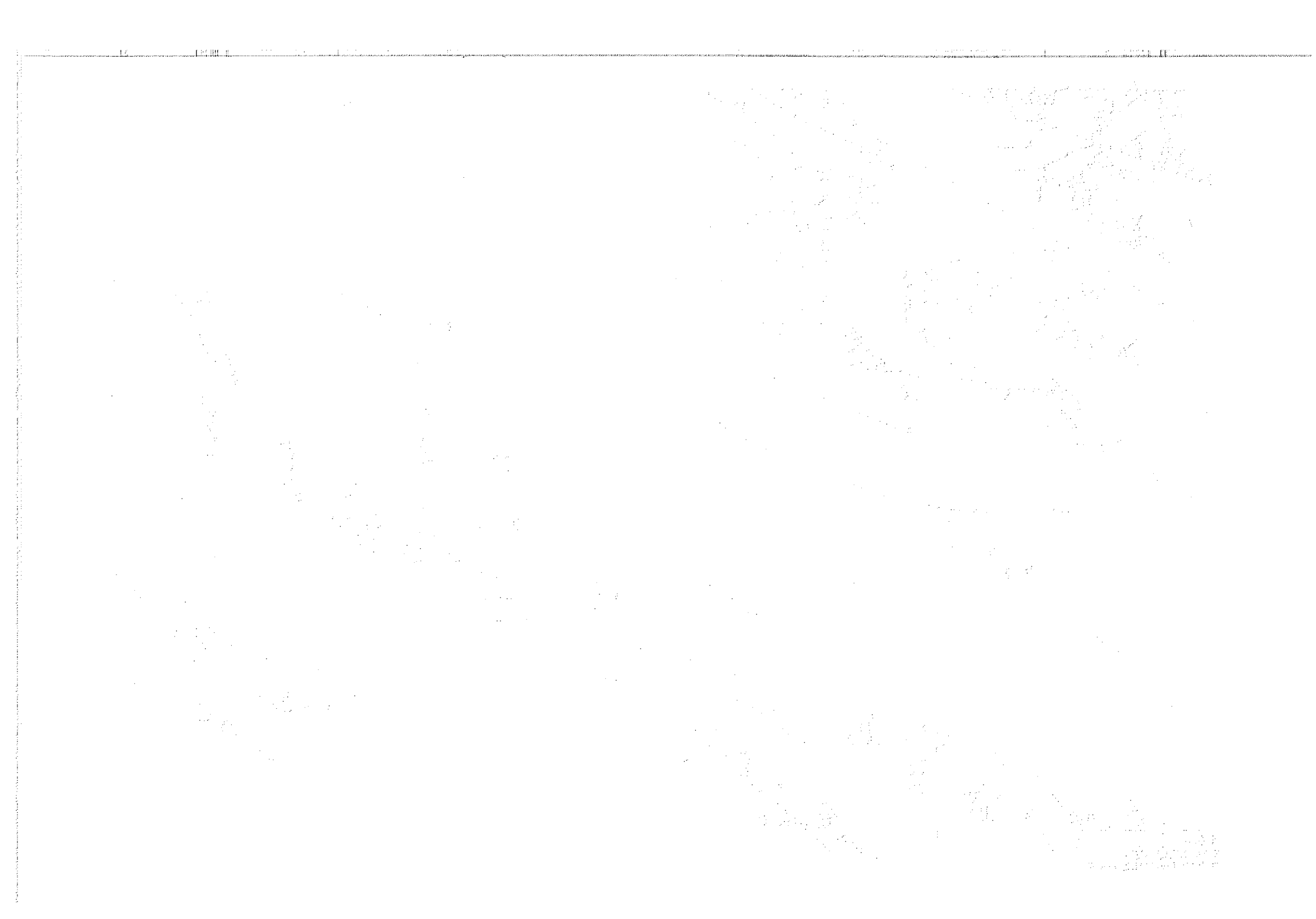

FORSCHUNGSZENTRUM JÜLICH GmbH

KFA

Jül-2731
February 1993
ISSN 0366-0885